



NTNU – Trondheim
Norwegian University of
Science and Technology

Fragment Based Approach in the Search for New Kinase Inhibitors

Ingri Ullestad Moen

Chemical Engineering and Biotechnology

Submission date: June 2014

Supervisor: Bård Helge Hoff, IKJ

Co-supervisor: Steffen Bugge, IKJ

Norwegian University of Science and Technology
Department of Chemistry

I hereby declare that this master thesis is an independant work, according to the exam regulations of the Norwegian University of Science and Technology.

Trondheim, June 13, 2014

Ingri Ullestad Moen

Preface

This master's thesis has been performed at the Department of Chemistry at NTNU, Trondheim, in spring 2014. The work has been supervised by Associate Professor Bård Helge Hoff and PhD Student Steffen Bugge.

I wish to thank Associate Professor Bård Helge Hoff for giving me the opportunity to be a part of the research group “Hoff/Sundby-familien”, and for inspirational and constructive guidance in the work. For good help and instructions in the lab and for always taking the time to give wise answers to all my questions, I would like to thank PhD Student Steffen Bugge. I am also grateful to the rest of the research group for providing a wonderful environment, socially as well as professionally. Thanks to Steffen Bugge and Fredrik Willumsen for enjoyable days in the lab, and to staff engineer Roger Aarvik for supplying all the chemicals I requested, and for handing me those extra NMR tubes. Susana Villa Gonzales also deserve a thank you for MS results, and for acting the role as MS-detective helping me to identify some mysterious by-products.

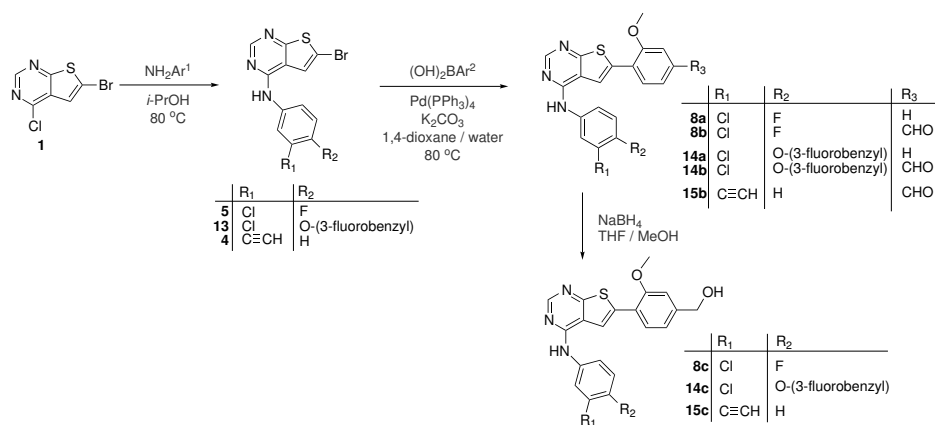
To Kent-Ove, Henrik, Trygve and the rest of the inhabitants of the reading hall; thanks for keeping spirits high every day. Thanks to Thomas Bakka for inappropriate jokes during coffee breaks. I also wish to thank my girls for refreshing lunch breaks in the sun, and for always having been there for me these past five years.

Finally, a special thanks to Håvard for keeping on saying “You can do it!”, even when I don't believe you. Thank you for always being right.

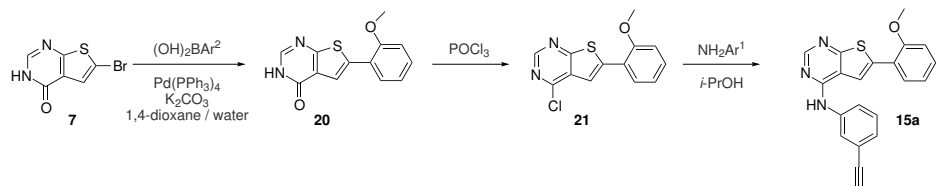
Abstract

This master's thesis has been performed in cooperation with a larger research group, as part of an ongoing study. The group is engaged in developing biologically active compounds with potency of inhibiting epidermal growth factor receptor tyrosine kinase (EGFR TK), for potential use as anti-cancer agents.

The primary goal of this master's thesis has been the identification of new active EGFR tyrosine kinase inhibitors. This has been done by use of a fragment based approach. Selected aniline fragments present in commercially available EGFR inhibitors have been introduced to a thienopyrimidine scaffold, forming building blocks for further combination with potency inducing fragments identified by the research group. A total of nine target compounds and one building block have been synthesized in this work.



The target compounds have been synthesized from **1** using a thermal amination succeeded by a Suzuki cross-coupling reaction. Compounds **8c**, **14c** and **15c** were obtained by reduction of the formyl group in **8b**, **14b** and **15b**, respectively. The building blocks **4** and **5** had been prepared earlier, but were used in further syntheses in this work. The aniline fragment found in **13** has also been made in this thesis work. Owing to dimerization of the product, compound **15a** had to be synthesized using an alternative route, starting from **7**.

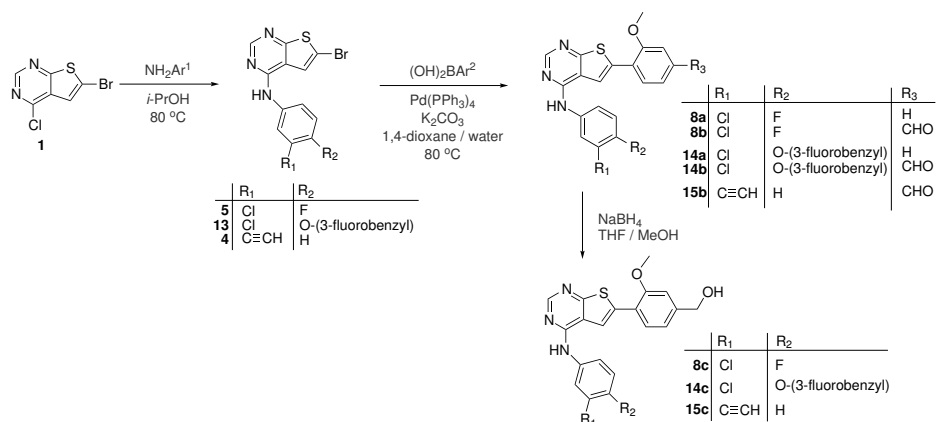


Most of the synthesized compounds have been tested for *in vitro* enzymatic inhibition activity. A second goal in this thesis has been to investigate the concept of fragment based drug design, based on these inhibition results. Combinations of potent substituent groups were found to give target compounds of high potency. The best compound tested gave an IC_{50} -value of 2.4 nM.

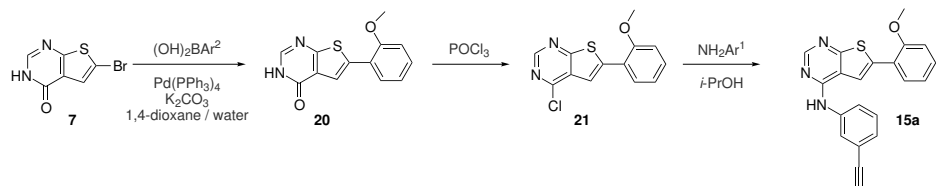
Samandrag

Arbeidet med denne masteroppgåva har vorte utført i samarbeid med ei større forskingsgruppe, som del av pågåande undersøkingar. Gruppa arbeider med utvikling av biologisk aktive stoff med evne til å hemme epidermal vekstfaktorreseptor tyrosin kinase (EGFR TK), for potensiell bruk innan kreftbehandling.

Hovudmålet med denne oppgåva har vore identifisering av nye aktive EGFR tyrosin kinasehemmarar. Dette har vorte gjort ved hjelp av ei fragmentbasert tilnærming. Utvalde anilinfragment funne i kommersielt tilgjengelege EGFR-hemmarar har vorte introdusert på ein tienopyrimidin grunnstruktur for å danne byggjesteinar som vidare har vorte substituert med aktivitetfremjande fragment, identifisert av forskingsgruppa. Totalt ni målmolekyl og éin byggjestein har vorte syntetiserte i dette arbeidet.



Målmolekyla har vorte framstilte ved bruk av ein termisk aminering etterfylgt av ein Suzuki koplingsreaksjon. Sambindingane **8c**, **14c** og **15c** vart framstilt ved reduksjon av formylgruppa i dei respektive aldehyda **8b**, **14b** og **15b**. Byggjesteinane **4** og **5** hadde vorte laga tidlegare, men vart nytta i vidare reaksjonar i dette masterarbeidet. Anilinfragmentet nytta i syntesa av **13** har også vorte syntetisert i dette arbeidet. Grunna dimerisering av produktet, vart **15a** framstilt ved bruk av ei alternativ synteserute med utgangspunkt i **7**.



Storparten av dei framstilte stoffa har vorte testa for *in vitro* EGFR hemmingsaktivitet. Eit delmål i denne oppgåva har vore å undersøke fragmentbasert medisindesign som konsept, basert på desse hemmingsdataa. Det vart funne at kombineringsav potente substituentar førte til målmolekyl med høgare hemmingsevne. Det målmolekylet som oppnådde best hemmingsaktivitet hadde ein IC_{50} -verdi på 2,4 nM.

Contents

Preface	iii
Abstract	v
Symbols and Abbreviations	xiii
Numbered Compounds	xv
1 Introduction	1
2 Theory	3
2.1 The Importance of Thiophene and Fluorine in Medicinal Chemistry	3
2.2 Drug Development	5
2.2.1 Structure-based drug design	5
2.2.2 Fragment-based drug design	6
2.3 Tyrosine Kinase and Tyrosine Kinase Inhibitors	7
2.4 Previous Work in the Research Group	11
2.4.1 Results from the pre-project autumn 2013	11
2.4.2 Results from the research group	13
2.5 Synthesis of Substituted Thieno[2,3- <i>d</i>]pyrimidines	16
2.5.1 Choice of reaction sequence	18
2.5.2 Thermal coupling of halogenated thienopyrimidines with anilines	19
2.5.3 Alternative methods of amination	22
2.5.4 Suzuki coupling	24
2.5.5 Williamson ether synthesis	29
2.5.6 Alternative methods of ether synthesis	31
3 Results and Discussion	33
3.1 Compounds Based on the Gefitinib Fragment	35
3.1.1 Purification of compound 5 ·HCl	35
3.1.2 Suzuki coupling of 5	36
3.1.3 Reduction of compound 8b - Synthesis of 8c	38
3.1.4 Overall remarks on the Gefitinib fragment based compounds	40

3.2	Compounds Based on the Lapatinib Fragment	41
3.2.1	Synthesis of the building block 13 ·HCl	41
3.2.2	Suzuki coupling of 13 - Synthesis of 14a and 14b	50
3.2.3	Reduction of 14b - Synthesis of 14c	51
3.2.4	Overall remarks on the Lapatinib fragment based compounds	53
3.3	Compounds Based on the Erlotinib Fragment	54
3.3.1	Synthesis of 15a	54
3.3.2	Synthesis of 15b	63
3.3.3	Synthesis of compound 15c	64
3.3.4	Overall remarks on the Erlotinib fragment based compounds	65
3.4	<i>In vitro</i> Inhibition Testing	67
3.5	Compound Characterization	71
3.5.1	Characterisation of Compound 8a	73
3.5.2	Characterisation of Compound 8b	76
3.5.3	Characterisation of Compound 8c	78
3.5.4	Characterisation of Compound 13 ·HCl	80
3.5.5	Characterisation of Compound 14a	82
3.5.6	Characterisation of Compound 14b	84
3.5.7	Characterisation of Compound 14c	86
3.5.8	Characterisation of Compound 20	88
3.5.9	Characterisation of Compound 21	90
3.5.10	Characterisation of Compound 15a	92
3.5.11	Characterisation of Compound 15b	94
3.5.12	Characterisation of Compound 15c	96
4	Conclusion	99
5	Future Work	101
6	Experimental	103
6.1	General Information	103
6.1.1	Separation techniques	103
6.1.2	Chromatographic and spectroscopic analyses	103
6.1.3	Melting point	104

6.1.4	<i>In vitro</i> EGFR inhibition testing	104
6.2	Synthetic Procedures	106
6.2.1	Purification of 6-bromo- <i>N</i> -(3-chloro-4-fluorophenyl)thieno[2,3- <i>d</i>]pyrimidine-4-amine·HCl (5 ·HCl)	106
6.2.2	Synthesis of <i>N</i> -(3-chloro-4-fluorophenyl)-6-(2-methoxyphenyl)thieno[2,3- <i>d</i>]pyrimidin-4-amine (8a)	106
6.2.3	Synthesis of 4-(4-((3-chloro-4-fluorophenyl)amino)thieno[2,3- <i>d</i>]pyrimidin-6-yl)-3-methoxybenzaldehyde (8b)	107
6.2.4	Synthesis of (4-(4-((3-chloro-4-fluorophenyl)amino)thieno[2,3- <i>d</i>]pyrimidin-6-yl)-3-methoxyphenyl)methanol (8c)	108
6.2.5	Synthesis of 2-chloro-1-((3-fluorobenzyl)oxy)-4-nitrobenzene (11)	109
6.2.6	Synthesis of 3-chloro-4-((3-fluorobenzyl)oxy)aniline (12)	109
6.2.7	Synthesis of 6-bromo- <i>N</i> -(3-chloro-4-((3-fluorobenzyl)oxy)phenyl)thieno[2,3- <i>d</i>]pyrimidin-4-amine·HCl (13 ·HCl)	110
6.2.8	Synthesis of <i>N</i> -(3-chloro-4-((3-fluorobenzyl)oxy)phenyl)-6-(2-methoxyphenyl)thieno[2,3- <i>d</i>]pyrimidin-4-amine (14a)	111
6.2.9	Synthesis of 4-(4-((3-chloro-4-((3-fluorobenzyl)oxy)phenyl)amino)thieno[2,3- <i>d</i>]pyrimidin-6-yl)-3-methoxybenzaldehyd (14b)	112
6.2.10	Synthesis of (4-(4-((3-chloro-4-((3-fluorobenzyl)oxy)phenyl)amino)thieno[2,3- <i>d</i>]pyrimidin-6-yl)-3-methoxyphenyl)methanol (14c)	113
6.2.11	Synthesis of 6-(2-methoxyphenyl)thieno[2,3- <i>d</i>]pyrimidin-4(3 <i>H</i>)-one (20)	113
6.2.12	Synthesis of 4-chloro-6-(2-methoxyphenyl)thieno[2,3- <i>d</i>]pyrimidine (21)	114
6.2.13	Synthesis of <i>N</i> -(3-ethynylphenyl)-6-(2-methoxyphenyl)thieno[2,3- <i>d</i>]pyrimidin-4-amine·HCl (15a ·HCl)	115
6.2.14	Synthesis of 4-(4-((3-ethynylphenyl)amino)thieno[2,3- <i>d</i>]pyrimidin-6-yl)-3-methoxybenzaldehyde (15b)	115
6.2.15	Synthesis of (4-(4-((3-ethynylphenyl)amino)thieno[2,3- <i>d</i>]pyrimidin-6-yl)-3-methoxyphenyl)methanol (15c)	116

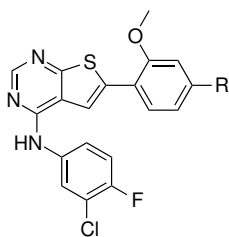
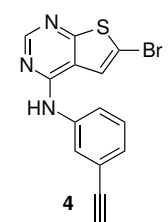
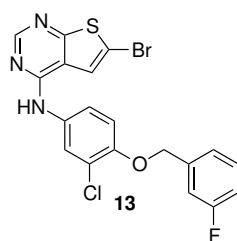
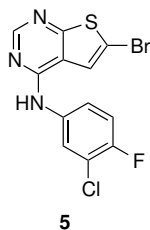
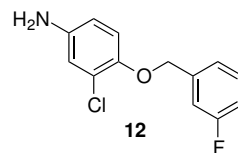
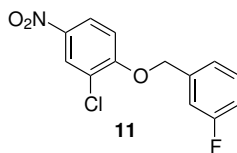
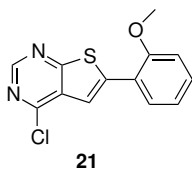
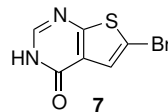
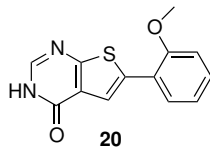
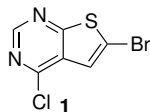
References	119
A Spectroscopic Data - Compound 5·HCl	II
B Spectroscopic Data - Compound 8a	IV
C Spectroscopic Data - Compound 8b	XIII
D Spectroscopic Data - Compound 8c	XXII
E Spectroscopic Data - Compound 11	XXXII
F Spectroscopic Data - Compound 12	XXXV
G Spectroscopic Data - Compound 13·HCl	XXXVIII
H Spectroscopic Data - Compound 14a	XLVIII
I Spectroscopic Data - Compound 14b	LVIII
J Spectroscopic Data - Compound 14c	LXIX
K Spectroscopic Data - Compound 20	LXXX
L Spectroscopic Data - Compound 21	LXXXVIII
M Spectroscopic Data - Compound 15a·HCl	XCVI
N Spectroscopic Data - Compound 15b	CIII
O Spectroscopic Data - Compound 15c	CX
P Risk Assessment Form	CXVIII

Symbols and Abbreviations

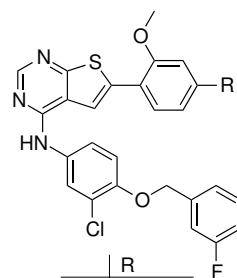
ACN	Acetonitrile
ADP	Adenosine diphosphate
Ar	Aryl
ATP	Adenosine triphosphate
bp	Boiling point
br	Broad signal
corr.	Correlation
COSY	^1H - ^1H correlation spectroscopy
d	Doublet
DCM	Dichloromethane
dd	Doublet of doublets
dec.	Decompose, decoupled (in ^{19}F -NMR)
DMF	Dimethyl formamide
DMSO	Dimethyl sulphoxide
EGF	Epidermal growth factor
EGFR	Epidermal growth factor receptor
eq.	Equivalents
<i>et al.</i>	<i>Et alii</i> (and others)
FBDD	Fragment-based drug design
FTIR	Fourier transform infrared spectroscopy
h	Hour
HMBC	Heteronuclear (^1H - ^{13}C) multiple bond coherence
HPLC	High performance liquid chromatography
HRMS	High resolution mass spectroscopy
HSQC	Heteronuclear (^1H - ^{13}C) single quantum coherence
HTS	High-throughput screening
IC ₅₀	The inhibitor concentration needed to reduce target function by 50%
int.	Integral
IR	Infrared spectroscopy
<i>J</i>	Coupling constant
lit.	Literature
m	Multiplet, medium (IR intensity)

m/z	Mass over charge ratio
min	Minute
mp	Melting point
MS	Mass spectroscopy
mult.	Multiplicity
NMR	Nuclear magnetic resonance
ppm	Parts per million
R_f	Retention factor
rt	Room temperature
RTK	Receptor tyrosine kinase
s	Singlet, strong (IR intensity)
S_N2	Nucleophilic substitution
S_NAr	Nucleophilic aromatic substitution
t	Triplet
THF	Tetrahydrofuran
TK	Tyrosine kinase
TKI	Tyrosine kinase inhibitor
TLC	Thin layer chromatography
TMS	Trimethylsilyl
t_R	Retention time
UV	Ultraviolet
δ	Chemical shift
ν	Wave number

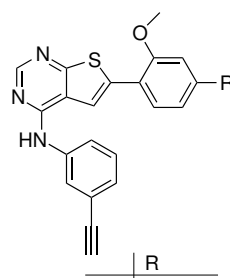
Numbered Compounds



	R
8a	H
8b	CHO
8c	CH ₂ OH



	R
14a	H
14b	CHO
14c	CH ₂ OH



	R
15a	H
15b	CHO
15c	CH ₂ OH

1 Introduction

Every diagnosed case of cancer brings fear, pain and horror to the patient and the surrounding friends and family. In many cases, the cancer also leads to death. In 2008, 13% of all deaths worldwide were estimated to be cancer related, with lung, breast, stomach, liver and colon cancer being the main diagnoses.¹ In the search for effective treatments, several tyrosine kinase inhibitors have been developed. By abrputing cellular functions in sick cells, tyrosine kinase inhibitors may provide a more target spesific and effective cancer treatment.²

The research group has developed several thienopyrimidine based compounds with high tyrosine kinase inhibition potency. The focus in this master's thesis has been to synthesize and characterize new compounds with potential biologic activity, based on potent fragementes discovered in the group and fragments present in commercially available tyrosine kinase inhibitors. The compounds synthesized in this thesis will thereby support the ongoing structure-activity study, and potentially lead to compounds of increased potency.

The target molecules have been synthesised using nucleophilic aromatic substitution reactions and Suzuki coupling reactions. In addition, Williamson ether synthesis has been applied to synthesize one of the anilines used in the nucleophilic aromatic substitution. The synthesized compounds are illustrated in Figure 1.1.

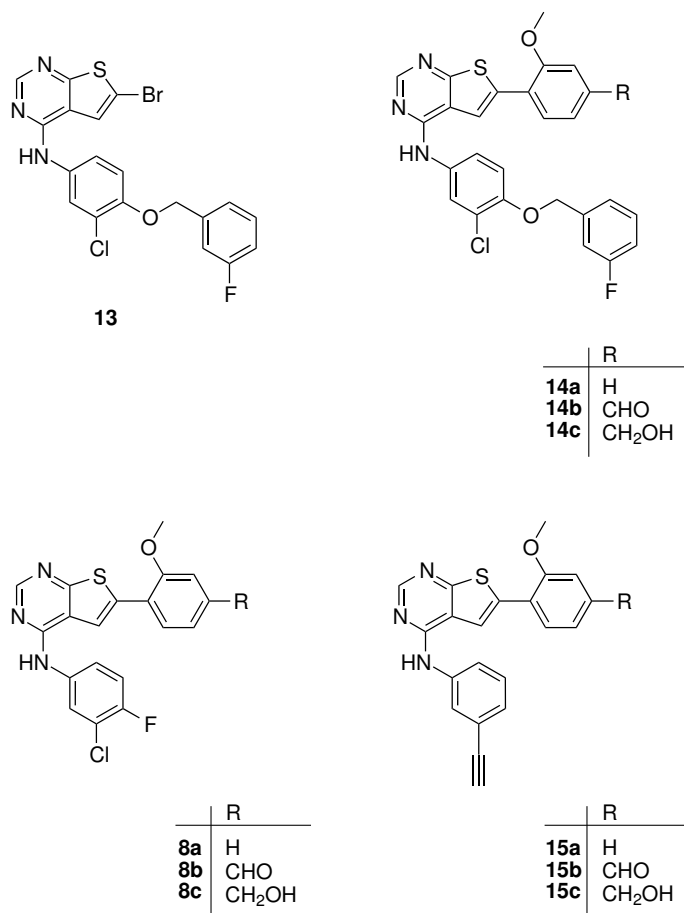


Figure 1.1: Potential tyrosine kinase inhibitors synthesized in this master's thesis.

2 Theory

2.1 The Importance of Thiophene and Fluorine in Medicinal Chemistry

Thiophenes constitute an important class of heterocyclic compounds. They are stable, easily functionalized and readily available.³ With its six π -electrons, thiophene is an electron rich compound, and a biostere to benzene. Thiophene can thus replace benzene in biological active compounds without drastically altering the chemical and physical properties of the compound.⁴ In addition, thiophene is less toxic than benzene,⁴ due to its lower resonance energy. This makes thiophene and its derivatives important compounds in pharmaceutical chemistry.

Among the many classes of thiophene derivatives possessing bioactive properties, thienopyrimidines make up an important branch.⁵ Numerous derivatives of thienopyrimidine are found to have biological activity, with effects ranging from antiinflammatory,⁶ antibacterial⁷ and analgesic agents,⁸ to preventing cartilage destruction in articular diseases⁹ and increasing the sexual activity among male rats.¹⁰ Another important function of thienopyrimidine derivatives are their ability to act as tyrosine kinase inhibitors (TKIs), low molecular weight anti-cancer agents.¹¹⁻¹³ The structures of thiophene and thieno[2,3-*d*]pyrimidine are illustrated in Figure 2.1.

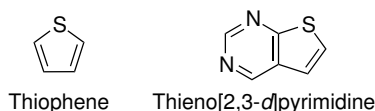


Figure 2.1: The structures of thiophene and thieno[2,3-*d*]pyrimidine.

For a drug to be effective, appropriate binding to the target site is essential, but there are also other factors influencing the obtained effect from a certain drug. The inhibitors must be transported to the correct location in the body, without decomposing. Oral drugs must thus tolerate the acidic conditions in the stomach. Further on, the drug must be hydrophilic enough for being dissolved and transported in the blood stream. On the other hand, the water solubility must

not be too high, causing the drug to be excreted from the body too fast, or causing hydrogen bonding with water to be more favourable than binding to the target site. If the target destination of the drug is inside the cell, the compound also must be hydrophobic enough to be transported through the lipophilic cell membrane. Finally, the drug should not form toxic compounds when metabolized.^{14,15}

Fluorine is a biostere to both hydrogen and hydroxyl (Figure 2.2), and such an atom replacement is one of the more commonly employed in medicinal chemistry.¹⁶ The reason for this being that introduction of fluorine in a pharmaceutical can be used to alter one or more of the qualities mentioned above, thereby improving the drug potency of the molecule. In fact, 20-25% of all commercially available drugs contain one or more fluorine atoms, despite the low natural abundance of organofluorine compounds.¹⁵ The possibility to tune the properties of a drug molecule is caused by the prominent difference in electronegativity between hydrogen and fluorine.



Figure 2.2: Fluorine is a biostere to hydrogen and hydroxyl.

Among the characteristics that can be affected by introduction of fluorine are binding affinity, bioavailability of oral drugs (% of the dose reaching the circulatory system) and metabolic stability. The electronegativity of fluorine can lead to a decrease in pK_a value for a compound.¹⁷ Such an increase in basicity is beneficial for the bioavailability of oral drugs. Altered acidity can also affect binding affinities of a molecule, as can properties such as conformation, electrostatic interactions and possibility of hydrogen bond formation. Poor metabolic stability is a common problem in drug development, but can in many cases be overcome by blocking metabolically labile sites with fluorine atoms.¹⁵ The electronegativity of fluorine can, as an example, deactivate aromatic rings towards metabolism.

2.2 Drug Development

Medicinal chemistry is the science that deals with discovery and design of new therapeutic chemicals, and their development into substances used to treat diseases, substances we call medicines.¹⁸

The process of developing a new, efficient drug can be approached in different ways. Identification of the drug target and the mechanism of drug action may be informative as to designing a suitable drug.¹⁹ Several kinase inhibitors have been discovered by targeting enzyme catalytic domains with similar ATP binding sites.^{20,21}

In the early years, drug discovery was based on a random approach; trial and error independent from any preset strategy. Later on, as a result of advances in areas such as synthesis, computational chemistry, biology and biochemical techniques, more rational approaches of drug design have developed.¹⁸ One such method is the high-throughput screening (HTS), which was particularly popular in the 1990s. HTS made it possible to screen hundreds of thousands of compounds in order to identify drug-like molecules with pharmacological activity. Although it has provided good results, this method is highly expensive and time consuming.^{22,23} Nowadays methods such as structure-based drug design and fragment-based drug design are becoming increasingly more widespread, and they provide a powerful complement to the HTS approach.²⁴⁻²⁶

2.2.1 Structure-based drug design

The goal in structure-based drug design (SBDD) is to develop novel molecules that fit into the desired binding site. Understanding the three-dimensional structure of the active site in the target is thus the key in this method of drug design. This information can be obtained through X-ray crystallography or NMR spectroscopy.^{24,25} Identification and depiction of the binding pocket is thus the primary step in a structure-based design. The next step is generation of molecular structures based on atoms or fragments that result in favourable interactions with the active site, and finally the generated structures are evaluated for their

desired properties and synthetic accessibility.²⁵

Structure based drug design is often used to increase efficiency and/or selectivity in lead structures already known to possess some form of bioactivity. The central idea in this approach is that a drug must contain chemical and structural features that are significantly complementary to those found in the target receptor,²⁷ in order to bind and act. A hydrogen bond acceptor must, for instance, interact with a hydrogen bond donor in order to contribute to binding of the drug. By altering the lead compounds and analysing the effects, substitution patterns that improve or worsen the properties of the potential drug can be identified. Subsequent combination of favourable fragments may thus lead to the preparation of molecules displaying better potency, based on already existing drugs, or other potent compounds.

Imatinib (Gleevec[®]) is an example of a drug discovered as a result of structure-based drug design. Commercialized in 2001, Imatinib was the first tyrosine kinase inhibitor in clinical use as an anti-tumor agent.²⁴

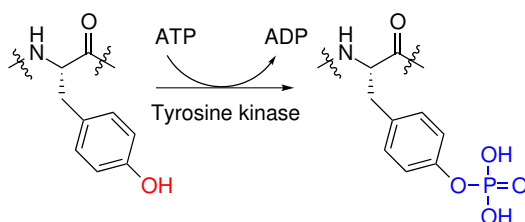
2.2.2 Fragment-based drug design

As suggested by the name, small molecular fragments form the starting point of a fragment-based drug design (FBDD).²⁵ Small fragments with no appreciable pharmacological activity are tested for weak binding to potential drug targets. The weak binders act as essential starting points from which larger drug-like binders can be created. Since their inception,²⁸ FBDD have been adopted by several drug companies, such as Abbott, Astex, Plexxikon and Vernalis.²⁹ One drug, Zelboraf (PLX4032), found by FBDD are commercially available, and several are undergoing clinical trials.^{26,29,30}

Deriving fragments from known inhibitors is a popular technique of finding a starting fragment, but screening by use of fragment libraries are also possible. If comparing screening of small fragments (having up to 12 heavy atoms) with that of potential drug-like compounds (having up to 30 heavy atoms), fragment screening is found much more efficient. Estimations suggest there are 10^7 potential fragments, while there are 10^{60} potential drug-like molecules.²⁶

2.3 Tyrosine Kinase and Tyrosine Kinase Inhibitors

Tyrosine kinases are enzymes that participate in the regulation of several cellular functions. The enzyme officiates by catalysing the transfer of a γ -phosphate group from adenosine triphosphate (ATP) to a surface hydroxyl group in the amino acid tyrosine, found in proteins (Scheme 2.1). This activates the protein for cellular actions eventually leading to e. g. differentiation, migration and proliferation.^{11,31} Tyrosine kinases thereby acts as an on/off switch for these cellular functions.



Scheme 2.1: Transfer of a phosphate group from ATP to a protein, catalyzed by tyrosine kinase.

One type of TK is the receptor tyrosine kinase (RTK), which works as a receptor in addition to being an enzyme. RTKs are transmembrane receptors, consisting of an extracellular binding site for signal molecules and an intracellular region involved in further downstream signalling.

The epidermal growth factor receptor (EGFR) is one type of RTK, belonging to the ErbB family. When a signal molecule, such as epidermal growth factor (EGF), bind to the outer binding site of the RTK, a ligand induced dimerization of the kinase activates signalling to the intracellular part.³² Binding of ATP then activates the inner region for autophosphorylation, eventually leading to cellular actions³³ (Figure 2.3).

Tyrosine kinases are essential in several different cellular activities, e.g. cell growth, survival and formation of blood vessels.² Mutations may cause disturbances in tyrosine kinase activity. Overactive TKs lead to abnormal cell growth, which in turn can cause malignant cancer tumors. EGFR is involved in cell proliferation, and it is found to be overexpressed in many malignant tumors.^{2,35}

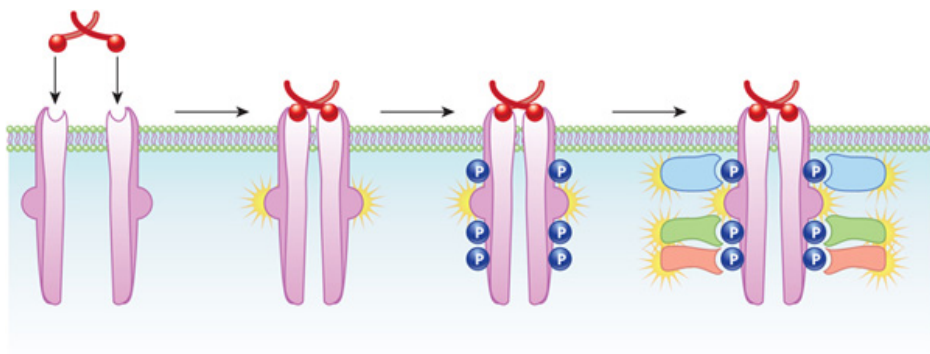


Figure 2.3: Receptor tyrosine kinase is activated by a signal molecule, leading to dimerization of the kinase. Phosphorylation of proteins is catalyzed by the kinase, activating the proteins for cellular action.³⁴

Inhibiting EGFR is thus a possible method of obstructing the abnormal cell growth. This makes EGFR a key target for anti-cancer drugs.^{36–38}

Most enzyme targeting drugs are inhibitors,³⁹ which functions by abruptly essential substrate binding. Two different types of EGFR inhibitors have been developed for use in cancer treatment; low molecular weight tyrosine kinase inhibitors (TKIs) and monoclonal antibodies.²⁰ Monoclonal antibodies block the extracellular binding site, thereby stopping further downstream signalling and cellular actions.⁴⁰ Panitumumab (Vectitix[®]) and Cetuximab (Erbix[®]) are examples of commercially available monoclonal antibodies that acts as such inhibitors.^{13,41}

The intracellular kinase domain represents another possible site of inhibition. Low molecular weight compounds can diffuse through the cellular membrane and act as tyrosine kinase inhibitors by blocking the site for binding of ATP. Thereby further signalling and cell activity are stopped.^{2,36} Both monoclonal antibodies and low molecular weight TKIs are selective to tumor cells, thus not affecting rapidly dividing host cells. Thereby side effects are efficiently reduced.³³ However, low molecular weight TKIs are attractive compared to monoclonal antibodies due to their more moderate cost profile, and their intracellular mode of action.

There are several commercially available TKIs. Erlotinib (Tarceva[®]), Gefitinib (Iressa[®]) and Lapatinib (Tykerb[®]), as illustrated in Figure 2.4, are all commercially available EGFR TKIs. Both Gefitinib and Erlotinib are used in treatment of non-small cell lung cancer (NSCLC), while Lapatinib is used to treat breast cancer.^{42–44} These structures are all based on a quinazoline core, substituted in 4-, 6- and 7-position.⁴⁵ The other structures shown, AEE-788, **I** and **II**, are examples of low molecular weight compounds based on pyrrolo- and thienopyrimidine core structures. These compounds have also shown promising EGFR inhibiting potency.^{46–48}

Although several TKIs are currently being used in cancer therapy, new inhibitors are needed. Reducing side effects compared to existing drugs is desirable, but other aspects are even more vital. Cancer cells are not dependant on only one signalling pathway, thus restraining growth can be a complex matter. In addition, mutations frequently occur in tumor cells, causing reduced drug response or even immunity to the drugs.^{49,50} Resistance to Erlotinib has been observed in several tumors.⁴⁹ New drugs are therefore crucial.

Resistance studies suggest that combination treatment, or multitarget drugs are needed in order to make significant advances in cancer treatment with TKIs.⁵¹ Drugs that can inhibit multiple kinases and/or work together with other drugs are thus desired. However, a multitarget drug may cause unexpected toxicity, and combination treatments can give undesirable drug-drug interactions.

Different kinases have been found to be of importance in different types of cancer. As an example over-expression of HER2, another member of the ErbB family, is often found in certain types of breast cancer,⁵² while the Src (sarcoma) family of kinases often are activated in acute myeloid leukemia.⁵³ Development of new drugs can thus contribute to the treatment of different cancers, depending on the selectivity profile of the drug.

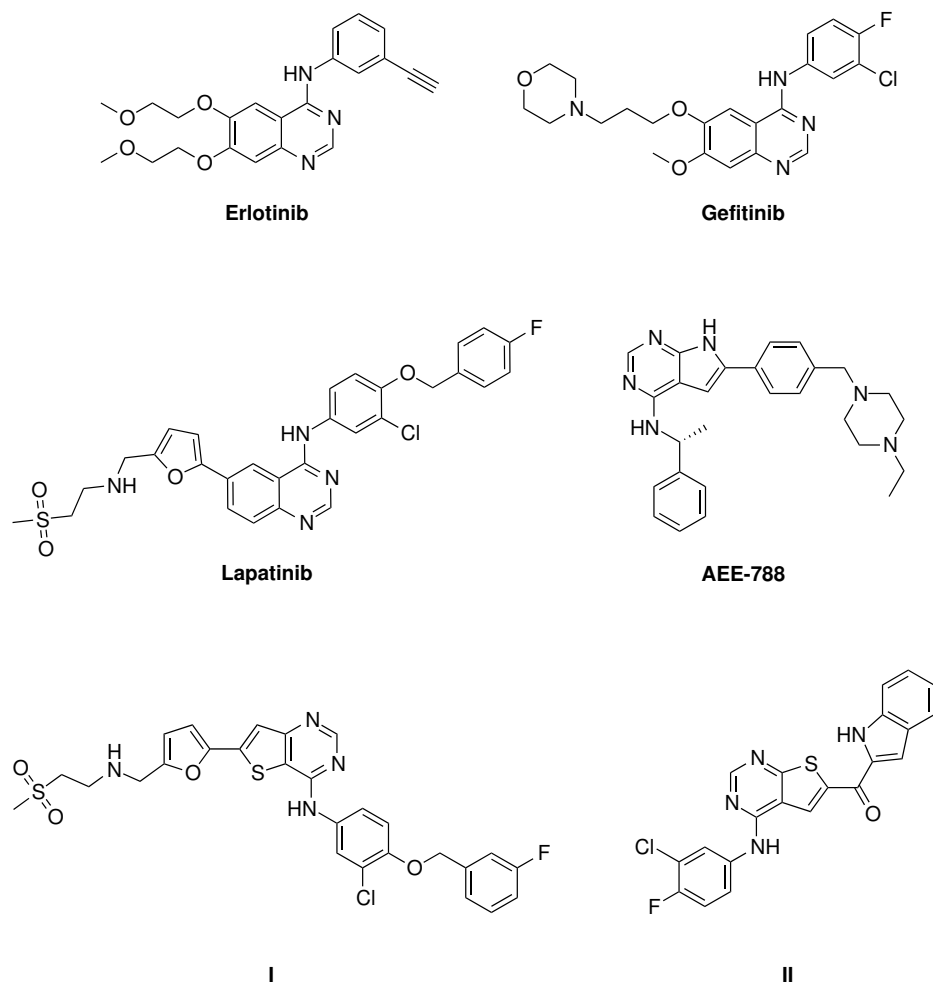


Figure 2.4: Examples of commercially available EGFR tyrosine kinase inhibitors (Erlotinib, Gefitinib and Lapatinib) and other potent EGFR inhibitors (AEE-788, I and II).⁴⁵⁻⁴⁸

2.4 Previous Work in the Research Group

2.4.1 Results from the pre-project autumn 2013

A pre-project to this master's thesis was performed in autumn 2013. In this project, compounds **2**, **3a-d**, **4**, **5** and **6** were synthesized from the starting material **1** (Figure 2.5). All synthesized compounds were characterized, and the building blocks **4** and **5** have been used in further syntheses in this master's thesis.

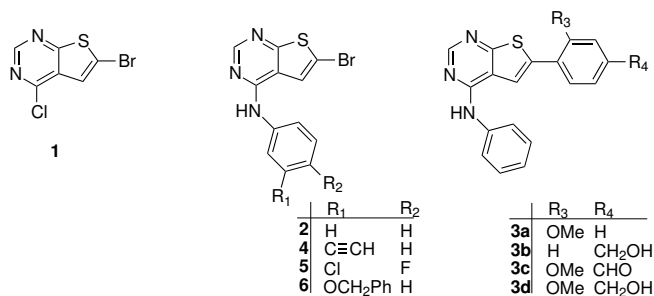
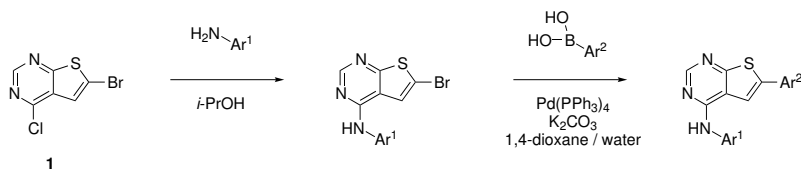


Figure 2.5: Compounds synthesized in the pre-project of autumn 2013.⁵⁴

The synthesized compounds were prepared as illustrated in Scheme 2.2 through a nucleophilic aromatic substitution with aniline, followed by Suzuki coupling reactions (to yield compounds **3a-d**).

The reaction conditions normally used for amination in the group were found unsuitable for amination using anilines. An attempt of reacting 3-ethynylaniline with **1** resulted in severe polymerization applying the original conditions. New reaction conditions were thus developed, leading to higher yields and purity of the obtained products. No changes were made to the Suzuki coupling conditions, on account of high yields and no occurred problems in the reactions. The same conditions for both amination and Suzuki coupling have thus been continued used in the master's thesis.

Scheme 2.2: Route of synthesis used in the pre-project of autumn 2013.⁵⁴

Poor solubility was a general problem for the target compounds in the pre-project, the Suzuki substituted compounds **3a-d** in particular. This resulted in substantial loss during purification by column chromatography. For compound **3b** recrystallization was performed in addition to column chromatography in order to get the desired purity of the compound, though resulting in only 7% final yield.

Enzymatic EGFR testing was applied to compounds **2**, **4**, **6** and **3a-d** to determine inhibitory activity. The results from this testing as well as obtained yields and purities, are presented in Table 2.1. Due to low inhibition activity, the building block **6** was not applied in further syntheses in this master's thesis.

Table 2.1: Results from the pre-project performed in autumn 2013.

Compound	Yield [%]	Purity [%]	Inhibition at 100 nM [%]	IC ₅₀ [nM]
2	78	99	74	80.5
3a	69	98	53	173.0
3b	7	96	89	20.7
3c	55	98	88	19.5
3d	96	96	>99	3.1
4 ·HCl ^a	76	96	84	23.4
5 ·HCl	101	85	N/D ^b	N/D ^b
6 ·HCl	100	98	N/D ^b	> 10.000

^a Yield and purity are average values from five different reactions. Inhibition at 100 nM are measured for compound of 97% purity.

^b N/D: not determined.

2.4.2 Results from the research group

The work performed in this master's thesis is part of an ongoing study run by a larger research group. Based on thieno-, pyrrolo- and furopyrimidine scaffolds, the group is working on synthesizing new potential tyrosine kinase inhibitors. Figure 2.6 shows some of the compounds that have been synthesized.⁵⁵⁻⁶⁰

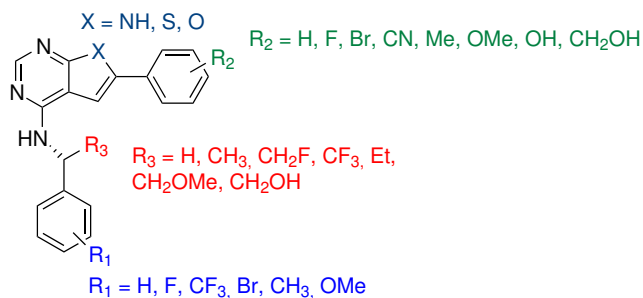


Figure 2.6: Compounds synthesized in the research group.⁵⁵⁻⁶⁰

More than 200 different compounds have been prepared, and a large number of these have undergone biological activity testing. The activities are reported using IC_{50} -values; the concentration of compound needed to reduce the target enzyme activity by 50%.¹⁴ Thus a lower value means better inhibition activity of the compound.

The obtained test results can be summarized in structure-activity relationships as illustrated in Figure 2.7. Fragment A has been found to tolerate aromatic substitution poorly. Except for substitution with fluorine, all groups tested resulted in drastic decrease in activity. The tolerance for different groups in fragment C is somewhat larger than for fragment A. Both hydrogen, methyl, ethyl and *tert*-butyl groups have shown good potency, but the best results have been obtained for hydroxymethyl in this position. The stereochemistry is also of great importance, as drawn in Figure 2.7 efficient inhibition is obtained, but changing the stereochemistry causes a drastic drop in activity.⁵⁵ In fragment B the substitution tolerance is distinctly higher, both potency increasing and decreasing substituents have been identified.

Inhibition data for some of the thienopyrimidines synthesized are presented in Table 2.2. The presented results are for compounds having a general structure as shown in Figure 2.7, without substitution in fragment A.

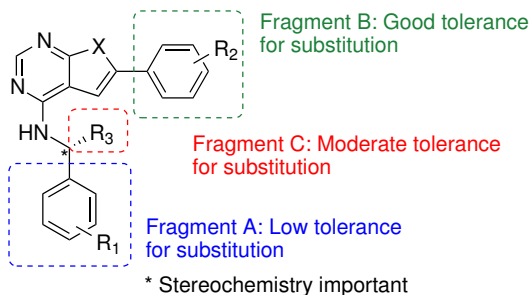


Figure 2.7: Structure-activity relationships (SARs) found from EGFR inhibition testing.

Table 2.2: EGFR-TK inhibition data for some compounds synthesized in the research group.⁵⁹

#	Stereochemistry	R ₂	R ₃	IC ₅₀ [nM]
1	<i>R</i>	H	CH ₃	58
2	<i>R</i>	<i>o</i> -CH ₂ OH	CH ₃	38
3	<i>R</i>	<i>m</i> -CH ₂ OH	CH ₃	9
4	<i>R</i>	<i>p</i> -CH ₂ OH	CH ₃	7
5	<i>R</i>	<i>p</i> - <i>t</i> Bu	CH ₃	1000
6	<i>R</i>	<i>o</i> -OMe	CH ₃	9
7	<i>R</i>	<i>m</i> -OMe	CH ₃	37
8	<i>R</i>	<i>p</i> -OMe	CH ₃	54
9	<i>rac</i>	<i>o</i> -OH	CF ₃	1000
10	<i>R</i>	<i>o</i> -OH	CH ₂ CH ₃	33
11	<i>R</i>	<i>o</i> -OH	CH ₃	35
12	<i>S</i>	<i>o</i> -OH	CH ₂ OH	3

Based on trends found by systematic evaluation and comparison of the obtained test results, the group has been able to identify highly potent EGFR TKIs. An example of how combining substituent groups from different active compounds can lead to highly potent compounds, is presented in Figure 2.8. In fragment B, a methoxy group displayed highest potency of inhibition when in *o*-position, while *p*-position was found most favourable for substitution with a hydroxymethyl group. A combination of both these groups, and the hydroxymethyl in fragment

C, yielded a highly potent EGFR inhibitor.

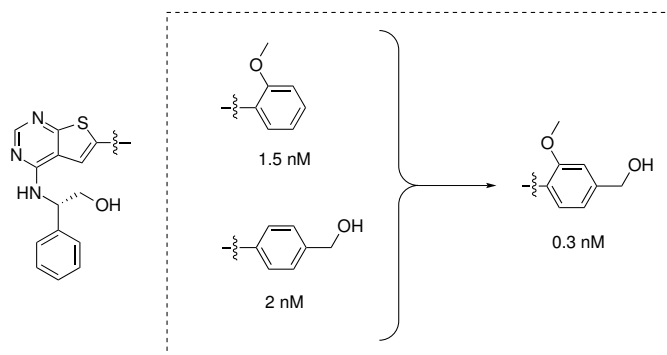


Figure 2.8: Example of how combination of substituents from potent compounds can result in a product of high inhibition potency, IC₅₀ values are given.

2.5 Synthesis of Substituted Thieno[2,3-*d*]pyrimidines

The goal in this master's thesis has been the synthetic study, optimisation and characterisation of new potential EGFR TKIs, as a continuation of the work performed in the pre-project. General structures of the target compounds in this thesis are illustrated in Figure 2.9.

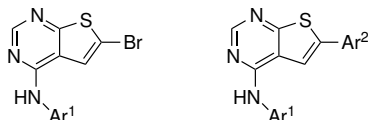
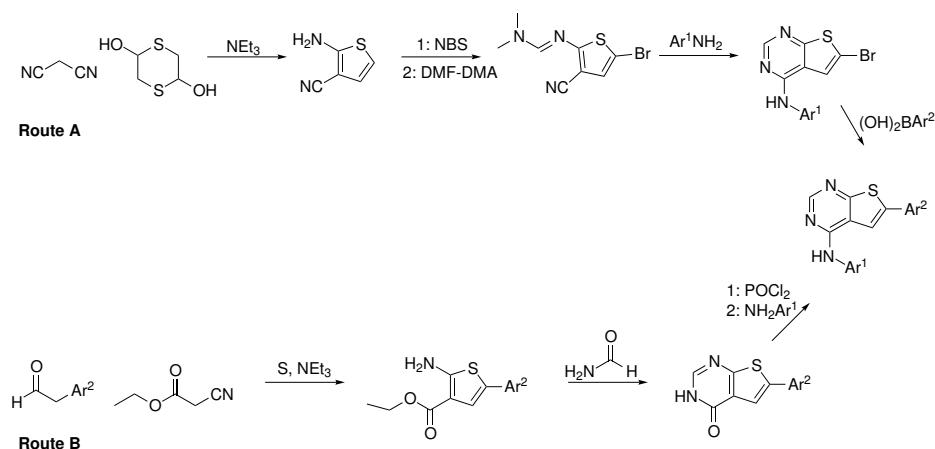


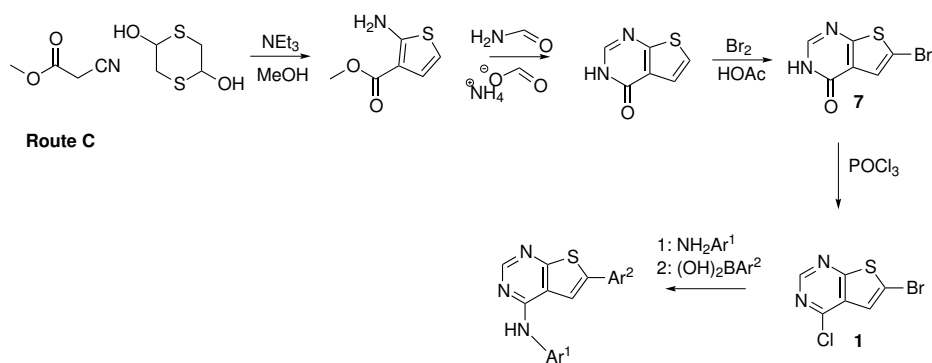
Figure 2.9: General structures of the target compounds in this master's thesis.

There are several synthetic routes available for obtaining these compounds, two of which are presented in Scheme 2.3. In Route A the aryl groups are introduced in the two final steps,⁶¹ while in Route B one of the aryls (Ar^2) is introduced with the starting material.⁶² This is an important difference to consider. If a compound library with variation in both substituents is to be made, Route B would entail starting from the beginning every time the Ar^2 group was to be changed. Route A would in contrast only need the final two steps repeated.



Scheme 2.3: Alternative synthetic routes for obtaining the disubstituted thienopyrimidine.^{61,62}

As the research group is currently investigating the structure-activity relationship for substituted thieno[2,3-*d*]pyrimidines, a route of synthesis having few steps is beneficial for efficiency. Therefore, a different synthetic route has been developed in the group (Route C, Scheme 2.4), leading to the building block **1**.⁵⁷ Compound **1** is easily substituted in one or both positions, permitting the introduction of a large variety of groups. This is convenient when numerous different compounds are to be made. The number of synthetic steps required to make the starting material is also of importance, particularly in multistep synthesis following a consecutive strategy as the ones illustrated in Scheme 2.3 and Scheme 2.4. The obtained total yield is strongly dependent on the number of steps in the synthesis,⁶³ favouring few steps. Route A (Scheme 2.3) gives the same product as Route C (Scheme 2.4) in two fewer steps. Route A may thus be favourable if the whole synthetic route was to be performed.



Scheme 2.4: Synthetic route used in the research group.

2.5.1 Choice of reaction sequence

Compound **1** made by Route C (Scheme 2.4) has been used as starting material in both the pre-project and the master's thesis. In order to introduce the desired substituents, two different types of reactions have been applied; nucleophilic aromatic substitution of a halogen with an aniline (Section 2.5.2) and Suzuki coupling of two aryl molecules (Section 2.5.4). The target molecules are obtained by performing one or both types of reactions, thus introducing one or two new substituents on the starting material **1**. The substituents are introduced to positions 4 and 6 in **1**. The structure of **1** with numbering of positions is shown in Figure 2.10.

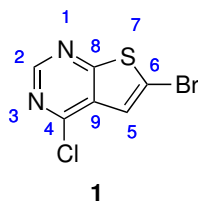
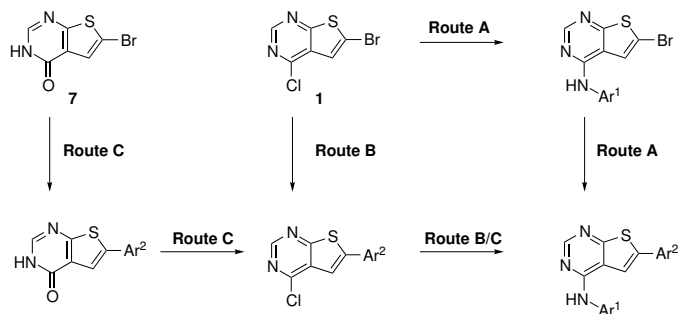


Figure 2.10: The starting material **1** with numbered positions.

The substituents can be introduced in two different orders, as illustrated in Scheme 2.5 Routes A and B. The general procedure in both the pre-project and master's thesis, has been to perform the amination reaction first. This is based on a study by Bugge *et al.*⁵⁷ where different routes for synthesis of disubstituted thienopyrimidines were investigated. The study found that amination preceding Suzuki coupling (Route A in Scheme 2.5) gave a higher overall yield, and the best functional group tolerance. In addition, problems concerning selectivity of the Suzuki coupling and hydrolysis at C-4 of the starting material were avoided using this route. Consequently, it was concluded that amination followed by Suzuki coupling is the preferential sequence of reactions when compounds with diverse substituents at C-6 are to be synthesized.

However, if for some reason the Suzuki coupling is needed to precede the amination, selective coupling at C-6 can be obtained by using **7** as starting material⁵⁷ (Route C in Scheme 2.5). This route is also beneficial if a large number of

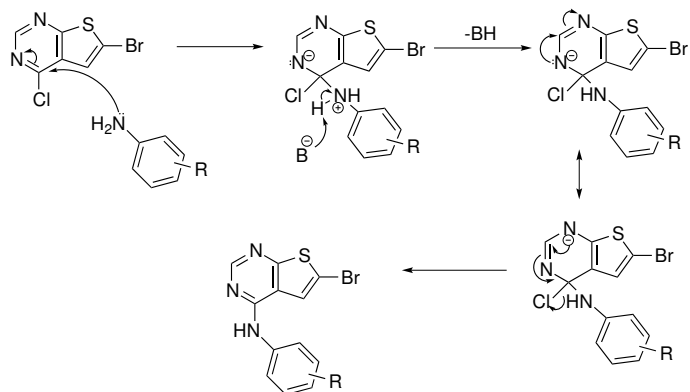


Scheme 2.5: Possible routes for synthesizing disubstituted thienopyrimidines from **1** or **7**.

analogues having the same C-6 substituent, but diverse C-4 substituents, are desired. Even so, this route may be challenging if the C-6 aryl holds functional groups sensitive to the subsequent chlorination step.

2.5.2 Thermal coupling of halogenated thienopyrimidines with anilines

The substitution of chlorine in the starting material **1** with an amine is a nucleophilic aromatic substitution, S_NAr , presumably proceeding by an addition-elimination mechanism, as shown in Scheme 2.6. Here the amine acts as a nucleophile, attacking the pyrimidine ring, which is the electrophile. The relative stability of the negatively charged intermediates (Meisenheimer complexes) formed in this reaction, is dependent on the types of substituents on the ring, and also on what kind of heteroatoms the system includes. As illustrated in Scheme 2.6, the negative charge is delocalized on the nitrogen atoms, thereby stabilising the complex.³⁹ If there is a potential leaving group at the site where the attack takes place, aromaticity of the ring can be regenerated, as is the case in the example shown in Scheme 2.6.⁶⁴



Scheme 2.6: Mechanism for the substitution of chlorine with an amine on the pyrimidine ring of halogenated thienopyrimidines.

The reactivity of a nucleophilic aromatic substitution is dependent on three factors⁶⁵

- The activation/deactivation of the electrophile
- The nucleophilic reagent
- The leaving group

Benzene has six π -electrons equally distributed over the six carbon atoms in the ring. In comparison, pyrimidine is an electron deficient compound. There are six π -electrons in the ring, distributed over four carbon atoms and two nitrogen atoms. Nitrogen being a more electronegative element than carbon, causes the electron density on the carbon atoms to be reduced relative to that found in benzene. Hence pyrimidine can be regarded as an electron deficient compound. Thiophene, on the other hand, is an electron rich compound; six π -electrons are distributed over five atoms.^{39,66} Pyrimidine is therefore the most electrophilic of these compounds, and will thus favour a nucleophilic attack. A comparison of the π -electron density at each atom in pyrimidine, benzene and thiophene is illustrated in Figure 2.11.

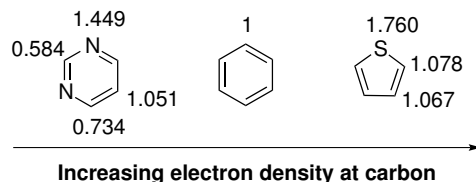


Figure 2.11: Electronic properties of pyrimidine, benzene and thiophene.

Addition of the nucleophile is the rate determining step in addition-elimination reactions.⁶⁴ A more electron deficient character on the electrophilic site will thus facilitate an attack. Figure 2.12 shows the relative reactivity of some halogenated diazines and pyridines, with the 4-substituted pyrimidine as the most reactive compound.³⁹

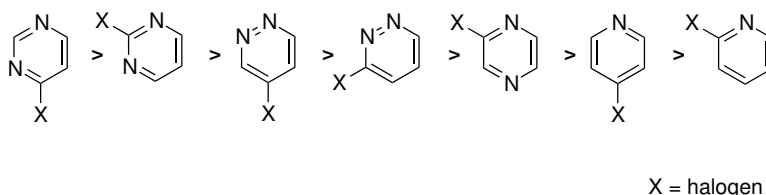


Figure 2.12: Relative reactivity of substitution in different halogenated diazines and pyridines.³⁹

Anilines are generally less reactive than aliphatic amines when it comes to aromatic substitution.⁶⁵ This is due to the fact that conjugation of the ring makes aniline less basic than aliphatic amines, and thereby less nucleophilic and more stable. The reaction time for aromatic substitutions with aniline as the nucleophile may thus be longer than for corresponding reactions with an aliphatic amine as nucleophile.

Lastly, the reactivity is affected by the group being substituted in the reaction. The halogens have different ability to act as leaving groups, the relative reaction rate being: $F \gg Cl > Br > I$. In nucleophilic aromatic substitutions the breaking of the halogen-carbon bond is not part of the rate determining step, as it is in normal S_N2 reactions. Therefore, the strength of this bond does not affect the reactivity. More important is the electronegative property of the halogen. A more electronegative halogen increases reactivity by activating the ring for addition by

inductive effect.⁶⁴ In this master's thesis, nucleophilic aromatic substitution has been performed at the 4-position of pyrimidine, with chloride as leaving group and substituted anilines as nucleophiles. Both the position and the leaving group thus indicates good reactivity for this reaction, while the applied amines are less favourable.

2.5.3 Alternative methods of amination

If one or both of the reagents in the amination are of low reactivity, e.g. if the amine is a weak nucleophile, high reaction temperatures are required for the nucleophilic aromatic substitution to occur. This may lead to formation of by-product, or decomposition of certain starting materials. To avoid this, acid or base catalysis can be used.⁶⁷ The proposed mechanisms for the acid catalysed reaction is shown in Figure 2.13. Figure 2.14 shows the mechanism with an alcohol operating as the acid catalyst.

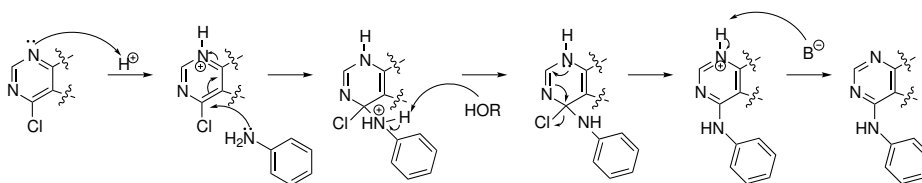


Figure 2.13: Proposed mechanism for acid catalyzed nucleophilic aromatic substitution reaction.⁶⁷

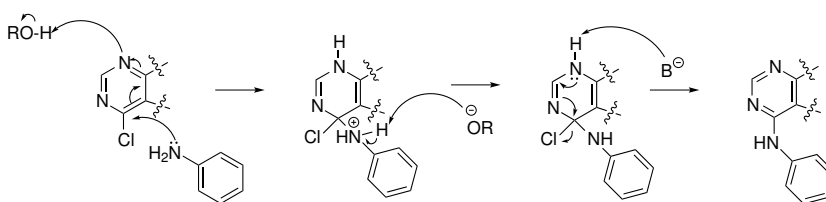


Figure 2.14: Proposed mechanism for nucleophilic aromatic substitution reaction catalysed by an alcohol.

The classical nucleophilic aromatic substitution reaction requires an electron poor aryl halide in combination with a strong nucleophile. However, unactivated, electron rich aryl halides may also undergo amination by use of an alternative type

of reaction; the Goldberg reaction. This was the first method of catalysed aryl amination, using copper as catalyst.⁶⁸ As for the nucleophilic aromatic substitution with unactivated substrate, harsh conditions such as high temperatures are required in the classic Goldberg reaction. In addition, a stoichiometric amount of copper is needed for the reactions to proceed in satisfactory yields.⁶⁹ From an environmental point of view, extensive use of copper is unfavourable.⁶⁸ Development of new ligands has made the reaction conditions milder; reduced reaction time and temperature. The amount of catalyst needed has also been reduced due to increased solubility of the copper caused by the ligands.⁶⁹

Catalysed amination of aryl halides may also be performed with palladium catalysis, as in the Buchwald-Hartwig reaction. This reaction constitutes a convenient method of synthesis, and due to greater diversity of ligands, conditions can be tuned to match a number of different substrates and reagents.⁷⁰ The ligands are thus expanding the repertoire of possible *N*-aryl bond formations. The high functional group tolerance makes this reaction highly important in areas such as synthesis of pharmaceuticals.^{71,72} The mechanism of the Buchwald-Hartwig reaction consists of a catalytic cycle,⁷⁰ resembling the one presented for the Suzuki mechanism in Figure 2.16.

The substrate **1** used for amination in both the pre-project and this master's thesis holds two halogen substituents; one situated on the electron rich thiophene part of the molecule, and the other situated on the electron deficient pyrimidine part (Figure 2.10). In the Goldberg reaction the loss of the leaving group constitutes the rate determining step, unlike in the S_NAr . Thereby the reactivity of the reaction follows this trend $I > Br > Cl \gg F$.⁷³ If the Goldberg reaction was to be used on **1**, this would most likely yield the 6-aminated product, illustrated in Figure 2.15.

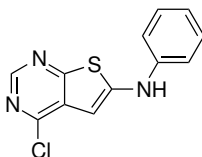


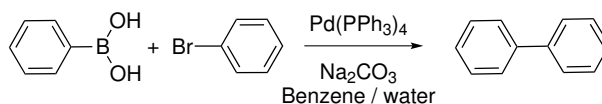
Figure 2.15: Probable product from a Goldberg amination of **1** and aniline.

It is also likely that the palladium catalysed Buchwald-Hartwig reaction would give both 4- and 6-aminated products.

2.5.4 Suzuki coupling

Generation of carbon-carbon bonds is an important aspect of organic chemistry, particularly when more complex carbon structures are to be synthesized. Palladium catalysed reactions are essential in such matters. Several types of palladium catalysed reactions are applicable for this purpose, e.g. the Negishi, Stille and Sonogashira couplings,⁶⁴ but in recent years the Suzuki cross-coupling reaction has become of the most preferable.⁷⁴ This is the method of choice for synthesis of biaryls.⁷⁵

In the Suzuki cross-coupling reaction a carbon-carbon bond is formed between an organohalide and a boron compound.⁶⁴ Common reactions include bond forming between aryl- or vinylhalides and aryl- or vinylboronic acids, but coupling with other types of compounds, such as alkenes, alkynes and amines⁷⁶⁻⁷⁸ are also possible. Scheme 2.7 shows one of the first biaryl compounds made using Suzuki coupling.⁷⁹



Scheme 2.7: Synthesis of biaryl compound using Suzuki coupling between an arylhalide and an aryl boronic acid.⁷⁹

Both boronic esters⁸⁰ and boranes⁷⁷ can be applied in Suzuki cross-couplings, but boronic acids are the most commonly used of the boronic compounds.⁸¹ Important advantages of boronic acids include mild reaction conditions, a wide range of commercially available compounds, as well as boronic acids being more environmentally friendly than organometallic reagents used in other palladium catalysed cross-coupling reactions⁷⁴ (e.g. organotin compounds used in the Stille coupling). In addition, many of the potential by-products formed in the Suzuki reaction are water soluble and thus easy to remove.⁸² The reaction is also well suited for industrial scale-up.^{83,84}

Mechanism

The mechanism with which this reaction proceeds, can be described by a catalytic cycle having four distinct steps.^{77,85} This is illustrated in Figure 2.16. The first reaction step is an *oxidative addition* of palladium to the arylhalide, forming an organopalladium compound where palladium is oxidized from Pd(0) to Pd(II). Following, addition of base gives an active intermediate in the *metathesis* step. In addition, the base creates a complex with the boronic acid, thereby activating it for further reaction, as illustrated at the center of Figure 2.16. The third step consists of *transmetalation* between palladium and the alkyl boron complex, while in the fourth and final step, the carbon-carbon bond is created in a *reductive elimination*, regenerating the catalyst (Pd(0)).

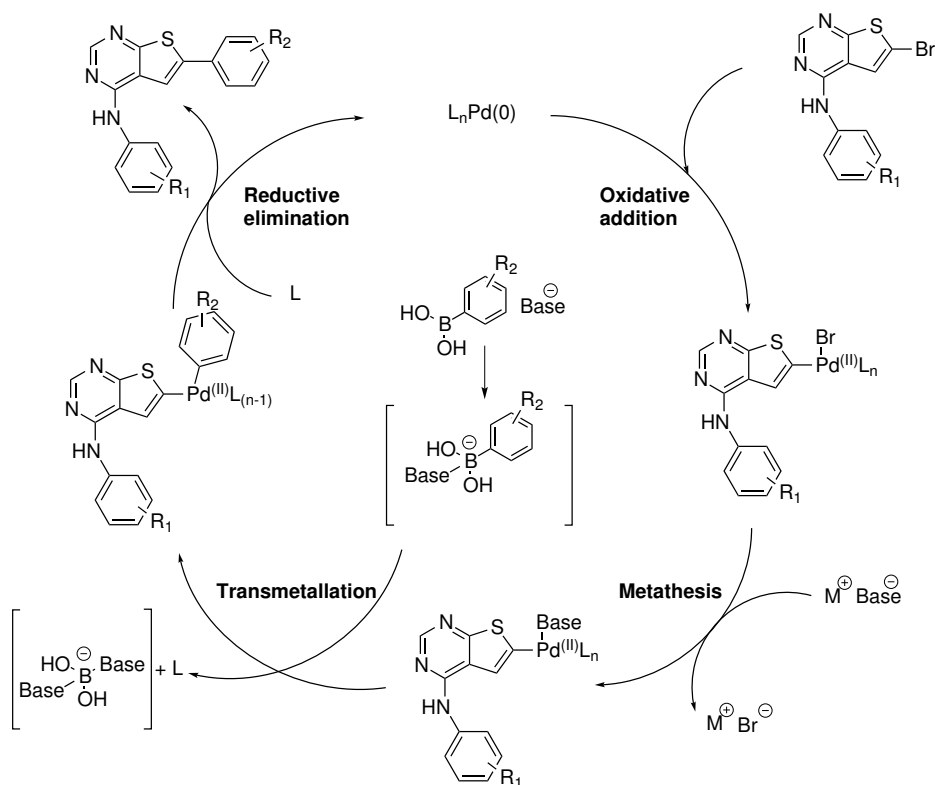
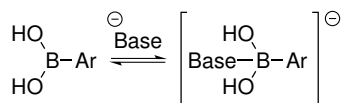


Figure 2.16: Mechanism for the Suzuki cross coupling reaction of halogenated thienopyrimidines with aryl boronic acids.

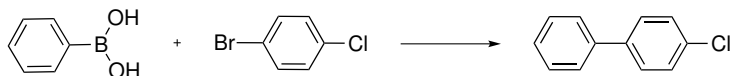
Electronic effects on reactivity and selectivity

Organoboron compounds are in general highly electrophilic, but the organic groups held by boron are weakly nucleophilic.⁷⁷ Thus the reactivity is low. By coordination of a negatively charged base to the boron atom, nucleophilicity of the organic substituents are increased (Scheme 2.8 and in the center of Figure 2.16). Thereby the compounds is activated for transmetalation, and the desired product can form.⁸⁶



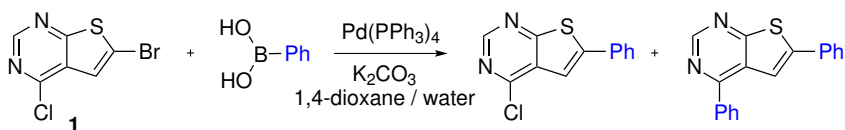
Scheme 2.8: Coordination of a negatively charged base activates the boron compound for transmetalation.

Oxidative addition is often the rate determining step,⁸⁷ while the relative reactivity follows this trend $\text{I} > \text{Br} \gg \text{Cl}$, opposite that of the $\text{S}_{\text{N}}\text{Ar}$.⁷⁷ Thus, if more than one halide is present in the substrate, coupling is favoured at the more reactive site (Scheme 2.9).



Scheme 2.9: Selectivity of the Suzuki reaction when the substrate holds more than one halide.

The reactivity of the aryl halide is also affected by proximal substituent groups. The presence of an electron donating group will decrease the reactivity towards oxidative addition by reducing the electrophilicity of the halide site. Contrarily, an electron withdrawing group will increase the reactivity.⁷⁷ Consequently, even though less preferred, substitution of a chlorine group is possible if the aryl holds electron withdrawing groups. Substitution of chlorine on an electron deficient aromatic compound such as pyrimidine is thus possible.⁸⁸ A Suzuki reaction performed on the starting material **1** is therefore likely to yield a mixture of 4- and 6-substituted products, as observed by Bugge *et al.* (Scheme 2.10).⁵⁷ Jang *et al.* reports of selective Suzuki coupling at C-6 of **1**, but due to low yields and the formation of by-products, another synthetic route was used in the subsequent syntheses.⁸⁹ This might indicate a nonselective coupling.



Scheme 2.10: Unsuccessful attempt of selective Suzuki coupling on **1**, performed by Bugge *et al.*⁵⁷

Other aspects of the reaction mixture can also be tuned to control the rate of reaction. The electronic properties of the arylboronic acid influences the nucleophilicity of the boronic acid; thus an electron rich boronic acid increases the rate relative to an electron poor boronic acid.^{77,81} One of the most important factors of rate control is the type of ligands used with the palladium catalyst. Trialkyl phosphine ligands, such as triphenyl phosphine (Figure 2.17), were the most used type of ligand in the Suzuki cross-coupling reaction up until the end of the 1990s. Since then, more electron rich dialkylbiaryl ligands, such as SPhos and XPhos (Figure 2.17), have been developed. The alkyl groups (Cy in SPhos and XPhos) increase electron density at phosphorous, thereby increasing the rate of oxidative addition, while an increased size of these groups increases the rate of reductive elimination.⁹⁰ The *ortho* substituents on the lower aryl ring also increases stability and activity by preventing palladacycle formation.⁹¹

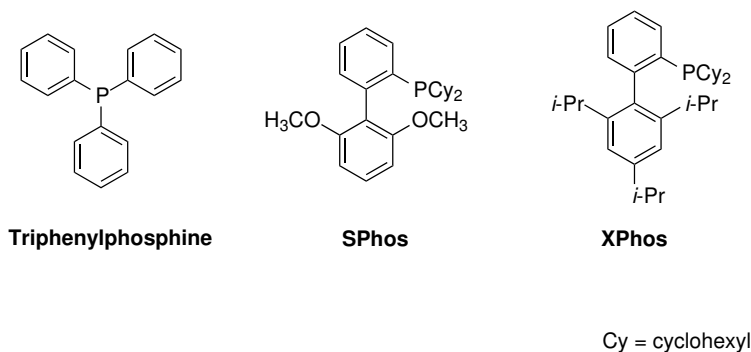


Figure 2.17: Common ligands used in the Suzuki cross-coupling reaction.

Side reactions

Several side reactions may occur in a Suzuki cross-coupling, Figure 2.18 illustrates this. A common by-product is biaryls formed by homocoupling of the arylboronic acid. Deboronation of the arylboronic acid may also take place by heat, base or the palladium catalyst,⁹² precluding cross-coupling. Electron poor and *ortho*-substituted arylboronic acids are particularly affected by this.⁹³

The aryl halide can also be involved in the making of by-products by homocoupling, reduction or hydrolysis of the halide function. Formation of these by-products is reduced by use of arylboronic acids as the boron compound.^{74,94}

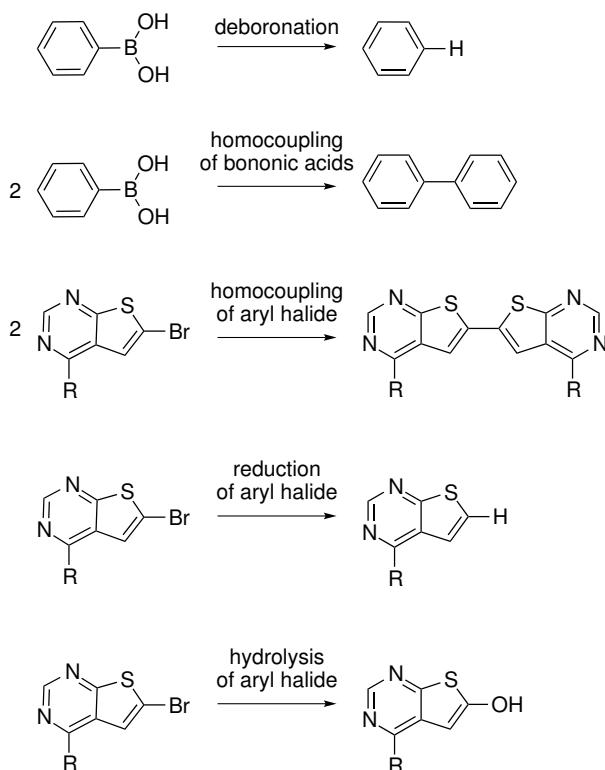


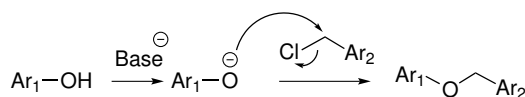
Figure 2.18: Possible side reactions to the Suzuki cross-coupling reaction.^{74,94}

Ligands from the catalyst may also be coupled to the aryl halide. This happens generally if the metathesis step of the catalytic cycle is slow due to e.g. steric hin-

derance. The rate of the metathesis can be increased by changing to a stronger base, thus preventing the formation of this side reaction.⁹³ All side reactions contribute to a poorer yield in the reaction, and to making the reaction mixture more intricate. Thus possibly complicating purification of the desired product. Side reactions are more susceptible to occur in slow reactions, therefore shortening the reaction time helps minimizing the amount of by-products formed in the Suzuki coupling.⁹³

2.5.5 Williamson ether synthesis

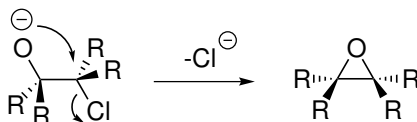
In 1850 Alexander Williamson developed a method for synthesizing ethers from organohalides and alcohols,^{95,96} a reaction later known as the Williamson ether synthesis. This reaction is a nucleophilic substitution, following a standard S_N2 type mechanism, as shown in Scheme 2.11.⁹⁷ A base is normally needed to activate the alcohol for substitution by deprotonation, unless applying an alkoxide, such as sodium ethoxide, instead of an alcohol.⁹⁸ Williamson ether synthesis also helped 19th century chemists better to understand the characteristics of the chemicals involved. In fact, due to the applicability of sodium ethoxide in the synthesis, the structure of the alkoxide could be determined as monovalent at sodium ($\text{CH}_3\text{CH}_2\text{ONa}$). Previously it was believed that sodium was multivalent in the alkoxide ($(\text{C}_2\text{H}_4\text{Na})\text{OH}$),⁹⁸ Wanklyn⁹⁹ even believed in a septivalent sodium atom.



Scheme 2.11: Mechanism of the Williamson ether synthesis.

The Williamson ether synthesis is among the simplest, most popular methods of ether preparation and can be applied in synthesis of both symmetrical and asymmetrical ethers. According to the S_N2 approach of the reaction, primary alkyl halides are the most preferable and the relative reactivity of the halide leaving group follows this trend: $\text{I} > \text{Br} > \text{Cl} \gg \text{F}$. The reaction is favoured in polar, aprotic solvents; solvation of the nucleophilic alkoxide anion is minimal and

thus the nucleophilicity is greatest. Secondary and tertiary halides are likely to undergo E2 elimination, due to the strongly basic nature of the alkoxide ion. The steric bulk of the alkoxide is of less importance for the reaction.⁹⁷ Intramolecular Williamson ether synthesis can be used to form cyclic ethers, such as epoxides (Scheme 2.12).



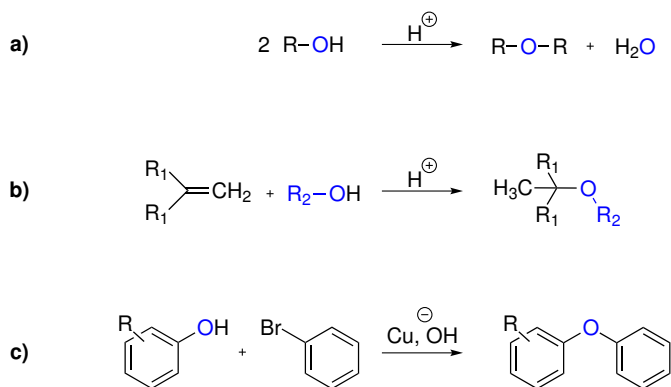
Scheme 2.12: Intramolecular Williamson ether synthesis.

Modifications of the Williamson ethers synthesis have been developed for improving synthesis with secondary and tertiary halide substrates. This can be done by use of phase transfer catalysts^{100,101} or miscellar catalysis.¹⁰² In recent years, an increased focus on green chemistry has led to the discovery of a combinatory microwave and ultrasound assisted Williamson ether synthesis. This method renders an efficient and environmental friendly way of preparing ethers without using organic auxiliary substances nor organic solvents. In addition the selectivity and reactivity of the reaction is enhanced, yields are increased and the reaction time can be shortened from hours to a few minutes.¹⁰³

Aryl ethers are best synthesized by the Williamson ether synthesis, given that the alkyl halide readily reacts by an $\text{S}_{\text{N}}2$ mechanism. Potassium carbonate is a suitable base for this reaction.⁹⁷ In this master's thesis the Williamson ether synthesis have been applied for synthesis of an aryl ether (Scheme 2.11). This reaction constituted one out of two steps performed in the formation of an aniline used in several of the target compounds. In this aryl ether synthesis potassium carbonate was applied as base, and the solvents used was polar aprotic (dimethyl formamide or acetonitrile). Thus, the applied conditions are appropriate for the performed reaction.

2.5.6 Alternative methods of ether synthesis

Acid catalysed condensation of primary alcohols is a common industrial method of preparing symmetrical ethers (Scheme 2.13 a)). Diisopropyl ether is also prepared in good yields using this method, but other approaches are required for synthesis of more substituted ethers. In such cases, acid catalysed addition of an alcohol to alkenes is useful (Scheme 2.13 b)).⁹⁷



Scheme 2.13: Methods of ether synthesis, alternative to the Williamson ether synthesis. a) Acid catalysed condensation of alcohols, yielding symmetrical ethers. b) Acid catalysed addition of an alcohol to alkene. c) Ullmann condensation.

The Ullmann condensation provides a method for preparing diaryl ethers from phenols and aryl halides.^{104,105} This reaction makes use of copper catalysis, and is in such analogous to the Goldberg reaction for anilines or aryl amides.¹⁰⁶ The Ullmann condensation is illustrated in Scheme 2.13 c).

3 Results and Discussion

The main goal of this master's thesis has been to identify new active tyrosine kinase inhibitors. This has been done following a fragment based approach, using aniline fragments found in the commercially available TKIs Gefitinib, Lapatinib and Erlotinib. By combining these fragments with potency inducing substituents identified by the research group, new thienopyrimidine based TKIs have been synthesized (Figure 3.1).

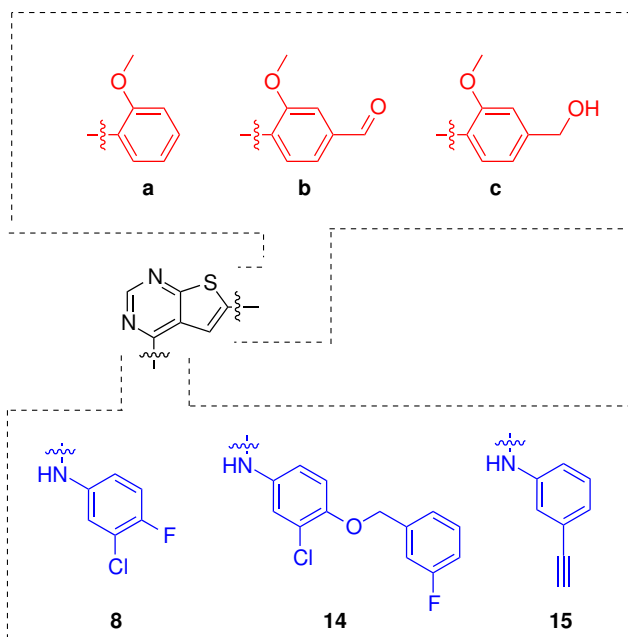


Figure 3.1: Fragments from Gefitinib, Lapatinib and Erlotinib (blue) have been combined with potency inducing fragments identified by the research group (red) to make new TKIs.

A second goal has been to investigate the concept of fragment based drug design. This was attempted done based on the inhibition performance of the synthesized compounds. However, three key compounds, **13**·HCl and **15b-c**, were not obtained in high purity ($\geq 96\%$ by HPLC) in time for shipment, thus inhibition data for these compounds are missing. In addition, some of the IC_{50} -values ordered for other compounds were not returned before the deadline of this thesis.

The attainment of this second objective is therefore limited.

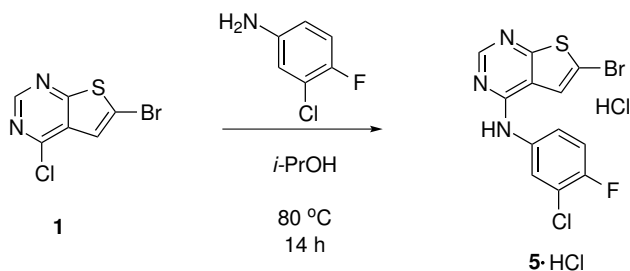
Throughout this laboratory work, obtaining pure compounds has been of higher priority than excellent yields. Purification of the obtained compounds has been one of the most challenging parts of the work, and are therefore described in detail for some compounds. Due to low solubility, most of the purification has been performed by crystallization, thus few by-products have been isolated and identified.

This section consists of five main parts. The first three parts concern the syntheses of the target compounds based on fragments from Gefitinib, Lapatinib and Erlotinib, respectively. Next follows a discussion of the obtained results from enzymatic inhibition testing of the synthesized molecules, and the final section summarizes the spectroscopic characterisation of the new compounds synthesized in this master's thesis.

3.1 Compounds Based on the Gefitinib Fragment

3.1.1 Purification of compound **5**·HCl

The building block **5**·HCl was synthesized during the pre-project autumn 2013, as illustrated in Scheme 3.1. Due to time constraints, however, high purity was not obtained at that point (only 85% by HPLC). Further purification was thus needed.



Scheme 3.1: Conditions for synthesis of compound **5**·HCl.

By comparison of HPLC retention times, the main impurity was identified as being remains of the aniline reagent. Solubility properties of **5**·HCl and the 3-chloro-4-fluoroaniline were investigated, and significant differences were discovered; the aniline showed high solubility in hot *n*-pentane, while **5**·HCl seemed insoluble.

The impure **5**·HCl was thus boiled in *n*-pentane for a few minutes, filtered and the solid was dried under reduced pressure. This yielded 94% of **5**·HCl, having an HPLC-purity of 98%. ¹H-NMR analysis of the filtrate confirmed this to contain 3-chloro-4-fluoroaniline, in addition to trace amounts of **5**·HCl.

The presence of **5** as its hydrochloric salt was confirmed by ¹H-NMR analysis of the free base. A small sample was free based using a saturated solution of sodium bicarbonate. When comparing ¹H-NMR spectra of the free base with that of the presumed hydrochloric salt, some differences in shifts were observed, thus indicating that the salt had been obtained in the reaction (Figure 3.2). As a control, the sample was acidified and reanalyzed by ¹H-NMR. The resulting

spectrum was identical to that of the product obtained in the reaction, thereby confirming that the obtained product was **5**·HCl.

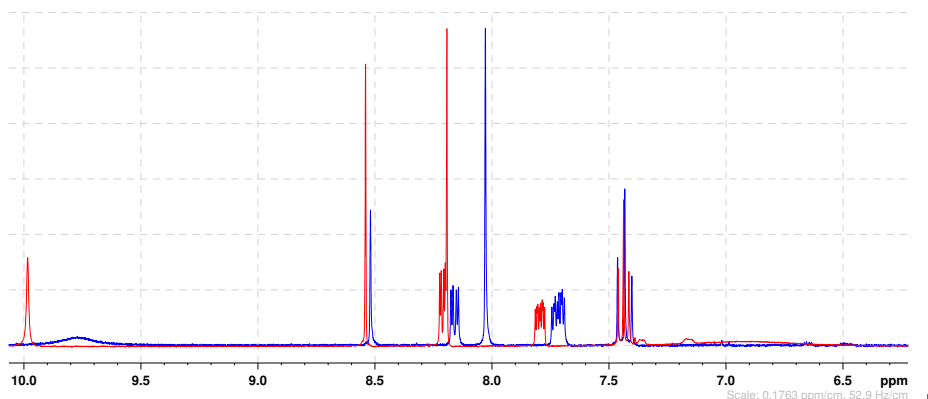


Figure 3.2: Comparison of ^1H -NMR shifts for **5**·HCl (red line) and free based **5** (blue line), section of spectra.

3.1.2 Suzuki coupling of **5**

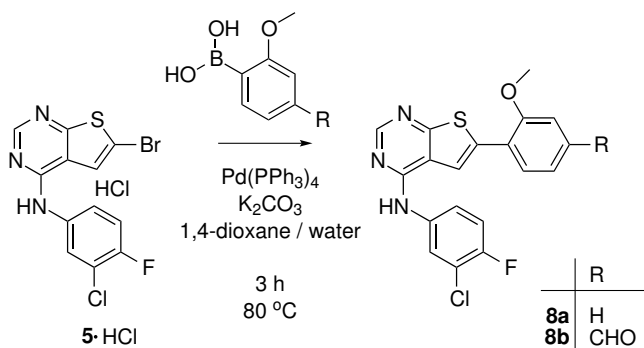
Synthesis of compound **8a**

Compound **8a** was synthesized from the building block **5**·HCl in a Suzuki coupling reaction, performed on a 200 mg scale. **5**·HCl was mixed with (2-methoxyphenyl) boronic acid, catalyst and potassium carbonate in a 50/50 mixture of 1,4-dioxane and water, and stirred at 80 °C for three hours (Scheme 3.2).

Yellow solids precipitated from the solution, and within 15 minutes the reaction mixture appeared thick and yellow. By the end of the reaction, the mixture had the appearance of custard. Water was added to the reaction mixture to ensure complete precipitation prior to filtration. The obtained crude solid was washed with water, dried in air and followingly under reduced pressure. This yielded 78% of **8a** as an orange-yellow solid. After a failed attempt of crystallization from methanol, the crude product was successfully purified by crystallization from THF. The yield of **8a** after crystallization was 26%, having an HPLC-purity of 98%. Addition of an anti-solvent would most likely increase the yield

in the purification step, but as procuring products of high purity was the goal throughout this thesis, this possibility was not explored.

TLC analysis of the reaction mixture had shown full conversion of **8a**, but the isolated crude material only constituted 78% of theoretical yield. This indicates formation of water soluble by-products that might have been removed during work-up, or loss of compound due to some solubility of **8a** in water. The work-up filtrate was not analysed for potential product or by-products.



Scheme 3.2: Conditions for synthesis of compounds **8a** and **8b**.

Synthesis of compound **8b**

Compound **8b** was synthesized as illustrated in Scheme 3.2, using (4-formyl-2-methoxyphenyl)boronic acid and the same procedure as described for compound **8a**. The synthesis was performed on a 500 mg scale.

During the reaction, large amounts of solid formed in the flask, causing poor stirring of the mixture. More solvent was added in order to improve this. Dilution of the reaction mixture can lead to longer reaction times, as can the electron withdrawing aldehyde function in the boronic acid, but this was not observed for this reaction. Conversion was completed within three hours, the same as for **8a**. Work-up was performed as described for **8a**.

As for compound **8a**, purification was accomplished by crystallization from THF, though the procedure was somewhat more troublesome. After dissolution of **8b** in THF (29 mL), the solution was slowly cooled to room temperature. When

no precipitation was observed the following day, the solution was cooled further, to -18°C . Still no solids had formed after three days at reduced temperature. It was thus decided to add an anti-solvent to the solution. Toluene (9 mL) was added, and the flask was kept cold for another three days. At this point a few tiny grains were observed, indicating that addition of anti-solvent had worked. Due to the small amount, more toluene (6 mL) was added and cooling continued overnight, but no significant difference was observed the next day.

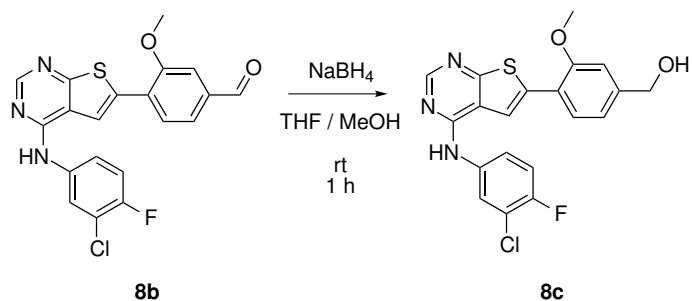
It was assumed that the amount of THF used to dissolve **8b** might have been larger than required, resulting in too good solubility of **8b**. Removal of solvent (7.35 g) by concentration was thus performed. After another two days at reduced temperature, a substantial amount of **8b** had precipitated. The mixture was filtered, and the product dried to yield 34% of a curry coloured solid. HPLC-purity was measured to 98%.

A pure product was obtained in sufficient yield, which was the goal of this reaction. The reaction procedure worked well, however, the purification step would most likely be less troublesome and time-consuming if dissolving the crude was achieved using less solvent. Continued cooling, removal of solvent or addition of anti-solvent would in all likelihood also result in an increased yield, but this was not investigated.

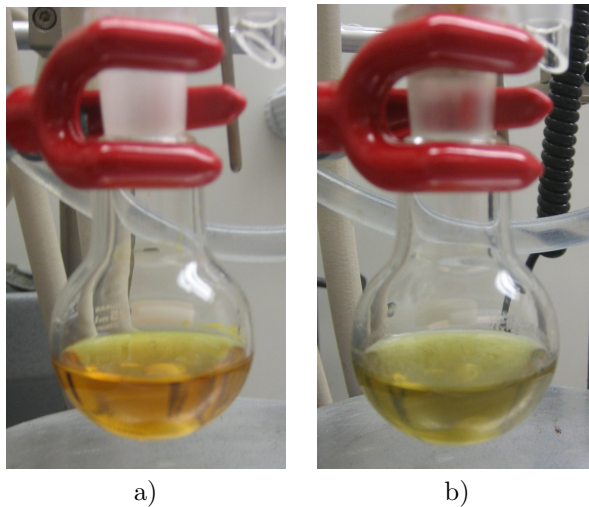
3.1.3 Reduction of compound **8b** - Synthesis of **8c**

Compound **8c** was obtained by reducing the aldehyde function of **8b**, as illustrated in Scheme 3.3. Compound **8b** was dissolved in methanol and THF, before two equivalents of sodium borohydride was added in two portions during an interval of 30 minutes.

The highly conjugated starting material **8b** had a bright yellow colour. As the reaction proceeded the colour gradually turned paler, indicating a reduced conjugation, see Figure 3.3. Upon completion, the reaction mixture was concentrated, and extracted with diethyl ether and water. The organic layer had a clouded appearance before washed with brine, then it became clear with a tint of yellow. Concentration of the organic layer yielded 93% of crude **8c**.

Scheme 3.3: Conditions for synthesis of **8c** from **8b**.

Purification by crystallization from THF, methanol and acetone was attempted unsuccessfully, but use of dimethyl formamide worked satisfactory. The solution was cooled to room temperature, and further to -18°C due to lack of precipitation. After four days at reduced temperature, a substantial amount of solid had formed, and the mixture was filtered. Addition of anti-solvent was thus not needed. Filtration and subsequent drying yielded 74% of **8c** as a pale yellow solid, having an HPLC-purity of $> 99\%$.

Figure 3.3: Reduction of **8b** to yield **8c** a) Reaction mixture by start of the reduction. b) Reaction mixture upon completed reduction.

3.1.4 Overall remarks on the Gefitinib fragment based compounds

In general, compounds **8a-c** were fairly easy to work with. All three reactions provided high crude yields, and high purity was obtained after a single crystallization for all compounds. THF was found to be a good crystallization solvent for both **8a** and **8b**, while DMF was used for **8c**. Investigations of the purification step would be the most beneficial for obtaining higher yields of pure compounds.

Table 3.1 presents the obtained yields and purities for the Gefitinib fragment based compounds **8a-c**. The melting points and colours of the compounds are also given, together with the reaction times.

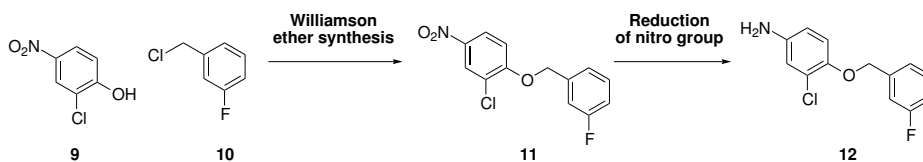
Table 3.1: Comparison of qualities for the synthesized compounds **8a**, **8b** and **8c**.

Compound	Reaction time [h]	Yield [%]	Purity [%]	Melting point [°C]	Colour
8a	3	26	98	243-245	Yellow
8b	3	34	98	252-254	Bright yellow, tint of green
8c	1	74	99	257-259	Pale yellow

3.2 Compounds Based on the Lapatinib Fragment

3.2.1 Synthesis of the building block **13**·HCl

Compound **13**·HCl was the only building block used in this master's thesis that had not been synthesized in the pre-project autumn 2013. All anilines used in the previous building block syntheses had been purchased from Sigma-Aldrich for reasonable prices. The 3-chloro-4-((3-fluorobenzyl)oxy)aniline (**12**) needed for **13**·HCl was also commercially available, but at a considerably higher price. Therefore, it was decided to synthesize **12** from the low-priced starting materials 2-chloro-4-nitrophenol (**9**) and 3-fluorobenzyl chloride (**10**), using a Williamson ether synthesis followed by a reduction of the nitro group (Scheme 3.4).



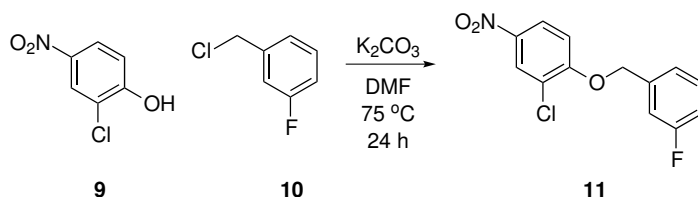
Scheme 3.4: Synthesis of **12** from 2-chloro-4-nitrophenol **9** and 3-fluorobenzyl chloride **10**.

Synthesis of **11**

The ether synthesis to make compound **11** was attempted three times, using two slightly different reaction conditions. The results and applied conditions for all three reactions are presented in Table 3.2. Firstly, a small scale test reaction was performed using reaction conditions as described by Shiao *et al.* for similar compounds.¹⁰⁷ The synthesis is illustrated in Scheme 3.5.

Table 3.2: Conditions and yield for the syntheses of **11**.

Entry	Solvent	Eq. of 10	Temperature	Rx. time	Yield
			[°C]	[h]	[%]
1	DMF	1.5	75	24	66
2	ACN	1.3	60	4	6
3	DMF	1.5	75	23	55

Scheme 3.5: Conditions for synthesis of **11**, as described by Shiao *et al.*¹⁰⁷

Compound **9** and the base, potassium carbonate, were dissolved in dimethyl formamide before **10** (1.5 eq.), also dissolved in dimethyl formamide, was added slowly. The reaction was monitored by $^1\text{H-NMR}$, but measuring the extent of conversion was difficult due to overlapping signals. Thin layer chromatography suggested full conversion of the limiting reagent **9** after five and a half hours, but the reaction was left overnight to make sure the conversion was complete.

Upon completion, the reaction mixture was concentrated to a about 5 mL of a dark yellow coloured liquid containing a substantial amount of solid. The mixture was diluted with ethyl acetate, dissolving all solid, and washed with water. The water layers took a pale yellow colour, while the organic layer was bright yellow. Concentration and drying under reduced pressure yielded 109% of crude product as sparkling yellow solid. $^1\text{H-NMR}$ analysis of the crude product showed trace amounts of dimethyl formamide in addition to some other impurities in the aromatic region. Thin layer chromatography and comparison of $^1\text{H-NMR}$ spectra was used to exclude the starting materials as origin of these impurity signals. Identification of the by-product was thus not obtained.

The crude material was attempted purified by crystallization from toluene. However, another method of purification was found in the literature before precipitation occurred. A patent by Fontana *et al.*¹⁰⁸ described procedures for both synthesis and work-up for compound **11**. The described work-up seemed quicker and easier than crystallization, and last but not least; the method was reported to work. The crystallization was aborted, and work-up as described by Fontana *et al.* was performed. Cold water was added to the solution, causing a yellow solid to precipitate. The mixture was then filtered, and the yellow filter cake washed with a cold acetonitrile/water solution. During this wash, the yellow

colour disappeared and a white solid remained, see Figure 3.4. Finally, the solid was washed with *n*-hexane and dried under reduced pressure. This yielded 66% of compound **11**. $^1\text{H-NMR}$ analysis of the obtained product coincided well with literature,¹⁰⁹ the previously observed aromatic impurities were no longer seen.

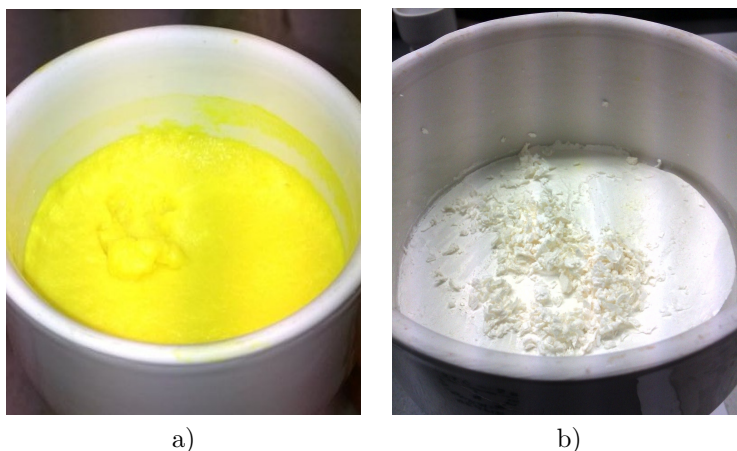
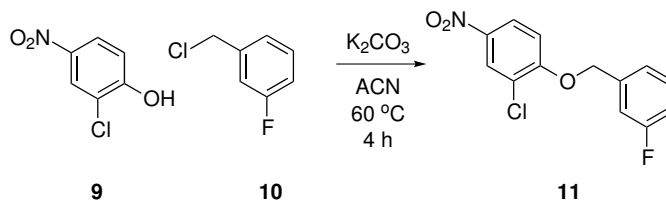


Figure 3.4: Work-up of compound **11**. a) Press cake after filtration, before washing. b) Press cake after washing with acetonitrile/water and *n*-hexane.

Fontana *et al.* reported a yield of 90%, and the reaction procedure described varies slightly from that of Shiao *et al.* Fontana *et al.* used acetonitrile as the reaction solvent, and reports of shorter reaction times (2 hours) and lower reaction temperature (60 °C). They also reports use of 3-fluorobenzyl bromide as reagent instead of 3-fluorobenzyl chloride (**10**). Due to a good experience with the work-up procedure, it was desirable to test the reaction conditions as well, hoping this would give a higher yield.



Scheme 3.6: Conditions for synthesis of **11**, as described by Fontana *et al.*¹⁰⁸

The second synthesis of **11** was thus performed using conditions as described by Fontana *et al.*, see Scheme 3.6. Compound **10** (1.3 eq.) dissolved in acetonitrile was added to **9** under nitrogen atmosphere, and the mixture was stirred until all solid was dissolved. Then, potassium carbonate was added, and the temperature was raised to 60 °C. The reaction mixture soon turned from yellow to an orange-red colour.

The conversion was monitored by TLC. After four hours no more **10** could be seen, which was peculiar since this reagent was added in excess. There seemed to be more of the other, limiting reagent in the mixture, but also this spot appeared different from earlier, thus it was difficult to conclude. The reaction was described by Fontana *et al.* to be completed in two hours, so when four hours had passed, the reaction was terminated. At this point, the reaction flask contained large amounts of orange solids, something which looked promising. Work-up was performed as described for the first reaction. Small amounts of an orange product (4%) was isolated. The filtrate was concentrated, and work-up was repeated. Now a white compound similar to that of the first reaction was isolated, in 6% yield. Once again the filtrate was concentrated to an orange solid and worked-up, but no more product was isolated.

Through $^1\text{H-NMR}$ and mass spectroscopy analyses, the orange by-product was identified to be the potassium salt of **9**, potassium 2-chloro-4-nitrophenolate (Figure 3.5).

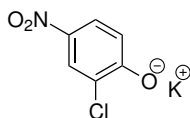


Figure 3.5: Reaction intermediate isolated in the second synthesis of **11**.

As the deprotonation of the phenol is the first step of the reaction mechanism for a Williamson ether synthesis (Scheme 2.11), this was not an unexpected product. The change in colour of the reaction mixture, from yellow to orange-red, indicated that a more conjugated electron system had been formed, as is the case for the deprotonated **9**. The fact that this colour change was observed shortly after addition of base, is also in consistency with the identified reaction intermediate.

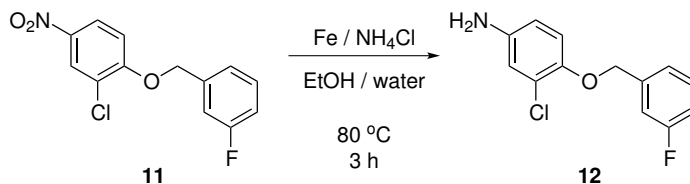
In retrospect, it is clear that longer reaction time would have been wise. As mentioned, the reaction described by Fontana *et al.* made use of 3-fluorobenzyl bromide in stead of 3-fluorobenzyl chloride (**10**), making bromide the leaving group, instead of chloride. According to theory (Section 2.5.5) longer reaction times are thus expected when having chloride as leaving group. This difference in reagents was not recollected as the reaction was performed, thus contributing to the decision of terminating the reaction after four hours.

It is likely that the second reaction conditions might have resulted in high yields if longer reaction time had been applied. However, the first conditions were chosen for the scale up of the reaction, simply because this had proven to work well in the small scale test reaction, and no more time was desired spent on investigation of reaction conditions for the intermediate **11**. The scale up reaction was thus performed as described for the first test reaction, and this yielded 53% of compound **11**. This white solid was highly static, something which made the transference of the compound difficult and led to large mechanical loss. The yield was still lower than expected. TLC analysis of the filtrate showed this to contain product as well as unreacted starting material. It was found that *n*-pentane could be used to extract the remaining product from the filtrate. This was performed, but only 2% of additional **11** was isolated. The work-up was also attempted once more, without positive result.

As remaining **9** was observed in the filtrate during work-up, the conversion was not complete. The yield of the reaction might thus have been higher if the reaction time had been longer, or if a larger excess of **10** had been applied. Since aromatic by-products were observed, other reaction conditions (solvent and temperature) might favour the formation of **11** to that of by-products, thereby increasing the yield.

Synthesis of **12**

Compound **12** was obtained by a reduction of the nitro group in **11**, performed as described by Fontana *et al.*¹⁰⁸ (Scheme 3.7). The reaction was done twice, firstly as a small scale test reaction, and secondly on a larger scale, Table 3.3.



Scheme 3.7: Conditions for reduction of **11** to yield compound **12**.

The reactions were monitored by TLC, and found to be completed after three hours for both scales. At this point, the mixtures were greyish black due to the iron. The fine iron particles were separated from the solutions by filtration through a short plug of celite. A mixture of ethanol and water (same ratio as used in the reaction) was used to wash all product through the celite (Figure 3.6).

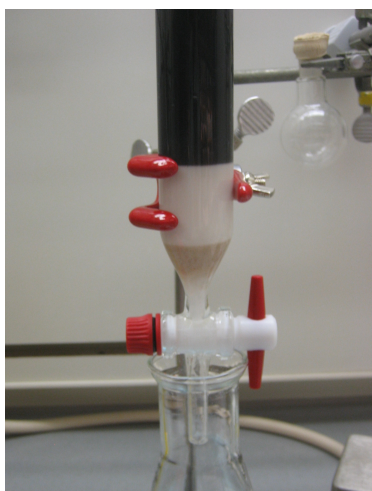


Figure 3.6: Celite filtration of reaction mixture in synthesis of **12**.

After concentration, the orange residue was extracted with dichloromethane, filtered and concentrated once more. Drying under reduced pressure yielded compound **12** as a redish brown solid. $^1\text{H-NMR}$ analysis indicated a pure product (see Addendix F), and the obtained signals corresponded well with literature values.¹⁰⁹ As no problems were encountered during the small scale reaction, the procedure was not changed before applied on a larger scale. However, due to

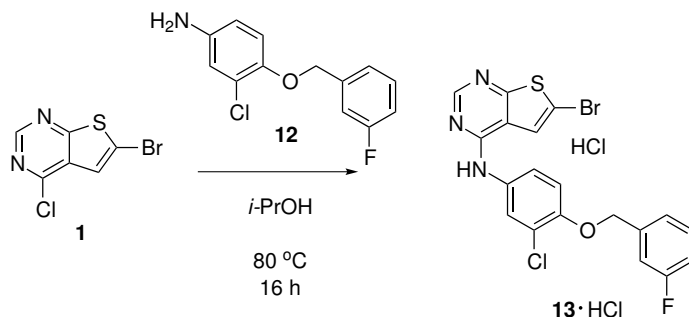
moderate yield in the small scale reaction, gentle heating was applied during extraction with dichloromethane in the work-up, to ensure better solubility of the product. This way, the yield was increased from 53% to 91%.

Table 3.3: Results from synthesis of **12**.

Entry	Scale [g]	Rx. time [h]	Yield [%]
1	0.200	3	53
2	1.29	3	91

Amination with **12** - Synthesis of **13·HCl**

Compound **13·HCl** was synthesized as illustrated in Scheme 3.8. The applied reaction conditions were developed in an improvement study performed in the pre-project autumn 2013.⁵⁴ Also this reaction was performed twice; the first time as a test reaction, and later on a larger scale, Table 3.4.



Scheme 3.8: Conditions for synthesis of compound **13·HCl**.

After five hours, the small scale test reaction had turned from a clear, slightly yellow solution to a clouded mixture. TLC analysis of the reaction mixture revealed remains of the starting material **1**. The reaction was thus left overnight. The following morning the mixture appeared thicker than the previous day, and TLC analysis now showed full conversion of **1**. The reaction mixture was concentrated, the residue triturated with diethyl ether, filtered and dried under reduced pressure. This yielded the hydrochloric salt of **13·HCl** as a pale yellow solid in 61% yield.

In the pre-project similar reactions gave yields in the range 76-100%, thus this moderate yield indicated that some of the product might have been lost during filtration. The yellow colour of the filtrate also pointed towards this, and TLC analysis of the filtrate proved this to contain the desired product, in addition to unreacted aniline (**12**). The filtrate was concentrated, and the residue was triturated with *n*-pentane, a less polar solvent than diethyl ether. This yielded an additional 6% of **13**·HCl, but with a darker, more brown colour than the first obtained product. Both batches of obtained solids were analysed by ¹H-NMR and found to be the desired compound **13**·HCl. No difference in purity could be seen from the ¹H-NMR analyses.

The larger scale reaction was performed as described for the small scale test reaction, but this time trituration was only performed with *n*-pentane since this had shown to give a higher yield. Trace amounts of starting material **1** was seen in TLC analysis of the filtrate, but no trace of the desired product was detected. The reaction yielded 92% of **13**·HCl as a sand coloured solid. The increase in yield compared with the first reaction is assumed mostly to be due to larger volumes, and thus smaller relative amounts lost in mechanical operations.

Table 3.4: Results from synthesis of **13**, prior to purification.

Entry	Scale [mg]	Rx. time [h]	Crude yield [%]
1	78	23	67
2	867	16	92

The presence of **13** as its hydrochloric salt was confirmed by ¹H-NMR analysis, as described for compound **5**·HCl in Section 3.1.1.

After work-up with *n*-pentane, **13**·HCl was dried under reduced pressure and HPLC-analysis was performed. The analysis showed compound **13**·HCl to have a purity of 93% at this point. Due to the darker colour observed in this product compared to that obtained in the small scale reaction worked-up using diethyl ether, it was believed that the latter work-up might result in a purer product, although no difference was observed in the ¹H-NMR analyses. The pale yellow solid obtained in the small scale test reaction was thus analysed with HPLC,

but also in this product the purity was found to be 93%. Further purification was thus needed for the building block **13**·HCl to undergo *in vitro* enzymatic inhibition testing.

Due to the poor solubility of **13**·HCl, purification using column chromatography was considered unsuitable. Hot filtration from both diethyl ether and *n*-pentane was performed, and in both cases the filtrates were analysed by TLC. In the diethyl ether, traces of both starting material **1** and aniline (**12**) was seen, as well as the desired product **13**, while in *n*-pentane only trace amounts of **1** were observed. HPLC-analyses showed no improvement in purity for either of the two methods.

Followingly, crystallization from both 1,4-dioxane and isopropanol was attempted unsuccessfully. Poor solubility of **13**·HCl was the problem in both cases. In 1,4-dioxane the colour of the solid seemed to be transferred to the solvent. Hot filtration was thus performed, but neither this led to any improvement in HPLC-purity.

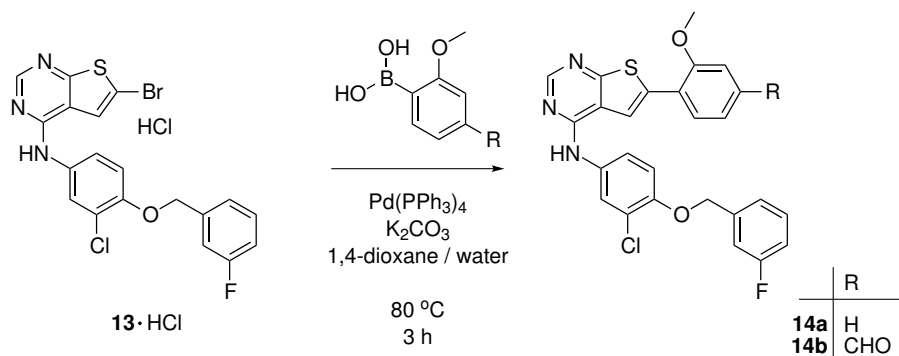
Finally, purification was managed through crystallization from dimethyl formamide, using water as anti-solvent. About 400 mg of **13**·HCl was dissolved in 4 mL of dimethyl formamide. During this process, upon addition of more solvent, a white cloud formed in the flask and disappeared again after a few seconds. When all solids were dissolved, water was added drop by drop until small solids formed and dissolved again in the flask. The solution was followingly left to cool in the hot oil-bath, to make the cooling process slow. The mixture was filtered two days later, to yield a big, fur ball looking, grey crystal like solid (216 mg, 13%), see Figure 3.7. ¹H-NMR analysis of this crystal showed it to be the free base of **13**. The purity was measured to 99% by HPLC.



Figure 3.7: Crystals of compound **13** obtained after crystallization from dimethyl formamide.

3.2.2 Suzuki coupling of **13** - Synthesis of **14a** and **14b**

Compounds **14a** and **14b** were synthesized as illustrated in Scheme 3.9.



Scheme 3.9: Conditions for synthesis of **14a** and **14b**.

Work-up of the reaction mixtures was performed by diluting with water and filtering, as for compounds **8a** and **8b**. Both **14a** and **14b** showed better solubility properties than the other target compounds synthesized in this thesis, and compound **14a** was found soluble enough to be purified by column chromatography. This gave a HPLC-purity of 91%, thus crystallization from 1,4-dioxane was performed in addition to obtain a satisfactory purity. Trace amounts of solvent

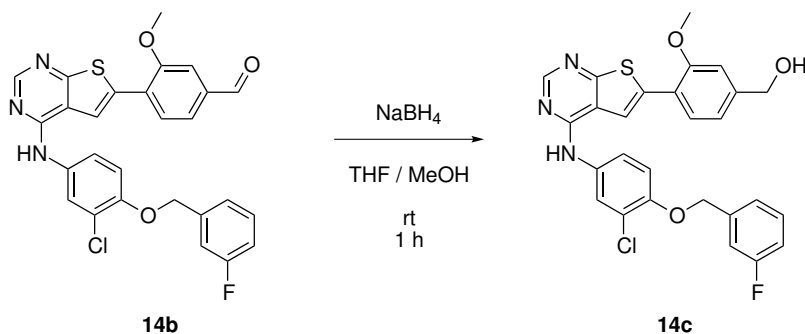
was removed from the obtained product by repeatedly adding dichloromethane, shaking the mixture in an ultrasound bath and concentrating. All solvent was removed after repeating three times, judging by $^1\text{H-NMR}$ analysis.

TLC analysis of the crude product of **14b** showed two weak spots in addition to the product spot. The R_f -value of one of by-products was found to be similar to that of compound **14a**, indicating loss of the formyl group. MS-analysis detected a mass corresponding to **14a**, thus supporting this theory. The other by-product was not identified.

The solubility of **14b** was not as good as that of **14a**. Therefore it was decided to attempt purification by crystallization. This was accomplished from THF, using *n*-pentane as anti-solvent. A bright yellow solid was obtained. The compound was highly static, causing an enlarged mechanical loss.

3.2.3 Reduction of **14b** - Synthesis of **14c**

Compound **14c** was obtained by reduction of **14b**, as illustrated in Scheme 3.10, following the same procedure as described for **8c** (Section 3.1.3).



Scheme 3.10: Conditions for synthesis of **14c** from **14b**.

After concentration and drying under reduced pressure, 90% of crude **14c** was obtained. Purification by crystallization from THF was attempted, yielding 43% of **14c**. Though the purity was measured to 92% by HPLC, requiring further purification of the product.

Due to the poor solubility of **14c**, repeated recrystallization was believed to be the best method of purification. Seeing as the first crystallization did not give a pure product, it was decided to try a different solvent, hoping the solubility properties of **14c** and the impurities would be more dissimilar. 1,4-Dioxane was chosen, due to good results in the purification of **14a**. Recrystallization was performed using 1.5 mL 1,4-dioxane for 51 mg product. After slowly cooling to room temperature, a substantial amount of yellow solid had formed. Filtering and elimination of trace solvent (as described for **14a** in Section 3.2.2) yielded less than 3% of **14c**. It was believed that more product could be obtained by use of an anti-solvent, or if dissolution of **14c** had been accomplished using a smaller amount of 1,4-dioxane. Further cooling of the crystallization flask would also most likely have given a higher yield. However, purity was again prioritized to higher yield, and the HPLC-purity of the obtained **14c** was now found to be > 99%.

Although the goal of pure product was met, the obtained amount of product was not sufficient for analyses and *in vitro* inhibition testing. The reaction thus had to be performed again. The second reaction was performed as described for the first, the sole difference being that crystallization was only performed once, from 1,4-dioxane. The crystallization was also done using less solvent. After elimination of trace solvent, 64% of **14c** was obtained, having an HPLC-purity of 96%.

The second product was slightly less pure than that of the first reaction. This implies that crystallization from THF also have contributed to the purification of **14c**. The fact that less 1,4-dioxane was used the second time can also have had a negative effect on the obtained purity, but most likely a positive effect on the yield. Table 3.5 summarizes yields, purities and crystallization solvents for both reductions.

Table 3.5: Results and method of purification for the two performed syntheses of **14c**.

Entry	Crude yield [%]	Final yield [%]	Purity [%]	Crystallization solvent
1	90	3	> 99	THF, 1,4-dioxane
2	100 ^a	64	96	1,4-dioxane

^a This number is probably too high, due to insufficient drying of the crude.

3.2.4 Overall remarks on the Lapatinib fragment based compounds

The compounds based on the Lapatinib aniline fragment were somewhat more challenging to work with than was the Gefitinib based compounds. Though solubility of compounds **14a-c** was slightly better, obtaining pure compounds was found more troublesome than for the Gefitinib based compounds. Reaction times, yields and purities for the building block and target compounds based on Lapatinib are presented in Table 3.6. The melting points and colours of the synthesized compounds are also given.

Table 3.6: Comparison of qualities for the synthesized compounds **13**, **14a**, **14b** and **14c**.

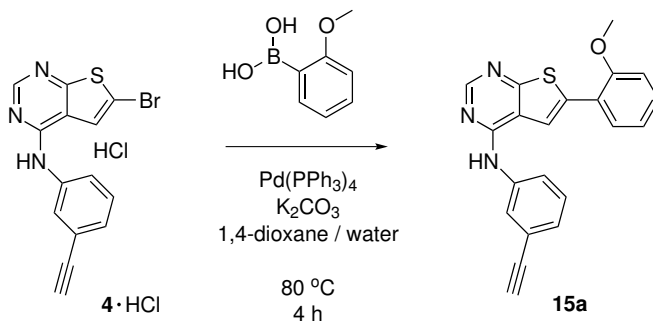
Compound	Reaction time [h]	Yield [%]	Purity [%]	Melting point [°C]	Colour
13	16	13	99	221-226	Grey
14a	3	26	97	163-165	White
14b	3	57	97	217-220	Bright yellow
14c^a	1	64	96	189-191	Pale yellow

^a Data from the second reaction (Entry 2 in Table 3.5).

3.3 Compounds Based on the Erlotinib Fragment

3.3.1 Synthesis of 15a

Compound **15a** was attempted synthesized using the same conditions as for the other Suzuki couplings performed in this master's thesis (Scheme 3.11).



Scheme 3.11: First attempt to synthesize **15a**, using standard conditions.

Full conversion was determined by thin layer chromatography after four hours, one hour longer than for the other performed Suzuki couplings. The reaction mixture was diluted with water, filtered and the obtained solid was dried under reduced pressure. After several failed attempts, crystallization of the sand coloured crude was obtained from dimethyl formamide. This yielded a brown solid with an appearance resembling instant coffee. The visual impression of the product suggested that the purification had not proceeded as intended. $^1\text{H-NMR}$ analysis resulted in a chaos of indistinct peaks in the aromatic region, confirming the formation of undesired by-products (Figure 3.8).

Due to the pronounced change in appearance over the crystallization process, it was assumed the product might have polymerized due to excess heating. Similar events had been observed in the pre-project for compounds containing the 3-ethynylaniline fragment when exposed to high temperatures. Unfortunately, no $^1\text{H-NMR}$ analysis was performed of the crude product, so this assumption could not be confirmed. The reaction was thus performed once more, using the same conditions as before (Scheme 3.11).

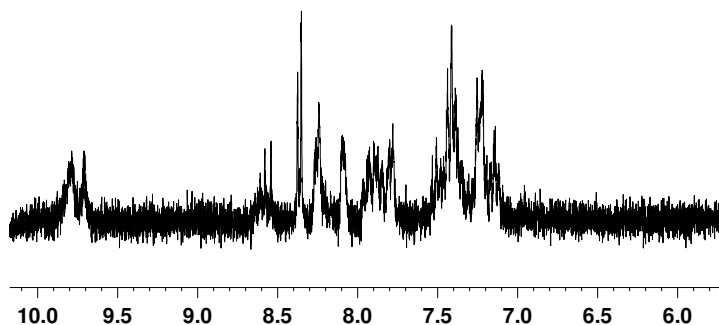


Figure 3.8: Section of ^1H -NMR spectra obtained after recrystallization of the first attempt to synthesize **15a**. Unit of the axis is ppm.

The crude product obtained in the second reaction had the same sand coloured appearance as in the first experiment. ^1H -NMR analysis was performed, but the result did not meet the expectations. Although not quite as bad as after recrystallization, the obtained spectrum resembled the one given in Figure 3.8. A new NMR sample was made to rule out contaminants in the tube, but the result was unchanged. Attempts were also made to perform NMR-analysis by use of another solvent to eliminate complexing as reason for the odd signals. However, this was not accomplished due to insolubility of the product mixture. All reagents used in the reaction; **4**-HCl, boronic acid, **15a**, catalyst, base and solvent, was the same as had been applied successfully in other reactions.

TLC analysis of the product showed three spots. Possibilities for purification by column chromatography were investigated, but the extremely poor solubility of the solid made this impossible. Mass spectroscopy analysis revealed the solid to contain the desired product **15a**, in addition to a dehalogenated version of **4** (**16** in Figure 3.9), a common by-product when longer reaction times are applied. The presence of water in the reaction mixture is reported to reduce the formation of this by-product.⁹⁰ All the Suzuki reactions in this thesis were performed with 50% water in the solvent mixture. Addition of more water would lead to lower solubility and most likely longer reaction times, thus possibly increasing the formation of other by-products.

The MS analysis also detected compounds of higher masses. Elemental calculations of some of these higher masses helped identify possible by-products formed by dimerization of **15a** and **16**. Suggested structures of two such by-products (**17** and **18**) are illustrated in Figure 3.9. These by-products are highly hypothetical, but mass and elemental composition are in agreement with MS findings. Two different bond formations are suggested, but the likelihood for either to occur is unknown.

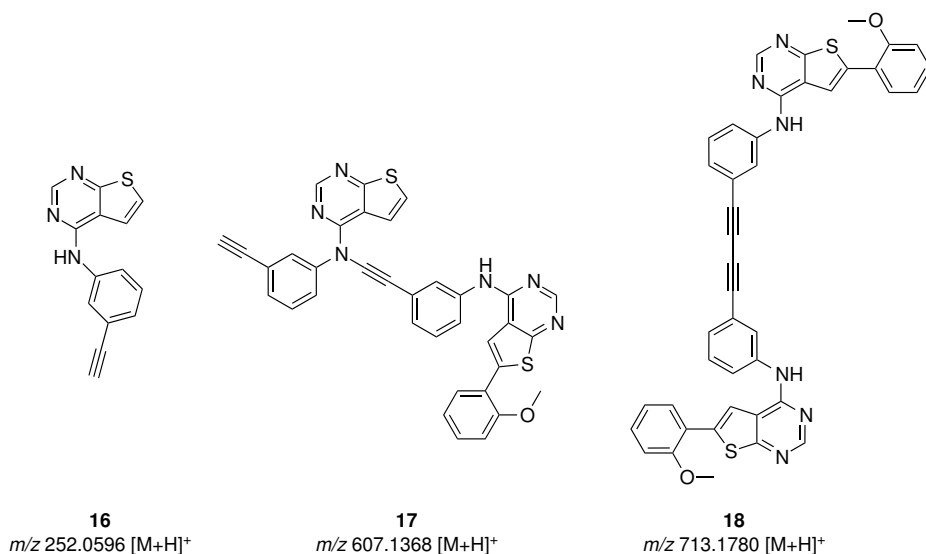
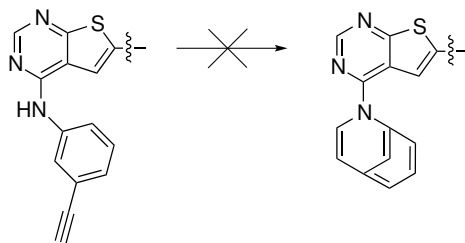


Figure 3.9: Suggested structures of by-products corresponding to peaks having m/z 252.0596, 607.1368 and 713.1780 for [M+H]⁺ in the MS-spectrum.

Alkynes are applicable in a number of different syntheses. They are extensively applied in cyclization reactions, and palladium is a favoured transition metal for catalysing addition to alkynes.⁸² Trost *et al.* have used palladium catalysed alkyne-alkyne coupling in intramolecular macrocyclizations.¹¹⁰ Soft nucleophiles, such as amines, tend to give 5- or 6-membered rings in intramolecular reactions catalysed by Pd(II).⁸² Due to intramolecular strain, this is unlikely to have happened in compound **15a** (Scheme 3.12).



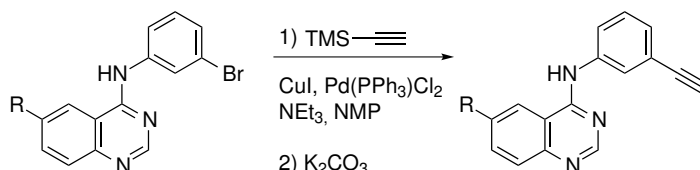
Scheme 3.12: Intramolecular alkyne-amine coupling is unlikely in this molecule, due to strain.

Homocoupling of terminal alkynes was first described by Glaser in 1869.¹¹¹ This reaction made use of a base, Cu(I) and oxygen in addition to the terminale alkyne. Variations of this reactions, such as the Hay reaction¹¹² has made it highly useful. Cadiot and Chodkiewicz developed a method for heterocoupling of terminale alkynes.¹¹³ Also this reaction is Cu-mediated. Yalagala *et al.* reports of palladium and copper mediated homotrimerization,¹¹⁴ while Atobe and co-workers have performed palladium catalysed homocoupling of terminale alkynes without copper, only base, solvent and Pd(PPh₃)₂Cl₂ was used.¹¹⁵

A control experiment was conducted as to see whether the dimerization was caused by the palladium catalyst, as seen for similar compounds and catalyst by Atobe *et al.*¹¹⁵ Compound **4**·HCl was mixed with the catalyst in the same solvent system as used in the Suzuki reaction, and the mixture was stirred at 80 °C. After four hours ¹H-NMR analysis gave a similarly chaotic spectrum as seen earlier, and after 24 hours it was even worse. This strongly suggests that the palladium catalyst was the reason for the failed reactions. However, this did not explain why dimerization was not a problem in the synthesis of **15b** (Section 3.3.2).

A more active catalyst, such as XPhos (Section 2.5.4), might have favoured the formation of product to dimerization, thus allowing the Suzuki coupling to be performed in the regular manner. Beckers *et al.* reports of an alternative method of synthesizing a molecule containing the same 3-ethynylaniline fragment as used in this thesis. Although no comments are made concerning problems of dimerization, in one of the syntheses the ethynyl function is introduced last in the reaction sequence (Scheme 3.13) by use of a palladium catalyzed Sonogashira

reaction with TMS-protected ethyne, followed by deprotection with potassium carbonate. This reaction was performed at 40 °C, thus dimerization due to heating could be avoided.

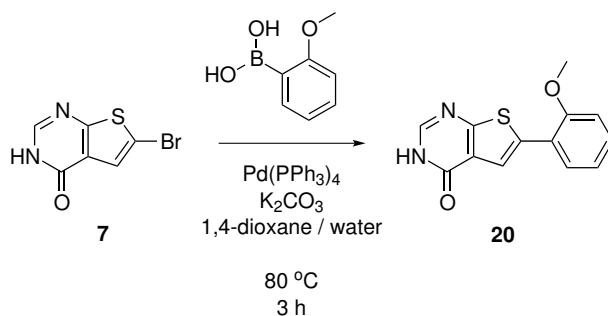


Scheme 3.13: Alternative introduction of the ethynyl function, as performed by Beckers *et al.*⁴⁷

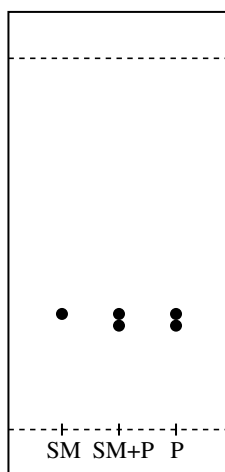
A new strategy of synthesis was needed to successfully synthesize **15a**. It was decided to attempt the alternative Route C as described in Section 2.5.1, and illustrated in Scheme 2.5. This method had been applied earlier in the research group, and all the needed reagents and starting material were available in house. In addition, this method avoided mixing palladium catalyst and ethynyl holding molecules, thus eliminating this as reason for the by-product formation.

Synthesis of **20**

Compound **7** had been synthesized in house at an earlier time. This compound had a brown sand like appearance, and was unpurified. With a melting point measured to 285-291 °C¹¹⁶ (lit. 301-304 °C¹¹⁷) it was clear that some impurities were present. Only signals from **7** were seen in the ¹H-NMR spectrum, thus the impurities were likely to be inorganic. The possibility of purification by column chromatography was investigated, but due to poor solubility properties of **7** this was not carried out. The unpurified **7** was thus used in the synthesis of **20**, this has also been done previously in the research group.⁵⁷ The synthesis of **20** was performed as illustrated in Scheme 3.14.

Scheme 3.14: Suzuki coupling conditions for synthesis of **20** from **7**.

Full conversion was determined by $^1\text{H-NMR}$ analysis after three hours. The brownish orange mixture was cooled to room temperature, before removal of 1,4-dioxane under reduced pressure. Following, the residue was filtered and the obtained solid was washed with water. TLC analysis of the crude product resulted in two spots. Further investigations by TLC indicated that this could be the desired product and remains of the starting material, Figure 3.10. Larger separation of the spots was not acquired, in most solvents only one spot was seen for the crude. Purification of **20** was not performed due to low solubility.

Figure 3.10: TLC analysis of crude product indicating remains of starting material **7**, SM is the starting material (**7**), while P is the crude product of **20**.

Through ^1H -, ^{13}C - and 2D-NMR analyses another by-product was assumed identified; biaryl of the boronic acid (**19**), Figure 3.11. The shifts obtained for **19** were in accordance with those estimated using ChemBioDraw 13.0, and was also close to the shifts of **20**.

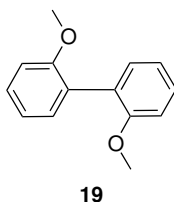
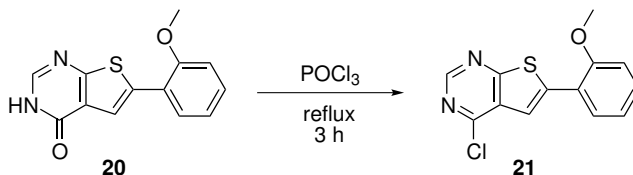


Figure 3.11: Biaryl by-product formed in the synthesis of **20**, identified by NMR analyses.

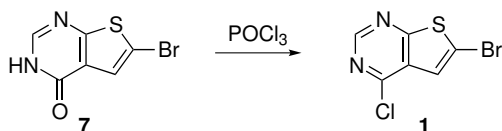
Synthesis of **21**

Compound **21** was obtained by refluxing **20** in phosphorous oxychloride for three hours (Scheme 3.15).



Scheme 3.15: Conditions for synthesis of **21**.

Upon completion, the reaction mixture was cooled to room temperature and quenched in ice water, before neutralized with sodium hydroxide and sodium bicarbonate solutions. Filtration yielded 92% of sand coloured crude product. Thin layer chromatography still showed two spots. This was expected, as it was already assumed that **20** contained some unreacted **7**; chlorination of **7** would give **1** (Scheme 3.16). A larger difference in R_f values of the two compounds was acquired. In addition, the chlorinated product **21** was significantly more soluble than **20**, thus purification by column chromatography (10:90 ethyl acetate:*n*-pentane) was applied to a fraction of the obtained material.



Scheme 3.16: Formation of **1** as a by-product in the synthesis of **21**.

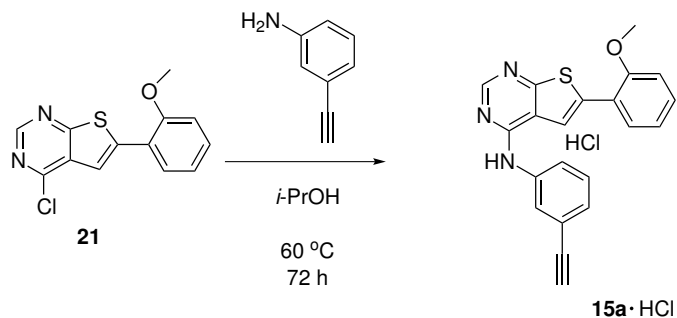
Two pure compounds were isolated during column chromatography, and $^1\text{H-NMR}$ analyses confirmed this to be **21** and **1**. One gram of crude product was applied to the column. From this only 152 mg (15 wt%) of **21** was isolated, and surprisingly 492 mg (49 wt%) of **1**. The fraction of **1** was not expected to be this large, seeing as no more of the starting material **7** was observed by $^1\text{H-NMR}$ upon termination of the synthesis of **20**.

As compound **21** eluted from the column, white solids precipitated in the spout of the column. These were attempted washed out using pure ethyl acetate. To some extent this method worked, but it is assumed that a fair amount of **21** might have been lost due to such precipitation. When product no longer eluted from the column, the eluent system was changed to pure ethyl acetate as a final attempt to isolate more **21**. Small amounts of additional product was obtained, however, the change in eluent caused impurities to elute together with **21**, resulting in yellow coloured product fractions. These fractions was thus not included in the final product.

Successful synthesis of **15a**

After having prepared and purified **21** in sufficient yield, the desired compound **15a** could eventually be synthesized by amination of **21** with 3-ethynylaniline, Scheme 3.17.

Due to problems with polymerization seen earlier, it was thought wise to lower the reaction temperature. Reaction temperatures as low as 60 °C had been tested in the pre-project, and found to work well, though resulting in longer reaction times.⁵⁴ A reaction temperature of 60 °C was thus chosen for the amination of **21**.

Scheme 3.17: Amination of **21** giving **15a**.

The conversion was monitored by ¹H-NMR and thin layer chromatography. By start of the reaction, the mixture was a white suspension. The low reaction temperature led to poor solubility of the starting material, but after 22 hours the mixture had turned more cream coloured. ¹H-NMR analysis suggested 20% conversion of **21** at this point. The following day, the reaction mixture had an appearance like custard, with a darker, more distinct yellow colour. Now ¹H-NMR analysis showed 90% conversion. The reaction was continued for another day, to get as high conversion as possible.

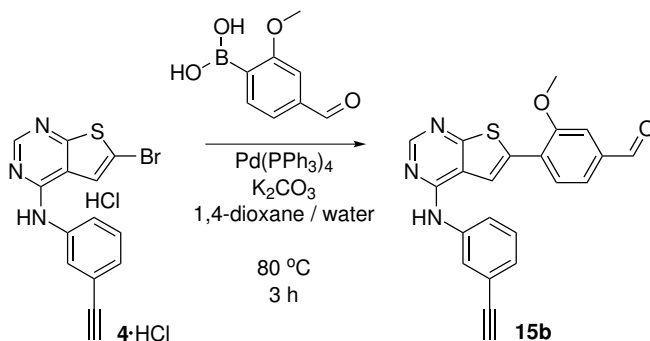
After 72 hours ¹H-NMR analysis indicated 82% conversion of **21**. Seeing as the mixture was a suspension, some margins of error in the measurement must be assumed. The measured conversions of 90% and 82% might thus lie within these margins, and followingly not mean a setback in conversion.

The reaction was terminated after 72 hours. After cooling the reaction mixture to room temperature, solvent was removed and the residue was triturated with diethyl ether. Filtration and subsequent drying yielded 41% of **15a·HCl**, having an HPLC-purity of > 99%.

The presence of **15a** as its hydrochloric salt was proved by free basing **15a·HCl** as described for compound **5·HCl** (Section 3.1.1).

3.3.2 Synthesis of **15b**

Compound **15b** was synthesized in a Suzuki coupling reaction, as illustrated in Scheme 3.18. This was the first Suzuki reaction performed in this master's thesis, thus the work-up applied differ from that described for the previous cross-coupling reactions.



Scheme 3.18: Suzuki coupling conditions for synthesis of **15b**.

Upon completion, the reaction mixture was concentrated and attempted dissolved in ethyl acetate for washing with water. The solubility of **15b** was poor, thus large amounts of solvent was needed to dissolve the solid. Heating was also applied to increase solubility. Washing with water caused precipitation of the product. Due to this precipitation, drying over anhydrous sodium sulfate was not performed.

Concentration of the organic layers yielded 300% of crude material. In addition to water residues, TLC analysis showed the crude to contain several different by-products. The high yield strongly suggested that the washing with water had been inadequate. As mentioned in Section 2.5.4, many common by-products in the Suzuki reaction are water soluble. Thus less by-products and lower yield might have been observed if more water had been applied in the washing of the organic layer. It is also likely that some of the excess mass of crude material results from potassium carbonate residues.

The crude product was purified by column chromatography. As experienced in the pre-project, the poor solubility led to low yields. In addition, the impurities

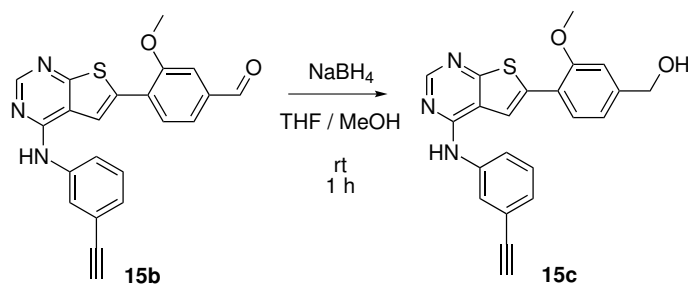
eluted over a large range, causing overlap with the desired product. Thus few of the collected fractions were pure. Only 32% of **15b** was obtained, having an HPLC-purity of 91%. Pure fractions of by-products were not obtained, thus non of these were identified.

Compound **15b** was to be used further in the synthesis of **15c**. In order to have enough starting material for this reaction, it was decided not to make further attempts to purify **15b**. As for the enzymatic testing, the alcohol function has earlier shown to be better than the formyl function. Having enough of **15b** for the synthesis of **15c** was thus prioritized to further purification of **15b**.

This unpractical, unsuccessful work-up and purification procedure resulted in a new method which was applied to all the other Suzuki couplings performed in this thesis. By taking advantage of the low solubility, work-up was performed by diluting with water and obtaining the crude product by filtration, as described earlier. Purification was in the subsequent reactions mostly performed by crystallization for the same reason.

3.3.3 Synthesis of compound 15c

Compound **15c** was synthesised by reduction of the aldehyde function in **15b** (Scheme 3.19), using the same procedure as described for **8c** (Section 3.1.3).



Scheme 3.19: Synthesis of **15c** by reduction of **15b**.

Upon completion, the reaction mixture was concentrated to about 5 mL, diluted with ethyl acetate and extracted with water. The organic layer was cloudy with

a greenish yellow colour, but turned clear yellow after washing with brine, as seen for compound **8c**. Concentration and drying yielded 98% of **15c** as a cream coloured solid.

Thin layer chromatography showed the product to contain some impurities, and purification by crystallization from methanol was applied. Only the desired product could be seen by TLC afterwards, and $^1\text{H-NMR}$ analysis also looked good. However, the HPLC-purity was only measured to be 86%. Further purification was thus needed. Recrystallization was attempted from several solvents, before being accomplished from dimethyl formamide, using water as anti-solvent. TLC analysis revealed the filtrate to contain product as well as another compound, while only one spot was seen for the isolated solid. The purity was now measured to be 92% by HPLC.

The purity requirement was still not met for **15c**. Due to time, additional purification was not managed before shipment to *in vitro* inhibition testing. Also, the amount of compound remaining was small (35 mg). Another recrystallization would most likely not yield enough compound, thus the necessary analyses was prioritized to pure compound.

3.3.4 Overall remarks on the Erlotinib fragment based compounds

The Erlotinib based compounds were the most challenging of the three compound series. Purification was difficult, and problems with dimerization caused **15a** to be synthesized using an alternative route. By the alternative strategy (Route C), pure compound was easily obtained. Good solubility of the intermediate **21** made column chromatography possible, yielding **21** of high purity. As seen in the pre-project, washing with diethyl ether was sufficient to yield **15a** with a purity of >99%.

Applying Route C in the syntheses of **15b** and **15c** would potentially also lead to compounds of high purity, given that the formyl and hydroxymethyl substituents are unaffected by the chlorination step. Though more steps are required, this is a good alternative if the aniline holds sensitive groups, or purification is difficult. For synthesizing a library of compounds having the same C-6 aryl group, Route

C would be beneficial. Exploring other routes of synthesis, like the one applied by Beckers *et al.*,⁴⁷ also provides an alternative strategy.

Obtained yields, purities, melting points and colours of the Erlotinib based compounds are given in Table 3.7.

Table 3.7: Obtained results for the syntheses of **15a-c**.

Entry	Yield [%]	Purity [%]	Melting point [°C]	Colour
15a	41	>99	223-233	Sandy yellow
15b	32	91	221-225	Yellow
15c	15	92	217-220	Pale yellow

3.4 *In vitro* Inhibition Testing

In vitro enzymatic EGFR inhibition activity testing has been applied for most of the target compounds synthesized in this thesis. Inhibition efficiencies at 100 nM concentration of the compounds have been measured (single point titration) in addition to IC₅₀-values. The single point results give an indication of the compound potencies, while the IC₅₀-values provide more reliable activity measurements. Unfortunately, some of the ordered IC₅₀-values were not obtained before deadline of this thesis. Table 3.9 and Table 3.10 presents the obtained data. Results from the pre-project are also included for comparison (compounds **2**, **3a**, **3c-d**, **5** and **4**), as is data for a selection of compounds previously synthesized in the research group (compounds **III-VI**).

Though the inhibition values are slightly lower, single point titration results obtained for the Gefitinib based series (**5**, **8a-c**) strongly resemble results previously obtained in the group (Table 3.9). This is also reflected in the IC₅₀-values given in Table 3.10.

The Erlotinib based building block **4** was found to be second best of the building blocks given. This is also the second best result ever obtained for a thienopyrimidine building block in the group. By comparison with **2**, it appears that some substitution on the aniline fragment is favourable.

From the IC₅₀-values given in Table 3.10 some trends can be observed. A more active building block leads to target compounds of higher potency. Additionally, the compounds holding the 2-methoxy-4-hydroxymethyl phenyl fragment **c** are the most potent compounds in each series. Judging by the single point titration (Table 3.9) this also appears to be valid for the Lapatinib and Erlotinib based compounds (**13**, **14a-c** and **4**, **15a-c**), though key data are missing in these series. If the Erlotinib based compounds follow this assumed potency trend, **15c** will be the most active of all the synthesized compounds.

However, although **3d** and **8c** show good inhibition activity, the activity is slightly lower than for **IVc** and **VIc**. This indicates that the hydroxymethyl group might be less favourable in the aniline substituted compounds than in the benzylamine substituted ones. Altering the amine fragment might have caused the compounds

to bind differently in the site, thus not obtaining optimal interaction of the hydroxymethyl group.

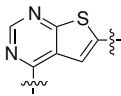
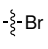
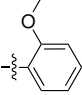
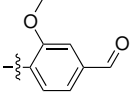
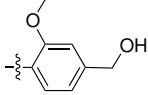
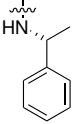
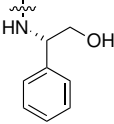
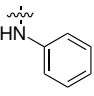
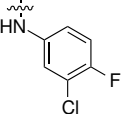
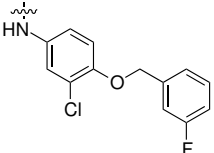
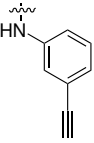
Inhibition activity testing towards the HER2 kinase have also been performed for the Lapatinib based compounds. As mentioned in Section 2.3, HER2 is often found to be overexpressed in certain types of breast cancer, and Lapatinib is an inhibitor acting on this kinase. The inhibition activities are measured at a 500 nM compound concentration, and the results are given in Table 3.8.

The Lapatinib based compounds show inhibition activity towards the HER2 kinase. Compounds **14b** and **14c** can be good lead compounds in the search for new HER2 inhibitors.

Table 3.8: HER2 inhibition efficiency for the Lapatinib based compounds **14a-c**, measured at a compound concentration of 500 nM.

Compound	HER2 inhibition efficiency (500 nM) [%]
14a	33
14b	63
14c	60

Table 3.9: Inhibition efficiency data [%] for the synthesized compounds, measured for compound concentrations of 100 nM. The number of the respective compounds are given in paranthesis. Data for compounds **III-VI** synthesized earlier in the research group and compounds **2, 3a-d** synthesized in the pre-project are given for comparison.

				
	59 ^a (III)	91 ^a (IVa)	88 ^a (IVb)	98 ^a (IVc)
	80 ^a (V)	>99 ^a (VIa)	90 ^a (VIb)	94 ^a (VIc)
	74 ^b (2)	53 ^b (3a)	89 ^b (3c)	>99 ^b (3d)
	40 (5)	92 (8a)	89 (8b)	93 (8c)
	N/D ^c (13)	55 (14a)	68 (14b)	82 (14c)
	84 ^b (4)	92 (15a)	N/D ^c (15b)	N/D ^c (15c)

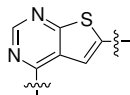
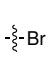
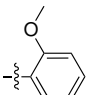
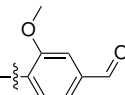
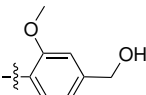
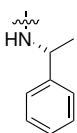
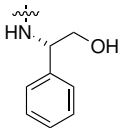
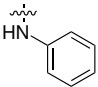
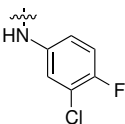
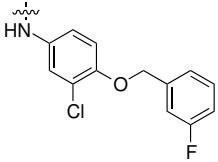
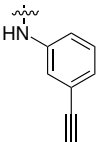
^a Results obtained earlier in the research group.

^b Results obtained in the pre-project.⁵⁴

^c N/D: Not determined.

3 RESULTS AND DISCUSSION

Table 3.10: IC₅₀ values for the synthesized compounds, measured for compound concentrations of 100 nM. The numbers of the respective compounds are given in paranthesis. Data for compounds **III-VI** synthesized earlier in the research group and compounds **2, 3a-d** synthesized in the pre-project are given for comparison.

				
	45 nM ^a (III)	9 nM ^a (IVa)	3 nM ^a (IVb)	0.7 nM ^a (IVc)
	16 nM ^a (V)	1.5 nM ^a (VIa)	0.8 nM ^a (VIb)	0.3 nM ^a (VIc)
	80 nM ^b (2)	173 nM ^b (3a)	20 nM ^b (3c)	3 nM ^b (3d)
	N/D ^c (5)	5.3 nM (8a)	5.3 nM (8b)	2.4 nM (8c)
	N/D ^c (13)	N/D ^c (14a)	52.5 nM (14b)	N/C ^c (14c)
	23.9 nM ^b (4)	N/D ^c (15a)	N/D ^c (15b)	N/D ^c (15c)

^a Results obtained earlier in the research group.

^b Results obtained in the pre-project.⁵⁴

^c N/D: Not determined.

3.5 Compound Characterization

Most of the target compounds synthesized in this master's thesis are new compounds, thus analytical and spectroscopic data were not found in the literature. Only compound **13** was known. ^1H -NMR data was found for **13**, but not for **13**·HCl. For the intermediate compounds **11**, **12**, **20** and **21**, only **11** and **12** were found in the literature. ^1H -NMR data were found for these compounds. Each new compound have been analysed by NMR, MS and IR. Melting points have also been measured.

NMR

^1H and ^{13}C shifts were assigned by use of ^1H -NMR, ^{13}C -NMR, ^1H - ^1H COSY, HSQC and HMBC spectra.

Some general trends were observed when comparing shifts for the elucidated compounds. In the heterocyclic core, both carbon and proton shifts are fairly constant, but shifts in positions 5 and 6 (Figure 3.12) were observed to vary according to the substitution pattern of the C-6 aryl. Shifts of the aryl substituents were also affected by different substituent groups, but were found to be similar for identical groups, regardless the aniline fragment.

The same observations were made for the C-4 aniline substituent; shifts varied according to the R_1 groups, but were found approximately constant within the same fragment, unaffected by the C-6 aryl substituent.

In some of the ^{13}C -NMR spectra an artefact signal appears around 83 ppm. This is believed to be caused by the detection method used in the analysis.

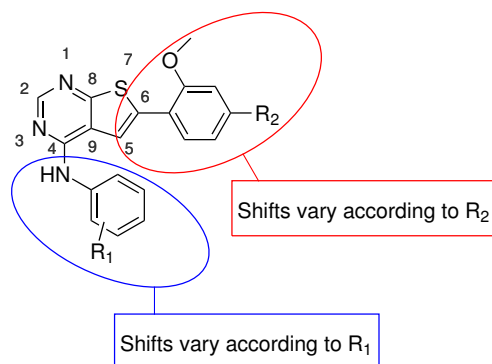


Figure 3.12: General structure of the target molecules with numbering of positions in the heteroaromatic core, showing which shifts are affected by the substituents R_1 and R_2 .

IR¹¹⁸

The IR analyses of the synthesized compounds share many of the same features, and are thus described ahead.

A weak, broad absorption around $3200\text{-}2500\text{ cm}^{-1}$ can be seen for all compounds containing a NH group, due to N-H stretching vibrations. N-H bending vibrations results in absorption just above 1600 cm^{-1} for the same compounds.

Aromatic C-H out of plane bending vibrations was observed in the area $900\text{-}675\text{ cm}^{-1}$ and in-plane bending in the region $1300\text{-}1000\text{ cm}^{-1}$ for all compounds.

Compounds holding a methoxy group displayed absorption due to C-O-C stretching in the regions $1300\text{-}1200\text{ cm}^{-1}$ and $1050\text{-}1000\text{ cm}^{-1}$. The aldehyde functions in **8b**, **14b** and **15b** showed C=O stretching around $1680\text{-}1670\text{ cm}^{-1}$. Hydroxyl groups in **8c**, **14c** and **15c** gave weak, broad absorptions around $3200\text{-}3100\text{ cm}^{-1}$.

Compounds **8a-c**, **13** and **14a-c** showed absorptions due to aromatic fluorine around $1250\text{-}1199\text{ cm}^{-1}$, while the ethynyl group in compounds **15a-c** gave absorption in the range $680\text{-}660\text{ cm}^{-1}$.

3.5.1 Characterisation of Compound **8a**

The structure of compound **8a** with numbering of positions is given in Figure 3.14. The melting point of **8a** was found to be 243-245 °C.

MS

High resolution mass spectroscopy gave m/z 386.0525 [M+H]⁺ for compound **8a**. With a calculated value of 386.0530, the molecular formula C₁₉H₁₃N₃OFSCl was confirmed with an accuracy of 1.3 ppm.

NMR

The findings from the ¹H- and ¹³C-NMR-analyses are presented in Table 3.11. ¹⁹F-NMR shift for **8a** was found to be -125.70 (s, dec.) ppm.

The assignment of shifts in the heterocyclic core was mostly based on long distance ¹H-¹³C correlations (HMBC). As seen in the pre-project,⁵⁴ H-2 was found to have the highest shift of the core protons, due to its placement between to heteroatoms. By the same reasoning, C-8 situated between sulfur and nitrogen, was found to have the highest shift of the carbons in the core. C-4 was assigned based on correlation to H-2 and H-10.

Introduction of fluorine causes signals from carbons 11 and 13-16 to give doublets in the ¹³C-NMR spectrum of **8a**. Carbon 12 was found not to couple to fluorine, it's ¹³C signal thus appears as a singlet. The doublets were identified by comparing obtained coupling constants with theoretical values. As illustrated in Figure 3.13, the coupling constant decreases with increasing distance from the fluorine atom. The coupling constants given in Figure 3.13 are valide for the unsubstituted fluorobenzene, variations may thus appear as the substitution pattern is changed, as seen for **8a**.

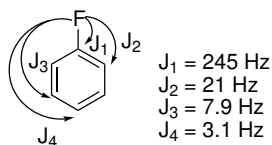
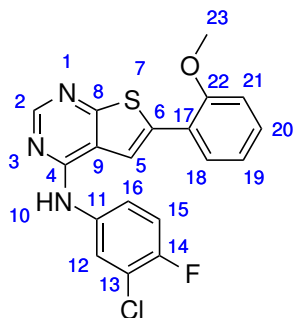


Figure 3.13: Carbon-fluorine coupling constants in fluorobenzene.

The splitting of carbon signals eased the assignment of carbon shifts on the fluorine containing ring. This made it possible to differentiate between C-14 and C-22, with ^{13}C signals at 154.25 and 154.26 ppm, respectively. Long range ^1H - ^{13}C correlations (HMBC) together with ^1H - ^1H correlations (COSY) were used to assign shifts at positions 17-22. Comparison of shifts with compounds having similar structures was used to confirm the assignment.

IR, MS and NMR spectra for compound **8a** are given in Appendix B.

Figure 3.14: Numbering of positions in compound **8a**.

3 RESULTS AND DISCUSSION

Table 3.11: ^1H - and ^{13}C -NMR data for compound **8a** (DMSO- d_6).

Position	^1H [ppm] (int., mult., J [Hz])	^{13}C [ppm] (mult., J [Hz])	COSY	HMBC
2	8.54 (1H, s)	153.8	-	4
4		151.8		
5	8.31 (1H, s)	116.6	-	6, 8, 9, 17
6		135.5		
8		166.5		
9		117.1		
10	9.79 (1H, s)	N	-	4, 12
11		136.7 (d, 3.6)		
12	8.24 (1H, dd, 6.8/2.8)	121.3	16	
13		118.9 (d, 18.4)		
14		154.25 (d, 242.8)		
15	7.49-7.41 (1H, m)	116.7 (d, 22.0)	16	11, 13
16	7.83-7.76 (1H, m)	121.24 (d, 6.8)	12, 15	
17		122.4		
18	7.83-7.76 (1H, m)	128.0	19	6, 20, 22
19	7.14 (1H, t, 7.6)	121.20	18, 20	17
20	7.49-7.41 (1H, m)	130.2	18, 19, 21	19, 22
21	7.24 (1H, d, 8.0)	112.6	20	19
22		154.26		
23	3.98 (3H, s)	55.9	-	22

3.5.2 Characterisation of Compound **8b**

The structure of compound **8b** with numbering of positions is given in Figure 3.15. The melting point of **8b** was found to be 252-254 °C.

MS

High resolution mass spectroscopy gave m/z 414.0471 $[M+H]^+$ for compound **8b**. With a calculated value of 414.0479, the molecular formula $C_{20}H_{13}N_3O_2FSCl$ was confirmed with an accuracy of 1.9 ppm.

NMR

The findings from the 1H - and ^{13}C -NMR analyses are presented in Table 3.12. ^{19}F -NMR shift for **8b** was found to be -125.40 (s, dec.) ppm.

Fluorine couplings were useful in the assignment of shifts on the aniline ring. Similar splitting as for **8a** was seen, with corresponding coupling constants. Comparison with other elucidated structures was helpful as to place C-6 and C-17. These carbons were only found to couple to C-5, and was thus identified by comparison with shifts in other structures.

IR, MS and NMR spectra for compound **8b** are given in Appendix C.

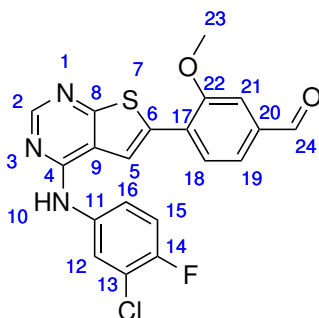


Figure 3.15: Numbering of positions in compound **8b**.

Table 3.12: ^1H - and ^{13}C -NMR data for compound **8b** (DMSO- d_6).

Position	^1H [ppm] (int., mult., J [Hz])	^{13}C [ppm] (mult., J [Hz])	COSY	HMBC
2	8.56 (1H, s)	153.5	-	4, 9
4		154.1		
5	8.50 (1H, s)	118.96	-	4, 6, 8, 9, 17
6		127.2		
8		167.5		
9		117.0		
10	9.87 (1H, s)	N	-	-
11		136.5 (d, 3.0)		
12	8.22 (1H, dd, 6.8/2.8)	122.6	16	11, 13, 14, 16
13		118.97 (d, 18.6)		
14		153.2 (d, 242.6)		
15	7.50-7.43 (1H, m)	116.8 (d, 21.9)	16	11, 14
16	7.83-7.78 (1H, m)	121.4 (d, 7.1)	12	12
17		133.9		
18	8.02-7.98 (1H, m)	128.4	19	17, 20, 22
19	7.73-7.67 (1H, m)	122.8	18	17, 18, 21
20		136.9		
21	7.73-7.67 (1H, m)	112.2	-	19, 20, 22
22		155.8		
23	4.08 (3H, s)	56.2	-	22
24	10.04 (1H, s)	192.2	-	18, 20, 21

3.5.3 Characterisation of Compound **8c**

The structure of compound **8c** with numbering of positions is given in Figure 3.16. The melting point of **8c** was found to be 257-259 °C.

MS

High resolution mass spectroscopy gave m/z 416.0630 $[M+H]^+$ for compound **8c**. With a calculated value of 416.0636, the molecular formula $C_{20}H_{15}N_3O_2FSCl$ was confirmed with an accuracy of 1.4 ppm.

NMR

The findings from the 1H - and ^{13}C -NMR analyses are presented in Table 3.13. ^{19}F -NMR shift for **8c** was found to be -125.75 (s, dec.) ppm.

The assignment of shifts was performed as described for **8a**. Fluorine coupling constants were found to be similar to those seen for compounds **8a** and **8b**.

IR, MS and NMR spectra for compound **8c** are given in Appendix D.

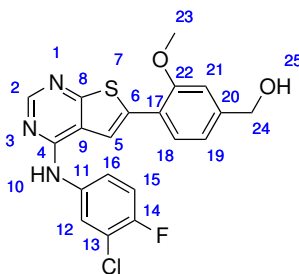


Figure 3.16: Numbering of positions in compound **8c**.

Table 3.13: ^1H - and ^{13}C -NMR data for compound **8c** (DMSO- d_6).

Position	^1H [ppm] (int., mult., J [Hz])	^{13}C [ppm] (mult., J [Hz])	COSY	HMBC
2	8.53 (1H, s)	153.7	-	4, 8
4		152.8		
5	8.29 (1H, s)	116.0	-	4, 6, 8, 9, 17
6		135.7		
8		166.3		
9		117.1		
10	9.77 (1H, s)	N	-	4, 12
11		136.7 (d, 3.0)		
12	8.23 (1H, dd, 6.8/2.8)	122.3	16	11, 13, 14
13		118.9 (d, 18.3)		
14		153.0 (d, 242.8)		
15	7.46 (1H, t, 9.2)	116.7 (d, 21.5)	16	11, 13, 14
16	7.84-7.78 (1H, m)	121.2 (d, 7.0)	12, 15	
17		119.8		
18	7.73 (1H, d, 8.0)	127.7	19	6, 20, 22
19	7.09 (1H, d, 8.0)	119.0	18	17, 21, 24
20		145.3		
21	7.18 (1H, s)	110.2	24	19, 20, 22, 24
22		155.5		
23	3.98 (3H, s)	55.8	-	22
24	4.57 (2H, d, 5.6)	62.5	25	19, 20, 21
25	5.33 (1H, t, 5.6)	O	24	-

3.5.4 Characterisation of Compound **13**·HCl

The structure of compound **13** with numbering of positions is given in Figure 3.17. The melting point of **13**·HCl was found to be 221-226 °C.

MS

High resolution mass spectroscopy gave m/z 463.9635 $[M+H]^+$ for compound **13**. With a calculated value of 463.9635, the molecular formula $C_{19}H_{12}N_3OFSClBr$ was confirmed with an accuracy of 0.0 ppm.

NMR

The findings from the 1H - and ^{13}C -NMR analyses are presented in Table 3.14. ^{19}F -NMR shift for **13**·HCl was found to be -115.34 (s, dec.) ppm.

Splitting of signals due to fluorine coupling was seen for all carbons in the lower ring holding fluorine, but also in the benzylic position C-17. Coupling constants made the assignment of these shifts fairly easy. The remaining shifts were assigned without any problems.

IR, MS and NMR spectra for compound **13**·HCl are given in Appendix G.

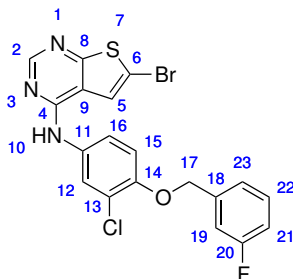


Figure 3.17: Numbering of positions in compound **13**.

Table 3.14: ^1H - and ^{13}C -NMR data for compound **13** (DMSO- d_6).

Position	^1H [ppm] (int., mult., J [Hz])	^{13}C [ppm] (mult., J [Hz])	COSY	HMBC
2	8.49 (1H, s)	153.3	-	4, 8, 9
4		152.9		
5	8.08 (1H, s)	123.1	-	8, 9
6		111.1		
8		165.8		
9		117.7		
10	9.73 (1H, s)	N	-	
11		132.7		
12	7.35-7.24 (1H, m)	114.5	16	11, 13, 14
13		121.2		
14		149.7		
15	8.05-8.00 (1H, m)	123.35	16	11, 13, 14
16	7.70-7.64 (1H, m)	121.6	12, 15	11, 14
17	5.24 (2H, s)	69.4 (d, 1.5)	19, 23	14, 18, 19, 23
18		139.6 (d, 7.4)		
19	7.35-7.24 (1H, m)	114.0 (d, 21.9)	-	
20		162.2 (d, 243.7)		
21	7.21-7.14 (1H, m)	114.7 (d, 21.1)	-	22
22	7.50-7.43 (1H, m)	130.6 (d, 8.6)	21, 23	18, 20
23	7.35-7.24 (1H, m)	1223.32 (d, 3.0)	22	

3.5.5 Characterisation of Compound 14a

The structure of compound **14a** with numbering of positions is given in Figure 3.18. The melting point of **14a** was found to be 163-165 °C.

MS

High resolution mass spectroscopy gave m/z 492.0946 $[M+H]^+$ for compound **14a**. With a calculated value of 492.0949, the molecular formula $C_{26}H_{19}N_3O_2SClF$ was confirmed with an accuracy of 0.6 ppm.

NMR

The findings from the 1H - and ^{13}C -NMR analyses are presented in Table 3.15. ^{19}F -NMR shift for **14a** was found to be -115.39 (s, dec.) ppm.

No problems were encountered during elucidation, but comparison of shifts found in **13**·HCl and **8a** was helpful to confirm the assignment.

IR, MS and NMR spectra for compound **14a** are given in Appendix H.

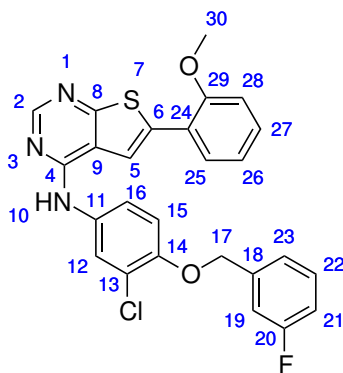


Figure 3.18: Numbering of positions in compound **14a**.

Table 3.15: ^1H - and ^{13}C -NMR data for compound **14a** ($\text{DMSO-}d_6$).

Position	^1H [ppm] (int., mult., J [Hz])	^{13}C [ppm] (mult., J [Hz])	COSY	HMBC
2	8.49 (1H, s)	153.1	-	4, 5, 8
4		154.0		
5	8.29 (1H, s)	116.7	-	4, 6, 8, 9, 24
6		135.2		
8		166.3		
9		116.9		
10	9.49 (1H, s)	N	-	4
11		133.4		
12	7.36-7.10 (1H, m)	114.5	16	11, 14, 16
13		121.5		
14		149.3		
15	8.06 (1H, d, 2.4)	123.0	16	11, 13, 14
16	7.72 (1H, dd, 9.2/2.4)	121.20	12, 15	14
17	5.25 (2H, s)	69.4 (d, 2.2)	-	14, 18, 19, 23
18		139.7 (d, 7.4)		
19	7.36-7.10 (1H, m)	114.0 (d, 21.9)	-	17
20		162.2 (d, 244.2)		
21	7.36-7.10 (1H, m)	114.7 (d, 21.0)	22	-
22	7.51-7.40 (1H, m)	130.6 (d, 8.0)	-	18, 20, 21
23	7.36-7.10 (1H, m)	123.3 (d, 3.0)	22	17
24		121.1		
25	7.77 (1H, dd, 1.6/7.6)	128.0	26	24, 27, 29
26	7.36-7.10 (1H, m)	121.18	25, 27	28
27	7.51-7.40 (1H, m)	130.1	26, 28	-
28	7.36-7.10 (1H, m)	112.6	27	27, 29
29		155.6		
30	3.97 (3H, s)	55.9	-	29

3.5.6 Characterisation of Compound 14b

The structure of compound **14b** with numbering of positions is given in Figure 3.19. The melting point of **14b** was found to be 217-220 °C.

MS

High resolution mass spectroscopy gave m/z 520.0888 $[M+H]^+$ for compound **14b**. With a calculated value of 520.0898, the molecular formula $C_{27}H_{19}N_3O_3FSCl$ was confirmed with an accuracy of 1.9 ppm.

NMR

The findings from the 1H - and ^{13}C -NMR analyses are presented in Table 3.16. ^{19}F -NMR shift for **14b** was found to be -115.38 (s, dec.) ppm.

In this compound the carbon shifts of C-13 and C-16 are too similar to be separated in the spectra, ppm values 121.19 and 121.21. The assignment was therefore done by comparing the relative shift values with those found for compounds **13** and **14a**. C-13 was thus assigned the higher shift, 121.21, and C-16 the lower. The remaining shifts were assigned as previously described for the other compounds.

IR, MS and NMR spectra for compound **14b** are given in Appendix I.

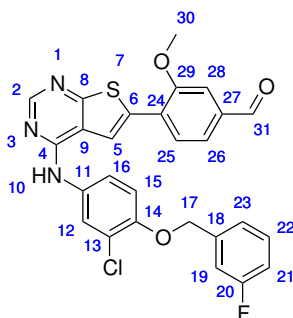


Figure 3.19: Numbering of positions in compound **14b**.

Table 3.16: ^1H - and ^{13}C -NMR data for compound **14b** ($\text{DMSO-}d_6$).

Position	^1H [ppm] (int., mult., J [Hz])	^{13}C [ppm] (mult., J [Hz])	COSY	HMBC
2	8.51-8.47 (1H, m)	153.7	-	4, 8
4		154.3		
5	8.51-8.47 (1H, m)	119.1	-	4, 6, 8, 9, 24
6		127.2		
8		166.9		
9		116.9		
10	9.74 (1H, s)	N	-	
11		133.2		
12	7.35-7.25 (1H, m)	114.5	16	11, 14, 16
13		121.21		
14		149.4		
15	8.07-8.03 (1H, m)	123.0	16	11, 13, 14
16	7.74-7.68 (1H, m)	121.19	12, 15	14
17	5.25 (2H, s)	69.4 (d, 2.0)	19, 23	14, 18, 19, 23
18		139.6 (d, 7.3)		
19	7.35-7.25 (1H, m)	114.0 (d, 21.9)	-	17
20		162.2 (d, 243.7)		
21	7.23-7.15 (1H, m)	114.7 (d, 21.1)	22	
22	7.51-7.43 (1H, m)	130.5 (d, 8.3)	21, 23	18, 20, 21
23	7.35-7.25 (1H, m)	123.3 (d, 2.5)	22	17
24		133.5		
25	8.02-7.97 (1H, m)	128.4	26, 28	24, 27, 29
26	7.74-7.68 (1H, m)	122.8	25	27, 28, 31
27		136.8		
28	7.74-7.68 (1H, m)	112.2	-	27, 29, 31
29		155.8		
30	4.08 (3H, s)	56.2	-	29
31	10.04 (1H, s)	192.2	-	

3.5.7 Characterisation of Compound **14c**

The structure of compound **14c** with numbering of positions is given in Figure 3.20. The melting point of **14c** was found to be 189-191 °C.

MS

High resolution mass spectroscopy gave m/z 522.1046 $[M+H]^+$ for compound **14c**. With a calculated value of 522.1054, the molecular formula $C_{27}H_{21}N_3O_3FSCl$ was confirmed with an accuracy of 1.5 ppm.

NMR

The findings from the 1H - and ^{13}C -NMR analyses are presented in Table 3.17. ^{19}F -NMR shift for **14c** was found to be -115.39 (s, dec.) ppm.

The assignment was performed without any problems aided by fluorine couplings and comparison with data for other structures.

IR, MS and NMR spectra for compound **14c** are given in Appendix J.

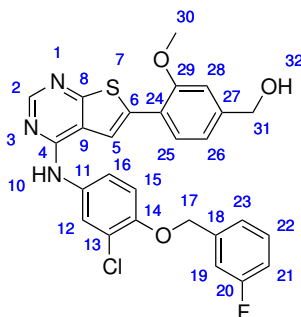


Figure 3.20: Numbering of positions in compound **14c**.

Table 3.17: ^1H - and ^{13}C -NMR data for compound **14c** ($\text{DMSO-}d_6$).

Position	^1H [ppm] (int., mult., J [Hz])	^{13}C [ppm] (mult., J [Hz])	COSY	HMBC
2	8.48 (1H, s)	153.0	-	4, 5, 8
4	-	153.9		
5	8.27 (1H, s)	116.2	-	6, 9, 24
6	-	135.3		
8	-	166.1		
9	-	117.0		
10	9.62 (1H, s)	N	-	4, 15, 16
11	-	133.5		
12	7.36-7.24 (1H, m)	114.6	16	11, 14, 16
13	-	121.2		
14	-	149.8		
15	8.08-8.03 (1H, m)	122.9	16	11, 14
16	7.74-7.69 (1H, m)	121.1	15	14, 15
17	5.25 (2H, s)	69.4 (d, 2.0)	-	14, 15, 18
18	-	139.7 (d, 7.3)		
19	7.36-7.24 (1H, m)	114.0 (d, 21.9)	-	
20	-	162.2 (d, 243.7)		
21	7.21-7.14 (1H, m)	114.7 (d, 21.0)	22	
22	7.51-7.44 (1H, m)	130.6 (d, 8.5)	21, 23	18, 19, 20
23	7.36-7.24 (1H, m)	123.3 (d, 2.9)	22	
24	-	119.8		
25	7.74-7.69 (1H, m)	127.7	26	27, 29
26	7.08 (1H, d, 8.0)	119.0	25	254, 28, 31
27	-	145.2		
28	7.21-7.14 (1H, m)	110.2	-	24, 27, 29, 31
29	-	155.5		
30	3.97 (3H, s)	55.8	-	29
31	4.57 (2H, d, 5.6)	62.5	32	26, 27, 28
32	5.32 (1H, t, 5.6)	O	-	27, 31

3.5.8 Characterisation of Compound 20

The structure of compound **20** with numbering of positions is given in Figure 3.21. The compound was found to decompose at 270-317 °C.

MS

High resolution mass spectroscopy gave m/z 259.0537 $[M+H]^+$ for compound **20**. With a calculated value of 259.0541, the molecular formula $C_{13}H_{11}N_2O_2S$ was confirmed with an accuracy of 1.5 ppm.

NMR

The findings from the 1H - and ^{13}C -NMR analyses are presented in Table 3.18.

Compound **20** had a low purity, something which complicated the assignment of shifts. By comparing integrals in the 1H -NMR spectrum, signals originating from the desired compound could be identified. This eased the rest of the assignment. Short range 1H - 1H correlations (COSY) were used to determine the relative order of the protons 11 - 14, while a comparison of shifts found in other structures was needed to identify protons 11 and 14, due to inconclusive long range 1H - ^{13}C correlations (HMBC). Carbons 10 and 12 were found to have very similar shifts, some uncertainty is therefore associated with the assignment of these shifts. By extensive zooming in the short range 1H - ^{13}C correlations spectrum, the shifts were assumed to be 121.3 and 121.2 for carbon 10 and 12, respectively.

IR, MS and NMR spectra for compound **20** are given in Appendix K.

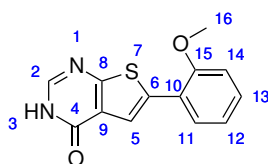


Figure 3.21: Numbering of positions in compound **20**.

Table 3.18: ^1H - and ^{13}C -NMR data for compound **20** (DMSO- d_6).

Position	^1H [ppm] (int., mult., J [Hz])	^{13}C [ppm]	COSY	HMBC
2	8.11 (1H, s)	146.3	-	4
4		157.9		
5	7.85-7.79 (1H, m)	118.9	-	6, 8, 9, 10
6		134.9		
8		163.9		
9		124.8		
10		121.3		
11	7.85-7.79 (1H, m)	128.0	12	13, 15
12	7.09-7.01 (1H, m)	121.2	11, 13	10
13	7.43-7.33 (1H, m)	129.7	12, 14	
14	7.21-7.17 (1H, m)	112.4	13	10, 12
15		155.3		
16	3.95 (3H, s)	55.8	-	15

3.5.9 Characterisation of Compound **21**

The structure of compound **21** with numbering of positions is given in Figure 3.22. The melting point of **21** was found to be 165-168 °C.

MS

High resolution mass spectroscopy gave m/z 277.0197 $[M+H]^+$ for compound **21**. With a calculated value of 277.0202, the molecular formula $C_{13}H_{10}N_2OSCl$ was confirmed with an accuracy of 1.8 ppm.

NMR

The findings from the 1H - and ^{13}C -NMR analyses are presented in Table 3.19.

The elucidation of structure **21** was fairly straight forward, the only exception being the shift assignment of carbons 6 and 9. These atoms both showed long range correlations with proton 5 (HMBC), but no other signals were seen for neither carbon. The difference in shift values of the carbons was significant, 141.2 and 129.2 ppm, something which eased the assignment. By comparing with other structures the higher of the shifts (141.2 ppm) was identified as carbon 6 and the lower (129.2 ppm) as carbon 9. This also corresponded well with the shift values estimated using ChemBioDraw 13.0.

IR, MS and NMR spectra for compound **21** are given in Appendix L.

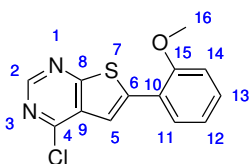


Figure 3.22: Numbering of positions in compound **21**.

Table 3.19: ^1H - and ^{13}C -NMR data for compound **21** (DMSO- d_6).

Position	^1H [ppm] (int., mult., J [Hz])	^{13}C [ppm]	COSY	HMBC
2	8.91 (1H, s)	152.6	-	4, 8
4		153.0		
5	7.99 (1H, s)	115.9	-	4, 6, 8, 9, 10
6		141.2		
8		168.2		
9		129.2		
10		120.3		
11	8.03 (1H, dd, 1.2/8.0)	128.9	12, 13	13, 15
12	7.13 (1H, t, 7.6)	121.3	11, 13, 14	10, 11, 14
13	7.53-7.46 (1H, m)	131.5	11, 12, 14	11, 15
14	7.26 (1H, d, 8.4)	112.6	12, 13	12, 15
15		155.9		
16	4.00 (3H, s)	56.0	-	15

3.5.10 Characterisation of Compound 15a

The structure of compound **15a** with numbering of positions is given in Figure 3.23. The melting point of **15a** was found to be 223-233 °C (dec.).

MS

High resolution mass spectroscopy gave m/z 358.1010 $[M+H]^+$ for compound **15a**. With a calculated value of 358.1014, the molecular formula $C_{22}H_{15}N_3O_2S$ was confirmed with an accuracy of 1.1 ppm.

NMR

The findings from the 1H - and ^{13}C -NMR analyses are presented in Table 3.20.

No problems were encountered during the assigning of shifts, but comparison with shift values in other compounds was useful as to separate carbons 20 and 23.

IR, MS and NMR spectra for compound **15a** are given in Appendix M.

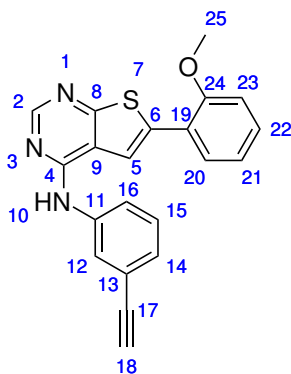


Figure 3.23: Numbering of positions in compound **15a**.

Table 3.20: ^1H - and ^{13}C -NMR data for compound **15a** (DMSO- d_6).

Position	^1H [ppm] (int., mult., J [Hz])	^{13}C [ppm]	COSY	HMBC
2	8.67-8.62 (1H, m)	151.3	-	4, 8
4		154.1		
5	8.67-8.62 (1H, m)	117.4	-	4, 6, 8, 9, 19
6		135.9		
8		162.9		
9		117.4		
10	10.45 (1H, s)	N	-	4
11		139.0		
12	8.11-8.08 (1H, m)	124.6	16	11, 13, 17
13		122.4		
14	7.29-7.22 (1H, m)	129.1	15	17
15	7.47-7.41 (1H, m)	127.9	14, 16	11
16	7.97-7.91 (1H, m)	122.7	15	12
17		83.4		
18	4.21 (1H, s)	80.8	-	13, 17
19		121.3		
20	7.86-7.82 (1H, m)	127.1	21	22, 24
21	7.14 (1H, t, 7.6)	121.1	20, 22	20, 23
22	7.47-7.41 (1H, m)	130.3	21	20, 21, 23, 24
23	7.29-7.22 (1H, m)	112.6	22	6, 24
24		155.8		
25	3.99 (3H, s)	56.0	-	24

3.5.11 Characterisation of Compound **15b**

The structure of compound **15b** with numbering of positions is given in Figure 3.24. The melting point of **15b** was found to be 221-225 °C.

MS

High resolution mass spectroscopy gave m/z 386.0959 $[M+H]^+$ for compound **15b**. With a calculated value of 386.0963, the molecular formula $C_{22}H_{15}N_3O_2S$ was confirmed with an accuracy of 1.0 ppm.

NMR

The findings from the 1H - and ^{13}C -NMR analyses are presented in Table 3.21.

The NMR-sample was slightly weak, causing few observed correlations in the long distance 1H - ^{13}C spectrum (HMBC). This made the assignment of shifts more difficult, specially for the tertiary carbons situated in the molecular core (C-4, C-6, C-9 and C-19). Assignment of these shifts was possible due to comparable shift values in the similar compounds synthesized. Carbons 9, 13 and 19 were the last shifts to be assigned. Carbon 13 was identified due to lack of long range coupling to C-5, which was present for both C-9 and C-19.

IR, MS and NMR spectra for compound **15b** are given in Appendix N.

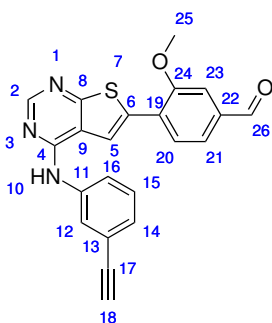


Figure 3.24: Numbering of positions in compound **15b**.

Table 3.21: ^1H - and ^{13}C -NMR data for compound **15b** (DMSO- d_6).

Position	^1H [ppm] (int., mult., J [Hz])	^{13}C [ppm]	COSY	HMBC
2	8.60-8.54 (1H, m)	153.6	-	
4		154.3		
5	8.12-8.10 (1H, m)	123.9	-	
6		127.2		
8		167.1		
9		117.1		
10	9.82 (1H, s)	N	-	
11		139.5		
12	8.60-8.54 (1H, m)	119.1	-	
13		121.9		
14	7.23 (1H, d, 7.6)	126.4	15	
15	7.46-7.40 (1H, m)	129.1	14, 16	11, 16
16	7.92-7.88 (1H, m)	121.7	15	
17		83.5		
18	4.22 (1H, s)	80.7	-	
19		133.7		
20	8.05-8.01 (1H, m)	128.4	21	22, 24
21	7.74-7.70 (1H, m)	122.8	20	
22		136.9		
23	7.74-7.70 (1H, m)	112.2	-	21
24		155.8		
25	4.09 (3H, s)	56.2	-	24
26	10.05 (1H, s)	192.2	-	22

3.5.12 Characterisation of Compound **15c**

The structure of compound **15c** with numbering of positions is given in Figure 3.25. The melting point of **15c** was found to be 217-220 °C.

MS

High resolution mass spectroscopy gave m/z 388.1113 $[M+H]^+$ for compound **15c**. With a calculated value of 388.1120, the molecular formula $C_{22}H_{17}N_3O_2S$ was confirmed with an accuracy of 1.8 ppm.

NMR

The findings from the 1H - and ^{13}C -NMR analyses are presented in Table 3.22.

The assignment was performed without any problems. Long range 1H - ^{13}C couplings were used to place the quaternary carbons.

IR, MS and NMR spectra for compound **15c** are given in Appendix O.

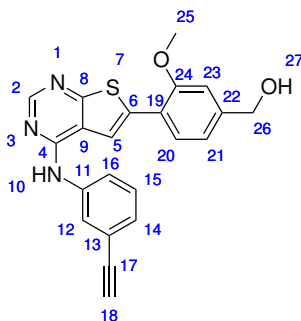


Figure 3.25: Numbering of positions in compound **15c**.

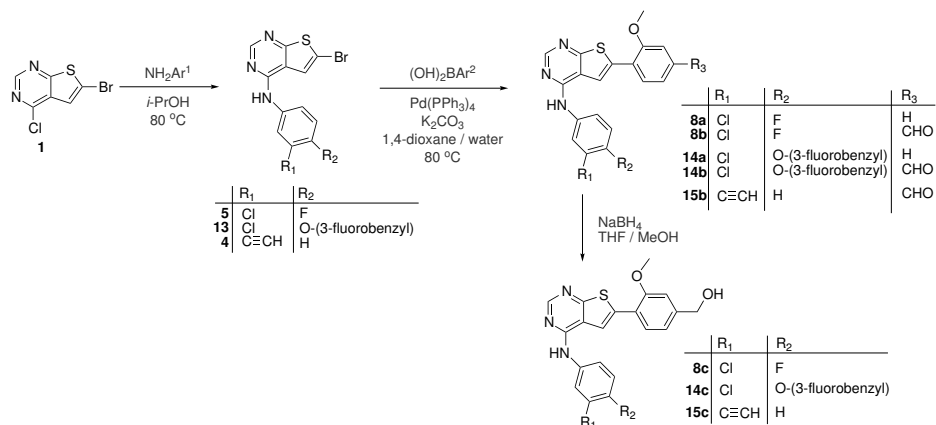
Table 3.22: ^1H - and ^{13}C -NMR data for compound **15c** ($\text{DMSO-}d_6$).

Position	^1H [ppm] (int., mult., J [Hz])	^{13}C [ppm]	COSY	HMBC
2	8.53 (1H, s)	152.9	-	4, 8
4		153.9		
5	8.33 (1H, s)	116.2	-	4, 6, 8, 9, 19
6		135.5		
8		166.4		
9		117.2		
10	9.68 (1H, s)	N	-	4, 12
11		139.7		
12	8.12-8.08 (1H, m)	123.7	-	
13		121.9		
14	7.23-7.17 (1H, m)	126.2	15	12, 15, 16, 17, 18
15	7.41 (1H, t, 8.0)	129.1	14, 16	11, 16
16	7.93-7.89 (1H, m)	121.5	15	12
17		83.5		
18	4.21 (1H, s)	80.6	-	
19		119.8		
20	7.74 (1H, d, 8.0)	127.7	21	6, 22, 24
21	7.09 (1H, d, 8.8)	119.0	20	19, 23, 26
22		145.2		
23	7.23-7.17 (1H, m)	110.2	-	19
24		155.6		
25	3.98 (3H, s)	55.8	-	24
26	4.57 (1H, d, 5.6)	62.6	27	21, 22, 23
27	5.33 (1H, t, 5.6)	O	26	22, 26

4 Conclusion

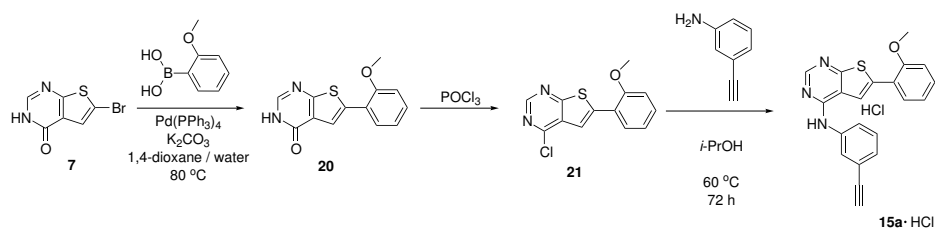
In this master's thesis a fragment based approach was applied in the identification of new active epidermal growth factor receptor tyrosine kinase inhibitors (EGFR TKIs). Using a thienopyrimidine as core molecular scaffold, aniline fragments found in the commercially available TKIs Gefitinib, Erlotinib and Lapatinib were combined with potency inducing fragments identified by the research group, to yield the new inhibitors.

The compounds were synthesized from the starting material **1** using a thermal amination followed by a Suzuki coupling reaction. Compounds **8c**, **14c** and **15c** were obtained by reducing the formyl group in **8b**, **14b** and **15b**, respectively. The synthesis route is illustrated below. The aniline used in the syntheses of **13** was also made in this thesis, and two different methods were investigated for synthesizing this aniline. The building blocks **4** and **5** were synthesized in the pre-project preceding this thesis, but used for further syntheses in this work.



Due to problems with dimerization, compound **15a** was synthesized using a different route, starting from **7**. Although including more steps, this route was found beneficial for synthesis of the Erlotinib fragment containing compound. High purity of **15a** was obtained as a result of eased purification preliminary to the amination step. Due to problematic purification, high purities were not obtained for the other target compounds in this series (**15b** and **15c**), thus an

alternative route of synthesis might be better for these compounds as well.



In vitro enzymatic inhibition testing of compounds obtained in high purity was performed. Although some key values were missing, the results indicated a structure-activity relationship that coincided with the method of fragment based drug design; combination of potent substituents led to increased potency for the resulting compound. However, the potencies did not increase as much as seen for other compounds synthesized in the group. This indicated a changed binding of the compound in the active site due to altered amine structure compared to the other compounds synthesized in the group. Target compounds based on the Lapatinib aniline fragment (**14b-c**) were identified as potential lead compounds in the search for new HER2 inhibitors.

The work performed in this thesis has contributed to the group's ongoing structure-activity relationship study, and some very potent TKIs have been identified. In addition, the concept of fragment based drug design has been investigated. This appears to be valid for the synthesized compounds, though missing inhibition data makes the attainment of this study limited.

5 Future Work

Several of the compounds synthesized in this thesis were found to be highly potent EGFR tyrosine kinase inhibitors. However, inhibition results were not obtained for all compounds. It is desirable to have the remaining compounds **13**·HCl, **15b** and **15c** tested to complete the fragment-activity study and possibly support the observed activity trend. Assuming this fragment-activity trend is followed, compound **15c**, will be the most potent of the compounds synthesized in this thesis. Obtaining inhibition results for **15c** is thus of high interest.

Since the Erlotinib based compounds were found to be highly potent, a reliable and efficient route of synthesis is desirable. Given the dimerization problems encountered for **15a** using standard conditions, altering the reaction conditions could be investigated. Since dimerization did not occur in the Suzuki reaction yielding **15b**, only small changes in the applied conditions might be needed, and changing the catalyst can be a good place to start. A more active catalyst might favour the Suzuki coupling to dimerization. Electron rich ligands such as dialkylbiaryl phosphines, are known to increase efficiency and selectivity in this cross-coupling reaction.⁹⁰ Reduced reaction times also minimizes the formation of by-products such as **16**.

However, since the palladium catalyst was found to be involved in the dimerization, alternative routes of synthesis could be preferential. Methods of introducing the ethynyl group subsequent to Suzuki coupling (e.g. as described by Beckers *et al.*⁴⁷) could be explored. This way all contact between the ethynyl substituent and palladium catalyst is avoided.

Combining the Erlotinib fragment with other potent C-6 aryls could lead to more potent target molecules. It was observed that the hydroxymethyl group did not increase compound potency as much as expected, and it is assumed this is a result of changed binding in the active site. Therefore, it would be interesting to see the effects of altering the position of this group, as illustrated in Figure 5.1. More favourable interactions in the active site could be obtained, thereby increasing inhibition potency.

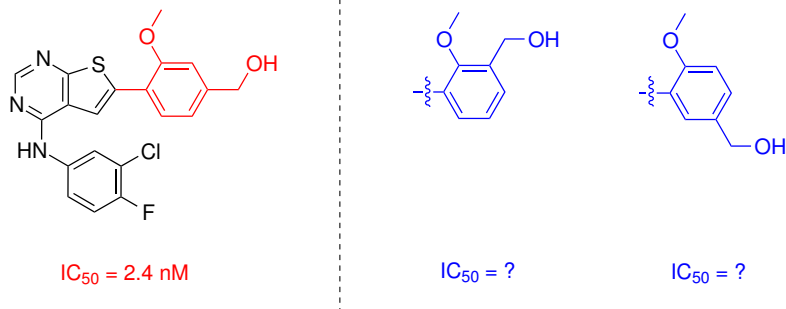


Figure 5.1: Changing the substitution pattern will affect interactions in the active site, and thereby alter potency.

The Lapatinib fragment based compounds **14b** and **14c** were found to have inhibition activity towards HER2. These compounds can be used as lead compounds in a structure-based search for new HER2 inhibitors.

Further on, improving the solubility properties and reducing toxicity of the compounds is advisable as to making them more suited as drugs. A solubilizing tail on the aryl substituent might increase the bioavailability of the compounds, and substitution with fluorine can be used to block undesirable metabolism (Figure 5.2).

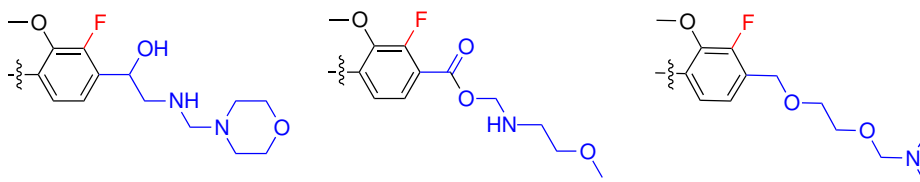


Figure 5.2: Introduction of fluorine can block undesirable metabolism and a solubilizing tail can increase bioavailability, making the compounds more suited as drugs.

Crystallization was the most used method of purification in this thesis. Pure compounds was mostly obtained, but the yields were at times very low. By optimizing the crystallization conditions in each reaction, the yields could be improved.

6 Experimental

6.1 General Information

Besides the building blocks **1**, **4**·HCl, **5**·HCl and **7** which previously had been synthesized in house, all reagents and solvents used are commercially available and were purchased from Sigma-Aldrich, VWR or Combi-Blocks. The purchased materials were of analytical quality and were used without further purification. Distilled water was used, and all reactions were stirred using a teflon coated magnetic stirrer. Temperatures above room temperature were regulated using an oil-bath. A risk assessment evaluation of the performed laboratory work is given in Appendix P.

6.1.1 Separation techniques

All reactions were monitored by thin layer chromatography (TLC; silica gel on aluminium plates, F_{254} , Merck). UV light (wave length 254 nm and 365 nm) was used for visualizing the plates. TLC was also used to find optimal separation conditions for column chromatography, and to tell apart fractions containing product from those containing impurities. Silica gel (40-63 mesh, 60 Å) was used as stationary phase for column chromatography, with eluent systems as described for each separation.

6.1.2 Chromatographic and spectroscopic analyses

HPLC analyses were performed using an Agilent 1100-Series instrument with a G1379A Degasser, G1311A Quatpumpe, G1313A ALS autosampler and a Agilent G1315D diode array detector. The software used was Agilent ChemStation. Spectra were recorded for wave lengths of 230 nm, 254 nm and 280 nm. A Poroshell C18 column (4.6 x 100 mm) was used, with a flow of 0.8 mL/min starting with H₂O/ACN (90:10)-(0:100) over 25 min, followed by 20 min of 100% ACN.

Infrared absorption spectra were recorded on a FTIR Thermo Nicolet Nexus FT-IR Spectrometer, using a Smart Endurance reflection cell. Frequencies between 4000-400 cm^{-1} are reported. Peaks are described as w (weak), m (medium), s (strong) and br (broad).

Accurate mass determination in positive and negative mode was performed on a "Synapt G2-S" Q-TOF instrument from Waters. Samples were ionized by use of an ASAP probe. No chromatography separation was used prior to the mass analyses.

1H and ^{13}C -NMR spectra were recorded using a Bruker Avance instrument operating at 400 MHz for 1H NMR and 100 MHz for ^{13}C NMR. ^{19}F -NMR analyses were performed on a Bruker Avance 500 operating at 564 MHz. Solvent used was DMSO- d_6 . Chemical shifts for 1H and ^{13}C are reported as δ [ppm] relative to DMSO- d_6 which is 2.50 ppm and 39.52 ppm for 1H and ^{13}C respectively, while shift values in ^{19}F -NMR are relative to hexafluorobenzene (-164.9 ppm). When using DMSO- d_6 as solvent, trace amounts of water can always be seen in 1H NMR at 3.33 ppm. Coupling constants (J) are reported in Hz. Peaks are described according to their multiplicity; s (singlet), d (doublet), dd (doublet of doublets), t (triplet), br (broad) and m (multiplet). For compounds isolated as HCl salts, all analyses were performed with the compound on this form, unless otherwise stated. The assignment of 1H and ^{13}C shifts have been done according to the numbering of the structures given in Section 3.5.

6.1.3 Melting point

Melting points were recorded using a Stuart automatic melting point SMP40 instrument (3 $^{\circ}C/min$).

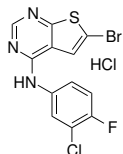
6.1.4 *In vitro* EGFR inhibition testing

The activity measurements of the compounds against EGFR were performed by Invitrogen (LifeTechnologies) using their Z'-LYTE[®] assay technology. The compounds were supplied in a 10 mM DMSO solution and tested for their inhibition

activity at 100 nM, in duplicate measurements. Some of the compounds were also subjected to a duplicate 10 points titration, using an ATP concentration equal to K_m . IC_{50} values were calculated from these data with a fourparameter logistic model, using SigmaPlot (Windows Version 11.0 from Systat Software, Inc.)

6.2 Synthetic Procedures

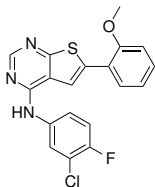
6.2.1 Purification of 6-bromo-*N*-(3-chloro-4-fluorophenyl)thieno[2,3-*d*]pyrimidine-4-amine·HCl (**5**·HCl)



Compound **5**·HCl⁵⁴ (3.21 g, HPLC-purity: 85%) was boiled in *n*-pentane (100 mL) for a few minutes, hot filtered and dried under reduced pressure. This yielded 3.01 g (7.62 mmol, 94%) of **5**·HCl as a greenish yellow solid, mp. 264-266 °C. HPLC-purity: 98%, $t_R = 29.5$ min.

Spectroscopic data for compound **5**·HCl (Appendix A): ¹H-NMR (400 MHz, DMSO-*d*₆) δ : 9.98 (s, 1H, NH), 8.54 (s, 1H, H-2), 8.23-8.17 (m, 2H, H-5/H-12), 7.83-7.77 (m, 1H, H-16), 7.47-7.40 (m, 1H, H-15); ¹³C-NMR (100 MHz, DMSO-*d*₆) δ : 167.1 (C-8), 153.4 (C-2), 153.2 (d, $J=242.9$, C-14), 152.0 (C-4), 136.3 (d, $J=2.9$, C-11), 122.9 (C-5), 122.6 (C-12), 121.5 (d, $J=7.1$, C-16), 118.9 (d, $J=18.3$, C-13), 117.9 (C-9), 116.8 (d, $J=21.9$, C-15), 111.3 (C-6). The data corresponds with that reported previously.⁵⁴

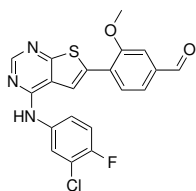
6.2.2 Synthesis of *N*-(3-chloro-4-fluorophenyl)-6-(2-methoxyphenyl)thieno[2,3-*d*]pyrimidin-4-amine (**8a**)



Compound **5**·HCl (200 mg, 0.506 mmol) was mixed with (2-methoxyphenyl)boronic acid (92 mg, 0.607 mmol, 1.2 eq.), Pd(PPh₃)₄ (6 mg, 5.2 μ g, 0.01 eq.) and K₂CO₃ (210 mg, 1.52 mmol, 3 eq.). Water (2 mL) and 1,4-dioxane (2 mL) was added under nitrogen atmosphere, and the mixture was agitated at 80 °C for 3 h. After cooling to rt, the reaction mixture was diluted with water (50 mL), filtered and the obtained product was dried under reduced pressure. The crude product (152 mg, 78%) was purified by crystallization from THF (5 mL), yielding 50 mg (0.130 mmol, 26%) of **8a** as a yellow solid, mp. 243-245 °C. HPLC-purity: 98%, $t_R = 32.4$ min.

Spectroscopic data for **8a** (Appendix B): $^1\text{H-NMR}$ (400 MHz, $\text{DMSO-}d_6$) δ : 9.79 (s, 1H, NH), 8.54 (s, 1H, H-2), 8.31 (s, 1H, H-5), 8.24 (dd, $J=6.8, 2.8$, 1H, H-12), 7.83-7.76 (m, 2H, H-16/H-18), 7.49-7.41 (m, 2H, H-15/H-20), 7.24 (d, $J=8.0$, 1H, H-21), 7.14 (t, $J=7.6$, 1H, H-19), 3.98 (s, 3H, H-23); $^{13}\text{C-NMR}$ (100 MHz, $\text{DMSO-}d_6$) δ : 166.5 (C-8), 154.26 (C-22), 154.25 (d, $J=242.8$, C-14), 153.8 (C-2), 151.8 (C-4), 136.7 (d, $J=3.6$, C-11), 135.5 (C-6), 130.2 (C-20), 128.0 (C-18), 122.4 (C-17), 121.3 (C-12), 121.24 (d, $J=6.8$, C-16), 121.20 (C-19), 118.9 (d, $J=18.4$, C-13), 117.1 (C-9), 116.7 (d, $J=22.0$, C-15), 116.6 (C-5), 112.6 (C-21), 55.9 (C-23); $^{19}\text{F-NMR}$ (564 MHz, $\text{DMSO-}d_6$, C_6F_6) δ : -125.70 (s, dec.); IR (cm^{-1}) ν : 3271 (w, br), 1249 (m), 1204 (m), 1021 (m), 744 (m); HRMS (ASAP+, m/z): detected 386.0525, calculated for $\text{C}_{19}\text{H}_{14}\text{N}_3\text{OFSCl}$ $[\text{M}+\text{H}]^+$ 386.0530.

6.2.3 Synthesis of 4-(4-((3-chloro-4-fluorophenyl)amino)thieno[2,3-*d*]pyrimidin-6-yl)-3-methoxybenzaldehyde (**8b**)



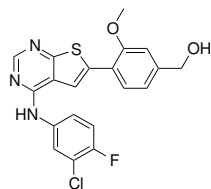
Compound **8b** was synthesized as described in Section 6.2.2, using **5**·HCl (500 mg, 1.27 mmol), (4-formyl-2-methoxyphenyl)boronic acid (273 mg, 1.52 mmol, 1.2 eq.), $\text{Pd}(\text{PPh}_3)_4$ (15 mg, 13 μmol , 0.01 eq.) and K_2CO_3 (525 mg, 3.80 mmol, 3 eq.). Crystallization from THF (29 mL), using toluene (15 mL) as anti-solvent, yielded 175 mg (0.423 mmol, 34%) of **8b** as a curry coloured solid, mp. 252-254 °C. HPLC-

purity: 98%, $t_R = 31.3$ min.

Spectroscopic data for **8b** (Appendix C): $^1\text{H-NMR}$ (400 MHz, $\text{DMSO-}d_6$) δ : 10.04 (s, 1H, H-24), 9.87 (s, 1H, NH), 8.56 (s, 1H, H-2), 8.50 (s, 1H, H-5), 8.22 (dd, $J=6.8, 2.8$, 1H, H-12), 8.02-7.98 (m, 1H, H18), 7.83-7.78 (m, 1H, H-16), 7.73-7.67 (m, 2H, H-19/H-21), 7.50-7.43 (m, 1H, H-15), 4.08 (s, 3H, H-23); $^{13}\text{C-NMR}$ (100 MHz, $\text{DMSO-}d_6$) δ : 192.2 (C-24), 167.1 (C-8), 155.8 (C-22), 154.1 (C-4), 153.5 (C-2), 153.2 (d, $J=242.6$, C-14), 136.9 (C-20), 136.5 (d, $J=3.0$, C-11), 133.9 (C-17), 128.4 (C-18), 127.2 (C-6), 122.8 (C-19), 122.6 (C-12), 121.4 (d, $J=7.1$, C-16), 118.97 (d, $J=18.6$, C-13), 118.96 (C-5), 117.0 (C-9), 116.8 (d, $J=21.9$, C-15), 112.2 (C-21), 56.2 (C-23); $^{19}\text{F-NMR}$ (564 MHz, $\text{DMSO-}d_6$, C_6F_6) δ : -125.40 (s, dec.); IR (cm^{-1}) ν : 3357 (w, br), 1674 (s), 1267 (m), 1199 (m), 775

(s); HRMS (ASAP+, m/z): detected 414.0471, calculated for $C_{20}H_{14}N_3O_2FSCl$ $[M+H]^+$ 414.0479.

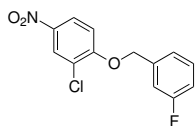
6.2.4 Synthesis of (4-(4-((3-chloro-4-fluorophenyl)amino)thieno[2,3-*d*]pyrimidin-6-yl)-3-methoxyphenyl)methanol (**8c**)



Compound **8b** (120 mg, 0.290 mmol) was dissolved in MeOH (2.5 mL) and THF (7.5 mL), and $NaBH_4$ (11 mg, 0.290 mmol, 1 eq.) was added. The reaction mixture was stirred for 30 min before additional $NaBH_4$ (11 mg, 0.290 mmol, 1 eq.) was added. The mixture was stirred for another 30 min, and concentrated to about 5 mL. The residue was diluted with EtOAc (100 mL) and washed with water (2x50 mL). The organic layer was washed with brine (50 mL), dried over anhydrous Na_2SO_4 , filtered and concentrated. This yielded a crude product of 113 mg (93%), crystallization from DMF (2 mL) gave **8c** in 89 mg (0.214 mmol, 74%) yield as a pale yellow solid, mp. 257-259 °C. HPLC-purity > 99%, t_R = 27.2 min.

Spectroscopic data for **8c** (Appendix D): 1H -NMR (400 MHz, $DMSO-d_6$) δ : 9.77 (s, 1H, NH), 8.53 (s, 1H, H-2), 8.29 (s, 1H, H-5), 8.23 (dd, $J=6.8, 2.8$, 1H, H-12), 7.84-7.78 (m, 1H, H-16), 7.73 (d, $J=8.0$, 1H, H-18), 7.46 (t, $J=8.0$, 1H, H-15), 7.18 (s, 1H, H-21), 7.09 (d, $J=8.0$, 1H, H-19), 5.33 (t, $J=5.6$, 1H, OH), 4.57 (d, $J=5.6$, 2H, H-24), 3.98 (s, 3H, H-23); ^{13}C -NMR (100 MHz, $DMSO-d_6$) δ : 166.3 (C-8), 155.5 (C-22), 153.7 (C-2), 153.0 (d, $J=242.8$, C-14), 152.8 (C-4), 145.3 (C-20), 136.7 (d, $J=3.0$, C-11), 135.7 (C-6), 127.7 (C-18), 123.3 (C-12), 121.2 (d, $J=7.0$, C-16), 119.8 (C-17), 119.0 (C-19), 118.9 (d, $J=18.3$, C-13), 117.1 (C-9), 116.7 (d, $J=21.5$, C-15), 116.0 (C-5), 110.2 (C-21), 62.5 (C-24), 55.8 (C-23); ^{19}F -NMR (564 MHz, $DMSO-d_6$, C_6F_6) δ : -125.75 (s, dec.); IR (cm^{-1}) ν : 3313 (w, br), 2862 (w, br), 1512 (s), 1199 (m), 776 (m); HRMS (ASAP+, m/z): detected 416.0630, calculated for $C_{20}H_{16}N_3O_2FSCl$ $[M+H]^+$ 416.0636.

6.2.5 Synthesis of 2-chloro-1-((3-fluorobenzyl)oxy)-4-nitrobenzene (**11**)

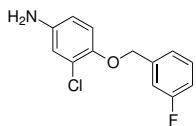


The synthesis was performed as described by Shiao *et al.*¹⁰⁷ for similar compounds. The work-up was performed as described by Fontana *et al.*¹⁰⁸

2-Chloro-4-nitrophenol (**9**) (1.50 g, 8.64 mmol) was mixed with K_2CO_3 (3.58 g, 25.9 mmol, 3 eq.), before DMF (90 mL) was added under nitrogen atmosphere. The mixture was heated to 75 °C, and 3-fluorobenzyl chloride (**10**) (1.87 g, 13.0 mmol, 1.5 eq.) dissolved in DMF (60 mL) was added slowly. The reaction mixture was stirred at 75 °C for 23 h, cooled to rt, poured into cold water (150 mL, < 5 °C) and filtered. The isolated solid was washed with an ACN:water mixture (1:1, 50 mL), and followingly with *n*-hexane (30 mL). The obtained white solid was dried under reduced pressure. This yielded 1.29 g (4.58 mmol, 53%) of **11** as a white solid, mp. 90-96 °C.

Spectroscopic data for **11** (Appendix E): 1H -NMR (400 MHz, DMSO- d_6) δ : 8.35 (d, $J=2.8$, 1H), 8.25 (dd, $J=8.8$, 2.8, 1H), 7.52-7.44 (m, 2H), 7.35-7.30 (m, 2H), 7.24-7.17 (m, 1H), 5.42 (s, 2H); ^{13}C -NMR (100 MHz, DMSO- d_6) δ : 162.2 (d, $J=243.7$), 158.6, 140.9, 138.4 (d, $J=8.1$), 130.7 (d, $J=8.1$), 125.4, 124.6, 123.5 (d, $J=2.9$), 122.0, 115.1 (d, $J=20.6$), 114.3 (d, $J=22.0$), 113.8, 70.1 (d, $J=2.1$); ^{19}F -NMR (564 MHz, DMSO- d_6 , C_6F_6) δ : -115.15 (s, dec.). 1H -NMR findings are in accordance with literature.¹⁰⁹

6.2.6 Synthesis of 3-chloro-4-((3-fluorobenzyl)oxy)aniline (**12**)



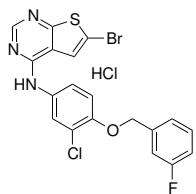
The synthesis was performed as described by Fontana *et al.*¹⁰⁸

Compound **11** (1.29 g, 4.57 mmol) was mixed with NH_4Cl (2.2 g, 41.2 mmol, 9 eq.) and iron powder (766 mg, 13.7 mmol, 3 eq.), before EtOH (19 mL) and water (4.5 mL) were added under nitrogen atmosphere. The reaction mixture was stirred at 78 °C for 3 h, cooled to rt, filtered through celite using a mixture of EtOH and water (4:1), and concentrated. The reaction residue was extracted with hot DCM (60 mL) and filtered. The filtrate was concentrated and dried under

reduced pressure. This yielded 1.05 g (4.17 mmol, 91%) of a sparkling greyish brown solid.

Spectroscopic data for **12** (Appendix F): $^1\text{H-NMR}$ (400 MHz, $\text{DMSO-}d_6$) δ : 7.46-7.39 (m, 1H), 7.28-7.23 (m, 2H), 7.17-7.11 (m, 1H), 6.91 (d, $J=8.8$, 1H), 6.65 (d, $J=2.4$, 1H), 6.46 (dd, $J=8.8$, 2.8, 1H), 5.03 (s, 2H), 4.94 (s, 2H); $^{13}\text{C-NMR}$ (100 MHz, $\text{DMSO-}d_6$) δ : 162.1 (d, $J=243.8$), 144.1, 140.3 (d, $J=7.4$), 130.3 (d, $J=8.1$), 123.3 (d, $J=2.8$), 122.5, 116.9, 114.9, 114.4 (d, $J=21.1$), 113.9 (d, $J=21.5$), 113.2, 70.3 (d, $J=1.7$); $^{19}\text{F-NMR}$ (564 MHz, $\text{DMSO-}d_6$, C_6F_6) δ : -115.61 (s, dec.). $^1\text{H-NMR}$ findings are in accordance with literature.¹⁰⁹ The carbon holding the amine group was not detected.

6.2.7 Synthesis of 6-bromo-*N*-(3-chloro-4-((3-fluorobenzyl)oxy)phenyl)thieno[2,3-*d*]pyrimidin-4-amine·HCl (**13**·HCl)

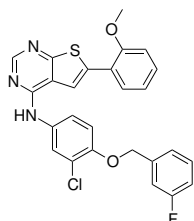


Compound **1** (867 mg, 3.48 mmol) was mixed with **12** (1.05 g, 4.17 mmol, 1.2 eq.), before *i*-PrOH (140 mL) was added under nitrogen atmosphere. The reaction mixture was agitated at 80 °C for 16 h, cooled to rt and concentrated. The reaction residue was triturated with *n*-pentane (250 mL) and filtered to yield the crude product (1.60 g, 92%). A fraction of the crude product (400 mg) was purified by crystallization from DMF (2 mL) using water (1 mL) as anti-solvent. This yielded 216 mg (0.431 mmol, 50%) of compound **13** as a grey crystal, mp. 221-226 °C. HPLC-purity: 99%, t_R = 30.6 min.

Spectroscopic data for **13**·HCl (Appendix G): $^1\text{H-NMR}$ (400 MHz, $\text{DMSO-}d_6$) δ : 9.73 (s, 1H, NH), 8.49 (s, 1H, H-2), 8.08 (s, 1H, H-5), 8.05-8.00 (m, 1H, H-15), 7.70-7.64 (m, 1H, H-16), 7.50-7.43 (m, 1H, H-22), 7.35-7.24 (m, 3H, H-12/H-19/H-23), 7.21-7.14 (m, 1H, H-21), 5.24 (s, 2H, H-17); $^{13}\text{C-NMR}$ (100 MHz, $\text{DMSO-}d_6$) δ : 165.8 (C-8), 162.2 (d, $J=243.7$, C-20), 153.3 (C-2), 152.9 (C-4), 149.7 (C-14), 139.6 (d, $J=7.4$, C-18), 132.7 (C-11), 130.6 (d, $J=8.6$, C-22), 123.35 (C-15), 123.32 (d, $J=3.0$, C-23), 123.1 (C-5), 121.6 (C-16), 121.2 (C-13), 117.7 (C-9), 114.7 (d, $J=21.1$, C-21), 114.5 (C-12), 114.0 (d, $J=21.9$, C-19), 111.1 (C-

6), 69.4 (d, $J=1.5$, C-17); ^{19}F -NMR (564 MHz, DMSO- d_6 , C_6F_6) δ : -115.34 (s, dec.); IR (cm^{-1}) ν : 3051 (w, br), 2394 (w, br), 1273 (s), 1199 (s), 805 (m); HRMS (ASAP+, m/z): detected 463.9635, calculated for $\text{C}_{19}\text{H}_{13}\text{N}_3\text{OFSClBr}$ $[\text{M}+\text{H}]^+$ 463.9635.

6.2.8 Synthesis of *N*-(3-chloro-4-((3-fluorobenzyl)oxy)phenyl)-6-(2-methoxyphenyl)thieno[2,3-*d*]pyrimidin-4-amine (**14a**)

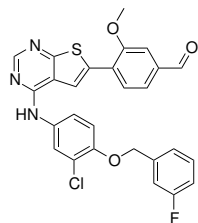


Compound **14a** was prepared as described in Section 6.2.2, using **13**·HCl (200 mg, 0.399 mmol), (2-methoxyphenyl)boronic acid (73 mg, 0.479 mmol, 1.2 eq.), $\text{Pd}(\text{PPh}_3)_4$ (5 mg, 4.3 μg , 0.01 eq.) and K_2CO_3 (165 mg, 1.20 mmol, 3 eq.). Purification by column chromatography (1:4 *n*-pentane:Et₂O, $R_f=0.22$) yielded 132 mg (67%) of **14a**, HPLC-purity: 91%. Following, a fraction of the product (112 mg) was crystallized from 1,4-dioxane (4 mL). The obtained white solid was dried under reduced pressure. Trace amounts of 1,4-dioxane was removed by repeatedly adding DCM (3x5mL) to the product, shaking the mixture for a few minutes in an ultrasound bath and concentrating. This gave the desired compound **14a** in 44 mg (0.089 mmol, 26%) yield, mp. 163-165 °C. HPLC-purity: 97%, $t_R = 35.1$ min.

Spectroscopic data for **14a** (Appendix H): ^1H -NMR (400 MHz, DMSO- d_6) δ : 9.49 (s, 1H, NH), 8.49 (s, 1H, H-2), 8.29 (s, 1H, H-5), 8.06 (d, $J=2.4$, 1H, H-15), 7.77 (dd, $J=7.6$, 1.6, 1H, H-25), 7.72 (dd, $J=9.2$, 2.4, 1H, H-16), 7.51-7.40 (m, 2H, H-22 / H-27), 7.36-7.10 (m, 6H, H-12/H-19/H-21/H-23/H-26/H-28), 5.24 (s, 2H, H-17), 3.97 (s, 3H, H-30); ^{13}C -NMR (100 MHz, DMSO- d_6) δ : 166.3 (C-8), 162.2 (d, $J=244.2$, C-20), 155.6 (C-29), 154.0 (C-4), 153.1 (C-2), 149.3 (C-14), 139.7 (d, $J=7.4$, C-18), 135.2 (C-6), 133.4 (C-11), 130.6 (d, $J=8.0$, C-22), 130.1 (C-27), 128.0 (C-25), 123.3 (d, $J=3.0$, C-23), 123.0 (C-15), 121.5 (C-13), 121.20 (C-16), 121.18 (C-26), 121.1 (C-24), 116.9 (C-9), 116.7 (C-5), 114.7 (d, $J=21.0$, C-21), 114.5 (C-12), 114.0 (d, $J=21.9$, C-19), 112.6 (C-28), 69.4 (d, $J=2.2$, C-17), 55.9 (C-30); ^{19}F -NMR (564 MHz, DMSO- d_6 , C_6F_6) δ : -115.39 (s, dec.); IR (cm^{-1}) ν : 3043 (w, br), 1610 (m), 1250 (s), 1024 (m), 755 (s); HRMS (ASAP+,

m/z): detected 492.0946, calculated for C₂₆H₂₀N₃O₂SClF [M+H]⁺ 492.0949.

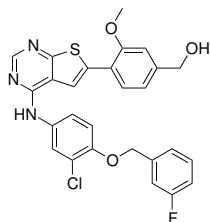
6.2.9 Synthesis of 4-(4-((3-chloro-4-((3-fluorobenzyl)oxy)phenyl)amino)thieno[2,3-*d*]pyrimidin-6-yl)-3-methoxybenzaldehyd (**14b**)



Compound **14b** was prepared as described in Section 6.2.2 using compound **13**·HCl (500 mg, 0.998 mmol), (4-formyl-2-methoxyphenyl)boronic acid (215 mg, 1.20 mg, 1.2 eq.), Pd(PPh₃)₄ (12 mg, 9.98 μmol, 0.01 eq.). Crystallization from THF (12 mL) using *n*-pentane (11 mL) as anti-solvent yielded 295 mg (0.567 mmol, 57%) of a bright yellow solid **14b**, mp. 217-220 °C. HPLC-purity: 97%, *t*_R = 34.2 min.

Spectroscopic data for **14b** (Appendix I): ¹H-NMR (400 MHz, DMSO-*d*₆) δ: 10.04 (s, 1H, H-31), 9.74 (s, 1H, NH), 8.51-8.47 (m, 2H, H-2/H-5), 8.07-8.03 (m, 1H, H-15), 8.02-7.97 (m, 1H, H-25), 7.74-7.68 (m, 3H, H-16/H-26/H-28), 7.51-7.43 (m, 1H, H-22), 7.35-7.25 (m, 3H, H-12/H-19/H-23), 7.23-7.15 (m, 1H, H-21), 5.25 (s, 2H, H-17), 4.08 (s, 3H, H-30); ¹³C-NMR (100 MHz, DMSO-*d*₆) δ: 192.2 (C-31), 166.9 (C-8), 162.2 (d, *J*=243.7, C-20), 155.8 (C-29), 154.3 (C-4), 153.7 (C-2), 149.4 (C-14), 139.6 (d, *J*=7.3, C-18), 136.8 (C-27), 133.5 (C-24), 133.2 (C-11), 130.5 (d, *J*=8.3, C-22), 128.4 (C-25), 127.2 (C-6), 123.3 (d, *J*=2.5, C-23), 123.0 (C-15), 122.8 (C-26), 121.21 (C-13), 121.19 (C-16), 119.1 (C-5), 116.9 (C-9), 114.7 (d, *J*=21.1, C-21), 114.5 (C-12), 114.0 (d, *J*=21.9, C-19), 112.2 (C-28), 69.4 (d, *J*=2.0, C-17), 56.2 (C-30); ¹⁹F-NMR (564 MHz, DMSO-*d*₆, C₆F₆) δ: -115.38 (s, dec.); IR (cm⁻¹) ν: 3380 (w, br), 1682 (m), 1260 (m), 1030 (m), 779 (s); HRMS (ASAP+, m/z): detected 520.0888, calculated for C₂₇H₂₀N₃O₃FSCl [M+H]⁺ 520.0898.

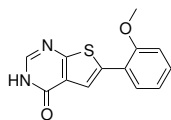
6.2.10 Synthesis of (4-(4-((3-chloro-4-((3-fluorobenzyl)oxy)phenyl)amino)thieno[2,3-*d*]pyrimidin-6-yl)-3-methoxyphenyl)methanol (**14c**)



Compound **14c** was prepared as described in Section 6.2.4 using **14b** (100 mg, 0.192 mmol) and NaBH₄ (10 mg, 0.257 mmol, 1.3 eq.) Crystallization from 1,4-dioxane (2 mL) yielded 64 mg (0.123 mmol, 64%) of **14c** as a pale yellow solid, mp. 189-191 °C. HPLC-purity: 96%, $t_R = 27.7$ min.

Spectroscopic data for **14c** (Appendix J): ¹H-NMR (400 MHz, DMSO-*d*₆) δ : 9.62 (s, 1H, NH), 8.48 (s, 1H, H-2), 8.27 (s, 1H, H-5), 8.08-8.03 (m, 1H, H-15), 7.74-7.69 (m, 2H, H-16/H-25), 7.51-7.44 (m, 1H, H-22), 7.36-7.24 (m, 3H, H-12/H-19/H-23), 7.21-7.14 (m, 2H, H-21/H-28), 7.08 (d, $J=8.0$, 1H, H-26), 5.32 (t, $J=5.6$, 1H, OH), 5.25 (s, 2H, H-17), 4.57 (d, $J=5.6$, 2H, H-31), 3.97 (s, 3H, H-30); ¹³C-NMR (100 MHz, DMSO-*d*₆) δ : 166.1 (C-8), 162.2 (d, $J=243.7$, C-20), 155.5 (C-29), 153.9 (C-2), 153.0 (C-4), 149.8 (C-14), 145.2 (C-27), 139.7 (d, $J=7.3$, C-18), 135.2 (C-6), 133.5 (C-11), 130.6 (d, $J=8.5$, C-22), 127.7 (C-25), 123.3 (d, $J=2.9$, C-23), 122.9 (C-15), 121.2 (C-13), 121.1 (C-16), 119.8 (C-24), 119.0 (C-26), 117.0 (C-9), 116.2 (C-5), 114.7 (d, $J=21.0$, C-21), 114.6 (C-12), 114.0 (d, $J=21.9$, C-19), 110.2 (C-28), 69.4 (d, $J=2.0$, C-17), 62.5 (C-31), 55.8 (C-30); ¹⁹F-NMR (564 MHz, DMSO-*d*₆, C₆F₆) δ : -115.39 (s, dec.); IR (cm⁻¹) ν : 3263 (w, br), 2863 (w, br), 1610 (m), 1204 (m), 775 (s); HRMS (ASAP+, m/z): detected 522.1046, calculated for C₂₇H₂₂N₃O₃FSCl [M+H]⁺ 522.1054.

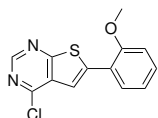
6.2.11 Synthesis of 6-(2-methoxyphenyl)thieno[2,3-*d*]pyrimidin-4(3*H*)-one (**20**)



Compound **20** was prepared as described in Section 6.2.2, using **7** (5.00 g, 21.6 mmol), (2-methoxyphenyl)boronic acid (3.95 g, 26.0 mmol, 1.2 eq.), Pd(PPh₃)₄ (250 mg, 0.216 mmol, 0.01 eq.) and K₂CO₃ (8.97 g, 63.1 mmol, 3 eq.). This yielded 6.25 g (112%) of **20** as a sand coloured solid, mp. 270-317 °C (dec.). **20** was used without further purification.

Spectroscopic data for **20** (Appendix K): $^1\text{H-NMR}$ (400 MHz, $\text{DMSO-}d_6$) δ : 8.11 (s, 1H, H-2), 7.85-7.79 (m, 2H, H-5/H-11), 7.43-7.33 (m, 1H, H-13), 7.21-7.17 (m, 1H, H-14), 7.09-7.01 (m, 1H, H-12), 3.95 (s, 3H, H-16), NH proton not detected; $^{13}\text{C-NMR}$ (100 MHz, $\text{DMSO-}d_6$) δ : 163.9 (C-8), 157.9 (C-4), 155.3 (C-15), 146.3 (C-2), 134.9 (C-6), 129.7 (C-13), 128.0 (C-11), 124.8 (C-9), 121.3 (C-10), 121.2 (C-12), 118.8 (C-5), 112.4 (C-14), 55.8 (C-16); IR (cm^{-1}) ν : 3069 (w, br), 1668 (s), 1264 (m), 1020 (m), 775 (s); HRMS (ASAP+, m/z): detected 259.0537, calculated for $\text{C}_{13}\text{H}_{11}\text{N}_2\text{O}_2\text{S}$ $[\text{M}+\text{H}]^+$ 259.0541.

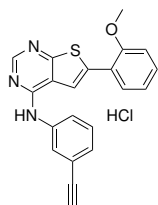
6.2.12 Synthesis of 4-chloro-6-(2-methoxyphenyl)thieno[2,3-*d*]pyrimidine (**21**)



Compound **20** (5.75 g, 22.3 mmol) was mixed with POCl_3 (20 mL) and heated to reflux for 3 h. The reaction mixture was cooled to rt and quenched in ice water, before neutralized using NaOH and NaHCO_3 . The solid in the mixture was isolated by filtered to yield 5.65 g (92%) of sand coloured crude product. A fraction of the crude product (1.00 g) was purified using column chromatography (10:90 EtOAc:*n*-pentane, $R_f = 0.21$). This yielded 152 mg (0.549 mmol, 15%) of the desired product **21** as a white solid, mp. 165-168 °C. HPLC-purity > 99%, $t_R = 27.0$ min.

Spectroscopic data for **21** (Appendix L): $^1\text{H-NMR}$ (400 MHz, $\text{DMSO-}d_6$) δ : 8.91 (s, 1H, H-2), 8.03 (dd, $J = 8.0, 1.2$, 1H, H-11), 7.99 (s, 1H, H-5), 7.53-7.46 (m, 1H, H-13), 7.26 (d, $J = 8.4$, 1H, H-14), 7.13 (t, $J = 7.6$, 1H, H-12), 4.00 (s, 3H, H-16); $^{13}\text{C-NMR}$ (100 MHz, $\text{DMSO-}d_6$) δ : 168.2 (C-8), 155.9 (C-15), 153.0 (C-4), 152.6 (C-2), 141.2 (C-6), 131.5 (C-13), 129.2 (C-9), 128.9 (C-11), 121.3 (C-12), 120.3 (C-10), 115.9 (C-5), 112.6 (C-14), 56.0 (C-16); IR (cm^{-1}) ν : 1253 (m), 1118 (m), 1021 (m), 740 (s); HRMS (ASAP+, m/z): detected 277.0197, calculated for $\text{C}_{13}\text{H}_{10}\text{N}_2\text{OSCl}$ $[\text{M}+\text{H}]^+$ 277.0202.

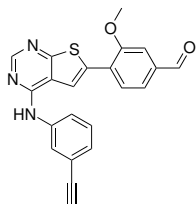
6.2.13 Synthesis of *N*-(3-ethynylphenyl)-6-(2-methoxyphenyl)thieno[2,3-*d*]pyrimidin-4-amine·HCl (**15a**·HCl)



Compound **15a**·HCl was synthesized as described in Section 6.2.7, using **21** (100 mg, 0.361 mmol) and 3-ethynylaniline (51 mg, 0.434 mmol, 1.2 eq.). The reaction mixture was stirred at 60 °C for 72 h, concentrated and triturated with Et₂O. The obtained product was dried under reduced pressure. This yielded 58 mg (0.147 mmol, 41%) of **15a**·HCl as sand yellow coloured solid, mp. 223-233 (dec.). HPLC-purity > 99%, *t*_R = 27.7 min.

Spectroscopic data for **15a**·HCl (Appendix M): ¹H-NMR (400 MHz, DMSO-*d*₆) δ: 10.45 (s, 1H, NH), 8.67-8.62 (m, 2H, H-2/H-5), 8.11-8.08 (m, 1H, H-12), 7.97-7.91 (m, 1H, H-16), 7.86-7.82 (m, 1H, H-20), 7.47-7.41 (m, 2H, H-15/H-22), 7.29-7.22 (m, 2H, H-14/H-23), 7.14 (t, *J*=7.6, 1H, H-21), 4.21 (s, 1H, H-18), 3.99 (s, 3H, H-25); ¹³C-NMR (100 MHz, DMSO-*d*₆) δ: 162.9 (C-8), 155.5 (C-24), 154.1 (C-4), 151.3 (C-2), 139.0 (C-11), 135.9 (C-6), 130.3 (C-22), 129.1 (C-14), 127.9 (C-15), 127.1 (C-20), 124.6 (C-12), 122.4 (C-13), 122.0 (C-16), 121.3 (C-19), 121.1 (C-21), 117.4 (C-9), 117.1 (C-5), 112.6 (C-23), 83.4 (C-17), 80.8 (C-18), 56.0 (C-25); IR (cm⁻¹) ν: 3064 (w, br), 2421 (m, br), 1246 (m), 1199 (m), 749 (s), 671 (m); HRMS (ASAP+, *m/z*): detected 358.1010, calculated for C₂₁H₁₆N₃OS [M+H]⁺ 358.1014.

6.2.14 Synthesis of 4-(4-((3-ethynylphenyl)amino)thieno[2,3-*d*]pyrimidin-6-yl)-3-methoxybenzaldehyde (**15b**)

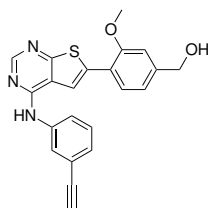


Compound **15b** was prepared as described in Section 6.2.2, using **4**·HCl (500 mg, 1.51 mmol), (4-formyl-2-methoxyphenyl)boronic acid (327 mg, 1.82 mmol, 1.20 eq.), Pd(PPh₃)₄ (17 mg, 0.015 mmol, 0.01 eq.) and K₂CO₃ (628 mg, 4.54 mmol, 3 eq.). The reaction residue was dissolved in hot EtOAc (950 mL). Water (400 mL) was added, and the layers were separated. The organic layer was washed with brine (200 mL), dried over anhydrous Na₂SO₄, filtered and concentrated. The crude

product was purified using silica-gel column chromatography (25:75 EtOAc:DCM, $R_f = 0.44$), and the obtained product was dried under reduced pressure. This yielded 168 mg (0.44 mmol, 32%) of **15b** as a yellow solid, mp. 221-225 °C. HPLC-purity: 91%, $t_R = 29.1$ min.

Spectroscopic data for **15b** (Appendix N): $^1\text{H-NMR}$ (400 MHz, $\text{DMSO-}d_6$) δ : 10.05 (s, 1H, H-26), 9.82 (s, 1H, NH), 8.60-8.54 (m, 2H, H-2/H-12), 8.12-8.10 (m, 1H, H-5), 8.05-8.01 (m, 1H, H-20), 7.92-7.88 (m, 1H, H-16), 7.74-7.70 (m, 2H, H-21/H-23), 7.46-7.40 (m, 1H, H-15), 7.23 (d, $J=7.6$, 1H, H-14) 4.22 (s, 1H, H-18), 4.09 (s, 3H, H-25); $^{13}\text{C-NMR}$ (100 MHz, $\text{DMSO-}d_6$) δ : 192.2 (C-26), 167.1 (C-8), 155.8 (C-24), 154.3 (C-4), 153.6 (C-2), 139.5 (C-11), 136.9 (C-22), 133.7 (C-19), 129.1 (C-15), 128.4 (C-20), 127.2 (C-6), 126.4 (C-14), 123.9 (C-5), 122.8 (C-21), 121.9 (C-13), 121.7 (C-16), 119.1 (C-12), 117.1 (C-9), 112.2 (C-23), 83.5 (C-17), 80.7 (C-18), 56.2 (C-25); IR (cm^{-1}) ν : 3226 (w, br), 1675 (s), 682 (m); HRMS (ASAP+, m/z): detected 386.0959, calculated for $\text{C}_{22}\text{H}_{16}\text{N}_3\text{O}_2\text{S}$ $[\text{M}+\text{H}]^+$ 386.0963.

6.2.15 Synthesis of (4-(4-((3-ethynylphenyl)amino)thieno[2,3-*d*]pyrimidin-6-yl)-3-methoxyphenyl)methanol (**15c**)



Compound **15c** was prepared as described in Section 6.2.4, using **15b** (100 mg, 0.361 mmol) and NaBH_4 (12 mg, 0.311 mmol, 1 eq.). This yielded 0.119 g (98%) of a cream coloured crude product. Crystallization from MeOH (18 mL), and again from DMF (2 mL) and water (1 mL) yielded compound **15c** as a pale yellow solid of 18 mg (0.046 mmol, 15%), mp. 217-225 °C. HPLC-purity: 92%, $t_R = 23.1$ min.

Spectroscopic data for **15c** (Appendix O): $^1\text{H-NMR}$ (400 MHz, $\text{DMSO-}d_6$) δ : 9.68 (s, 1H, NH), 8.53 (s, 1H, H-2), 8.33 (s, 1H, H-5), 8.12-8.08 (m, 1H, H-12), 7.93-7.89 (m, 1H, H-16), 7.74 (d, $J=8.0$, 1H, H-20), 7.41 (t, $J=8.0$, 1H, H-15), 7.23-7.17 (m, 2H, H-14/H-23), 7.09 (d, $J=8.8$, 1H, H-21) 5.33 (t, $J=5.6$, 1H, OH), 4.57 (d, $J=5.6$, 2H, H-26), 4.21 (s, 1H, H-18), 3.98 (s, 3H, H-27); $^{13}\text{C-NMR}$ (100 MHz, $\text{DMSO-}d_6$) δ : 166.4 (C-8), 155.6 (C-24), 153.9 (C-4), 152.9 (C-2),

145.2 (C-22), 139.7 (C-11), 135.5 (C-6), 129.1 (C-15), 127.7 (C-20), 126.2 (C-14), 123.7 (C-12), 121.9 (C-13), 121.5 (C-16), 119.8 (C-19), 119.0 (C-21), 117.2, (C-9), 116.2 (C-5), 110.2 (C-23), 83.5 (C-17), 80.6 (C-18), 62.6 (C-26), 55.8 (C-25); IR (cm^{-1}) ν : 3236 (w, br), 1005 (s), 774 (s), 657 (m); HRMS (ASAP+, m/z): detected 388.1113, calculated for $\text{C}_{22}\text{H}_{18}\text{N}_3\text{O}_2\text{S}$ $[\text{M}+\text{H}]^+$ 388.1120.

References

- [1] WorldHealthOrganization, Key facts about cancer. 2009, last checked 05/30/2014; <http://www.who.int/mediacentre/factsheets/fs297/en/>.
- [2] Guren, T.; Christoffersen, T.; Thoresen, G.; Wisløff, F.; Dajani, O.; Tveit, K. *Tidsskrift for den Norske Laegeforening* **2005**, *125*, 3115–3119.
- [3] Sperry, J.; Wright, D. *Current Opinion in Drug Discovery and Development* **2005**, *8*, 723–740.
- [4] Gronowitz, S., Ed. *Thiophene and its derivatives - part 1*; Heterocyclic Compounds; John Wiley and sons, 1985; Vol. 44.
- [5] Mishra, R.; Tomar, I.; Singhal, S.; Jha, K. *Der Pharma Chemica* **2011**, *3*, 38–54.
- [6] Rizk, O.; Shaaban, O.; El-Ashmawy, I. *European Journal of Medicinal Chemistry* **2012**, *55*, 85–93.
- [7] Veena, K.; Nargund, S.; Nargund, S.; Chandra, J.; Nargund, L. *Der Pharma Chemica* **2012**, *4*, 581–586.
- [8] El-Gazzar, A.-R.; Hussein, H.; Hafez, H. *Acta Pharmaceutica* **2007**, *57*, 395–411.
- [9] Panico, A.; Cardile, V.; Santagati, A.; Gentile, B. *Farmaco* **2001**, *56*, 959–964.
- [10] Vyawahare, N.; Hadambar, A.; Chothe, A.; Jalnapurkar, R.; Bhandare, A.; Kathiravan, M. *Journal of Chemical Biology* **2012**, *5*, 35–42.
- [11] Nedergaard, M. K.; Hedegaard, C. J.; Poulsen, H. S. *BioDrugs* **2012**, *26*, 83–99.
- [12] Warnault, P. *Current medicinal chemistry* **2013**, *20*, 2043–67.
- [13] Li, S.; Schmitz, K.; Jeffrey, P.; Wiltzius, J.; Kussie, P.; Ferguson, K. *Cancer Cell* **2005**, *7*, 301–311.

-
- [14] Patrick, G. L. *An Introduction to Medicinal Chemistry*, 4th ed.; Oxford University Press, 2009.
- [15] Purser, S.; Moore, P. R.; Swallow, S.; Gouverneur, V. *Chemical Society Reviews* **2008**, *37*, 320–330.
- [16] Patani, G. A.; LaVoie, E. J. *Chemical Reviews (Washington, D. C.)* **1996**, *96*, 3147–3176.
- [17] Chambers, R. D. *Fluorine in Organic Chemistry*; Blackwell Publishing, 2000.
- [18] Silverman, R. B. *The Organic Chemistry of Drug Design and Drug Action*, 2nd ed.; Elsevier/Academic Press, 2004.
- [19] Martell, R. b.; Brooks, D.; Wang, Y.; Wilcoxon, K. *Clinical Therapeutics* **2013**, *35*, 1271–1281.
- [20] Arora, A.; Scholar, E. c. *Journal of Pharmacology and Experimental Therapeutics* **2005**, *315*, 971–979.
- [21] Zhang, J.; Yang, P.; Gray, N. *Nature Reviews Cancer* **2009**, *9*, 28–39.
- [22] Mayr, L. M.; Bojanic, D. *Current Opinion in Pharmacology* **2009**, *9*, 580–588.
- [23] Pereira, D. A.; Williams, J. A. *British Journal of Pharmacology* **2007**, *152*, 53–61.
- [24] Ravina, E. *The Evolution of Drug Discovery: From Traditional Medicines to Modern Drugs*; WILEY-VCH, 2011.
- [25] Schneider, G. *De Novo Molecular Design*; WILEY-VCH, 2014.
- [26] Congreve, M.; Chessari, G.; Tisi, D.; Woodhead, A. J. *Journal of Medicinal Chemistry* **2008**, *51*, 3661–3680.
- [27] Kuntz, I. *Science* **1992**, *257*, 1078–1082.
- [28] Shuker, S. B.; Hajduk, P. J.; Meadows, R. P.; Fesik, S. W. *Science (Washington, D. C.)* **1996**, *274*, 1531–1534.

-
- [29] Loving, K.; Alberts, I.; Sherman, W. *Current Topics in Medicinal Chemistry (Sharjah, United Arab Emirates)* **2010**, *10*, 14–32.
- [30] Scott, D. E.; Coyne, A. G.; Hudson, S. A.; Abell, C. *Biochemistry* **2012**, *51*, 4990–5003.
- [31] StoreNorskeLeksikon, Fosfoproteiner. last checked 05/30/2014; <http://snl.no/fosfoproteiner>.
- [32] Patel, R.; Leung, H. *Current Pharmaceutical Design* **2012**, *18*, 2672–2679.
- [33] Baselga, J. *Oncologist* **2002**, *7*, 2–8.
- [34] Nature, RTK. 2010, last checked 05/22/2014; <http://www.nature.com/scitable/topicpage/rtk-14050230>.
- [35] Mukherji, D.; Spicer, J. *Expert Opinion on Investigational Drugs* **2009**, *18*, 293–301.
- [36] Blume-Jensen, P.; Hunter, T. *Nature* **2001**, *411*, 355–365.
- [37] Tsatsanis, C.; Spandidos, D. *International journal of molecular medicine* **2000**, *5*, 583–590.
- [38] Yewale, C.; Baradia, D.; Vhora, I.; Patil, S.; Misra, A. *Biomaterials* **2013**, *34*, 8690–8707.
- [39] Joule, J. A.; Mills, K. *Heterocyclic Chemistry*, 4th ed.; Blackwell Science, 2000.
- [40] Bier, H.; Hoffmann, T.; Haas, I.; Van Lierop, A. *Cancer Immunology Immunotherapy* **1998**, *46*, 167–173.
- [41] Yang, X.-D.; Jia, X.-C.; Corvalan, J.; Wang, P.; Davis, C.; Jakobovits, A. *Cancer Research* **1999**, *59*, 1236–1243.
- [42] Felleskatalogen, Gefitinib. last checked 05/30/2014; <http://www.felleskatalogen.no/medisin/iressa-astrazeneca-560272>.
- [43] Felleskatalogen, Erlotinib. last checked 05/30/2014; <http://www.felleskatalogen.no/medisin/tarceva-roche-564418>.

-
- [44] Felleskatalogen, Lapatinib. last checked 05/30/2014; <http://www.felleskatalogen.no/medisin/tyverb-glaxosmithkline-564901>.
- [45] Zhang, L.; Fan, C.; Guo, Z.; Li, Y.; Zhao, S.; Yang, S.; Yang, Y.; Zhu, J.; Lin, D. *European Journal of Medicinal Chemistry* **2013**, *69*, 833–841.
- [46] Traxler, P.; Allegrini, P.; Brandt, R.; Brueggen, J.; Cozens, R.; Fabbro, D.; Grosios, K.; Lane, H.; McSheehy, P.; Mestan, J.; Meyer, T.; Tang, C.; Wartmann, M.; Wood, J.; Caravatti, G. *Cancer Research* **2004**, *64*, 4931–4941.
- [47] Beckers, T.; Sellmer, A.; Eichhorn, E.; Pongratz, H.; Schächtele, C.; Totzke, F.; Kelter, G.; Krumbach, R.; Fiebig, H.-H.; Böhmer, F.-D.; Mahboobi, S. *Bioorganic and Medicinal Chemistry* **2012**, *20*, 125–136.
- [48] Rheault, T. R. et al. *Bioorganic and Medicinal Chemistry Letters* **2009**, *19*, 817 – 820.
- [49] Traxler, P. *Expert Opinion on Therapeutic Targets* **2003**, *7*, 215–234.
- [50] Ohashi, K.; Maruvka, Y.; Michor, F.; Pao, W. *Journal of Clinical Oncology* **2013**, *31*, 1070–1080.
- [51] Goffin, J.; Zbuk, K. *Clinical Therapeutics* **2013**, *35*, 1282–1303.
- [52] Nagy, P.; Jenei, A.; Kirsch, A.; Szöllosi, J.; Damjanovich, S.; Jovin, T. *Journal of Cell Science* **1999**, *112*, 1733–1741.
- [53] Boehrer, S.; Galluzzi, L.; Lainey, E.; Bouteloup, C.; Tailler, M.; Harper, F.; Pierron, G.; Adès, L.; Thépot, S.; Sébert, M.; Gardin, C.; De Botton, S.; Fenaux, P.; Kroemer, G. *Cell Cycle* **2011**, *10*, 3168–3175.
- [54] Moen, I. U. Project Thesis, Synthesis of Aniline Substituted Thienopyrimidines as Epidermal Growth Factor Tyrosine Kinase Inhibitors, NTNU, 2013.
- [55] Kaspersen, S. J.; Sørum, C.; Willassen, V.; Fuglseth, E.; Kjøbli, E.; Bjørkøy, G.; Sundby, E.; Hoff, B. H. *European Journal of Medicinal Chemistry* **2011**, *46*, 6002 – 6014.

-
- [56] Kaspersen, S. J.; Sundby, E.; Charnock, C.; Hoff, B. H. *Bioorganic Chemistry* **2012**, *44*, 35–41.
- [57] Bugge, S.; Kaspersen, S. J.; Sundby, E.; Hoff, B. H. *Tetrahedron* **2012**, *68*, 9226–9233.
- [58] Sørum, C.; Simic, N.; Sundby, E.; Hoff, B. H. *Magnetic Resonance in Chemistry* **2010**, *48*, 244–248.
- [59] Bugge, S.; Kaspersen, S. J.; Larsen, S.; Nonstad, U.; Bjørkøy, G.; Sundby, E.; Hoff, B. H. *European Journal of Medicinal Chemistry* **2014**, *75*, 354–374.
- [60] Kaspersen, S. J.; Rydså, L.; Bugge, S.; Hoff, B. H.; Han, J.; Nørsett, K. G.; Kjøbli, E.; Bjørkøy, G.; Sundby, E. *European journal of pharmaceutical sciences : official journal of the European Federation for Pharmaceutical Sciences* **2014**, *59C*, 69–82.
- [61] Zhan, D.; Li, S.; Zhao, H.; Lan, M. b. *Chinese Journal of Organic Chemistry* **2011**, *31*, 207–211.
- [62] Hess, J.; Grembecka, J.; Cierpicki, T. *PCT Int. Appl. WO2011029054* **2011**,
- [63] Smith, M. B. *Organic Synthesis*, 3rd ed.; Elsevier/Academic Press, 2010.
- [64] Carey, F. A.; Sundberg, R. J. *Advanced Organic Chemistry, Part B: Reactions and Synthesis*; Springer, 2007.
- [65] Bunnett, J. F.; Zahler, R. E. *Chemical Reviews (Washington, DC, United States)* **1951**, *49*, 273–412.
- [66] Gilchrist, T. L. *Heterocyclic Chemistry*, 3rd ed.; Pearson Education, 1997.
- [67] Guo, C.; Dong, L.; Marakovits, J.; Kephart, S. *Tetrahedron Letters* **2011**, *52*, 1692–1696.
- [68] Kunz, K.; Scholz, U.; Ganzer, D. *Synlett* **2003**, 2428–2439.
- [69] Sperotto, E.; Van Klink, G.; Van Koten, G.; De Vries, J. *Dalton Transactions* **2010**, *39*, 10338–10351.

-
- [70] Surry, D.; Buchwald, S. *Angewandte Chemie - International Edition* **2008**, *47*, 6338–6361.
- [71] Carey, J.; Laffan, D.; Thomson, C.; Williams, M. *Organic and Biomolecular Chemistry* **2006**, *4*, 2337–2347.
- [72] Torborg, C.; Beller, M. *Advanced Synthesis and Catalysis* **2009**, *351*, 3027–3043.
- [73] Goodbrand, H.; Hu, N.-X. *Journal of Organic Chemistry* **1999**, *64*, 670–674.
- [74] Kotha, S.; Lahiri, K.; Kashinath, D. *Tetrahedron* **2002**, *58*, 9633 – 9695.
- [75] Anslyn, D. A., E. V.; Dougherty *Modern Physical Organic Chemistry*; University Science Books, 2006.
- [76] Miyaura, N.; Suzuki, A. *Journal of the Chemical Society, Chemical Communications* **1979**, 866–7.
- [77] Miyaura, N.; Suzuki, A. *Chemical Reviews* **1995**, *95*, 2457–2483.
- [78] Miyaura, N.; Yamada, K.; Suzuki, A. *Tetrahedron Letters* **1979**, *20*, 3437 – 3440.
- [79] Miyaura, N.; Yanagi, T.; Suzuki, A. *Synthetic Communications* **1981**, *11*, 513–19.
- [80] Oh-e, T.; Miyaura, N.; Suzuki, A. *Synlett* **1990**, 221–3.
- [81] Hartwig, J. F. *Organotransition Metal Chemistry From Bonding to Catalysis*; University Science Books, 2010.
- [82] Hegedus, B. C. G., L. S.; Söderberg *Transition Metals in the Synthesis of Complex Organic Molecules*, 3rd ed.; University Science Books, 2010.
- [83] Magano, J.; Dunetz, J. *Chemical Reviews* **2011**, *111*, 2177–2250.
- [84] Lipton, M. F.; Mauragis, M. A.; Maloney, M. T.; Velej, M. F.; Vander-Bor, D. W.; Newby, J. J.; Appell, R. B.; Dausg, E. D. *Organic Process Research & Development* **2003**, *7*, 385–392.

-
- [85] Suzuki, A. *Journal of Organometallic Chemistry* **1999**, *576*, 147–168.
- [86] Braga, A. A. C.; Morgon, N. H.; Ujaque, G.; Maseras, F. *Journal of the American Chemical Society* **2005**, *127*, 9298–9307.
- [87] Fauvarque, J.-F.; Pflüger, F.; Troupel, M. *Journal of Organometallic Chemistry* **1981**, *208*, 419–427.
- [88] Colombo, M.; Giglio, M. b.; Peretto, I. *Journal of Heterocyclic Chemistry* **2008**, *45*, 1077–1081.
- [89] Jang, M.-Y.; Jonghe, S. D.; Belle, K. V.; Louat, T.; Waer, M.; Herdewijn, P. *Bioorganic and Medicinal Chemistry Letters* **2010**, *20*, 844 – 847.
- [90] Martin, R.; Buchwald, S. L. *Accounts of Chemical Research* **2008**, *41*, 1461–1473.
- [91] Strieter, E. R.; Buchwald, S. L. *Angewandte Chemie, International Edition* **2006**, *45*, 925–928.
- [92] Knapp, D. M.; Gillis, E. P.; Burke, M. D. *Journal of the American Chemical Society* **2009**, *131*, 6961–6963.
- [93] Hall, D. *Boronic Acids*; WILEY-VCH, 2005.
- [94] Ozawa, F.; Hidaka, T.; Yamamoto, T.; Yamamoto, A. *Journal of Organometallic Chemistry* **1987**, *330*, 253–63.
- [95] Williamson, A. *Philosophical Magazine series 3* **1850**, *37*, 350–336.
- [96] Williamson, A. W. *Quart. J., Chem. Soc., London* **1852**, *4*, 229–39.
- [97] Carey, F. A. *Organic Chemistry*, 7th ed.; McGraw-Hill: New York, 2008.
- [98] Dermer, O. C. *Chem. Rev.* **1934**, *14*, 385–430.
- [99] Wanklyn, J. A. *Journal of the Chemical Society, Transactions* **1869**, *22*, 199–202.
- [100] Freedman, H. H.; Dubois, R. A. *Tetrahedron Letters* **1975**, 3251–4.
- [101] Tan, S. N.; Dryfe, R. A.; Girault, H. H. *Helvetica Chimica Acta* **1994**, *77*, 231–42.

-
- [102] Jursic, B. *Tetrahedron* **1988**, *44*, 6677–80.
- [103] Peng, Y.; Song, G. *Green Chemistry* **2002**, *4*, 349–351.
- [104] Ullmann, F.; Sponagel, P. *Berichte der Deutschen Chemischen Gesellschaft* **1905**, *38*, 2211–12.
- [105] Brewster, R. Q.; Groening, T. *Organic Syntheses* **1934**, *14*, No pp. given.
- [106] Goldberg, I. *Berichte der Deutschen Chemischen Gesellschaft* **1906**, *39*, 1691–92.
- [107] Shiao, H.-Y. et al. *Journal of Medicinal Chemistry* **2013**, *56*, 5247–5260.
- [108] Fontana, F.; Leganza, A.; Osti, S. *Eur. Pat. Appl., patent EP2489661A1* **2012**,
- [109] Mahboobi, S.; Sellmer, A.; Winkler, M.; Eichhorn, E.; Pongratz, H.; Ciossek, T.; Baer, T.; Maier, T.; Beckers, T. *Journal of Medicinal Chemistry* **2010**, *53*, 8546–8555.
- [110] Trost, B. M.; Dong, G. *Journal of the American Chemical Society* **2010**, *132*, 16403–16416.
- [111] Stang, F., P. J.; Diederich, Ed. *Modern Acetylene Chemistry*; WILEY-VCH, Weinheim, 1995.
- [112] Hay, A. S. *Journal of Organic Chemistry* **1962**, *27*, 3320–1.
- [113] Dyker, G., Ed. *Handbook in C-H Transformations: Applications in Organic Synthesis*; WILEY-VCH Verlag, 2005.
- [114] Yalagala, R. S.; Zhou, N.; Yan, H. *Tetrahedron Letters* **2014**, *55*, 1883–1885.
- [115] Atobe, S.; Sonoda, M.; Suzuki, Y.; Yamamoto, T.; Masuno, H.; Shinohara, H.; Ogawa, A. *Research on Chemical Intermediates* **2013**, *39*, 359–370.
- [116] Skjønshjell, E. M. Syntese av halogenerte tienopyrimidiner. M.Sc. thesis, NTNU, 2012.

-
- [117] Atherall, J. F.; Hough, T. L.; Lindell, S. D.; O'Mahony, M. S.; Saville-Stones, E. A. *PCT Int. Appl. WO9849899* **1998**,
- [118] Silverstein, *Spectroscopic Identification of Organic Compounds*, 7th ed.; Wiley, 2005.



Appendices

A Spectroscopic Data - Compound 5·HCl

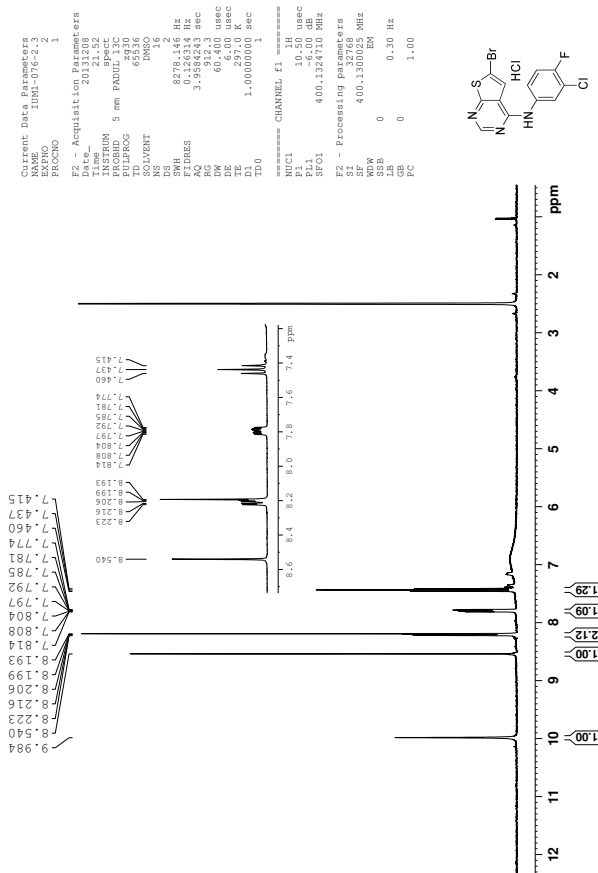


Figure A.1: ¹H-NMR spectrum of compound 5·HCl.

A SPECTROSCOPIC DATA - COMPOUND 5·HCL

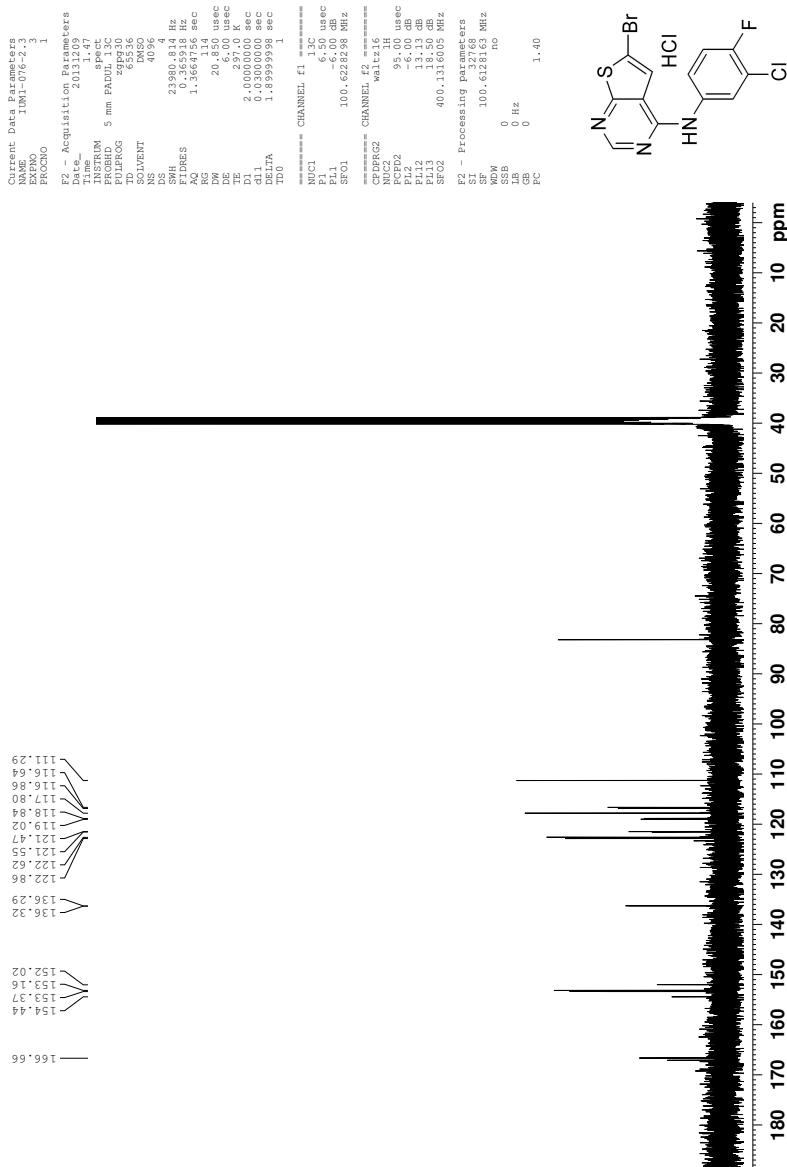


Figure A.2: ¹³C-NMR spectrum of compound 5·HCl.

B Spectroscopic Data - Compound 8a

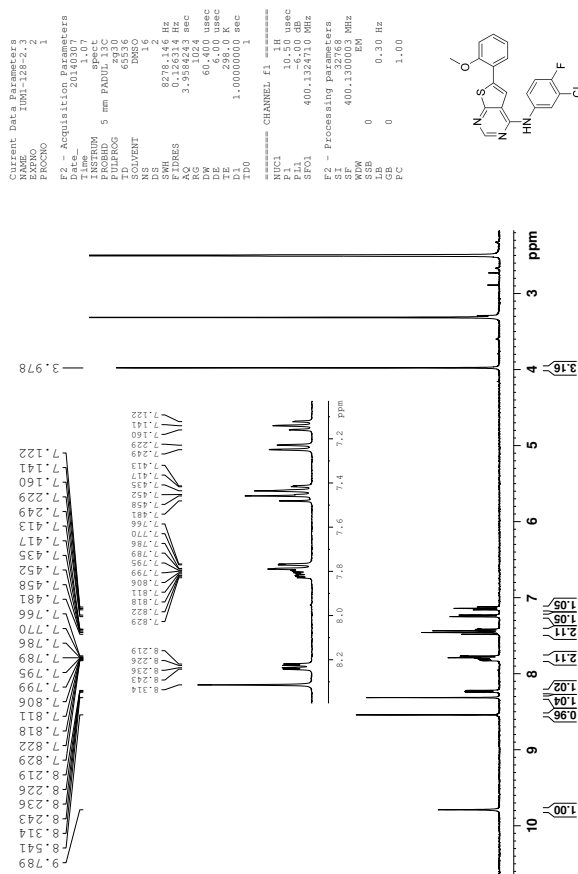


Figure B.1: ¹H-NMR spectrum of compound 8a.

B SPECTROSCOPIC DATA - COMPOUND 8A

```

Current Data Parameters
NAME      LUMI-128-2.4
EXNO     1
PROCNO   1

F2 - Acquisition Parameters
Date_    20140313
Time     3.53
INSTRUM  spect
PROBHD   5 mm PADUL13C
PULPROG  zgpg30
TD       65536
SOLVENT  DMSO
NS       10240
DS       4
SWH      23980.814 Hz
AQ       0.3285686 sec
RG       1.366756
RG       1.14
DM       20.850 usec
DE       600.0 usec
TE       298.0
D1       2.00000000 sec
d11      0.03000000 sec
DELTA    1.89999998 sec
TD0      1

===== CHANNEL f1 =====
NUC1     13C
P1       6.50 usec
PL1      -6.00 dB
SFO1     100.6228298 MHz

===== CHANNEL f2 =====
CFDPGR2  waltz16
NUC2     1H
PCPD2    92.00 usec
PL2      19.00 dB
PL12     13.13 dB
PL13     18.50 dB
SFO2     400.1316005 MHz

F2 - Processing parameters
SI       32768
SF       100.6128161 MHz
WDW      no
SSB      0
LB       0 Hz
GB       0
EC       1.40
    
```

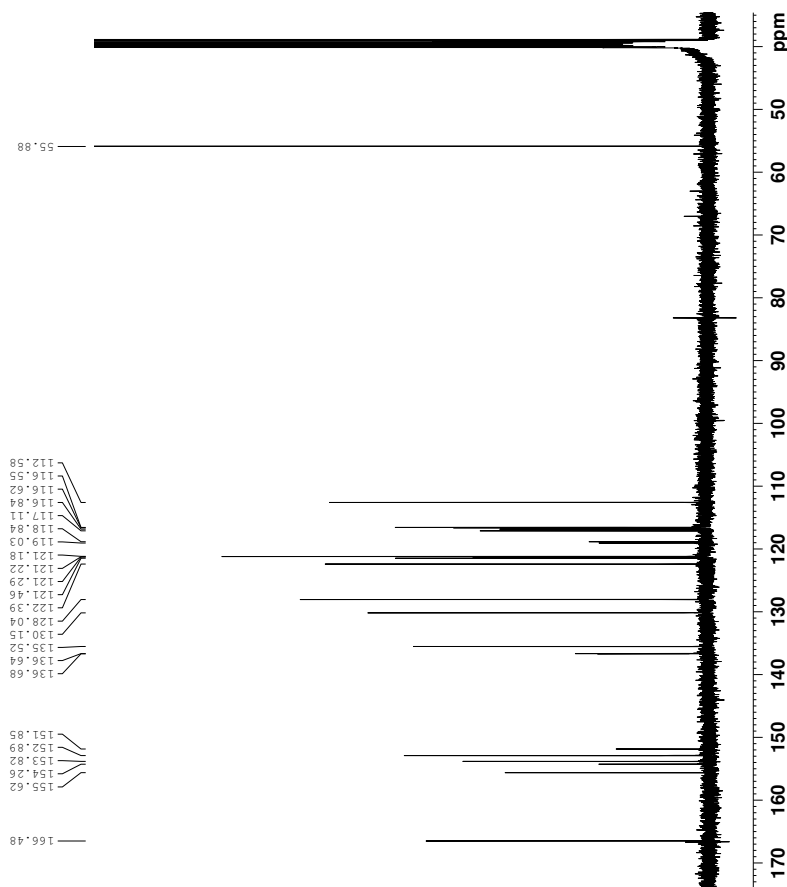
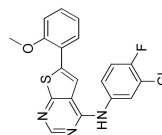


Figure B.2: ^{13}C -NMR spectrum of compound 8a.

B SPECTROSCOPIC DATA - COMPOUND **8a**

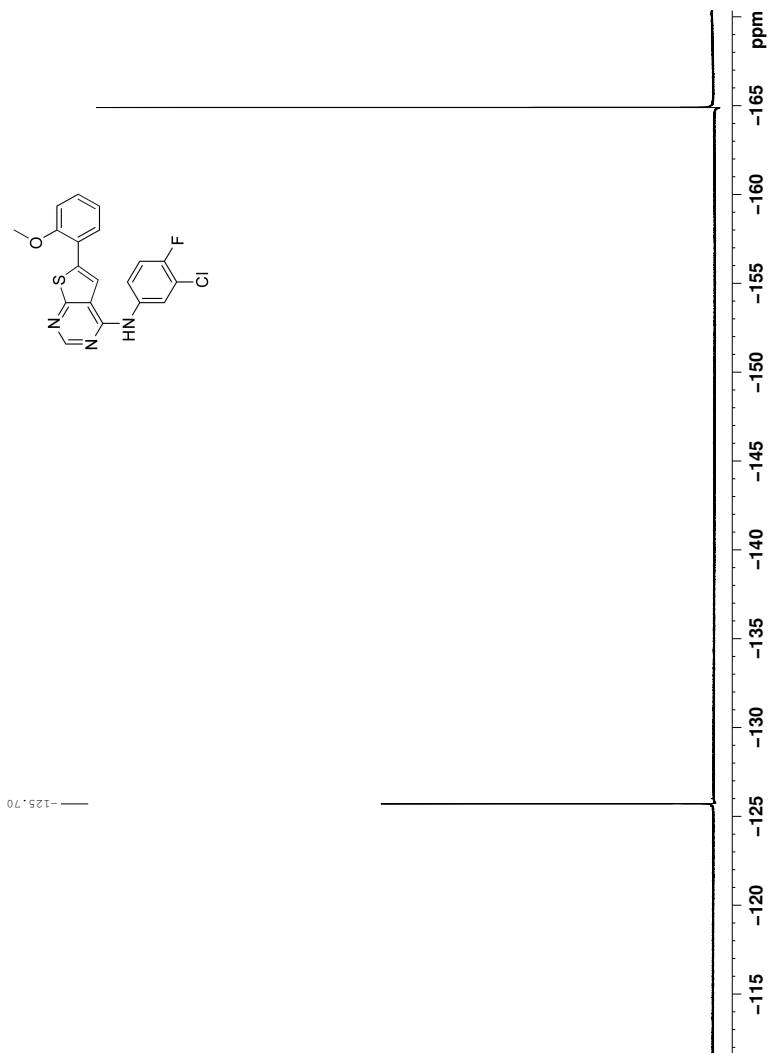


Figure B.3: ^{19}F -NMR spectrum of compound **8a** (decoupled).

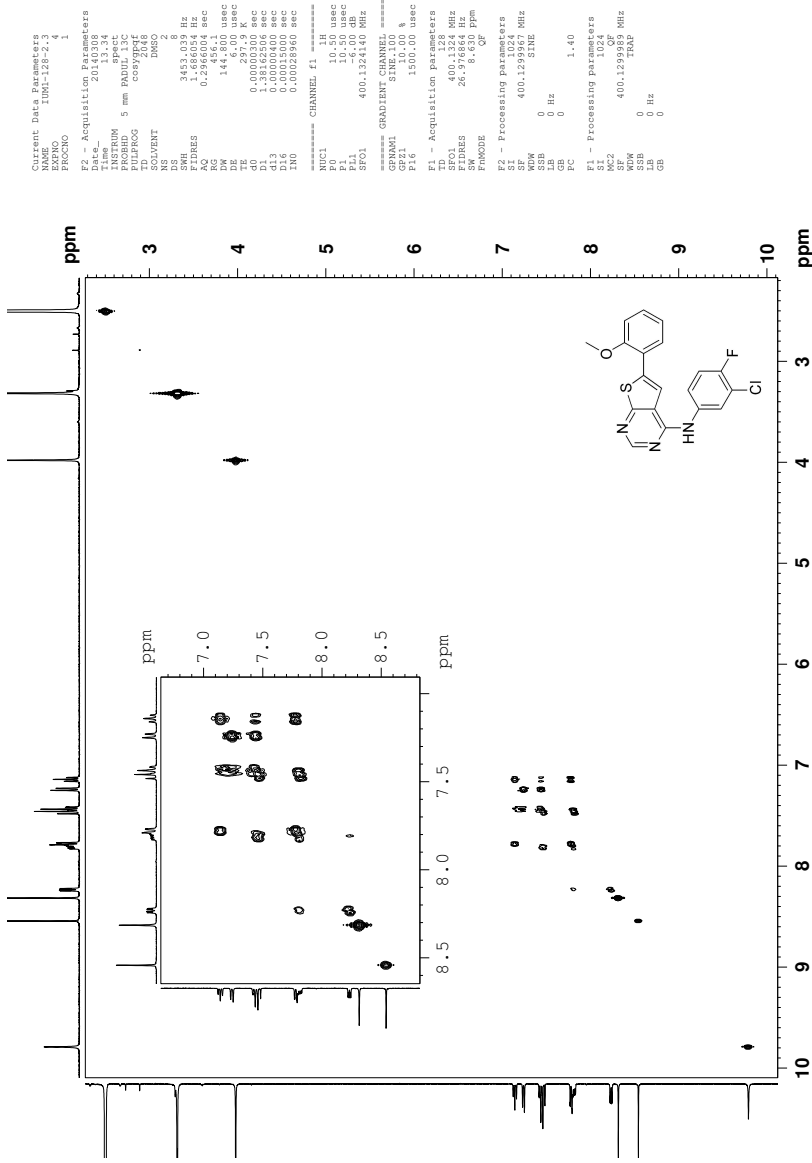


Figure B.4: COSY spectrum of compound 8a.

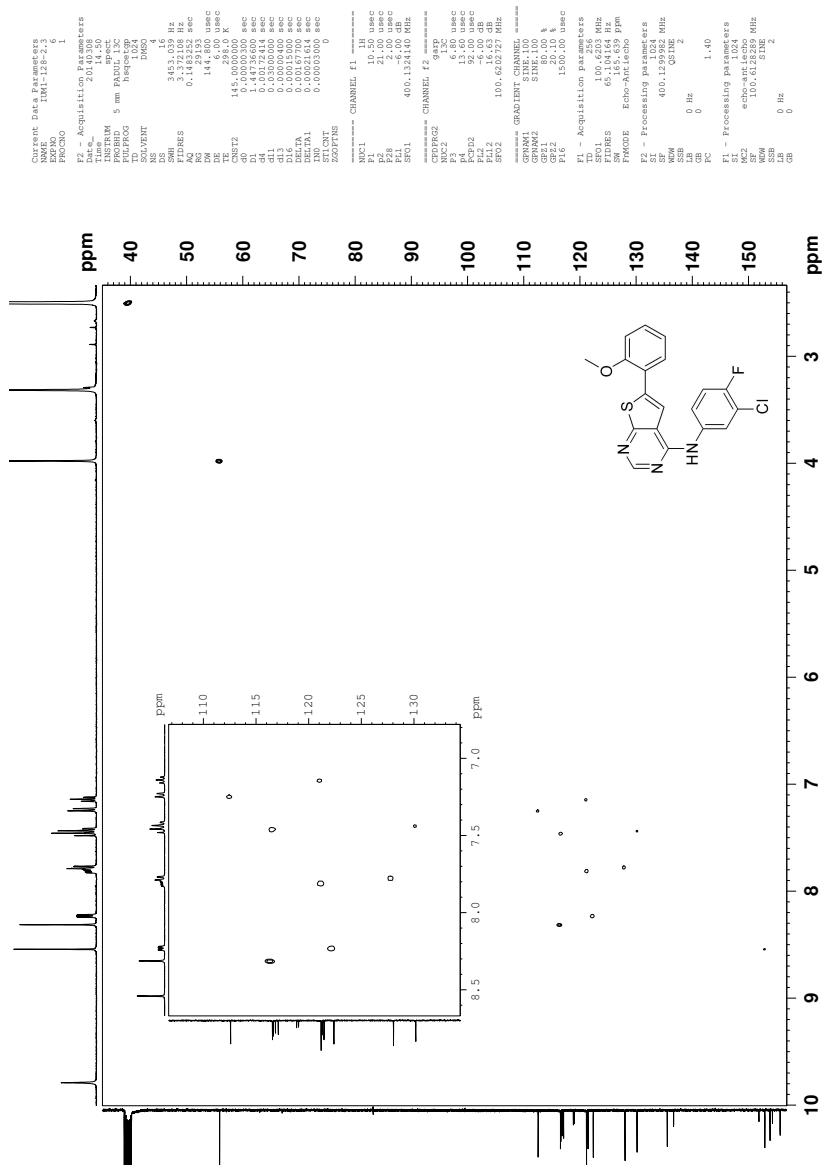


Figure B.5: HSQC spectrum of compound 8a.

B SPECTROSCOPIC DATA - COMPOUND 8A

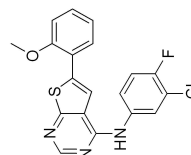
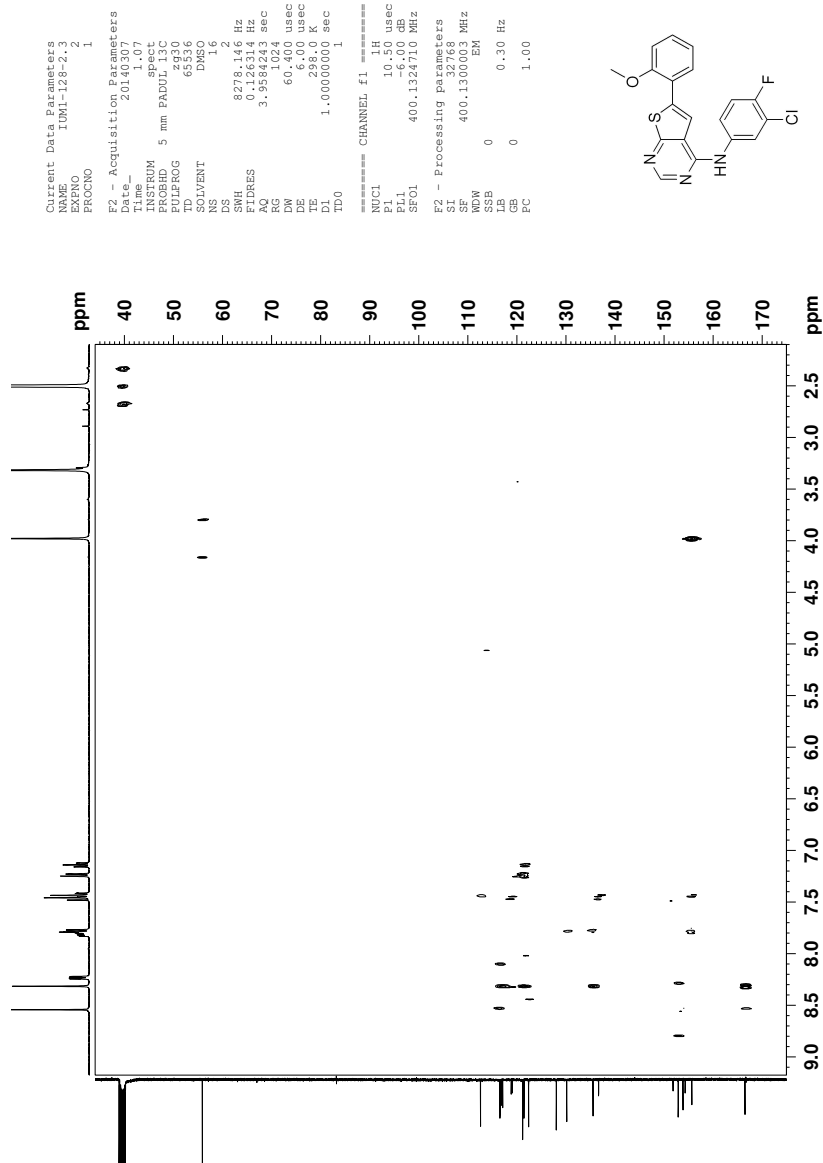


Figure B.6: HMBC spectrum of compound 8a.

B SPECTROSCOPIC DATA - COMPOUND 8A

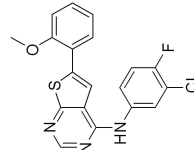
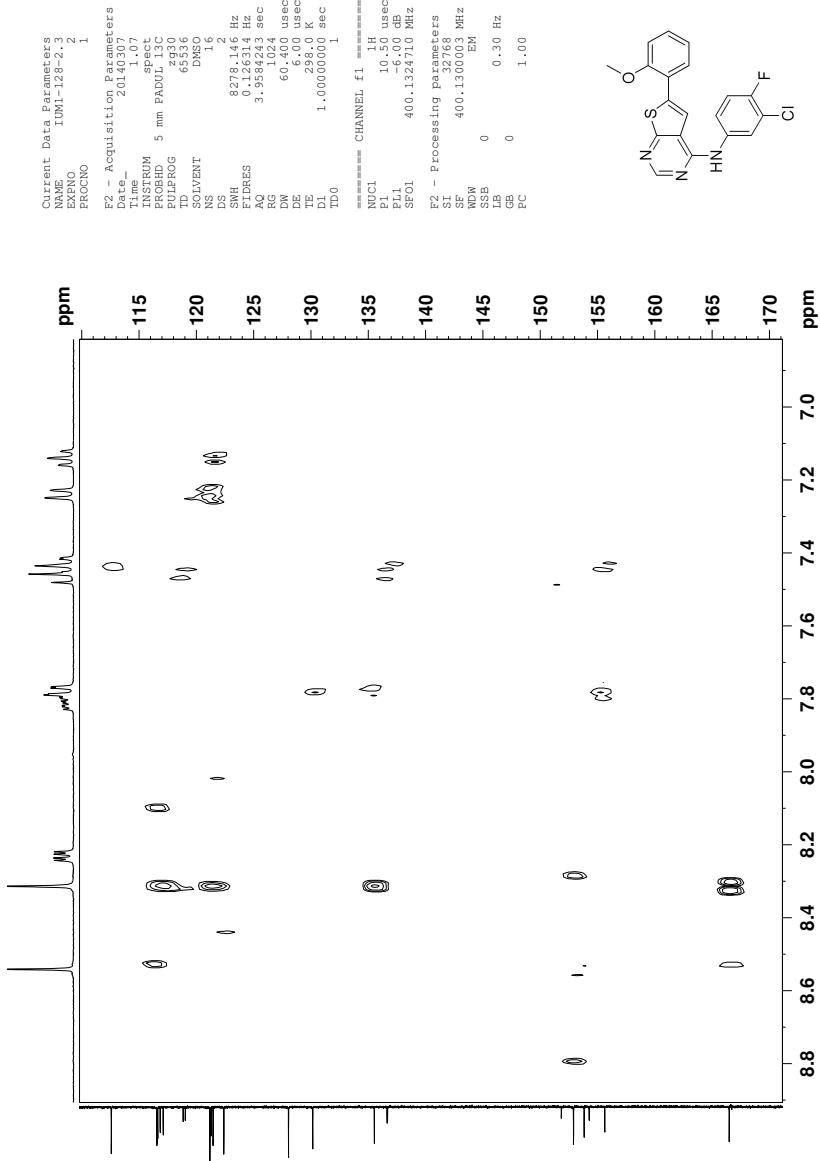
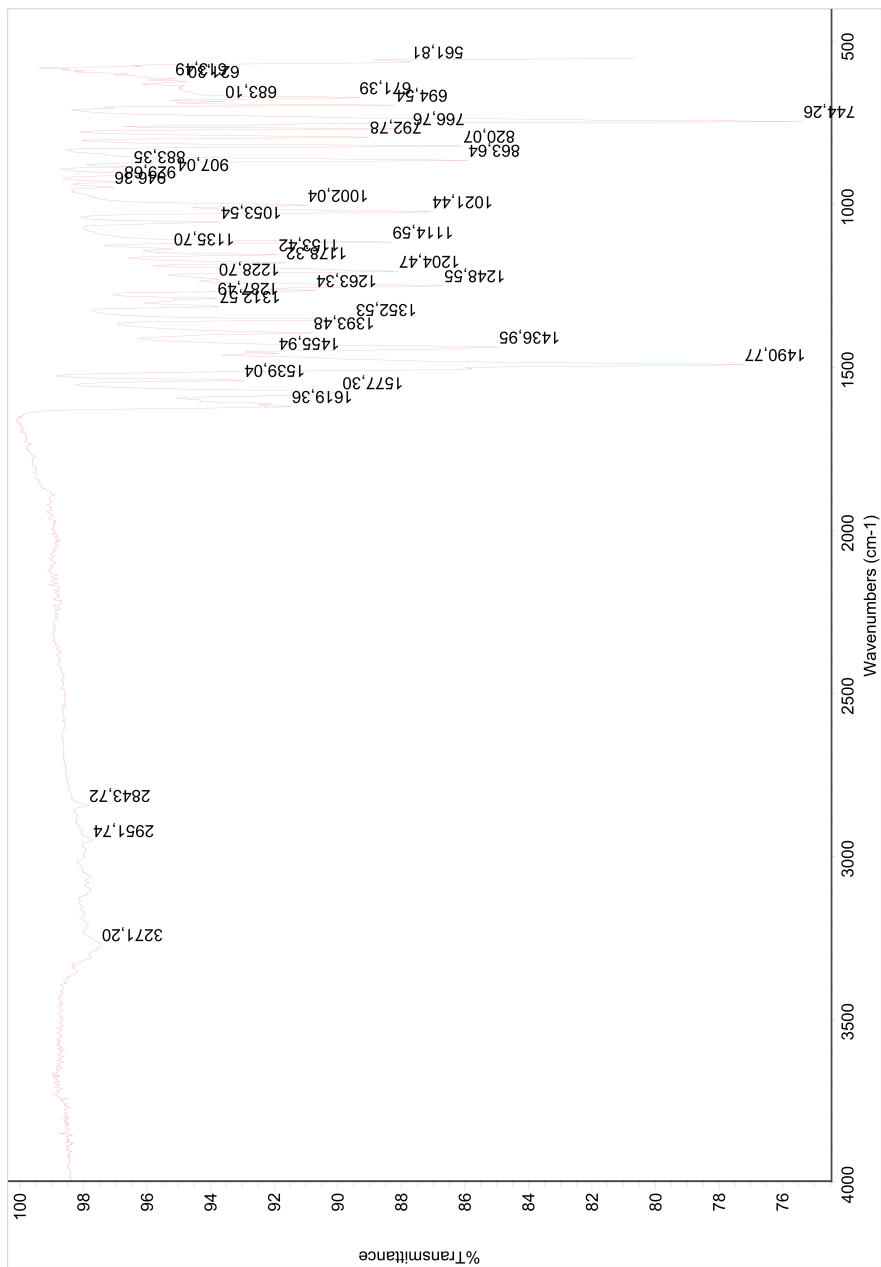


Figure B.7: Section of HMBC spectrum of compound 8a.

Figure B.8: IR spectrum of compound **8a**.

Elemental Composition Report

Single Mass Analysis

Tolerance = 2.0 PPM / DBE: min = -1.5, max = 50.0

Element prediction: Off

Number of isotope peaks used for i-FIT = 3

Monoisotopic Mass, Even Electron Ions

14728 formula(e) evaluated with 25 results within limits (all results (up to 1000) for each mass)

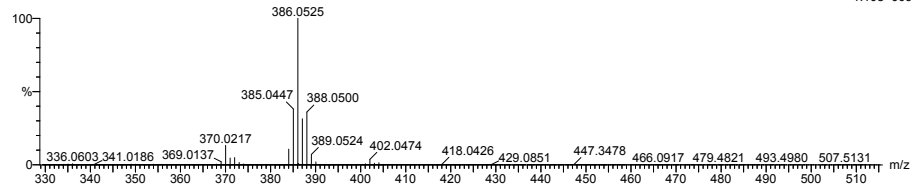
Elements Used:

C: 0-200 H: 0-1000 N: 0-10 O: 0-200 F: 0-3 S: 0-2 Cl: 0-2

NT-MSLAB-Operator-SVG

2014-41 125 (2.447) AM2 (Ar,35000.0,0.00,0.00); Cm (122:125)

1: TOF MS ASAP+
1.10e+006



Minimum: -1.5
Maximum: 50.0

Mass	Calc. Mass	mDa	PPM	DBE	i-FIT	Norm	Conf(%)	Formula
386.0525	386.0519	0.6	1.6	17.5	1136.9	0.390	67.71	C22 H13 N3 S Cl
	386.0530	-0.5	-1.3	13.5	1138.6	2.044	12.94	C19 H14 N3 O F S Cl
	386.0519	0.6	1.6	10.5	1139.4	2.896	5.53	C16 H12 N3 O3 F3 Cl
	386.0528	-0.3	-0.8	10.5	1139.8	3.293	3.71	C11 H10 N9 O4 F Cl
	386.0526	-0.1	-0.3	6.5	1140.0	3.441	3.20	C9 H12 N9 O F3 S Cl
	386.0524	0.1	0.3	4.5	1140.4	3.898	2.03	C11 H18 N5 O3 F S2 Cl
	386.0526	-0.1	-0.3	1.5	1141.2	4.713	0.90	C7 H15 N5 O9 F2 Cl
	386.0524	0.1	0.3	-0.5	1141.6	5.065	0.63	C9 H21 N O11 S Cl
	386.0521	0.4	1.0	12.5	1141.8	5.283	0.51	C19 H16 N O4 S2
	386.0529	-0.4	-1.0	0.5	1141.8	5.326	0.49	C5 H18 N9 O5 S Cl2
	386.0528	-0.3	-0.8	1.5	1142.1	5.563	0.38	C6 H15 N7 O5 F3 S2
	386.0519	0.6	1.6	9.5	1142.1	5.580	0.38	C11 H12 N7 O7 S
	386.0523	0.2	0.5	14.5	1142.5	5.942	0.26	C17 H10 N5 O2 F2 S
	386.0532	-0.7	-1.8	8.5	1142.5	5.979	0.25	C16 H17 N O5 F S2
	386.0530	-0.5	-1.3	5.5	1142.6	6.114	0.22	C8 H13 N7 O8 F S
	386.0526	-0.1	-0.3	9.5	1142.8	6.260	0.19	C18 H16 N O2 F2 Cl2
	386.0522	0.3	0.8	4.5	1142.9	6.370	0.17	C12 H18 N3 O7 Cl2
	386.0520	0.5	1.3	0.5	1143.0	6.470	0.15	C10 H20 N3 O4 F2 S Cl2
	386.0521	0.4	1.0	5.5	1143.0	6.496	0.15	C13 H15 N O7 F3 S
	386.0530	-0.5	-1.3	3.5	1143.2	6.721	0.12	C13 H22 N3 O2 S2 Cl2
	386.0519	0.6	1.6	2.5	1145.2	8.686	0.02	C5 H11 N7 O10 F3
	386.0525	0.0	0.0	18.5	1145.2	8.725	0.02	C19 H8 N5 O5
	386.0523	0.2	0.5	9.5	1145.5	8.938	0.01	C15 H13 N O10 F
	386.0530	-0.5	-1.3	23.5	1145.6	9.102	0.01	C25 H6 N3 F2
	386.0531	-0.6	-1.6	0.5	1145.8	9.254	0.01	C6 H16 N3 O16

Figure B.9: MS spectrum of compound 8a.

C Spectroscopic Data - Compound 8b

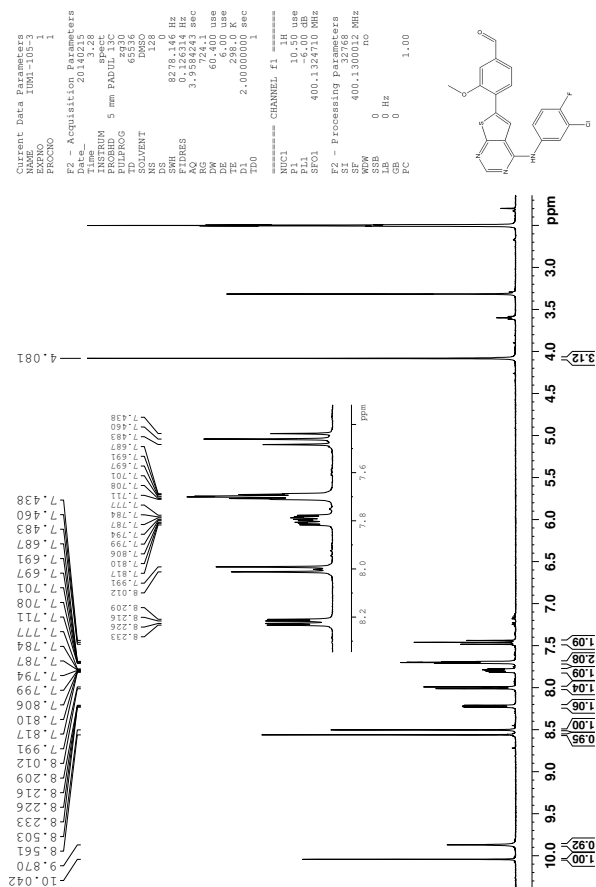


Figure C.1: ¹H-NMR spectrum of compound 8b.

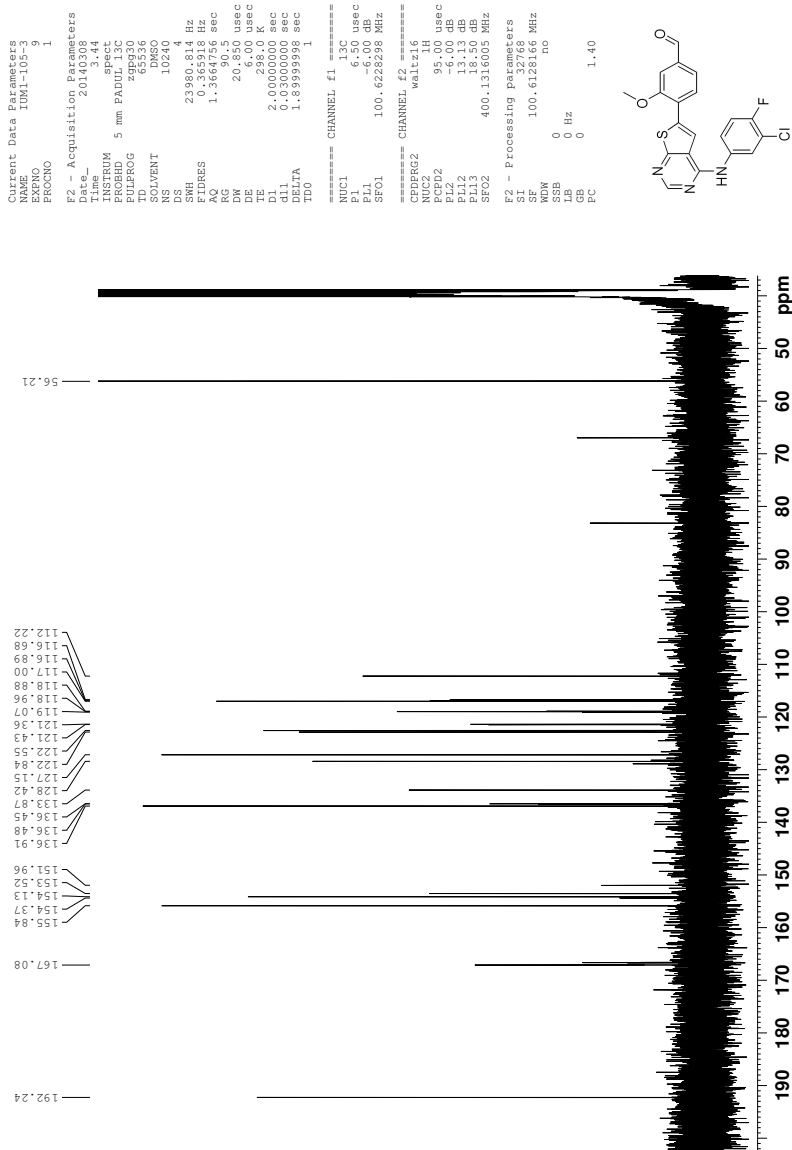
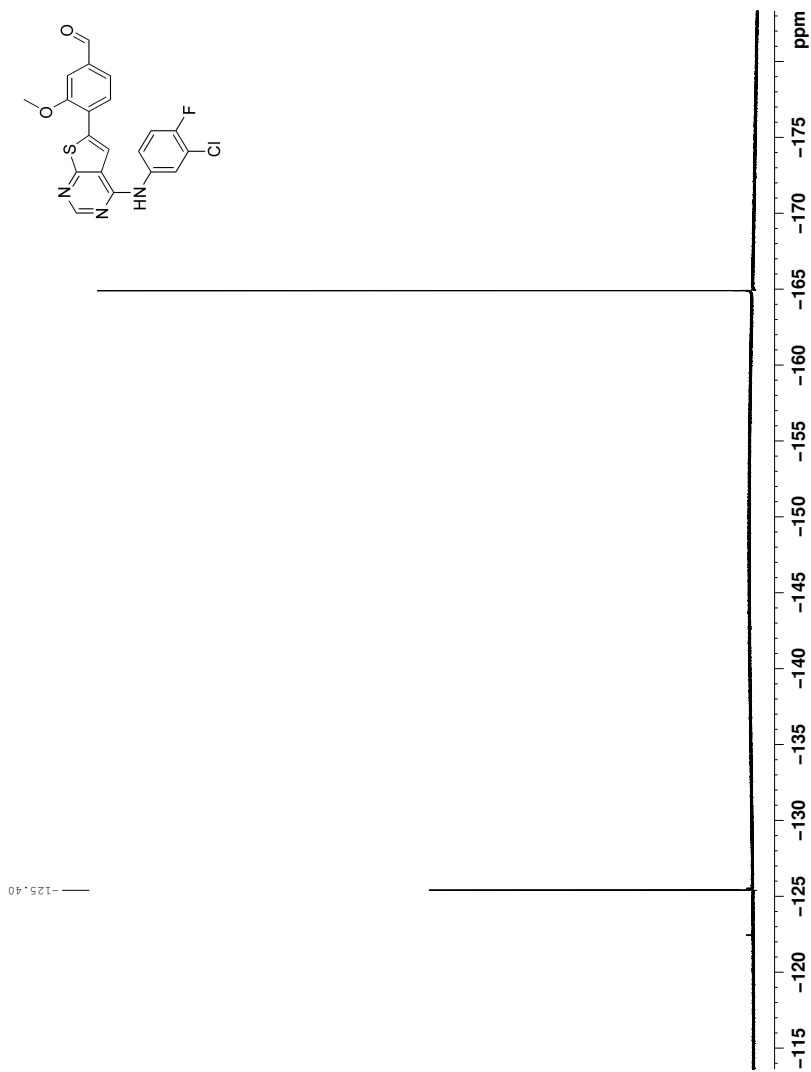


Figure C.2: ¹³C-NMR spectrum of compound 8b.

Figure C.3: ^{19}F -NMR spectrum of compound **8b** (decoupled).

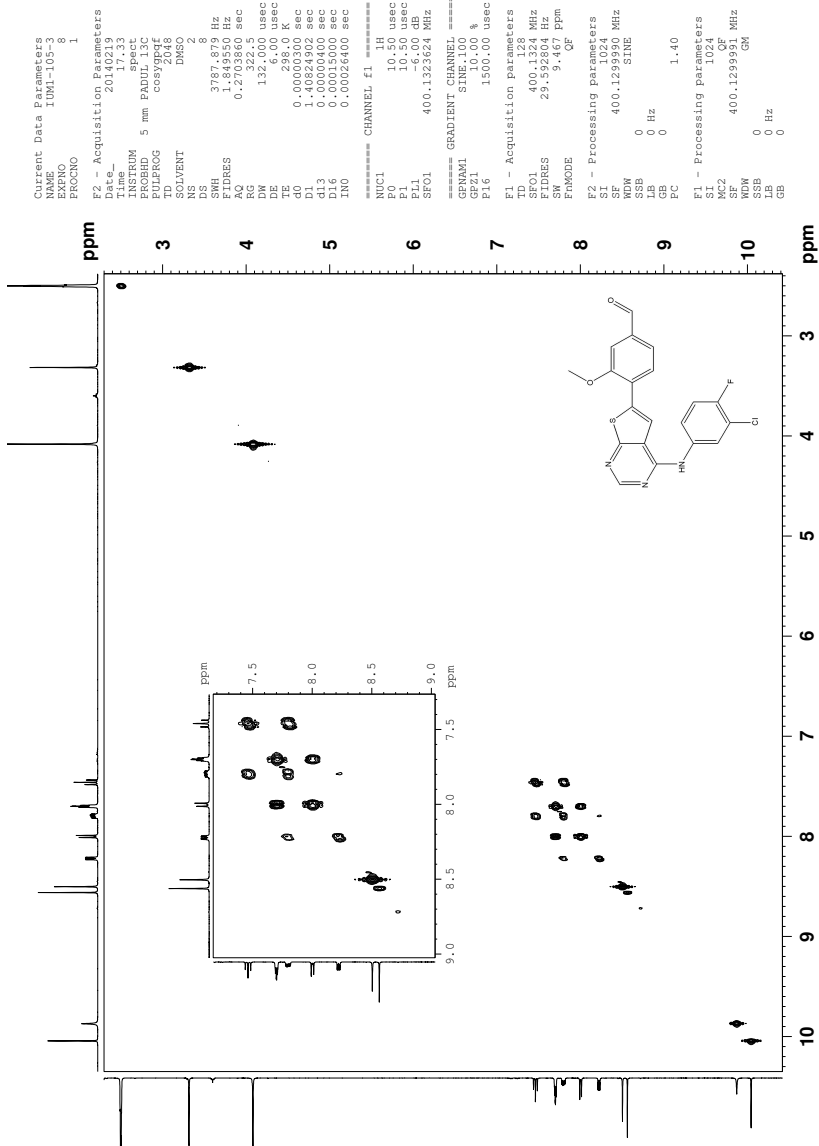


Figure C.4: COSY spectrum of compound 8b.

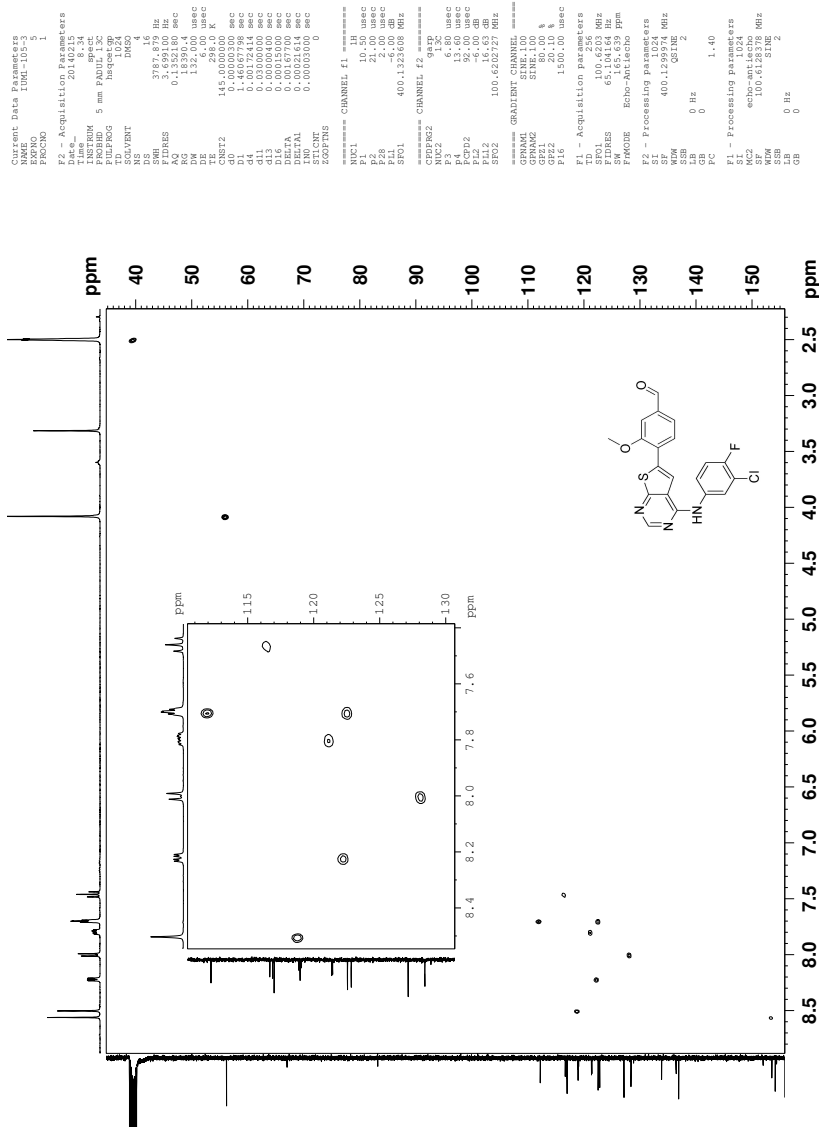


Figure C.5: HSQC spectrum of compound 8b.

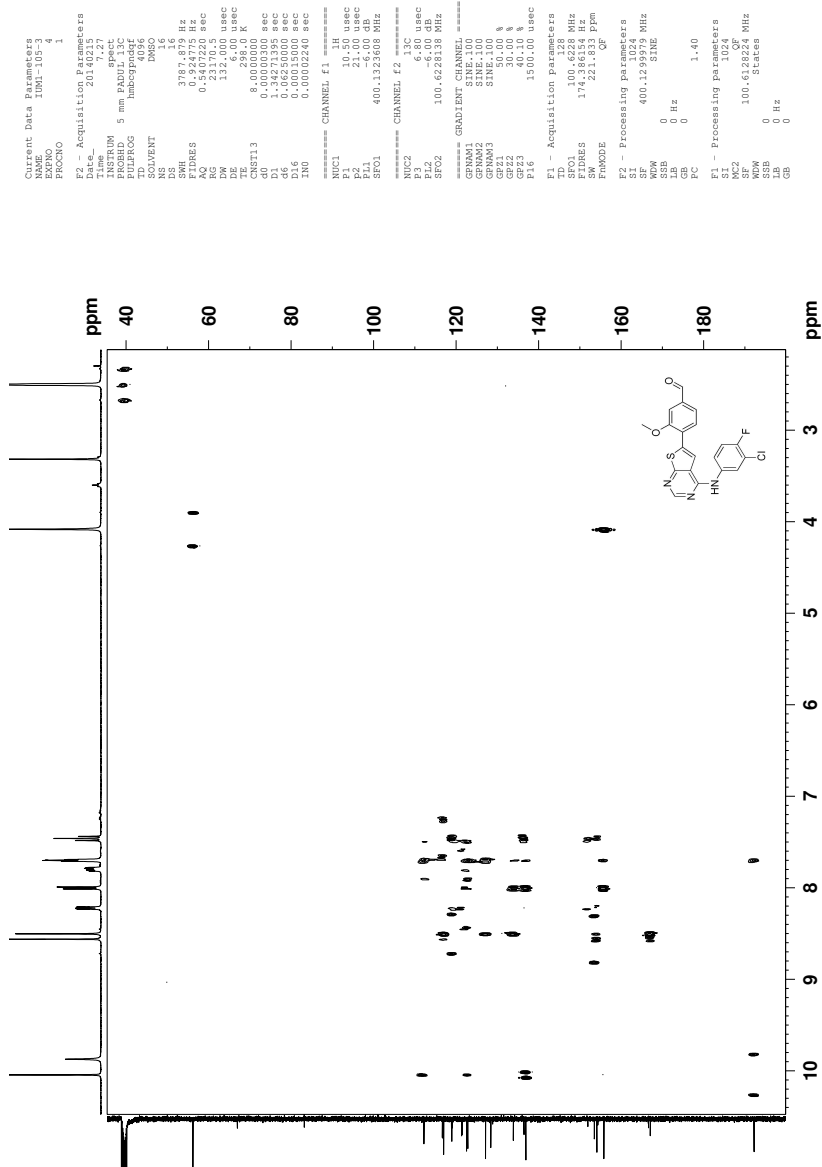


Figure C.6: HMBC spectrum of compound 8b.

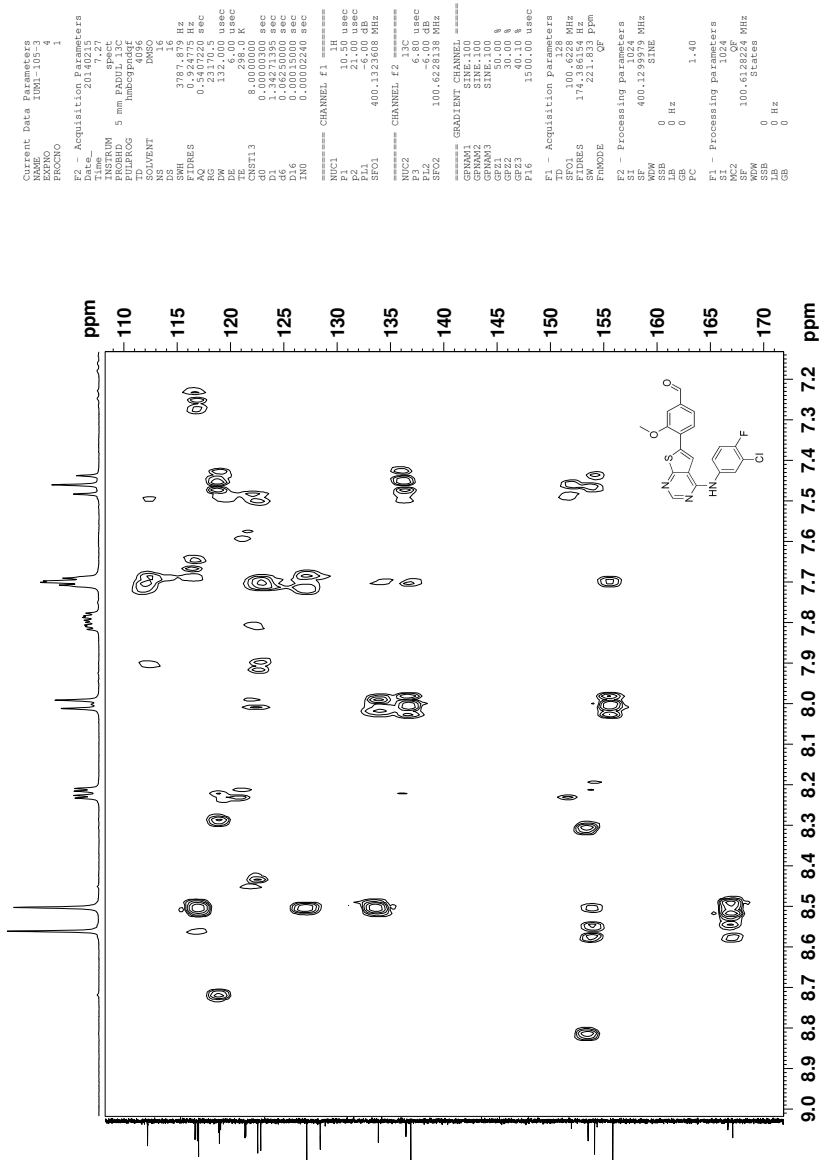
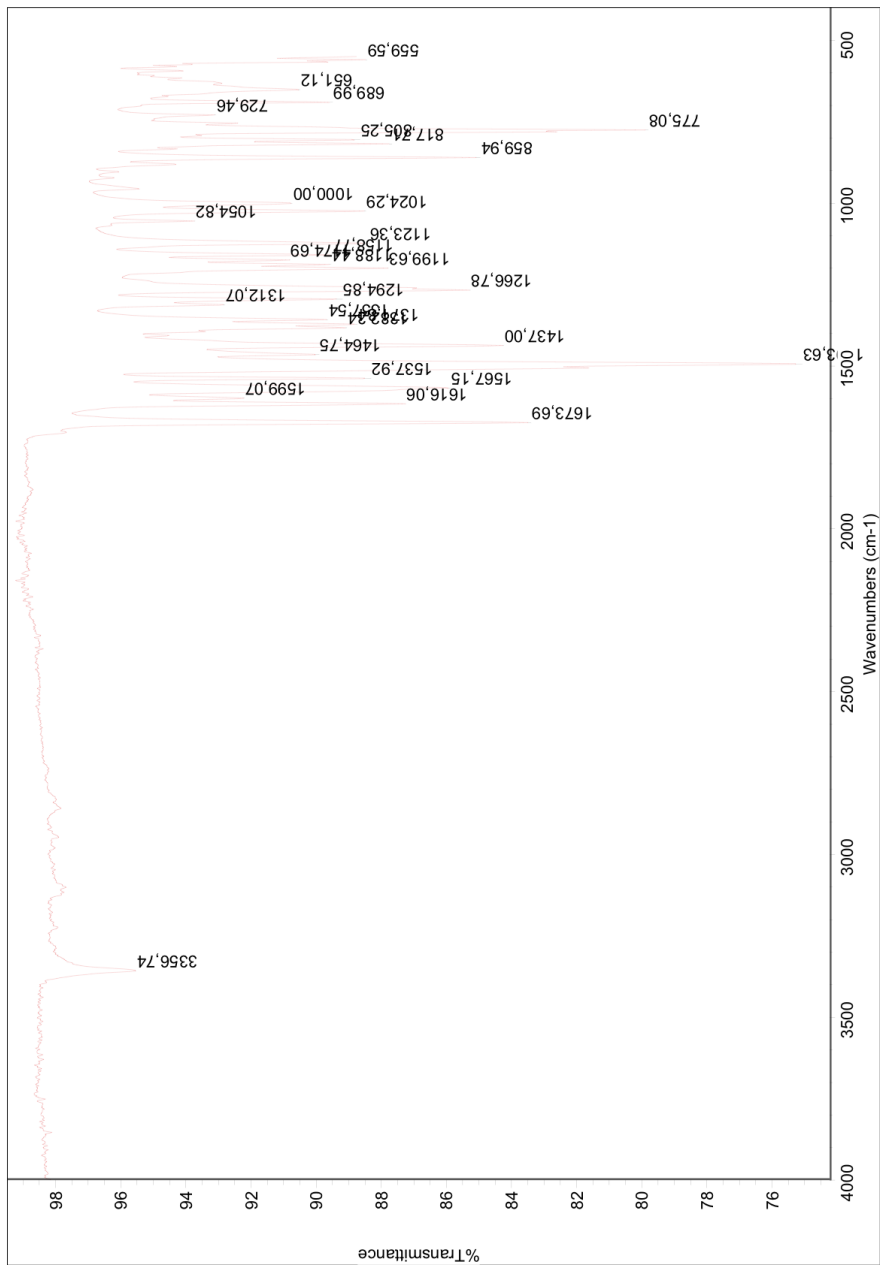


Figure C.7: Section of HMBC spectrum of compound 8b.

Figure C.8: IR spectrum of compound **8b**.

Elemental Composition Report

Single Mass Analysis

Tolerance = 3.0 PPM / DBE: min = -1.5, max = 50.0

Element prediction: Off

Number of isotope peaks used for i-FIT = 3

Monoisotopic Mass, Even Electron Ions

17012 formula(e) evaluated with 61 results within limits (all results (up to 1000) for each mass)

Elements Used:

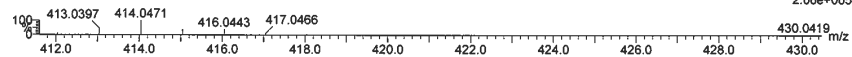
C: 0-500 H: 0-1000 N: 3-100 O: 0-100 F: 1-3 S: 0-3 Cl: 0-3

21-Feb-2014

2016-20 311 (6.047) AM2 (Ar,35000.0,0.00,0.00)

1: TOF MS ASAP+

2.06e+005



Minimum: -1.5
Maximum: 50.0

Mass	Calc. Mass	mDa	PPM	DBE	i-FIT	Norm	Conf (%)	Formula
414.0471	414.0464	0.7	1.7	-1.5	39.5	10.185	0.00	H13 N9 O16 F
	414.0479	-0.8	-1.9	24.5	39.5	10.178	0.00	C26 H6 N3 O F2
	414.0478	-0.7	-1.7	3.5	39.4	10.128	0.00	C H9 N13 O12 F
	414.0482	-1.1	-2.7	8.5	39.4	10.044	0.00	C7 H7 N11 O7 F3
	414.0469	0.2	0.5	3.5	39.3	10.035	0.00	C6 H11 N7 O11 F3
	414.0468	0.3	0.7	28.5	39.1	9.836	0.01	C29 H5 N3 F
	414.0471	0.0	0.0	12.5	38.9	9.631	0.01	C10 H6 N11 O6 F2
	414.0464	0.7	1.7	21.5	38.9	9.616	0.01	C19 H3 N9 F3
	414.0478	-0.7	-1.7	2.5	38.7	9.350	0.01	C11 H18 N5 O2 F3 Cl3
	414.0459	1.2	2.9	16.5	38.6	9.288	0.01	C13 H5 N11 O5 F
	414.0473	-0.2	-0.5	21.5	38.5	9.201	0.01	C14 H N15 O F
	414.0467	0.4	1.0	6.5	38.4	9.111	0.01	C14 H17 N5 O F2 Cl3
	414.0482	-1.1	-2.7	1.5	37.9	8.553	0.02	C10 H19 N3 O9 F Cl2
	414.0477	-0.6	-1.4	0.5	37.8	8.481	0.02	C12 H24 N3 F2 S3 Cl2
	414.0469	0.2	0.5	1.5	37.5	8.218	0.03	C11 H20 N3 O5 F2 S Cl2
	414.0466	0.5	1.2	1.5	37.5	8.165	0.03	C8 H17 N3 O13 F S
	414.0479	-0.8	-1.9	6.5	37.4	8.056	0.03	C9 H13 N7 O9 F S
	414.0482	-1.1	-2.7	6.5	37.3	8.005	0.03	C12 H16 N7 O F2 S Cl2
	414.0472	-0.1	-0.2	15.5	37.0	7.735	0.04	C18 H10 N5 O3 F2 S
	414.0471	0.0	0.0	10.5	36.9	7.609	0.05	C15 H15 N7 F S Cl2
	414.0477	-0.6	-1.4	2.5	36.9	7.555	0.05	C7 H15 N7 O6 F3 S2
	414.0460	1.1	2.7	7.5	36.7	7.422	0.06	C12 H13 N7 O2 F3 Cl2
	414.0475	-0.4	-1.0	0.5	36.7	7.359	0.06	C9 H21 N3 O8 F S3
	414.0464	0.7	1.7	1.5	36.6	7.268	0.07	C7 H19 N9 O2 F S2 Cl2
	414.0461	1.0	2.4	19.5	36.6	7.257	0.07	C21 H9 N5 O2 F S
	414.0479	-0.8	-1.9	11.5	36.6	7.245	0.07	C11 H10 N11 O F2 S2
	414.0466	0.5	1.2	6.5	36.5	7.224	0.07	C10 H14 N7 O5 F2 S2
	414.0468	0.3	0.7	15.5	36.1	6.789	0.11	C14 H9 N11 F S2
	414.0469	-0.5	-1.2	2.5	36.0	6.718	0.12	C8 H15 N5 O10 F2 Cl1
	414.0476	-0.5	-1.2	7.5	35.9	6.587	0.14	C7 H11 N13 O3 F Cl2
	414.0469	0.2	0.5	7.5	35.9	6.429	0.16	C3 H16 N9 O8 F2 Cl2
	414.0467	0.4	1.0	-1.5	35.7	6.425	0.16	C4 H12 N13 O4 F2 Cl2
	414.0480	-0.9	-2.2	3.5	35.7	6.425	0.16	C5 H13 N13 F3 S Cl2
	414.0467	0.4	1.0	3.5	35.6	6.258	0.19	C5 H13 N13 F3 S Cl2
	414.0471	0.0	0.0	1.5	35.5	6.232	0.20	C10 H20 N5 O F3 S3 Cl1
	414.0462	0.9	2.2	2.5	35.5	6.185	0.21	C9 H16 N5 O6 F3 S Cl1
	414.0466	0.5	1.2	12.5	35.4	6.138	0.22	C6 H5 N17 O3 F S
	414.0461	1.0	2.4	6.5	35.4	6.083	0.23	C6 H13 N13 O2 F S3
	414.0464	0.7	1.7	8.5	35.4	6.061	0.23	C4 H7 N17 F3 S2
	414.0464	0.7	1.7	6.5	35.3	6.011	0.25	C11 H14 N5 O9 F Cl1
	414.0473	-0.2	-0.5	5.5	35.2	5.923	0.27	C12 H18 N5 O4 F S2 Cl1
	414.0459	1.2	2.9	5.5	35.0	5.713	0.33	C13 H19 N5 F2 S3 Cl1
	414.0473	-0.2	-0.5	2.5	35.0	5.657	0.35	C3 H14 N13 O3 F2 S3
	414.0475	-0.4	-1.0	7.5	35.0	5.642	0.35	C10 H12 N9 O2 F3 S Cl1
	414.0480	-0.9	-2.2	1.5	34.9	5.620	0.36	C5 H18 N11 O2 F S3 Cl1
	414.0477	-0.6	-1.4	8.5	34.9	5.586	0.37	C3 H6 N17 O4 F2 S
	414.0477	-0.6	-1.4	11.5	34.8	5.459	0.43	C12 H10 N9 O5 F Cl1
	414.0471	0.0	0.0	2.5	34.4	5.127	0.59	C4 H14 N11 O7 F S Cl1
	414.0468	0.3	0.7	11.5	34.4	5.074	0.63	C17 H12 N3 O4 F3 Cl1
	414.0464	0.7	1.7	11.5	34.2	4.887	0.75	C13 H11 N9 O F2 S Cl1
	414.0460	1.1	2.7	3.5	34.1	4.791	0.83	C2 H12 N17 O F Cl3
	414.0482	-1.1	-2.7	3.5	33.9	4.567	1.04	C3 H12 N15 F3 S2 Cl1
	414.0464	0.7	1.7	3.5	33.9	4.556	1.05	C2 H10 N13 O8 F2 S
	414.0482	-1.1	-2.7	16.5	33.8	4.456	1.16	C18 H8 N7 F3 Cl1
	414.0462	0.9	2.2	8.5	33.7	4.362	1.28	C5 H7 N15 O4 F2 Cl1
	414.0479	-0.8	-1.9	14.5	33.7	4.360	1.28	C20 H14 N3 O2 F S Cl1
	414.0482	-1.1	-2.7	-1.5	33.6	4.291	1.37	C H15 N11 O8 F2 S Cl1

Figure C.9: MS spectrum of compound 8b.

D Spectroscopic Data - Compound 8c

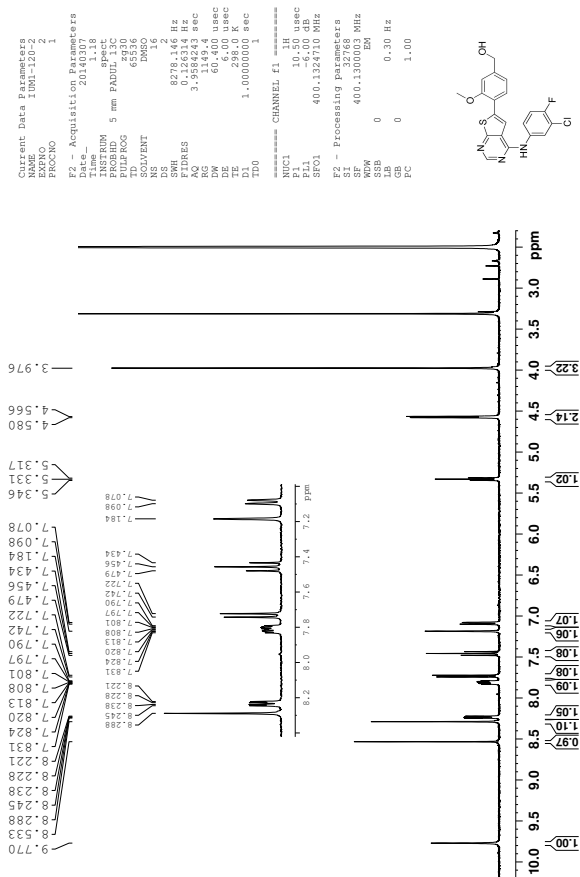


Figure D.1: ¹H-NMR spectrum of compound **8c**.

D SPECTROSCOPIC DATA - COMPOUND 8C

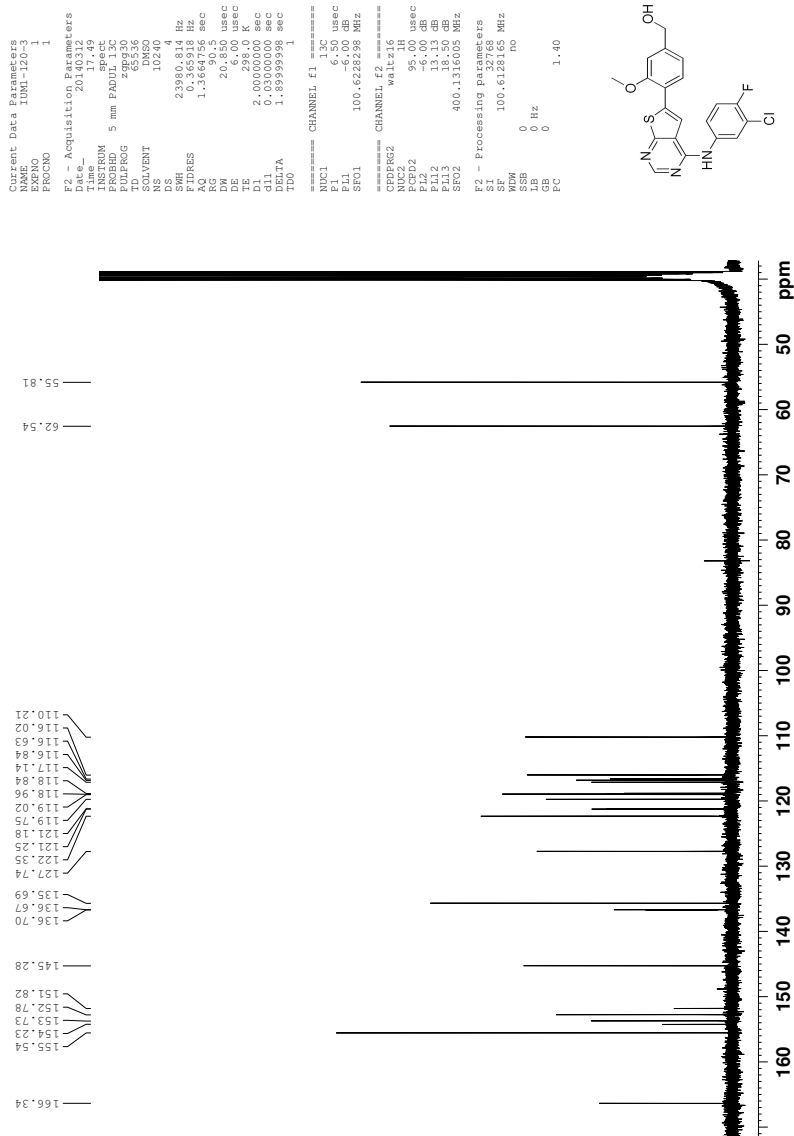
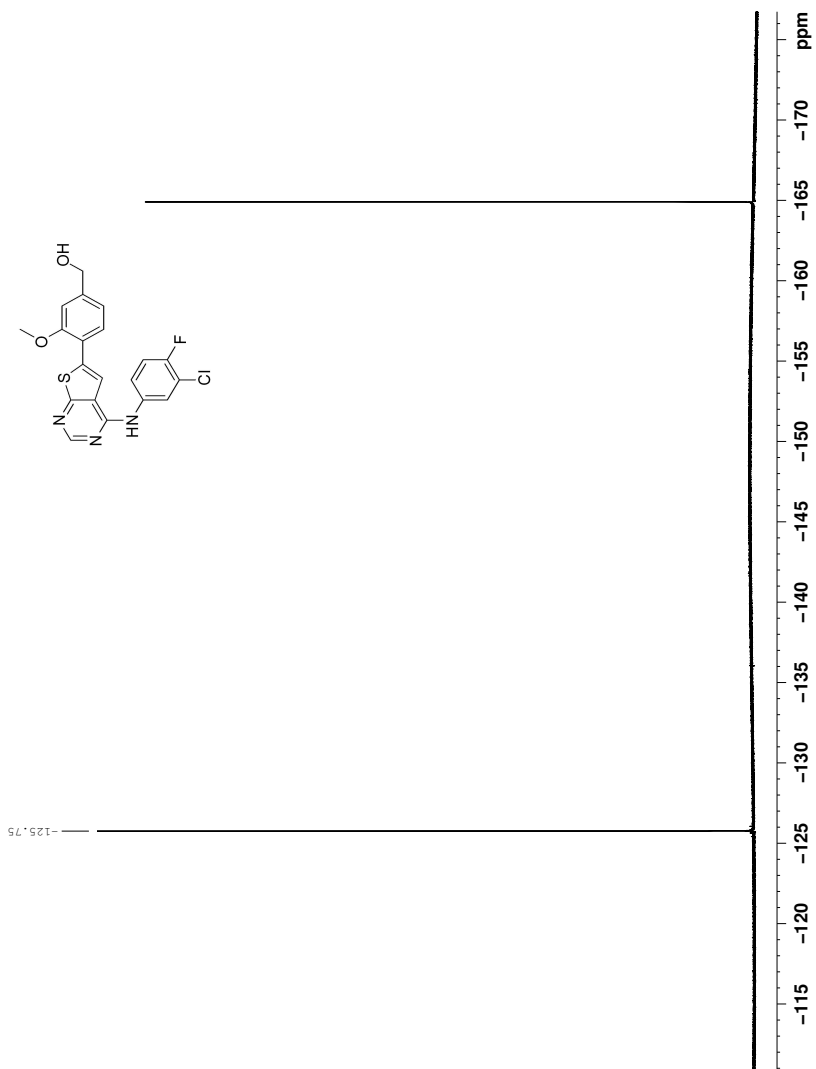


Figure D.2: ^{13}C -NMR spectrum of compound 8c.

Figure D.3: ^{19}F -NMR spectrum of compound **8c** (decoupled).

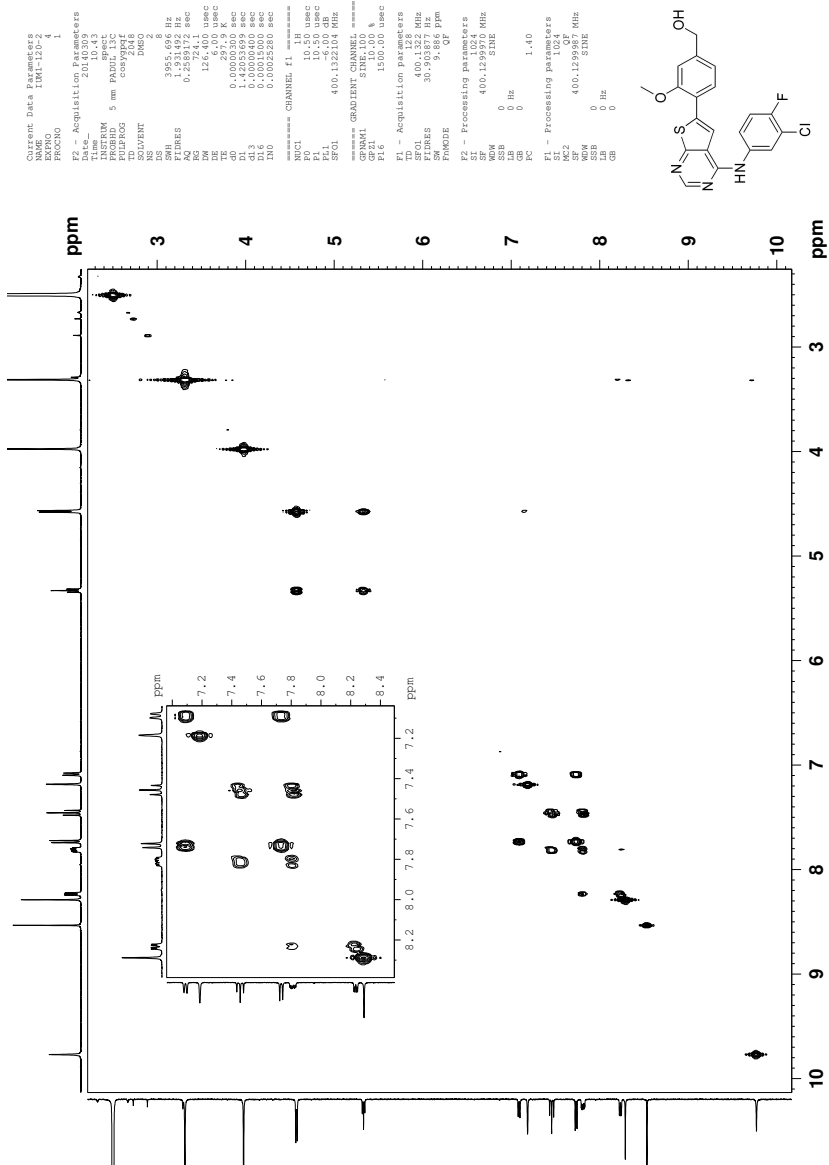


Figure D.4: COSY spectrum of compound 8c.

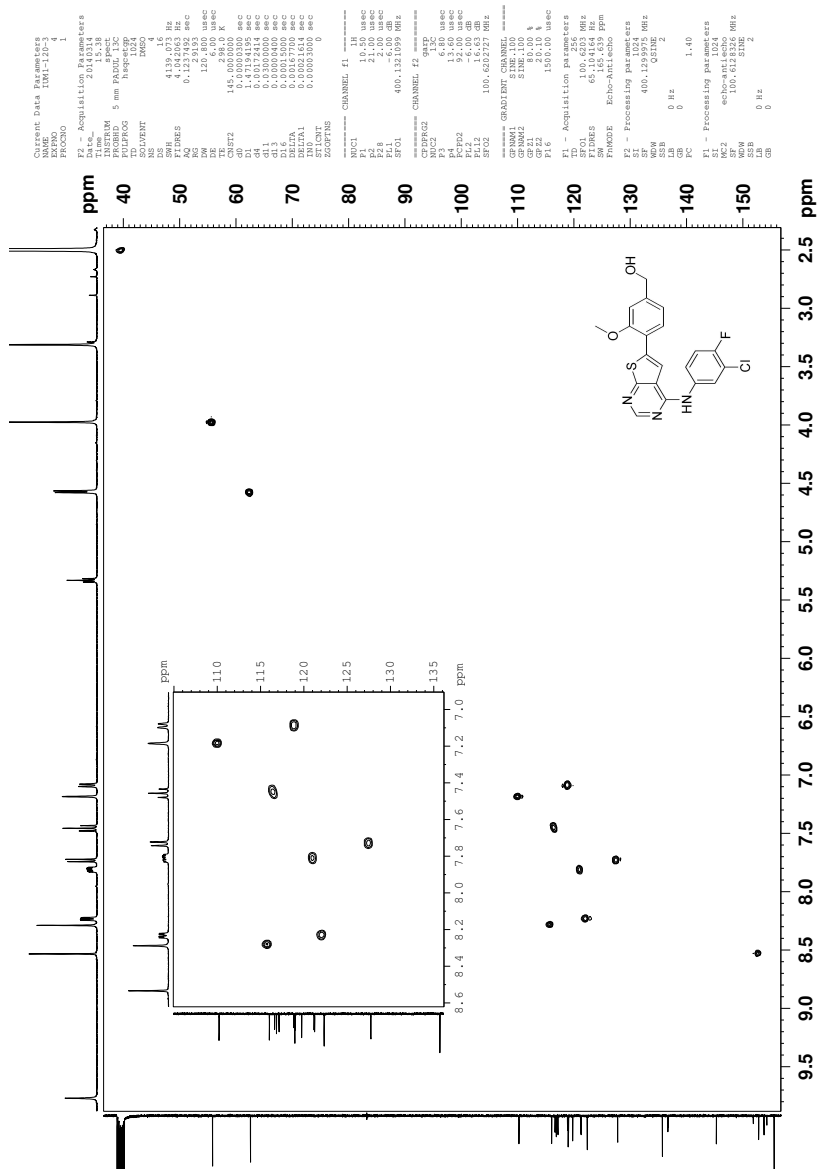


Figure D.5: HSQC spectrum of compound 8c.

D SPECTROSCOPIC DATA - COMPOUND 8C

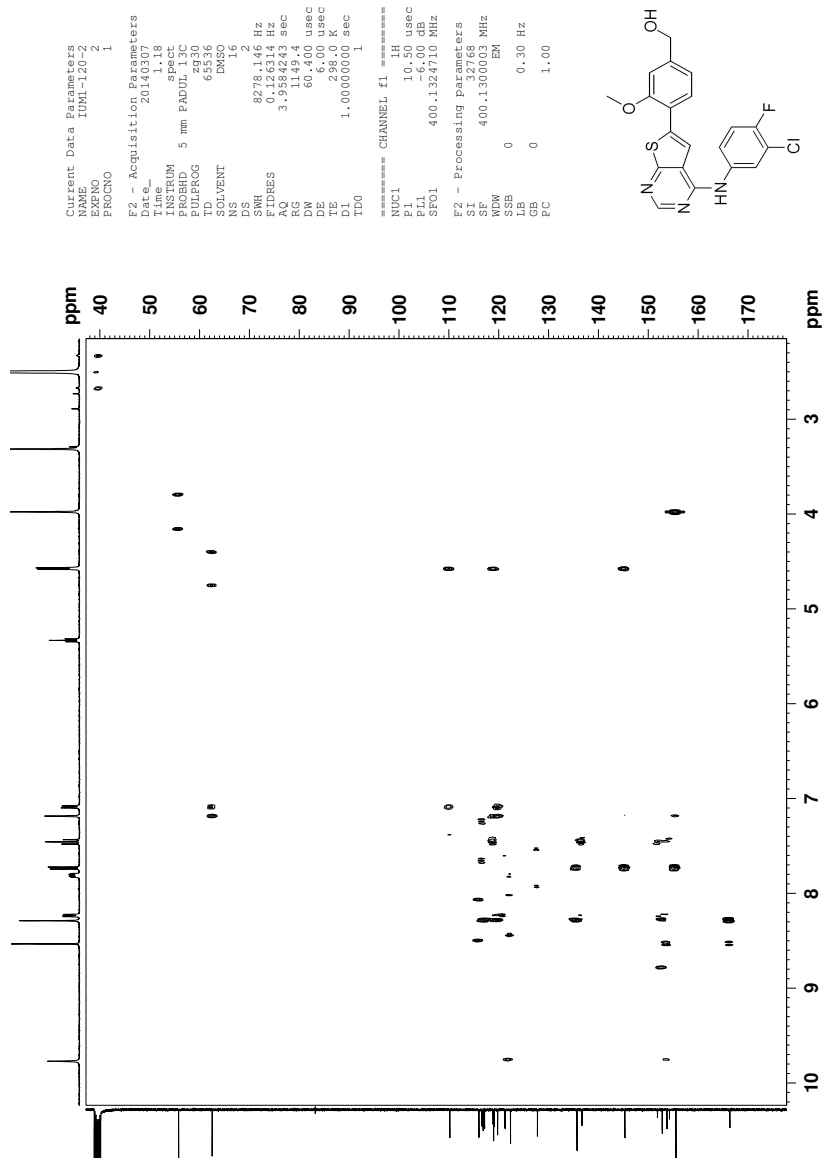


Figure D.6: HMBC spectrum of compound 8c.

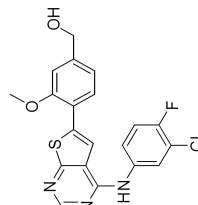
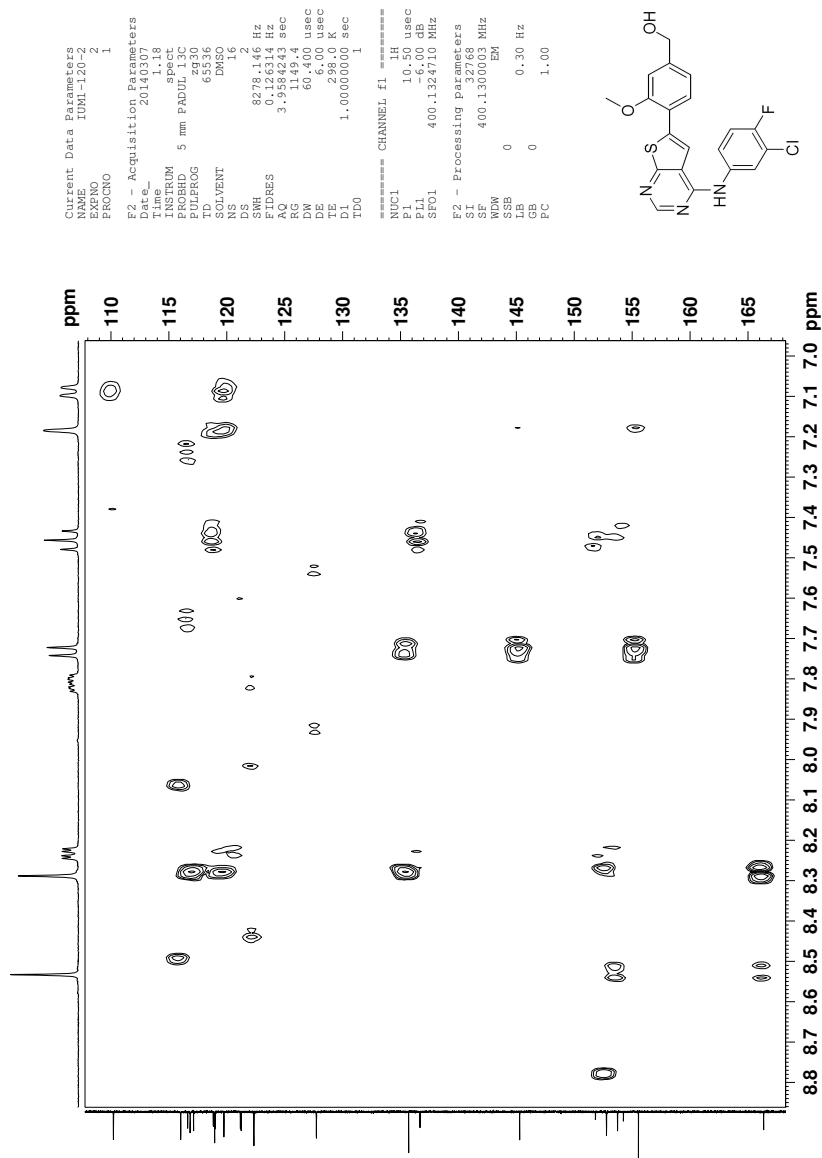
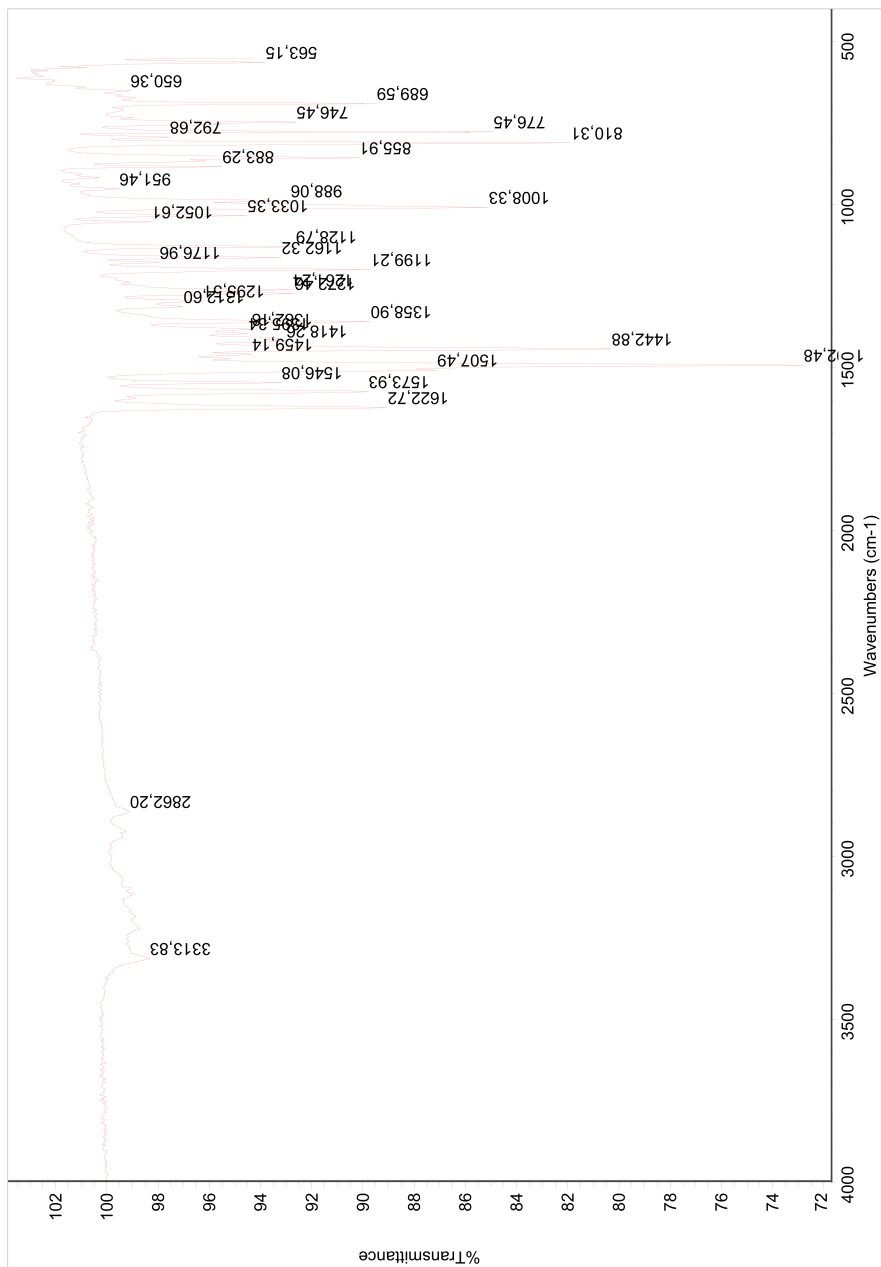


Figure D.7: Section of HMBC spectrum of compound 8c.

Figure D.8: IR spectrum of compound **8c**.

D SPECTROSCOPIC DATA - COMPOUND 8C

Elemental Composition Report

Page 1

Single Mass Analysis

Tolerance = 2.0 PPM / DBE: min = -1.5, max = 50.0

Element prediction: Off

Number of isotope peaks used for i-FIT = 3

Monoisotopic Mass, Even Electron Ions

47471 formula(e) evaluated with 67 results within limits (all results (up to 1000) for each mass)

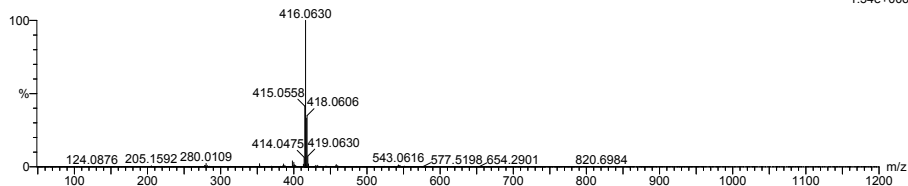
Elements Used:

C: 0-200 H: 0-1000 N: 0-10 O: 0-200 F: 0-3 S: 0-2 Cl: 0-2 K: 0-3

NT-MSLAB-Operator-SVG

2014-40 177 (3.464) AM2 (Ar,35000.0,0.00,0.00)

1: TOF MS ASAP+
1.54e+006



Minimum: -1.5
Maximum: 50.0

Mass	Calc. Mass	mDa	PPM	DBE	i-FIT	Norm	Conf(%)	Formula
416.0630	416.0624	0.6	1.4	17.5	1138.2	1.284	27.70	C23 H15 N3 O S Cl
	416.0638	-0.8	-1.9	15.5	1139.4	2.458	8.56	C18 H10 N7 F3 Cl
	416.0623	0.7	1.7	14.5	1139.4	2.536	8.08	C15 H11 N9 O4 Cl
	416.0636	-0.6	-1.4	13.5	1139.6	2.647	7.09	C20 H16 N3 O2 F S Cl
	416.0625	0.5	1.2	10.5	1140.1	3.178	4.17	C17 H14 N3 O4 F3 Cl
	416.0635	-0.5	-1.2	5.5	1140.4	3.506	3.00	C16 H24 N3 O S2 K
	416.0631	-0.1	-0.2	10.5	1140.5	3.554	2.86	C20 H18 N O2 F2 Cl K
	416.0634	-0.4	-1.0	10.5	1140.5	3.589	2.76	C12 H12 N9 O5 F Cl
	416.0623	0.7	1.7	-1.5	1140.6	3.672	2.54	C4 H18 N9 O7 F2 Cl K
	416.0630	0.0	0.0	2.5	1140.6	3.691	2.49	C16 H26 N O F S K3
	416.0631	-0.1	-0.2	-1.5	1140.6	3.718	2.43	C6 H22 N9 O F2 S2 K2
	416.0632	-0.2	-0.5	6.5	1140.8	3.851	2.13	C10 H14 N9 O2 F3 S Cl
	416.0622	0.8	1.9	-0.5	1141.0	4.068	1.71	C5 H18 N9 O6 F2 K2
	416.0633	-0.3	-0.7	2.5	1141.2	4.292	1.37	C8 H20 N9 O4 S K2
	416.0629	0.1	0.2	4.5	1141.2	4.307	1.35	C12 H20 N5 O4 F S2 Cl
	416.0624	0.6	1.4	18.5	1141.2	4.342	1.30	C24 H15 N3 S K
	416.0634	-0.4	-1.0	1.5	1141.4	4.460	1.16	C7 H20 N9 O5 S Cl K
	416.0629	0.1	0.2	-0.5	1141.4	4.503	1.11	C8 H22 N7 O4 F K3
	416.0627	0.3	0.7	5.5	1141.4	4.516	1.09	C14 H20 N3 O7 Cl K
	416.0638	-0.8	-1.9	6.5	1141.4	4.517	1.09	C13 H18 N7 F2 S Cl K
	416.0624	0.6	1.4	2.5	1141.5	4.567	1.04	C13 H22 N3 O3 F2 S K2
	416.0629	0.1	0.2	5.5	1141.5	4.600	1.00	C13 H20 N5 O3 F S2 K
	416.0631	-0.1	-0.2	11.5	1141.6	4.736	0.88	C21 H18 N O F2 K2
	416.0625	0.5	1.2	1.5	1141.9	4.948	0.71	C12 H22 N3 O4 F2 S Cl K
	416.0632	-0.2	-0.5	1.5	1141.9	4.995	0.68	C8 H17 N5 O10 F2 Cl
	416.0626	0.4	1.0	6.5	1141.9	5.009	0.67	C15 H20 N3 O6 K2
	416.0636	-0.6	-1.4	4.5	1141.9	5.038	0.65	C15 H24 N3 O2 S2 Cl K
	416.0635	-0.5	-1.2	14.5	1142.0	5.060	0.63	C21 H16 N3 O F S K
	416.0629	0.1	0.2	-1.5	1142.0	5.063	0.63	C7 H22 N7 O5 F Cl K2
	416.0631	-0.1	-0.2	7.5	1142.0	5.064	0.63	C11 H14 N9 O F3 S K
	416.0633	-0.3	-0.7	3.5	1142.0	5.090	0.62	C13 H20 N5 F3 Cl K2
	416.0622	0.8	1.9	15.5	1142.0	5.141	0.59	C16 H11 N9 O3 K
	416.0626	0.4	1.0	12.5	1142.1	5.229	0.54	C20 H18 N O5 S2
	416.0629	0.1	0.2	-0.5	1142.3	5.346	0.48	C10 H23 N O12 S Cl
	416.0622	0.8	1.9	5.5	1142.3	5.416	0.44	C10 H16 N7 O5 F2 S2
	416.0636	-0.6	-1.4	-1.5	1142.3	5.440	0.43	C10 H23 N3 O4 F3 S K2
	416.0638	-0.8	-1.9	1.5	1142.4	5.457	0.43	C11 H21 N3 O8 F Cl K
	416.0631	-0.1	-0.2	1.5	1142.5	5.625	0.36	C15 H26 N O2 F S Cl K2
	416.0625	0.5	1.2	9.5	1142.6	5.667	0.35	C12 H14 N7 O8 S
	416.0634	-0.4	-1.0	1.5	1142.6	5.739	0.32	C7 H17 N7 O6 F3 S2
	416.0633	-0.3	-0.7	11.5	1142.7	5.810	0.30	C13 H12 N9 O4 F K
	416.0624	0.6	1.4	11.5	1142.8	5.861	0.28	C18 H14 N3 O3 F3 K
	416.0634	-0.4	-1.0	0.5	1142.8	5.890	0.28	C6 H20 N9 O6 S Cl2
	416.0638	-0.8	-1.9	2.5	1142.8	5.905	0.27	C12 H21 N3 O7 F K2
	416.0629	0.1	0.2	0.5	1142.9	5.962	0.26	C11 H23 N O11 S K
	416.0638	-0.8	-1.9	8.5	1142.9	5.983	0.25	C17 H19 N O6 F S2
	416.0629	0.1	0.2	14.5	1142.9	5.991	0.25	C18 H12 N5 O3 F2 S
	416.0635	-0.5	-1.2	-1.5	1142.9	6.009	0.25	C10 H26 N5 O3 Cl K3
	416.0627	0.3	0.7	9.5	1143.1	6.224	0.20	C15 H17 N7 F S Cl2
	416.0636	-0.6	-1.4	5.5	1143.2	6.283	0.19	C9 H15 N7 O9 F S
	416.0623	0.7	1.7	0.5	1143.2	6.342	0.18	C8 H19 N3 O13 F S
	416.0631	-0.1	-0.2	2.5	1143.3	6.398	0.17	C9 H17 N5 O9 F2 K
	416.0627	0.3	0.7	5.5	1143.5	6.556	0.14	C14 H17 N O8 F3 K

Figure D.9: MS spectrum of compound 8c, page 1.

XXX

Elemental Composition Report

Page 2

Single Mass Analysis

Tolerance = 2.0 PPM / DBE: min = -1.5, max = 50.0

Element prediction: Off

Number of isotope peaks used for i-FIT = 3

Monoisotopic Mass, Even Electron Ions

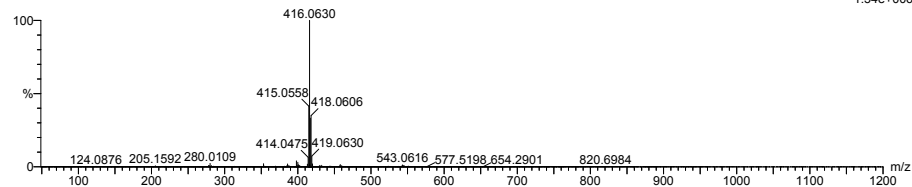
47471 formula(e) evaluated with 67 results within limits (all results (up to 1000) for each mass)

Elements Used:

C: 0-200 H: 0-1000 N: 0-10 O: 0-200 F: 0-3 S: 0-2 Cl: 0-2 K: 0-3

NT-MSLAB-Operator-SVG

2014-40 177 (3.464) AM2 (Ar,35000.0,0.00,0.00)

1: TOF MS ASAP+
1.54e+006

Minimum: -1.5
Maximum: 50.0

Mass	Calc. Mass	mDa	PPM	DBE	i-FIT	Norm	Conf(%)	Formula
416.0627	0.3	0.7	0.5	1143.5	6.641	0.13	C10 H25 N7 S2 Cl2 K	
416.0632	-0.2	-0.5	9.5	1143.6	6.653	0.13	C19 H18 N O3 F2 Cl2	
416.0623	0.7	1.7	6.5	1143.6	6.654	0.13	C15 H19 N5 F2 Cl2 K	
416.0627	0.3	0.7	4.5	1143.6	6.724	0.12	C13 H20 N3 O8 Cl2	
416.0625	0.5	1.2	0.5	1143.8	6.850	0.11	C11 H22 N3 O5 F2 S Cl2	
416.0634	-0.4	-1.0	2.5	1143.9	7.008	0.09	C12 H20 N5 O F3 Cl2 K	
416.0636	-0.6	-1.4	3.5	1144.0	7.096	0.08	C14 H24 N3 O3 S2 Cl2	
416.0632	-0.2	-0.5	0.5	1144.4	7.468	0.06	C14 H26 N O3 F S Cl2 K	
416.0624	0.6	1.4	27.5	1145.6	8.732	0.02	C29 H7 N3 F	
416.0631	-0.1	-0.2	18.5	1145.7	8.771	0.02	C20 H10 N5 O6	
416.0625	0.5	1.2	2.5	1145.7	8.808	0.01	C6 H13 N7 O11 F3	
416.0629	0.1	0.2	9.5	1145.9	9.006	0.01	C16 H15 N O11 F	
416.0635	-0.5	-1.2	23.5	1146.0	9.095	0.01	C26 H8 N3 O F2	
416.0636	-0.6	-1.4	0.5	1146.3	9.364	0.01	C7 H18 N3 O17	

Figure D.10: MS spectrum of compound 8c, page 2.


```

Current Data Parameters
NAME      TUM-11-7
EXPNO    1
PROCNO   1
F2 - Acquisition Parameters
Time     2013.53
PULPROG  zgpg30
PCPDPRG2 5 mm PAMPR13
SOLVENT   DMSO
NS        812
SMH       23880.814 Hz
FIDRES    0.36928 Hz
RG         1.0176
AQ         1.0176 sec
DWDW      20.860 usec
TE         298.0 K
DELTA     6.000000 sec
d11       1.8899998 sec
TD        100
===== CHANNEL f1 =====
NUC1      13C
P11       6.50 usec
PL1       6.50 dB
SFO1      100.6282629 MHz
===== CHANNEL f2 =====
NUC2      13C
P12       6.50 usec
PL2       6.50 dB
SFO2      100.6282629 MHz
F2 - Processing Parameters
SI         32768
SF         100.628170 MHz
GB         0 Hz
PC         1.40
  
```

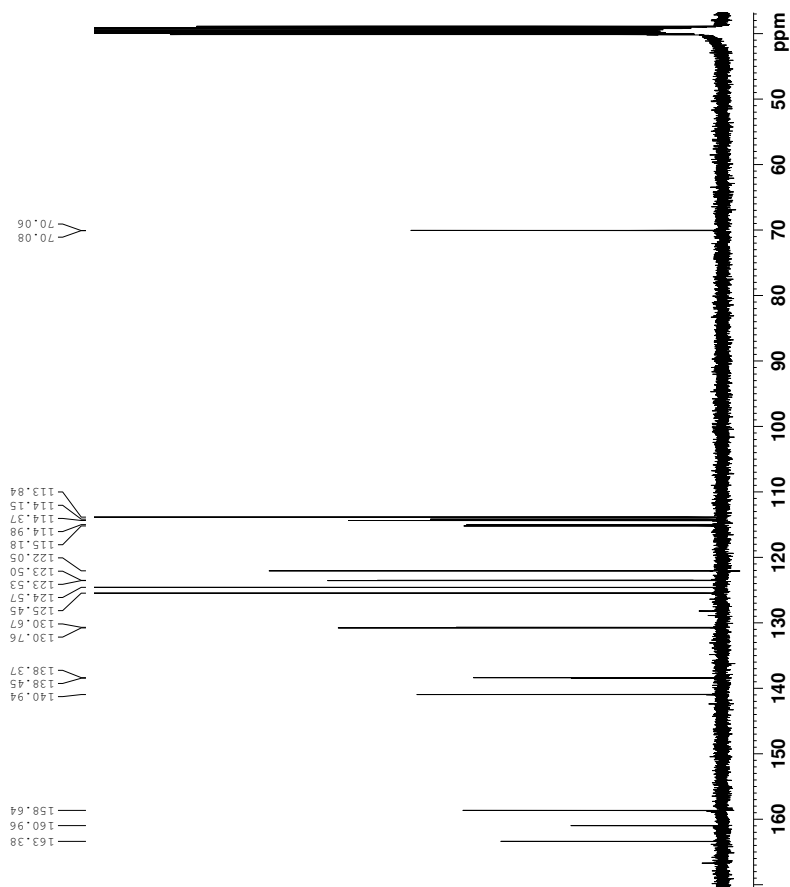
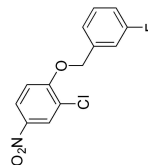
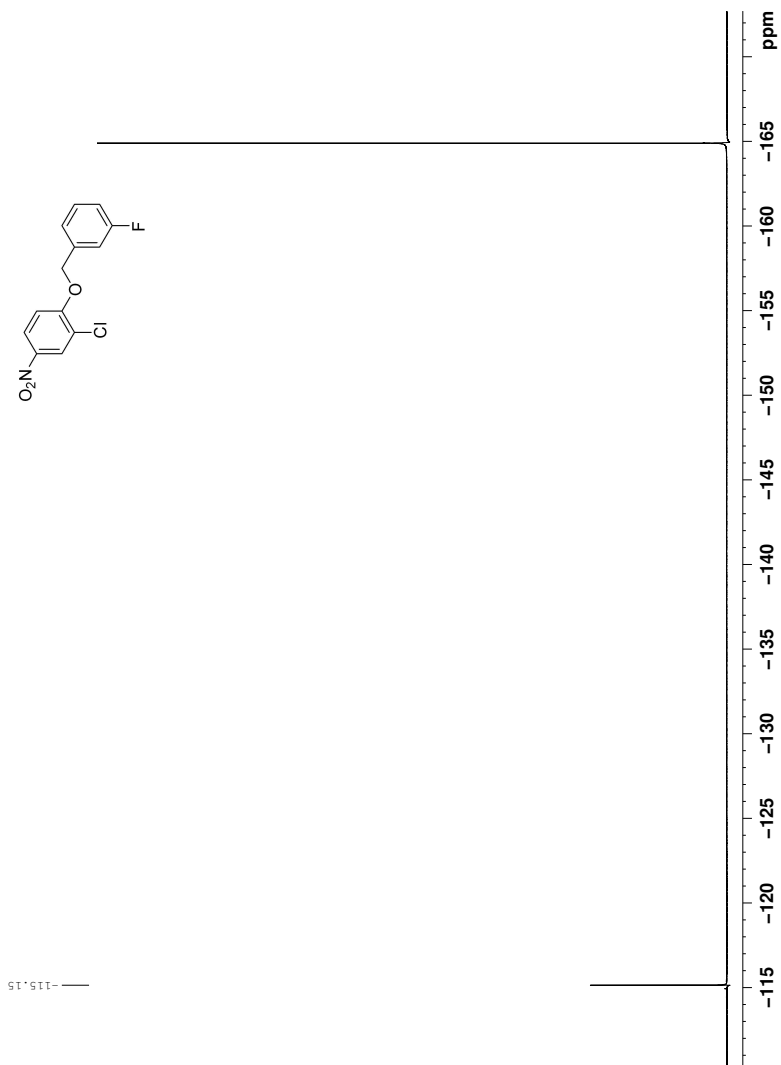
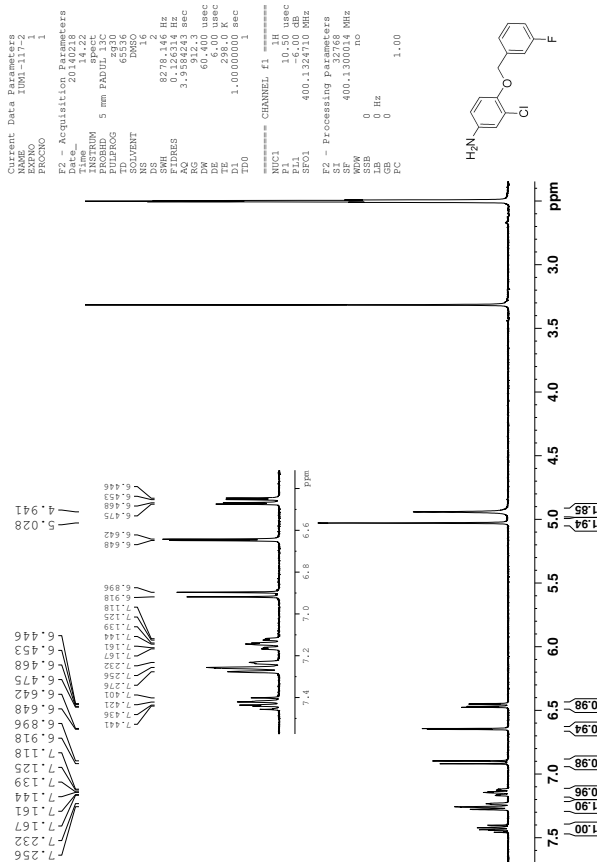


Figure E.2: ¹³C-NMR spectrum of compound 11.

Figure E.3: ^{19}F -NMR spectrum of compound 11 (decoupled).

F Spectroscopic Data - Compound 12

Figure F.1: $^1\text{H-NMR}$ spectrum of compound 12.

```

Current Data Parameters
NAME      IUMI-117-2
EXNO     3
PROCNO   1

F2 - Acquisition Parameters
Date_    20190224
Time     8:24
INSTRUM  spect
PROBHD   5 mm PABUL13
PULPROG  zgpg30
TD       65536
SOLVENT  DMSO
DS       51.4
SS       4
SMH      23980.814 Hz
AQC      0.665756 Hz
RG        128
RG2       128
RG3       128
AQ        20.850 usec
TE        300.0 K
D1        2.00000000 sec
DELTA     0.85999998 sec
TDO       1
===== CHANNEL f1 =====
NUC1      13C
P1        6.50 usec
SFO1     100.628298 MHz
===== CHANNEL f2 =====
CPDPRG2  waltz16
NUC2      1H
PCPD2    95.00 usec
P12      13.00 usec
PL12     13.13 dB
PL13     18.50 dB
SFO2     400.1315005 MHz
F2 - Processing parameters
SI        32768
WDW       0 Hz
SSB       0
GB        0
PC        1.40
    
```

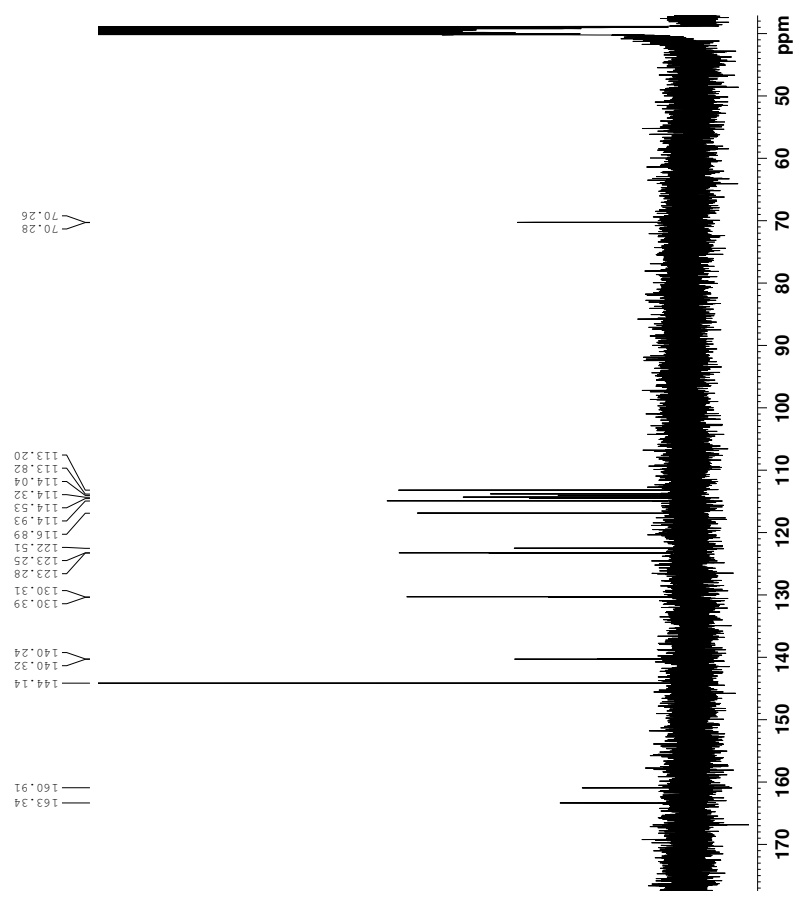
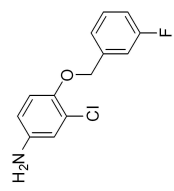


Figure F.2: $^{13}\text{C-NMR}$ spectrum of compound 12.

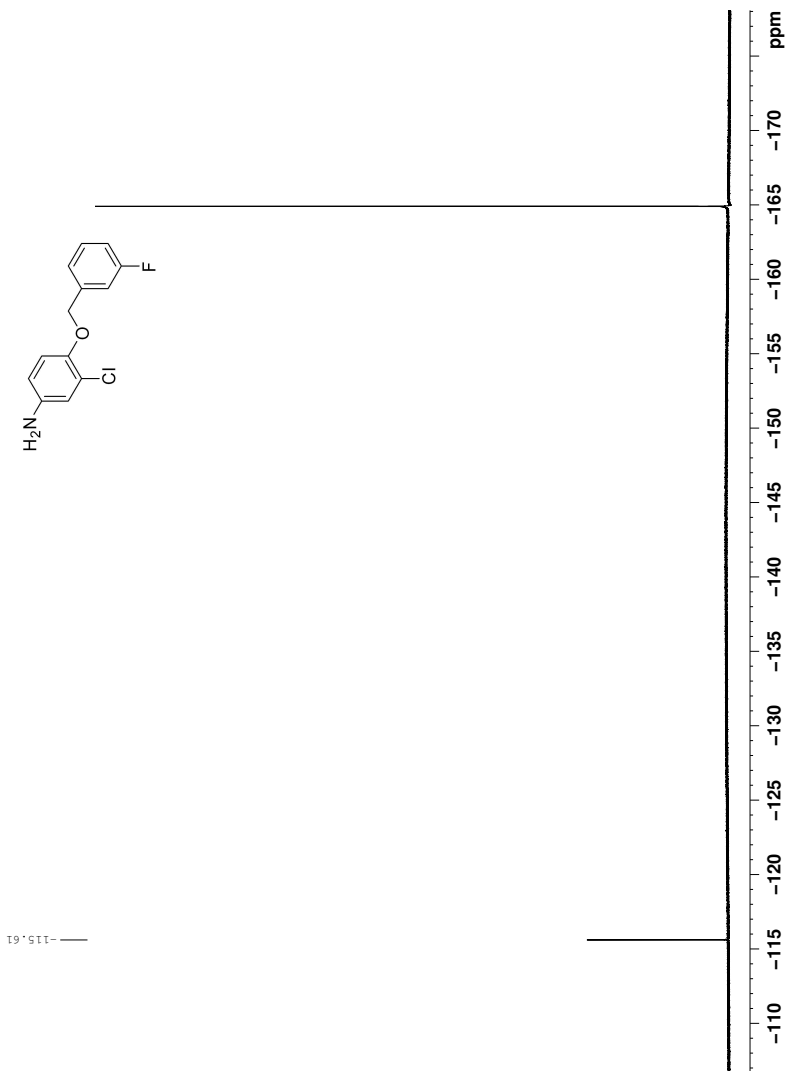
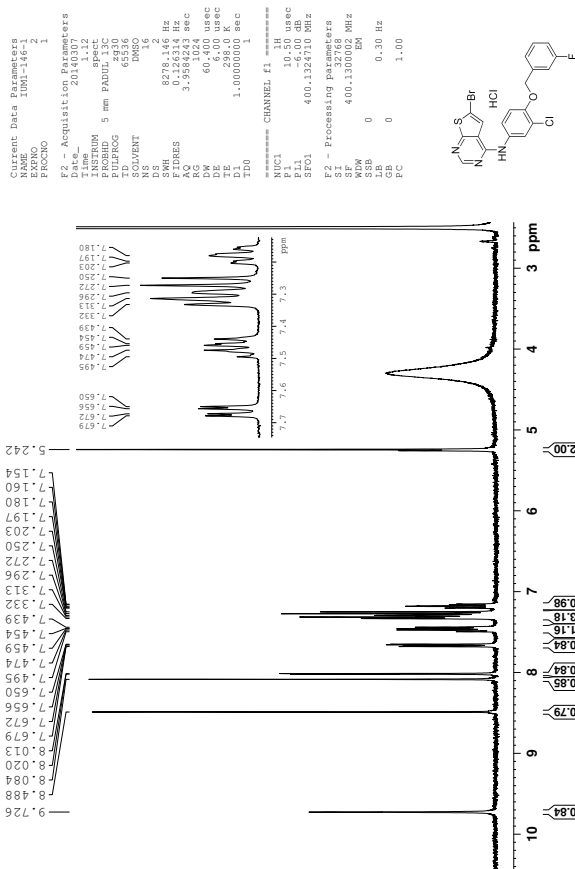


Figure F.3: ^{19}F -NMR spectrum of compound **12** (decoupled).

G Spectroscopic Data - Compound 13·HCl

Figure G.1: ¹H-NMR spectrum of compound 13·HCl.

G SPECTROSCOPIC DATA - COMPOUND 13·HCL

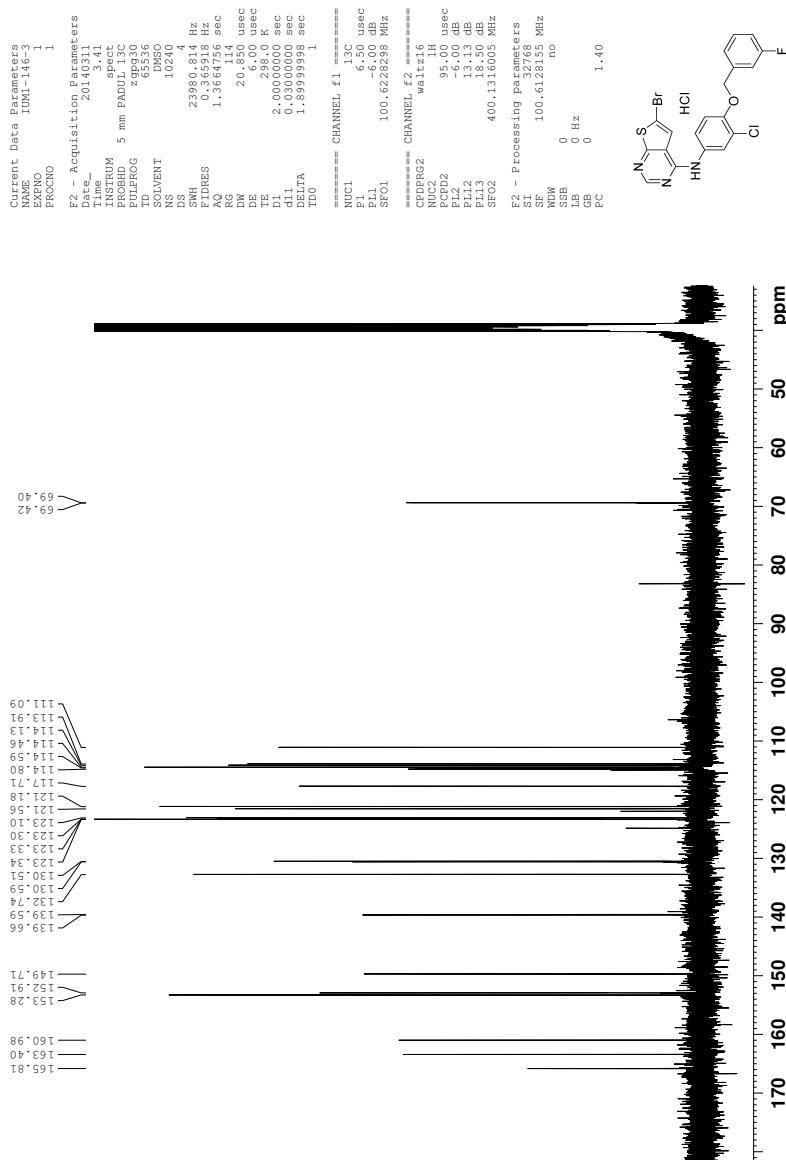
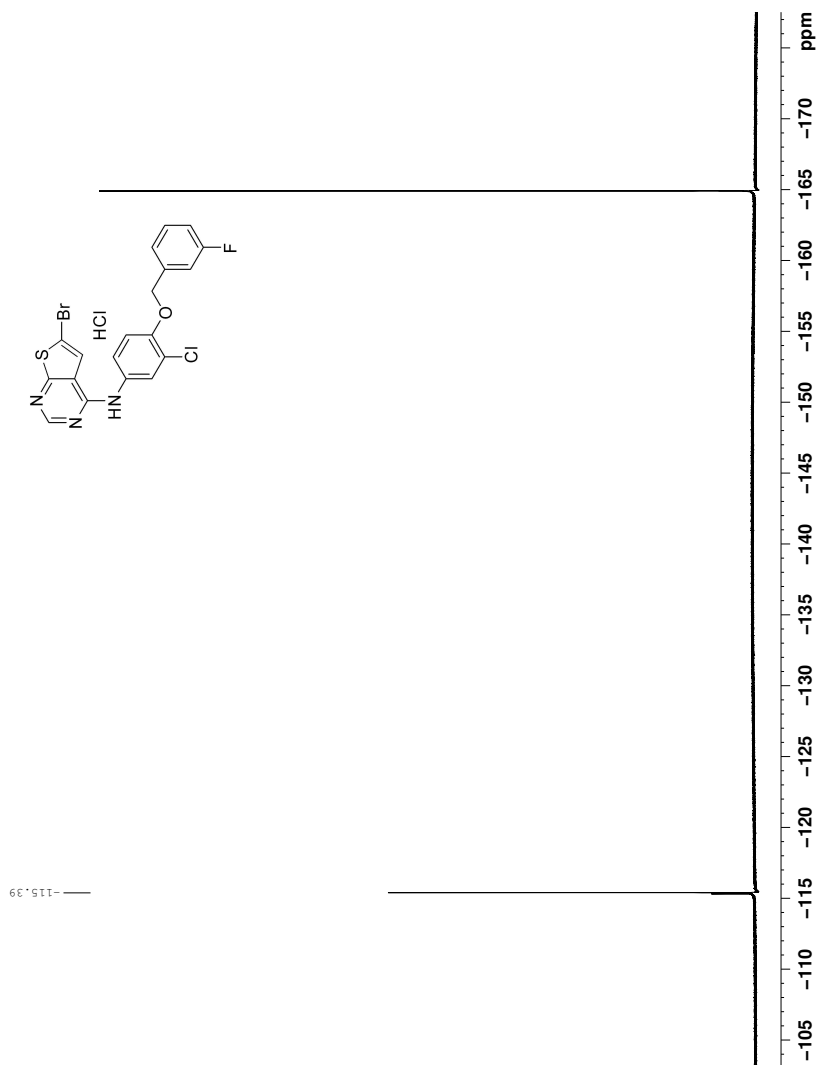


Figure G.2: ¹³C-NMR spectrum of compound 13·HCL.

Figure G.3: ^{19}F -NMR spectrum of compound 13·HCl (decoupled).

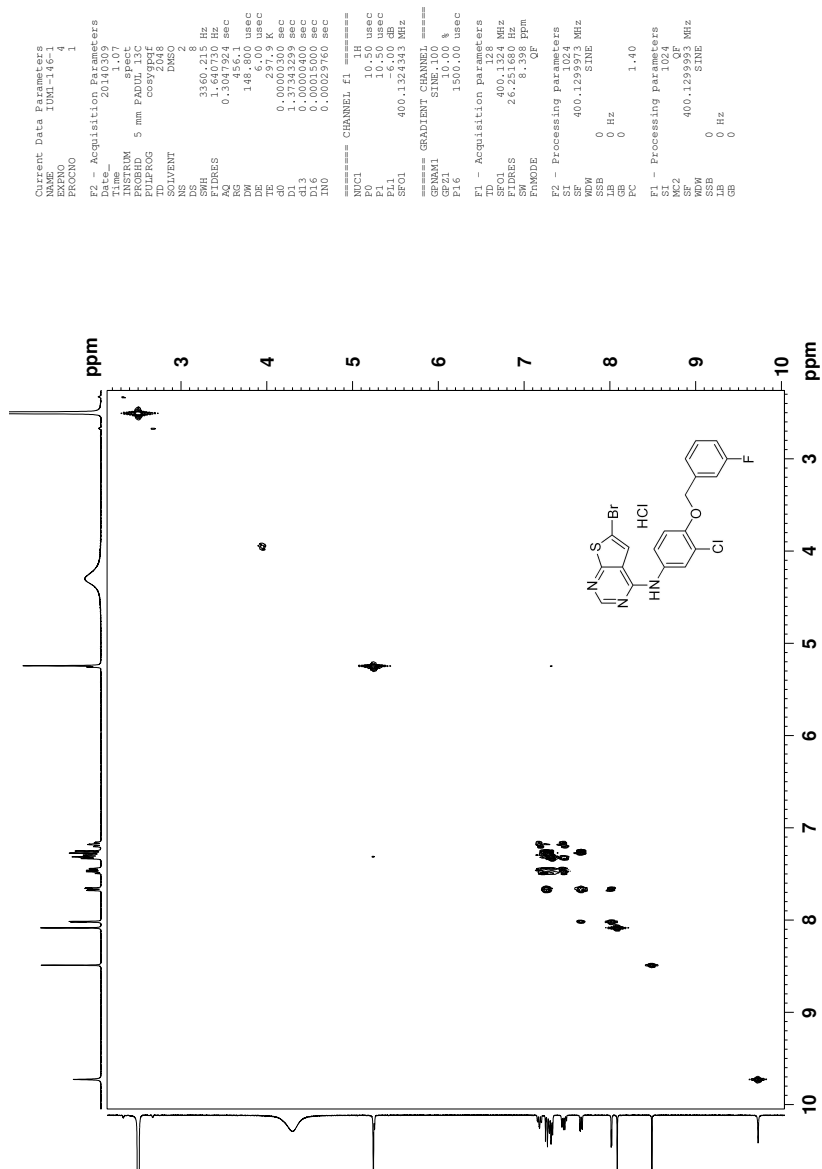


Figure G.4: COSY spectrum of compound 13·HCl.

G SPECTROSCOPIC DATA - COMPOUND 13·HCL

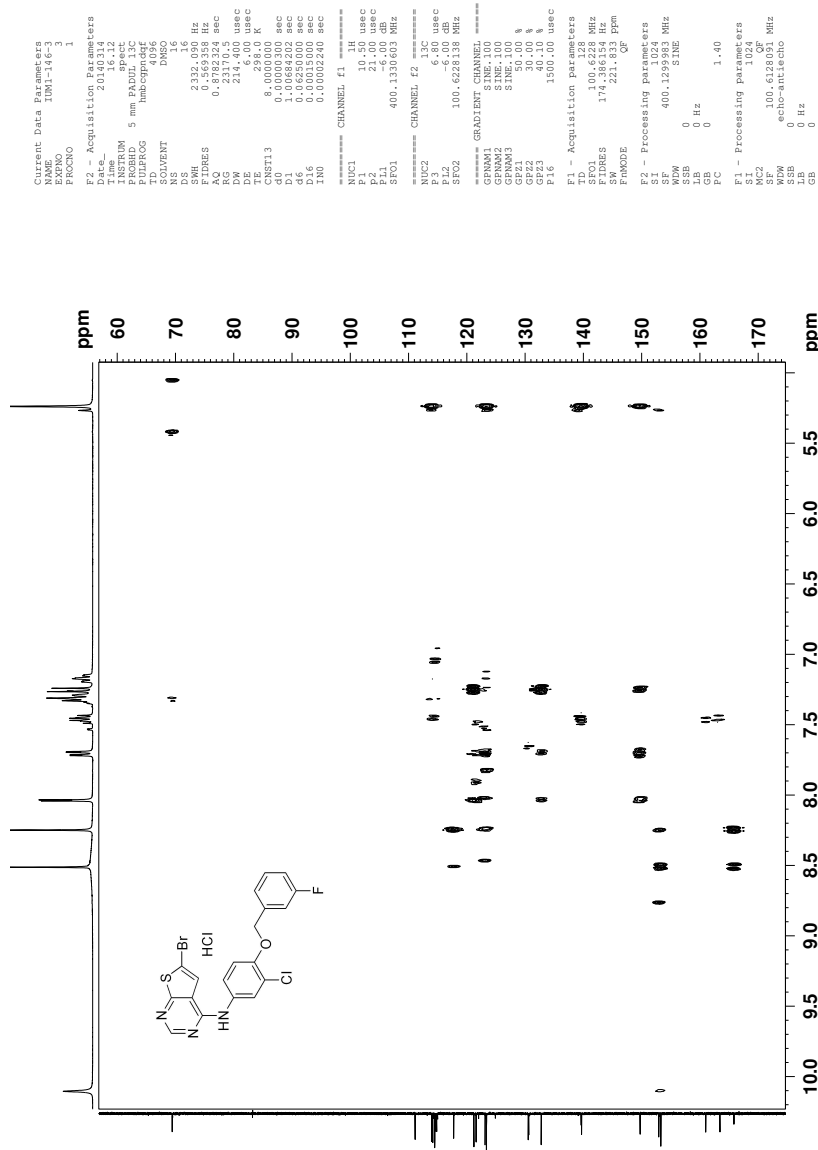


Figure G.6: HMBC spectrum of compound 13·HCl.

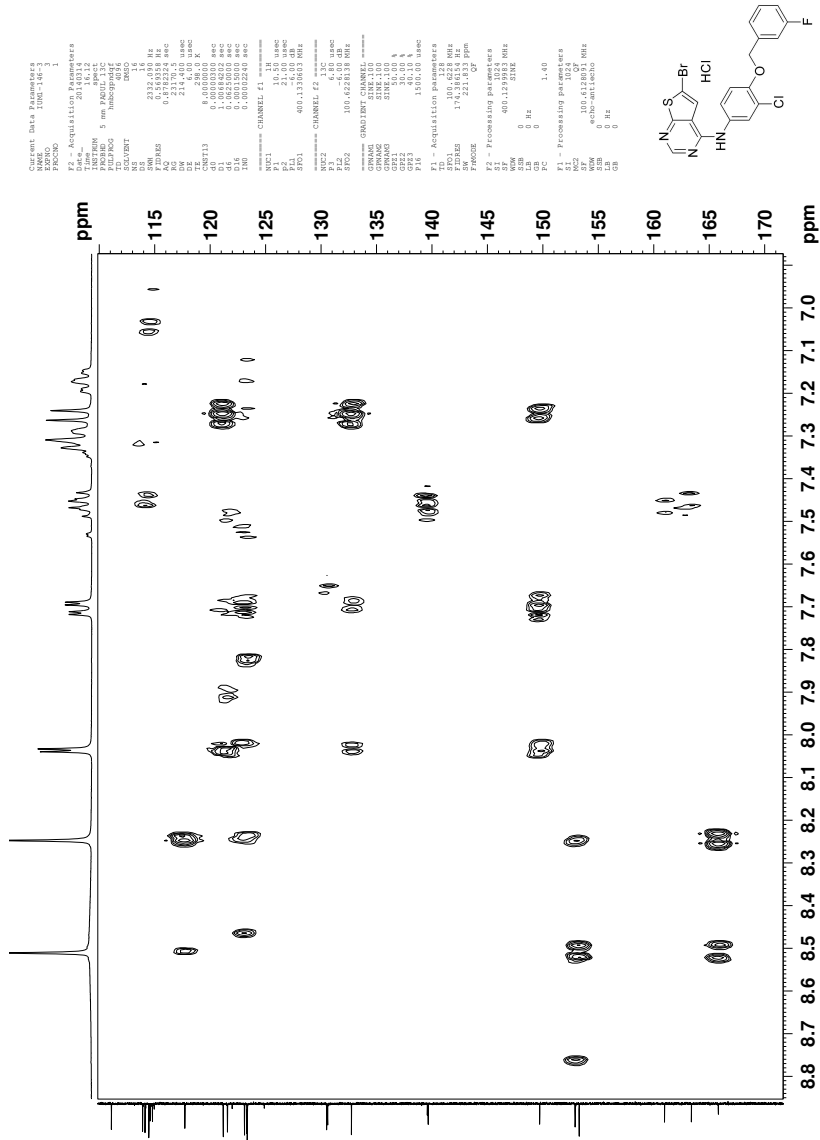


Figure G.7: Section of HMBC spectrum of compound 13·HCl.

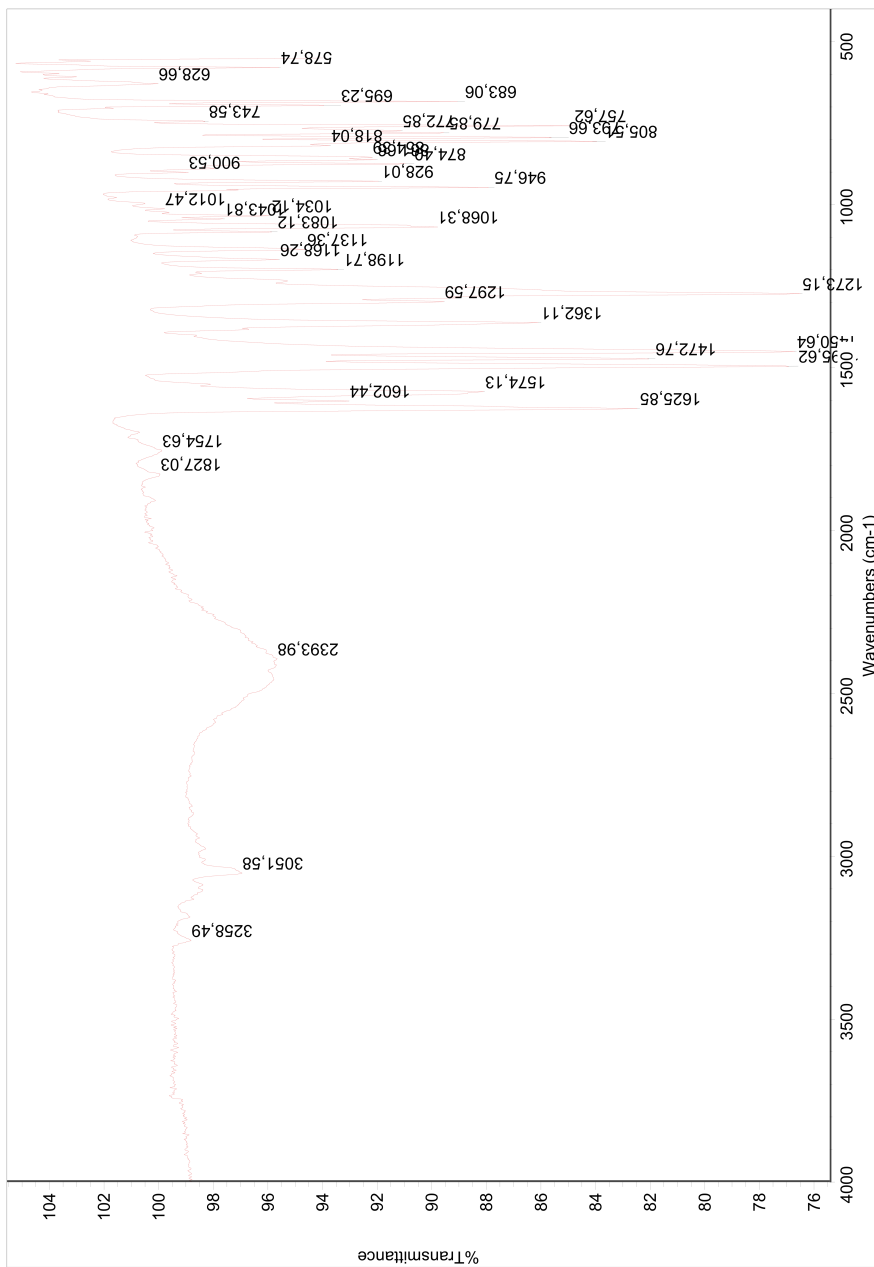


Figure G.8: IR spectrum of compound 13·HCL.

G SPECTROSCOPIC DATA - COMPOUND 13·HCL

Elemental Composition Report

Page 1

Single Mass Analysis

Tolerance = 2.0 PPM / DBE: min = -1.5, max = 50.0

Element prediction: Off

Number of isotope peaks used for i-FIT = 3

Monoisotopic Mass, Even Electron Ions

44862 formula(e) evaluated with 99 results within limits (all results (up to 1000) for each mass)

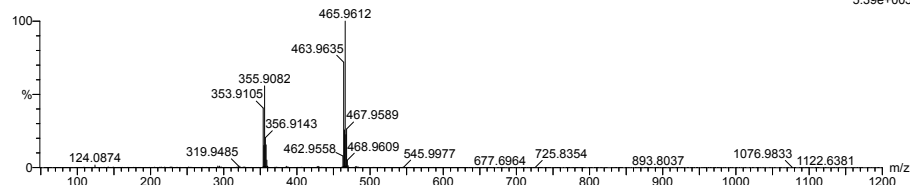
Elements Used:

C: 0-200 H: 0-1000 N: 0-10 O: 0-200 F: 0-3 S: 0-2 Cl: 0-2 Br: 0-2

NT-MSLAB-Operator-SVG

2014-42 124 (2.430) AM2 (Ar,35000,0,0.00,0.00)

1: TOF MS ASAP+
5.39e+005



Minimum:

Maximum: 5.0 2.0 -1.5

Mass	Calc. Mass	mDa	PPM	DBE	i-FIT	Norm	Conf (%)	Formula
463.9635	463.9635	0.0	0.0	5.5	1018.5	4.139	1.59	C8 H12 N7 O8 F S Br
463.9635	463.9635	0.0	0.0	23.5	1017.3	2.988	5.04	C25 H5 N3 F2 Br
463.9635	463.9635	0.0	0.0	13.5	1016.6	2.236	10.69	C19 H13 N3 O F S Cl Br
463.9635	463.9635	0.0	0.0	-1.5	1020.8	6.450	0.16	C H11 N5 O21 Cl
463.9635	463.9635	0.0	0.0	11.5	1020.3	5.923	0.27	C14 H9 N5 O6 F S Cl2
463.9635	463.9635	0.0	0.0	6.5	1021.2	6.827	0.11	C12 H12 N O14 Cl2
463.9635	463.9635	0.0	0.0	3.5	1020.4	6.082	0.23	C3 H8 N9 O13 F S Cl
463.9636	463.9636	-0.1	-0.2	0.5	1019.8	5.480	0.42	C6 H15 N3 O16 Br
463.9636	463.9636	-0.1	-0.2	16.5	1023.5	9.104	0.01	C17 H4 N3 O9 F2 S
463.9636	463.9636	-0.1	-0.2	3.5	1018.8	4.478	1.14	C13 H21 N3 O2 S2 Cl2 Br
463.9634	463.9634	0.1	0.2	2.5	1019.9	5.546	0.39	C10 H21 N7 S Cl Br2
463.9636	463.9636	-0.1	-0.2	21.5	1023.0	8.667	0.02	C19 H N7 O F3 S2
463.9634	463.9634	0.1	0.2	13.5	1024.5	10.167	0.00	C9 N9 O12 F2
463.9634	463.9634	0.1	0.2	21.5	1022.2	7.888	0.04	C20 H N5 O5 F2 Cl
463.9634	463.9634	0.1	0.2	0.5	1018.2	3.865	2.10	C5 H17 N9 O5 S Cl2 Br
463.9637	463.9637	-0.2	-0.4	-1.5	1019.1	4.739	0.88	H11 N7 O17 F S2
463.9637	463.9637	-0.2	-0.4	8.5	1017.9	3.580	2.79	C16 H16 N O5 F S2 Br
463.9637	463.9637	-0.2	-0.4	13.5	1020.4	6.036	0.24	C12 H3 N9 O4 F3 Cl2
463.9633	463.9633	0.2	0.4	1.5	1018.1	3.799	2.24	C6 H14 N7 O5 F3 S2 Br
463.9633	463.9633	0.2	0.4	-0.5	1018.8	4.429	1.19	C H10 N9 O10 F3 S2 Cl
463.9637	463.9637	-0.2	-0.4	6.5	1022.0	7.607	0.05	C11 H12 N3 O10 F S2 Cl
463.9637	463.9637	-0.2	-0.4	-1.5	1020.7	6.326	0.18	C12 H24 N F3 S Cl Br2
463.9633	463.9633	0.2	0.4	2.5	1020.9	6.569	0.14	C10 H14 N O11 F2 S Cl2
463.9633	463.9633	0.2	0.4	10.5	1017.7	3.321	3.61	C11 H9 N9 O4 F Cl Br
463.9637	463.9637	-0.2	-0.4	20.5	1019.9	5.521	0.40	C18 H4 N9 O S Cl2
463.9633	463.9633	0.2	0.4	4.5	1024.7	10.315	0.00	C5 H5 N5 O17 F3
463.9632	463.9632	0.3	0.6	12.5	1022.6	8.230	0.03	C16 H6 N O10 F3 Cl
463.9638	463.9638	-0.3	-0.6	0.5	1019.6	5.273	0.51	C9 H18 N3 O8 F Cl2 Br
463.9632	463.9632	0.3	0.6	11.5	1023.0	8.691	0.02	C11 H6 N5 O14 S
463.9632	463.9632	0.3	0.6	16.5	1022.7	8.304	0.02	C13 H3 N9 O6 F S2
463.9638	463.9638	-0.3	-0.6	20.5	1025.1	10.790	0.00	C19 H2 N3 O12
463.9632	463.9632	0.3	0.6	19.5	1022.1	7.751	0.04	C22 H7 N O7 S Cl
463.9638	463.9638	-0.3	-0.6	5.5	1018.6	4.270	1.40	C11 H15 N7 F2 S Cl2 Br
463.9632	463.9632	0.3	0.6	7.5	1020.0	5.618	0.36	C12 H11 N5 O3 F3 S2 Cl2
463.9632	463.9632	0.3	0.6	3.5	1019.8	5.421	0.44	C12 H18 N3 O4 F2 Br2
463.9639	463.9639	-0.4	-0.9	2.5	1020.7	6.374	0.17	C14 H22 N O3 F Cl Br2
463.9631	463.9631	0.4	0.9	18.5	1017.7	3.310	3.65	C19 H7 N5 O5 Br
463.9631	463.9631	0.4	0.9	9.5	1018.4	4.039	1.76	C18 H15 N O2 F2 Cl2 Br
463.9631	463.9631	0.4	0.9	6.5	1017.6	3.300	3.69	C9 H11 N9 O F3 S Cl Br
463.9639	463.9639	-0.4	-0.9	16.5	1020.3	5.987	0.25	C20 H7 N3 O F3 S Cl2
463.9639	463.9639	-0.4	-0.9	-0.5	1018.8	4.483	1.13	C5 H18 N9 O2 F2 S Br2
463.9631	463.9631	0.4	0.9	-0.5	1019.4	5.099	0.61	C2 H10 N7 O14 F2 Cl2
463.9639	463.9639	-0.4	-0.9	15.5	1021.7	7.319	0.07	C15 H7 N7 O5 S2 Cl
463.9639	463.9639	-0.4	-0.9	8.5	1021.9	7.555	0.05	C9 H6 N7 O8 F3 S Cl
463.9631	463.9631	0.4	0.9	1.5	1018.9	4.517	1.09	C7 H14 N5 O9 F2 Cl Br
463.9639	463.9639	-0.4	-0.9	17.5	1016.7	2.325	9.78	C20 H11 N5 S2 Br
463.9639	463.9639	-0.4	-0.9	3.5	1022.7	8.346	0.02	C7 H9 N3 O16 F2 Cl
463.9640	463.9640	-0.5	-1.1	28.5	1023.4	9.019	0.01	C29 H3 N O F S2
463.9630	463.9630	0.5	1.1	16.5	1022.0	7.632	0.05	C14 H3 N7 O10 Cl
463.9640	463.9640	-0.5	-1.1	-1.5	1019.4	5.062	0.63	C3 H14 N7 O9 F2 S2 Cl2
463.9630	463.9630	0.5	1.1	-1.5	1020.6	6.292	0.19	C9 H23 N5 O F Cl2 Br2
463.9630	463.9630	0.5	1.1	7.5	1022.8	8.443	0.02	C9 H8 N5 O11 F2 S2

Figure G.9: MS spectrum of compound 13·HCl, page 1.

XLVI

Elemental Composition Report

Page 2

Single Mass Analysis

Tolerance = 2.0 PPM / DBE: min = -1.5, max = 50.0

Element prediction: Off

Number of isotope peaks used for i-FIT = 3

Monoisotopic Mass, Even Electron Ions

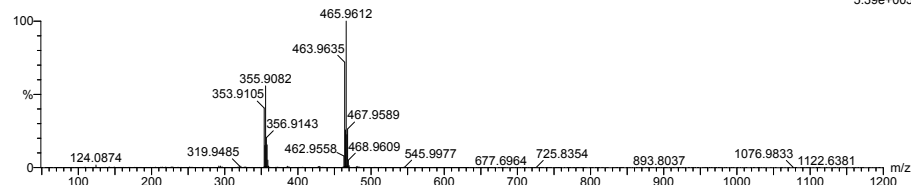
44862 formula(e) evaluated with 99 results within limits (all results (up to 1000) for each mass)

Elements Used:

C: 0-200 H: 0-1000 N: 0-10 O: 0-200 F: 0-3 S: 0-2 Cl: 0-2 Br: 0-2

NT-MSLAB-Operator-SVG

2014-42 124 (2,430) AM2 (Ar,35000,0,0,00,0,00)

1: TOF MS ASAP+
5.39e+005

Minimum:

Maximum: 5.0 2.0 -1.5

Mass	Calc. Mass	mDa	PPM	DBE	i-FIT	Norm	Conf (%)	Formula
463.9640	-0.5	-1.1	5.5	1019.6	5.211	0.55		C12 H13 N O11 F2 Br
463.9640	-0.5	-1.1	10.5	1018.3	3.942	1.94		C14 H10 N5 O3 F3 S Br
463.9640	-0.5	-1.1	9.5	1018.6	4.221	1.47		C13 H13 N7 O3 Cl2 Br
463.9640	-0.5	-1.1	0.5	1018.5	4.176	1.54		C9 H18 N5 O4 F2 S2 Cl Br
463.9630	0.5	1.1	15.5	1021.9	7.520	0.05		C20 H9 N O4 F2 S2 Cl
463.9630	0.5	1.1	24.5	1020.3	5.981	0.25		C25 H4 N3 O3 Cl2
463.9630	0.5	1.1	2.5	1023.4	9.083	0.01		C7 H11 N O19 F S
463.9641	-0.6	-1.3	20.5	1020.7	6.304	0.18		C22 H5 N3 O4 F Cl2
463.9629	0.6	1.3	-0.5	1019.1	4.763	0.85		C9 H20 N O11 S Cl Br
463.9629	0.6	1.3	32.5	1023.0	8.627	0.02		C32 H2 N S2
463.9629	0.6	1.3	4.5	1017.8	3.475	3.10		C11 H17 N5 O3 F S2 Cl Br
463.9641	-0.6	-1.3	3.5	1019.3	4.949	0.71		C7 H16 N9 O5 Br2
463.9641	-0.6	-1.3	3.5	1022.9	8.603	0.02		C6 H9 N5 O12 F3 S2
463.9641	-0.6	-1.3	11.5	1022.2	7.846	0.04		C17 H10 N O5 F3 S2 Cl
463.9641	-0.6	-1.3	-1.5	1023.8	9.484	0.01		C4 H12 N O20 F2 S
463.9629	0.6	1.3	9.5	1018.8	4.422	1.20		C15 H12 N O10 F Br
463.9629	0.6	1.3	25.5	1023.4	9.033	0.01		C26 H N O3 F3 S
463.9641	-0.6	-1.3	12.5	1022.3	7.920	0.04		C11 H4 N7 O11 F Cl
463.9628	0.7	1.5	-1.5	1023.1	8.745	0.02		C5 H13 N O16 F3 S2
463.9628	0.7	1.5	20.5	1020.0	5.663	0.35		C23 H6 N3 F2 S Cl2
463.9628	0.7	1.5	-1.5	1019.6	5.261	0.52		C6 H20 N5 O9 Br2
463.9642	-0.7	-1.5	4.5	1018.6	4.206	1.49		C10 H16 N5 O7 S Cl Br
463.9642	-0.7	-1.5	14.5	1018.4	4.090	1.67		C16 H8 N5 O6 F Br
463.9628	0.7	1.5	12.5	1021.7	7.362	0.06		C12 H5 N7 O7 F2 S Cl
463.9628	0.7	1.5	3.5	1018.8	4.419	1.20		C8 H17 N9 O F S Br2
463.9628	0.7	1.5	2.5	1019.6	5.265	0.52		C6 H13 N7 O8 F S2 Cl2
463.9628	0.7	1.5	14.5	1017.5	3.141	4.33		C17 H9 N5 O2 F2 S Br
463.9642	-0.7	-1.5	12.5	1018.1	3.714	2.44		C21 H17 N S Cl2 Br
463.9628	0.7	1.5	7.5	1022.4	8.049	0.03		C10 H8 N3 O15 F Cl
463.9628	0.7	1.5	6.5	1020.3	5.912	0.27		C17 H21 N O2 Cl Br2
463.9642	-0.7	-1.5	2.5	1020.2	5.851	0.29		C5 H12 N7 O12 S Cl2
463.9643	-0.8	-1.7	5.5	1019.2	4.850	0.78		C15 H16 N O3 F3 Cl2 Br
463.9643	-0.8	-1.7	12.5	1022.9	8.562	0.02		C10 H4 N9 O7 F2 S2
463.9627	0.8	1.7	4.5	1019.0	4.665	0.94		C12 H17 N3 O7 Cl2 Br
463.9643	-0.8	-1.7	25.5	1025.5	11.144	0.00		C25 N O7 F2
463.9643	-0.8	-1.7	6.5	1019.7	5.403	0.45		C15 H20 N3 O2 S Br2
463.9643	-0.8	-1.7	15.5	1022.4	8.098	0.03		C19 H8 N O8 F S Cl
463.9643	-0.8	-1.7	20.5	1022.0	7.612	0.05		C21 H5 N5 F2 S2 Cl
463.9643	-0.8	-1.7	7.5	1023.4	9.073	0.01		C8 H7 N5 O15 F S
463.9644	-0.9	-1.9	2.5	1025.4	11.008	0.00		C6 H10 N O23
463.9626	0.9	1.9	5.5	1018.7	4.351	1.29		C13 H14 N O7 F3 S Br
463.9644	-0.9	-1.9	-0.5	1020.3	5.984	0.25		C9 H19 N3 O5 F3 Br2
463.9644	-0.9	-1.9	23.5	1017.5	3.202	4.07		C20 H3 N9 O Br
463.9626	0.9	1.9	12.5	1017.1	2.705	6.69		C19 H15 N O4 S2 Br
463.9626	0.9	1.9	3.5	1022.1	7.742	0.04		C8 H10 N3 O12 F3 S Cl
463.9644	-0.9	-1.9	5.5	1020.5	6.201	0.20		C13 H16 N O9 S2 Cl2
463.9644	-0.9	-1.9	-1.5	1021.4	7.060	0.09		C7 H15 N O12 F3 S Cl2

Figure G.10: MS spectrum of compound 13·HCl, page 2.

XLVII

H Spectroscopic Data - Compound 14a

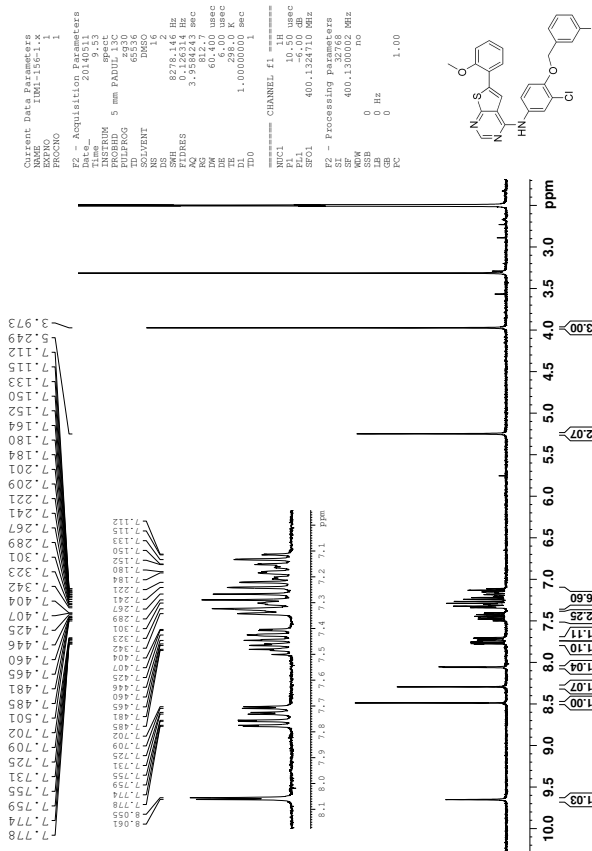


Figure H.1: ¹H-NMR spectrum of compound 14a.

H SPECTROSCOPIC DATA - COMPOUND 14A

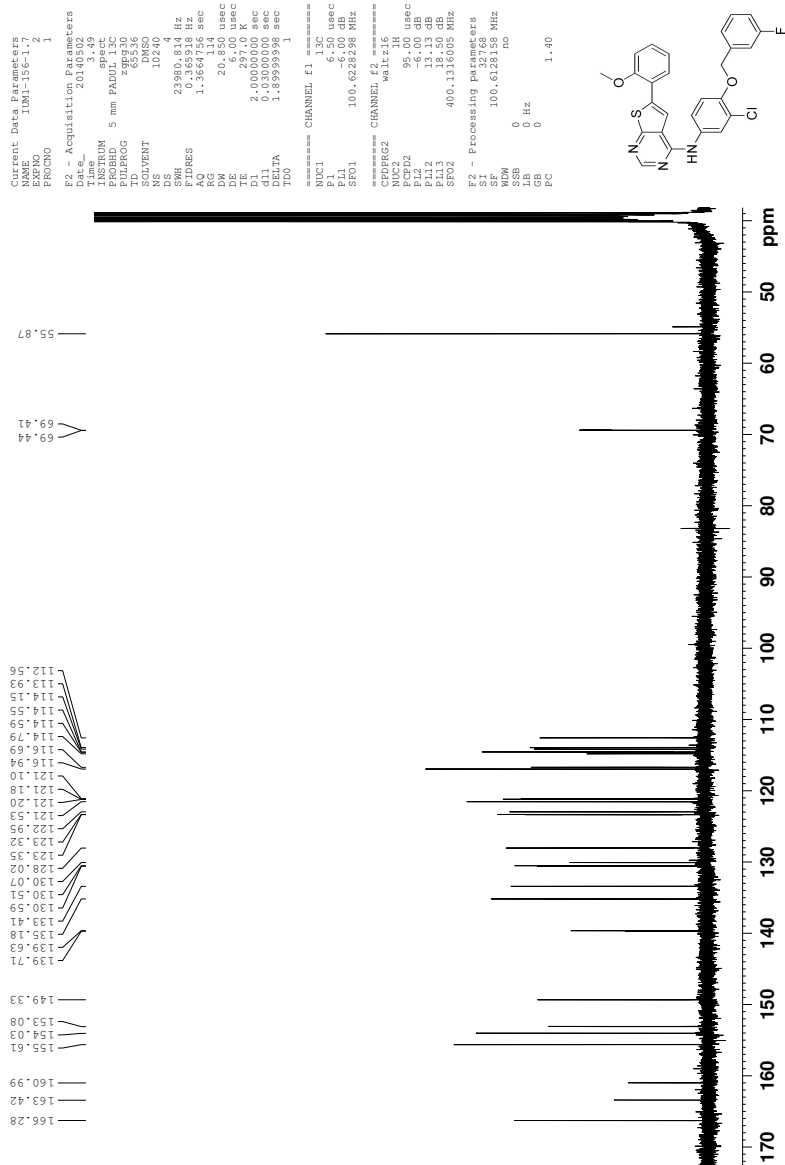


Figure H.2: ^{13}C -NMR spectrum of compound 14a.

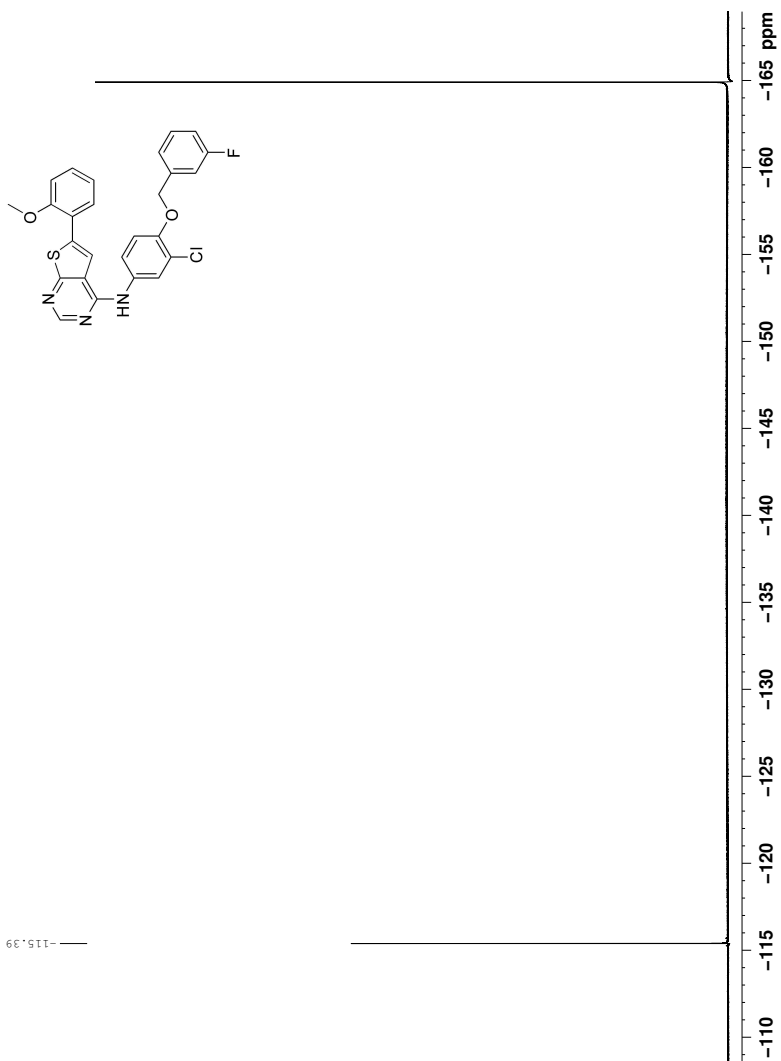


Figure H.3: ^{19}F -NMR spectrum of compound **14a** (decoupled).

H SPECTROSCOPIC DATA - COMPOUND 14A

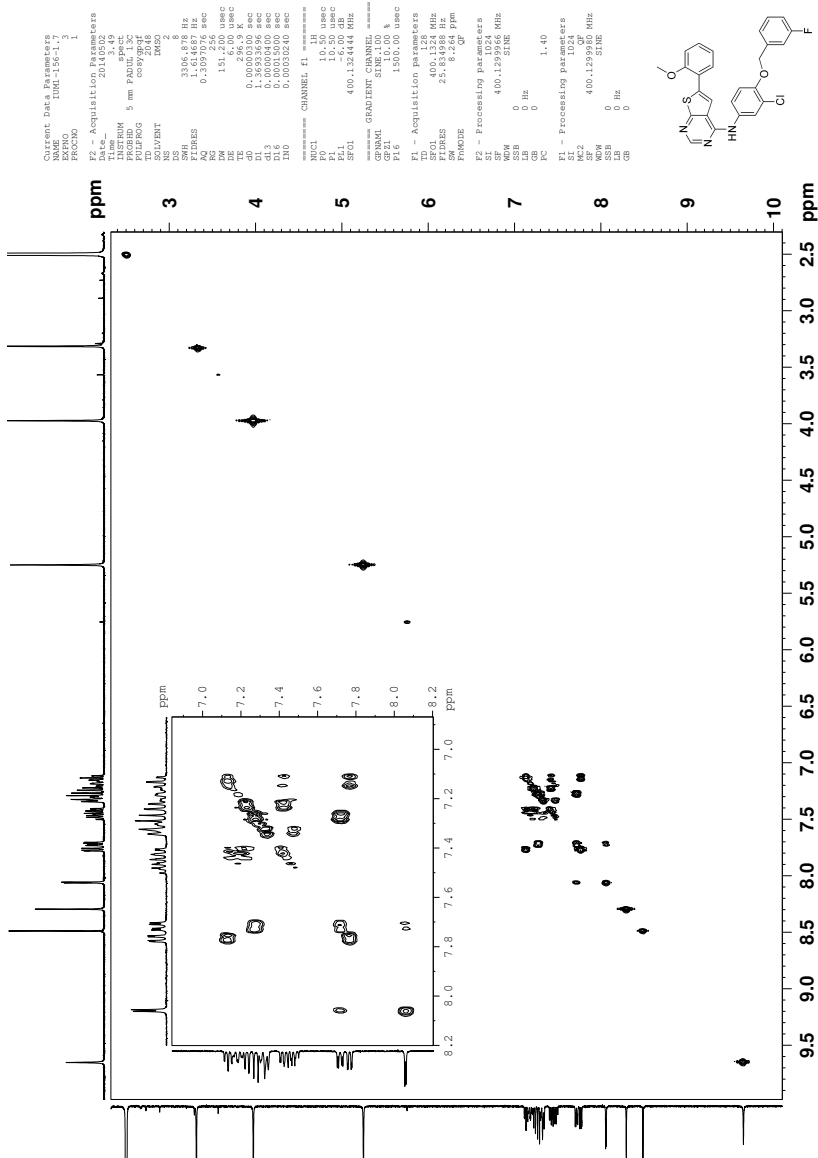


Figure H.4: COSY spectrum of compound 14a.

H SPECTROSCOPIC DATA - COMPOUND 14A

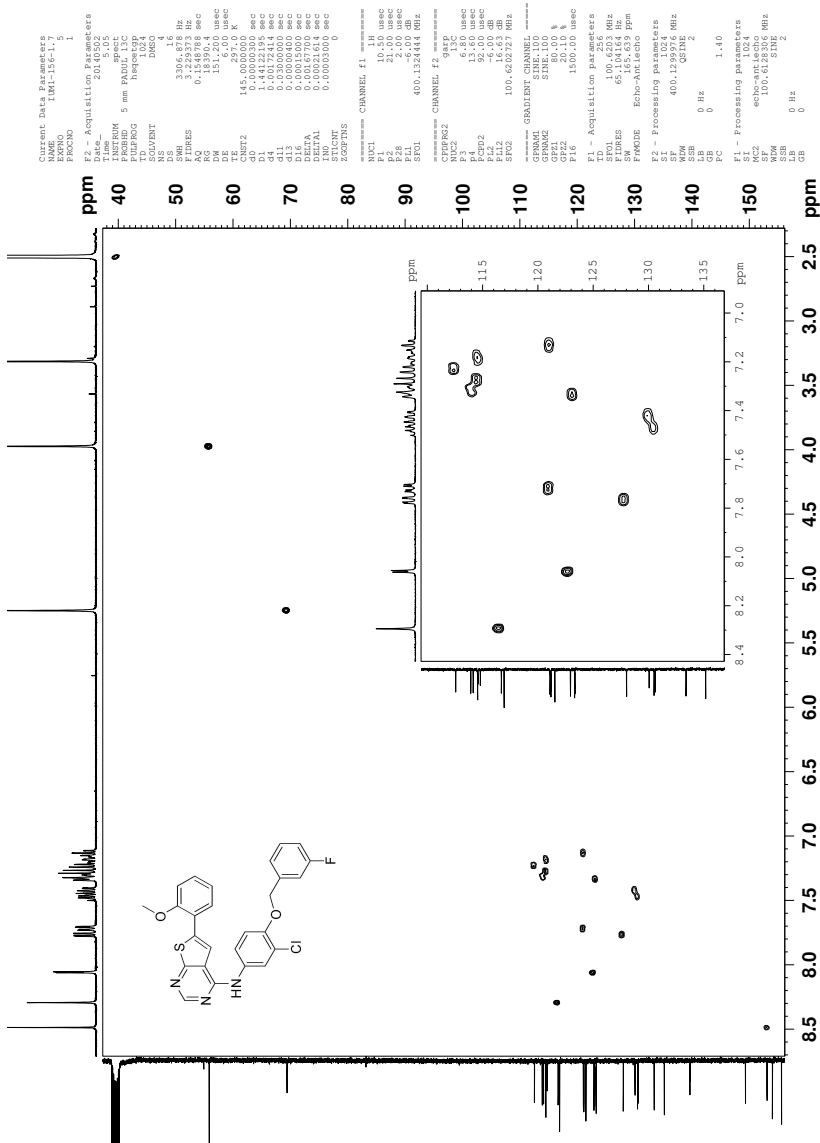


Figure H.5: HSQC spectrum of compound 14a.

H SPECTROSCOPIC DATA - COMPOUND 14A

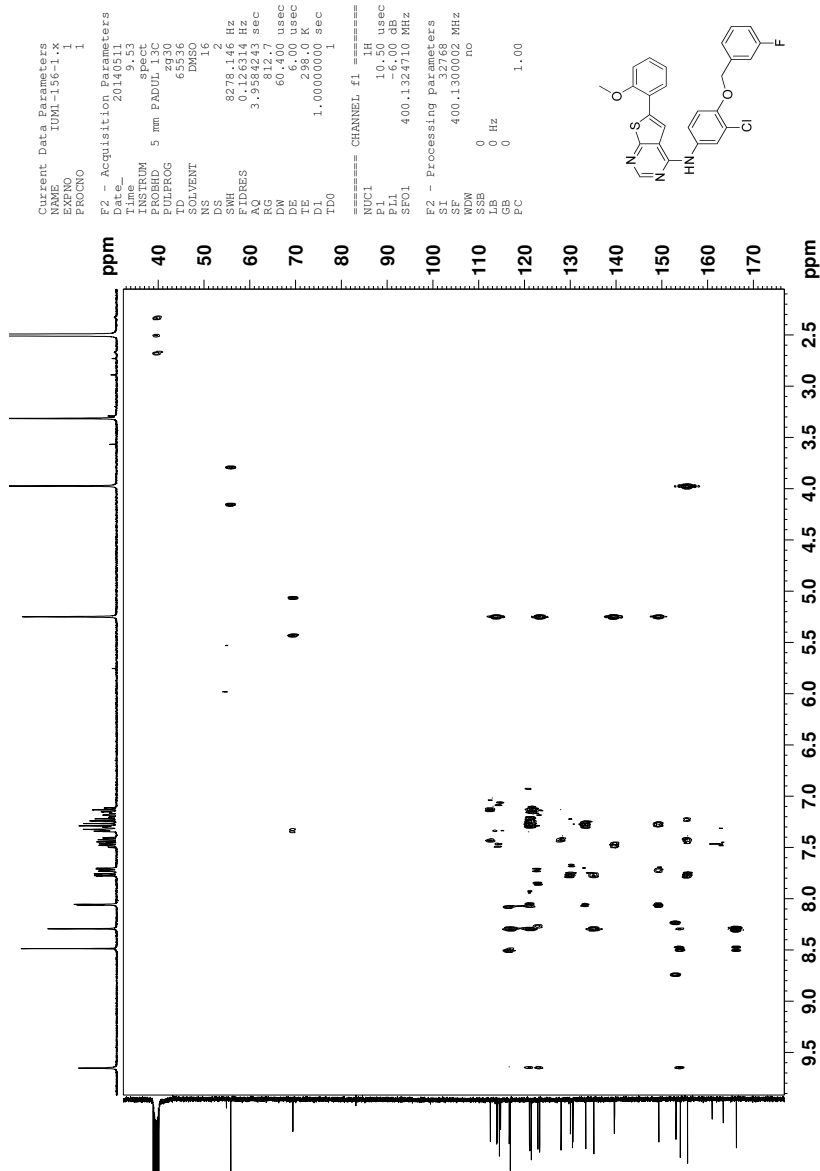


Figure H.6: HMBC spectrum of compound 14a.

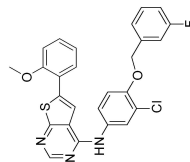
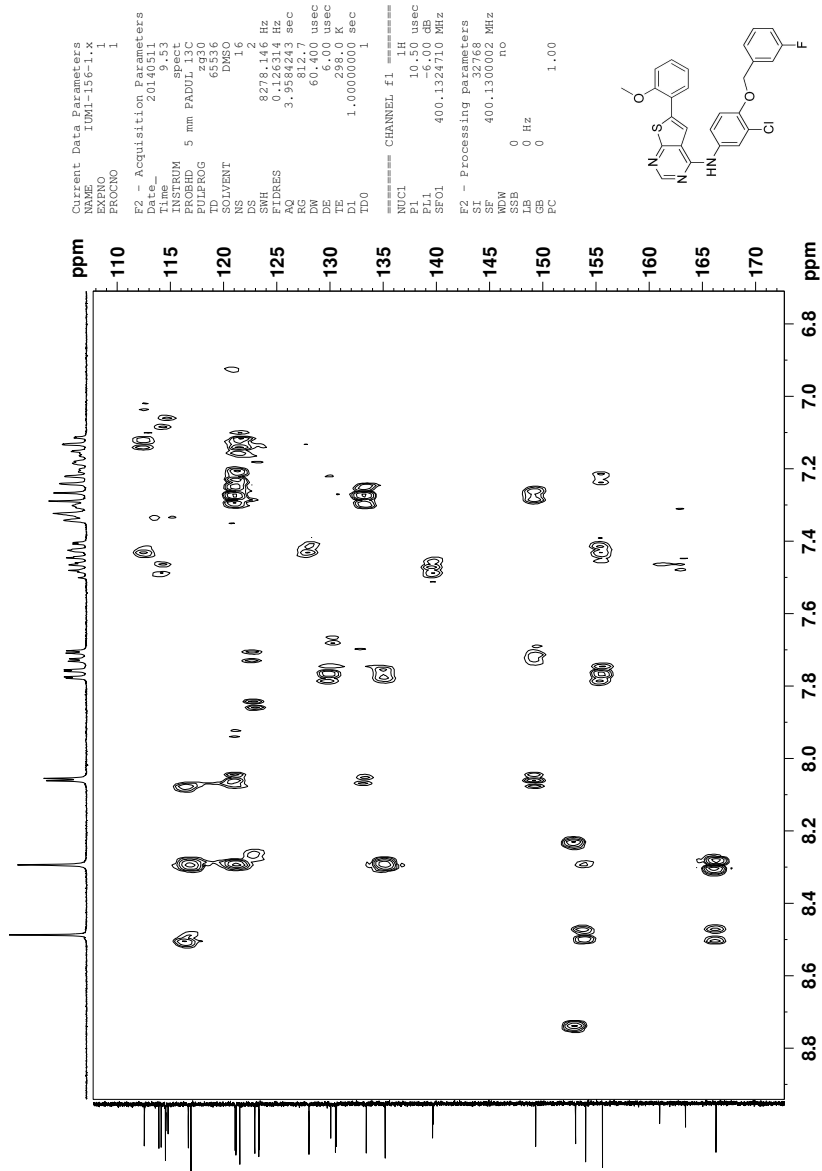


Figure H.7: Section of HMBC spectrum of compound 14a.

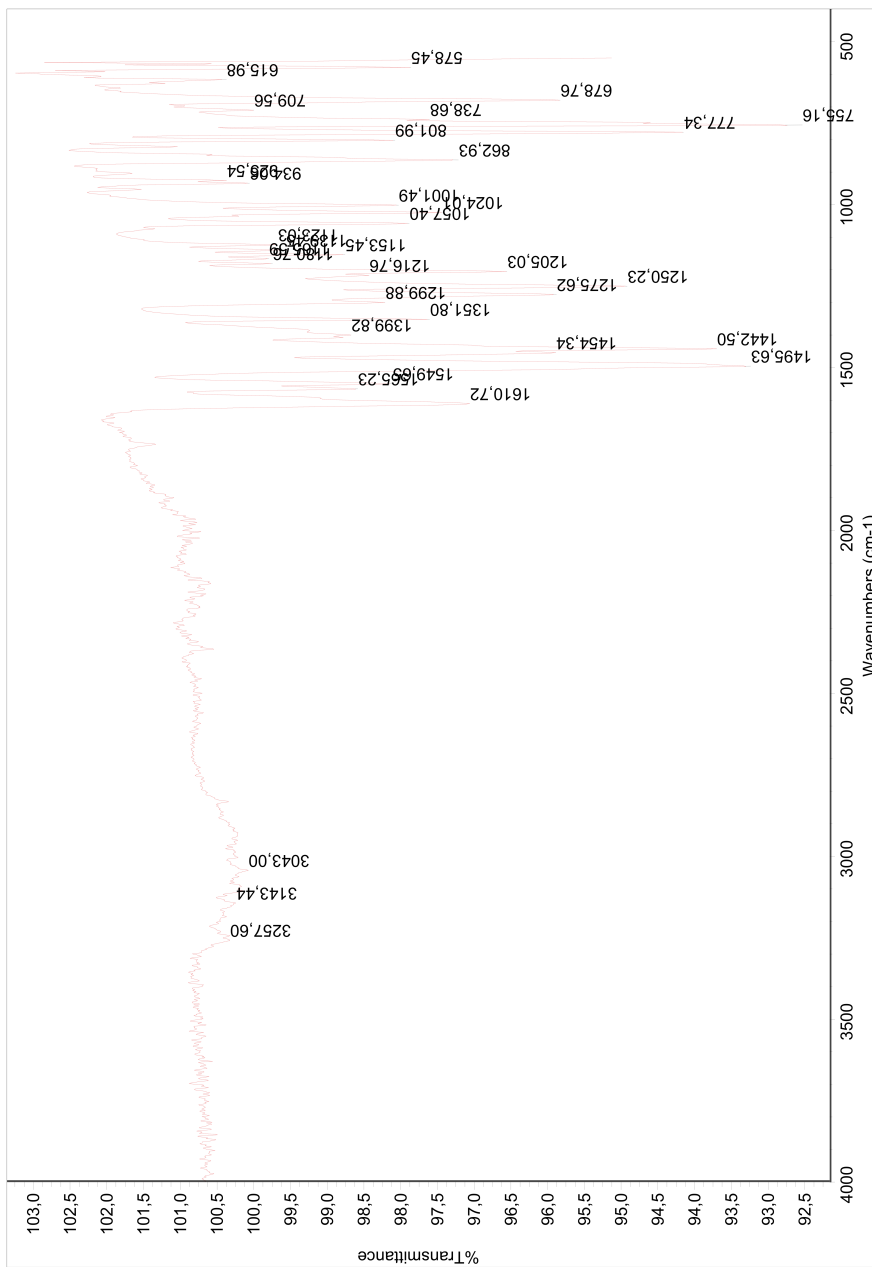


Figure H.8: IR spectrum of compound 14a.

H SPECTROSCOPIC DATA - COMPOUND 14A

Elemental Composition Report

Page 1

Single Mass Analysis

Tolerance = 2.0 PPM / DBE: min = -1.5, max = 50.0

Element prediction: Off

Number of isotope peaks used for i-FIT = 3

Monoisotopic Mass, Even Electron Ions

43061 formula(e) evaluated with 94 results within limits (all results (up to 1000) for each mass)

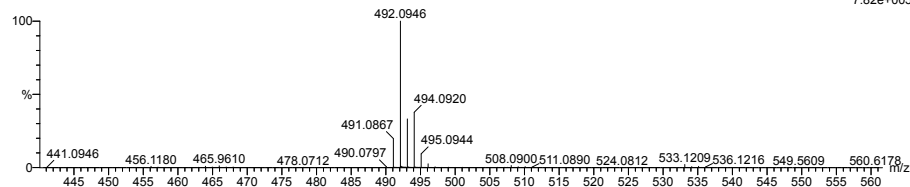
Elements Used:

C: 0-200 H: 0-1000 N: 0-100 O: 0-200 S: 0-2 Cl: 0-2 F: 0-3

NT-MSLAB-Operator-SVG

2014-43 153 (3.000) AM2 (Ar,35000.0,0.00,0.00); Cm (152:153)

1: TOF MS ASAP+
7.82e+005



Minimum: -1.5
Maximum: 5.0 2.0 50.0

Mass	Calc. Mass	mDa	PPM	DBE	i-FIT	Norm	Conf (%)	Formula
492.0946	492.0937	0.9	1.8	31.5	930.3	16.128	0.00	C35 H11 N3 F
	492.0955	-0.9	-1.8	26.5	917.6	3.402	3.33	C34 H16 N Cl F
	492.0948	-0.2	-0.4	27.5	930.5	16.356	0.00	C32 H12 N3 O F2
	492.0937	0.9	1.8	21.5	915.6	1.372	25.35	C29 H19 N3 O S Cl
	492.0956	-1.0	-2.0	16.5	925.0	10.858	0.00	C28 H24 N O S Cl2
	492.0953	-0.7	-1.4	21.5	924.7	10.499	0.00	C27 H18 N5 O S2
	492.0949	-0.3	-0.6	17.5	917.2	3.066	4.66	C26 H20 N3 O2 S Cl F
	492.0944	0.2	0.4	22.5	930.2	16.023	0.00	C26 H14 N5 O6
	492.0939	0.7	1.4	16.5	923.8	9.585	0.01	C26 H22 N O5 S2
	492.0945	0.1	0.2	13.5	924.0	9.833	0.01	C25 H22 N O3 Cl2 F2
	492.0942	0.4	0.8	18.5	926.0	11.838	0.00	C24 H16 N5 O3 S F2
	492.0951	-0.5	-1.0	19.5	916.7	2.551	7.80	C24 H14 N7 Cl F3
	492.0951	-0.5	-1.0	12.5	924.6	10.384	0.00	C23 H23 N O6 S2 F
	492.0956	-1.0	-2.0	18.5	930.5	16.355	0.00	C23 H15 N5 O7 F
	492.0938	0.8	1.6	14.5	918.0	3.838	2.15	C23 H18 N3 O4 Cl F3
	492.0942	0.4	0.8	13.5	930.3	16.122	0.00	C22 H19 N O11 F
	492.0949	-0.3	-0.6	23.5	915.3	1.126	32.44	C22 H11 N13 Cl
	492.0940	0.6	1.2	13.5	923.1	8.949	0.01	C21 H21 N7 S Cl2 F
	492.0953	-0.7	-1.4	14.5	926.5	12.316	0.00	C21 H17 N5 O4 S F3
	492.0940	0.6	1.2	9.5	926.0	11.785	0.00	C20 H21 N O8 S F
	492.0937	0.9	1.8	18.5	921.3	7.127	0.08	C20 H15 N11 S2 F
	492.0954	-0.8	-1.6	13.5	924.1	9.878	0.01	C20 H20 N7 O4 Cl2
	492.0949	-0.3	-0.6	7.5	924.5	10.358	0.00	C20 H28 N3 O3 S2 Cl2
	492.0942	0.4	0.8	24.5	929.7	15.519	0.00	C20 H7 N15 O F
	492.0940	0.6	1.2	8.5	923.9	9.699	0.01	C19 H24 N3 O8 Cl2
	492.0956	-1.0	-2.0	13.5	920.0	5.813	0.30	C19 H20 N9 S2 Cl F
	492.0951	-0.5	-1.0	18.5	925.6	11.458	0.00	C19 H14 N11 O4 S
	492.0954	-0.8	-1.6	9.5	930.6	16.465	0.00	C19 H20 N O12 F2
	492.0947	-0.1	-0.2	14.5	918.7	4.561	1.05	C18 H16 N9 O5 Cl F
	492.0938	0.8	1.6	13.5	925.2	11.013	0.00	C18 H18 N7 O8 S
	492.0942	0.4	0.8	8.5	919.9	5.768	0.31	C18 H24 N5 O4 S2 Cl F
	492.0952	-0.6	-1.2	9.5	923.9	9.731	0.01	C18 H22 N7 O S Cl2 F2
	492.0938	0.8	1.6	4.5	924.1	9.913	0.00	C17 H26 N3 O5 S Cl2 F2
	492.0953	-0.7	-1.4	20.5	930.0	15.816	0.00	C17 H8 N15 O2 F2
	492.0949	-0.3	-0.6	14.5	921.9	7.760	0.04	C17 H16 N11 O S2 F2
	492.0942	0.4	0.8	3.5	921.6	7.425	0.06	C16 H27 N O12 S Cl
	492.0945	0.1	0.2	10.5	919.0	4.799	0.82	C16 H18 N9 O2 S Cl F3
	492.0952	-0.6	-1.2	4.5	924.8	10.664	0.00	C16 H25 N3 O9 Cl2 F
	492.0940	0.6	1.2	15.5	930.0	15.784	0.00	C16 H12 N11 O6 F2
	492.0949	-0.3	-0.6	9.5	925.7	11.507	0.00	C15 H19 N7 O9 S F
	492.0954	-0.8	-1.6	4.5	921.7	7.505	0.06	C15 H25 N5 O5 S2 Cl F2
	492.0942	0.4	0.8	14.5	917.2	2.982	5.07	C14 H15 N15 O2 S Cl
	492.0945	0.1	0.2	5.5	921.1	6.942	0.10	C14 H21 N5 O10 Cl F2
	492.0950	-0.4	-0.8	0.5	924.7	10.507	0.00	C14 H27 N3 O6 S Cl2 F3
	492.0940	0.6	1.2	-0.5	922.1	7.914	0.04	C14 H29 N O9 S2 Cl F2
	492.0954	-0.8	-1.6	-0.5	923.3	9.139	0.01	C13 H28 N O13 S Cl F
	492.0947	-0.1	-0.2	5.5	922.3	8.104	0.03	C13 H21 N7 O6 S2 F3
	492.0952	-0.6	-1.2	11.5	930.3	16.134	0.00	C13 H13 N11 O7 F3
	492.0938	0.8	1.6	10.5	921.5	7.357	0.06	C13 H17 N13 O3 Cl2 F
	492.0949	-0.3	-0.6	4.5	930.5	16.300	0.00	C13 H22 N3 O17
	492.0945	0.1	0.2	16.5	916.7	2.531	7.96	C12 H9 N19 Cl F2
	492.0938	0.8	1.6	6.5	930.2	16.049	0.00	C12 H17 N7 O11 F3

Figure H.9: MS spectrum of compound 14a, page 1.

Elemental Composition Report

Single Mass Analysis

Tolerance = 2.0 PPM / DBE: min = -1.5, max = 50.0

Element prediction: Off

Number of isotope peaks used for i-FIT = 3

Monoisotopic Mass, Even Electron Ions

43061 formula(e) evaluated with 94 results within limits (all results (up to 1000) for each mass)

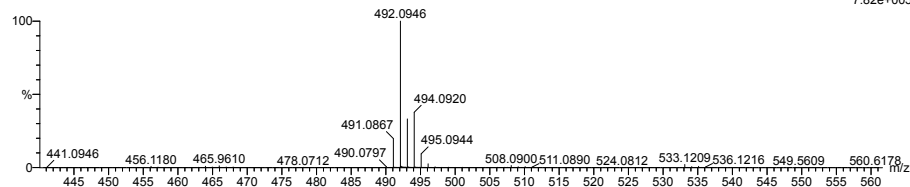
Elements Used:

C: 0-200 H: 0-1000 N: 0-100 O: 0-200 S: 0-2 Cl: 0-2 F: 0-3

NT-MSLAB-Operator-SVG

2014-43 153 (3.000) AM2 (Ar,35000,0,0.00,0.00); Cm (152:153)

1: TOF MS ASAP+
7.82e+005

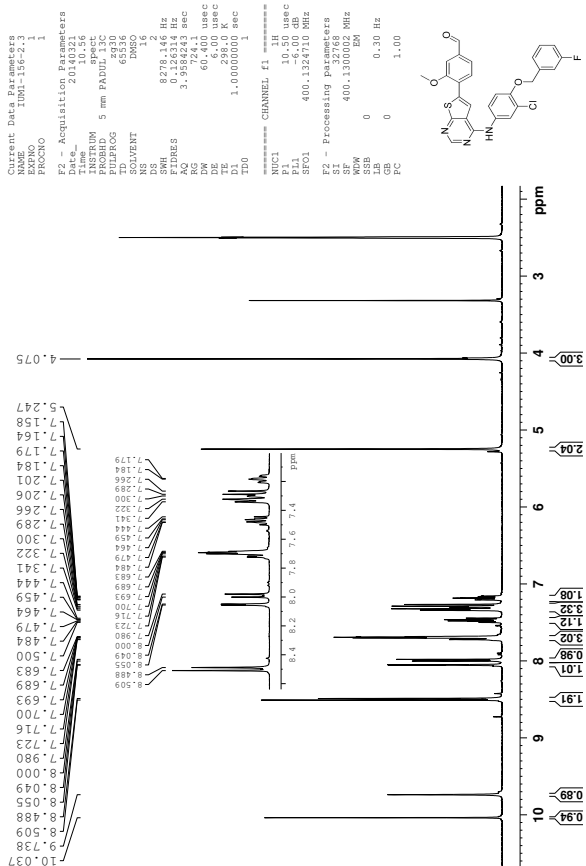


Minimum: -1.5
Maximum: 50.0

Mass	Calc. Mass	mDa	PPM	DBE	i-FIT	Norm	Conf (%)	Formula
492.0947	-0.1	-0.2	4.5	922.4	8.266	0.03		C12 H24 N9 O6 S Cl2
492.0944	0.2	0.4	9.5	920.0	5.841	0.29		C11 H18 N13 O6 S2
492.0949	-0.3	-0.6	15.5	929.8	15.649	0.00		C11 H10 N17 O7
492.0936	1.0	2.0	6.5	922.3	8.145	0.03		C11 H19 N13 S Cl2 F3
492.0954	-0.8	-1.6	10.5	918.9	4.750	0.86		C11 H16 N15 O3 S Cl F
492.0947	-0.1	-0.2	0.5	926.1	11.939	0.00		C11 H24 N3 O14 S F2
492.0940	0.6	1.2	5.5	918.9	4.740	0.87		C10 H20 N11 O7 S Cl F
492.0950	-0.4	-0.8	6.5	921.1	6.878	0.10		C10 H18 N13 O4 Cl2 F2
492.0945	0.1	0.2	0.5	922.0	7.796	0.04		C10 H26 N9 O3 S2 Cl2 F2
492.0938	0.8	1.6	17.5	928.6	14.441	0.00		C10 H5 N21 O F3
492.0947	-0.1	-0.2	11.5	921.6	7.469	0.06		C9 H12 N17 O4 S F2
492.0954	-0.8	-1.6	5.5	920.9	6.722	0.12		C9 H19 N11 O11 Cl
492.0949	-0.3	-0.6	-0.5	920.7	6.493	0.15		C9 H27 N7 O10 S2 Cl
492.0952	-0.6	-1.2	6.5	918.6	4.386	1.25		C9 H18 N15 S2 Cl F3
492.0936	1.0	2.0	1.5	922.4	8.249	0.03		C9 H22 N9 O8 Cl2 F2
492.0938	0.8	1.6	1.5	920.2	5.991	0.25		C8 H22 N11 O4 S2 Cl F3
492.0943	0.3	0.6	7.5	918.3	4.153	1.57		C8 H14 N15 O5 Cl F3
492.0941	0.5	1.0	0.5	920.5	6.287	0.19		C8 H23 N7 O15 Cl
492.0952	-0.6	-1.2	1.5	919.5	5.352	0.47		C7 H21 N11 O8 S Cl F2
492.0947	-0.1	-0.2	6.5	930.4	16.209	0.00		C7 H15 N13 O12 F
492.0954	-0.8	-1.6	16.5	919.5	5.358	0.47		C7 H7 N25 O Cl
492.0949	-0.3	-0.6	10.5	918.9	4.679	0.93		C7 H15 N21 S2 Cl
492.0942	0.4	0.8	0.5	920.6	6.411	0.16		C7 H23 N9 O11 S2 F
492.0945	0.1	0.2	6.5	921.7	7.542	0.05		C6 H17 N19 O S Cl2 F
492.0941	0.5	1.0	11.5	921.0	6.786	0.11		C6 H11 N21 O5 Cl
492.0945	0.1	0.2	2.5	923.9	9.736	0.01		C5 H17 N13 O9 S F3
492.0947	-0.1	-0.2	17.5	928.1	13.967	0.00		C5 H3 N27 O2 F
492.0954	-0.8	-1.6	0.5	921.8	7.610	0.05		C5 H24 N15 O4 S2 Cl2
492.0942	0.4	0.8	11.5	924.2	10.022	0.00		C5 H11 N23 O S2 F
492.0938	0.8	1.6	7.5	923.1	8.875	0.01		C4 H13 N21 O2 S Cl F2
492.0945	0.1	0.2	1.5	922.0	7.772	0.04		C4 H20 N15 O9 Cl2
492.0947	-0.1	-0.2	1.5	922.2	8.054	0.03		C3 H20 N17 O5 S2 Cl F
492.0952	-0.6	-1.2	7.5	923.0	8.775	0.02		C3 H12 N21 O6 Cl F
492.0943	0.3	0.6	6.5	925.9	11.752	0.00		C3 H14 N19 O9 S
492.0939	0.7	1.4	2.5	924.5	10.319	0.00		C2 H16 N17 O10 Cl F
492.0954	-0.8	-1.6	7.5	925.2	10.986	0.00		C2 H12 N23 O2 S2 F2
492.0945	0.1	0.2	8.5	930.8	16.642	0.00		C H8 N23 O7 F2
492.0940	0.6	1.2	2.5	926.6	12.374	0.00		C H16 N19 O6 S2 F2
492.0950	-0.4	-0.8	3.5	924.8	10.648	0.00		C H14 N21 O3 S Cl F3
492.0939	0.7	1.4	13.5	926.4	12.231	0.00		H4 N31 Cl F
492.0954	-0.8	-1.6	2.5	928.1	13.927	0.00		H15 N19 O10 S F
492.0936	1.0	2.0	-1.5	926.6	12.374	0.00		H18 N17 O7 S Cl F3

Figure H.10: MS spectrum of compound 14a, page 2.

I Spectroscopic Data - Compound 14b

Figure I.1: $^1\text{H-NMR}$ spectrum of compound 14b.

I SPECTROSCOPIC DATA - COMPOUND 14B

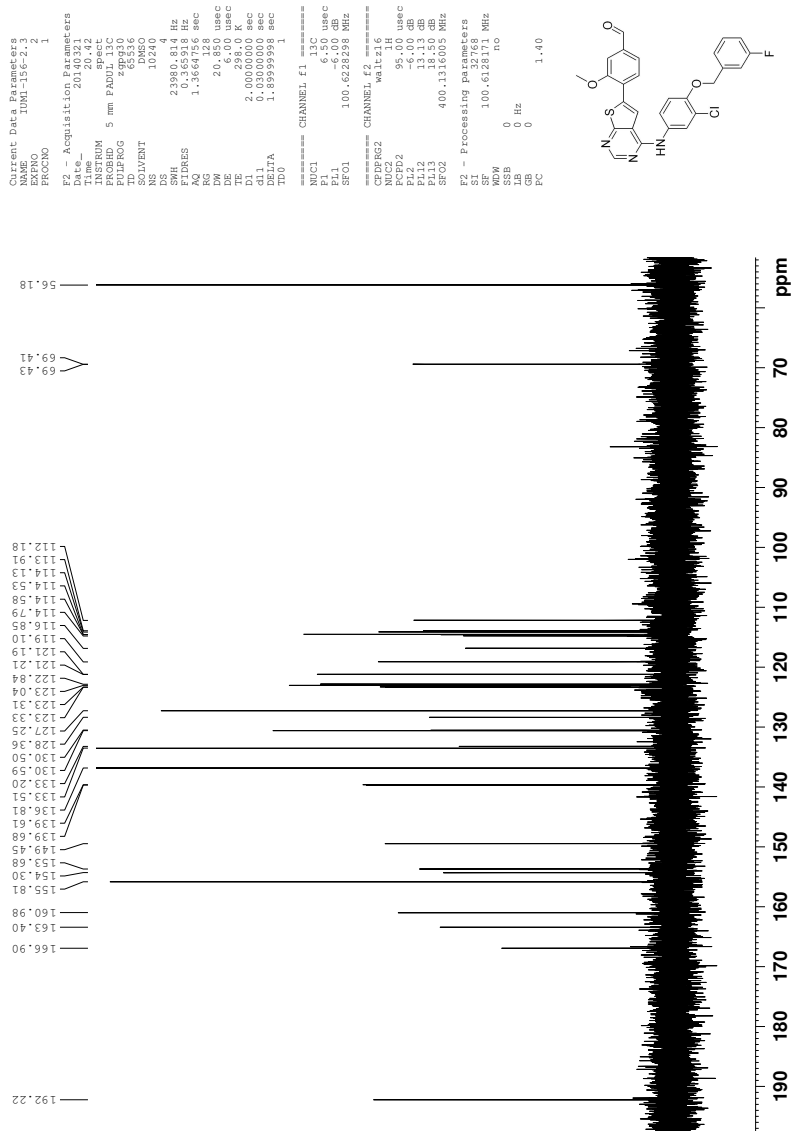
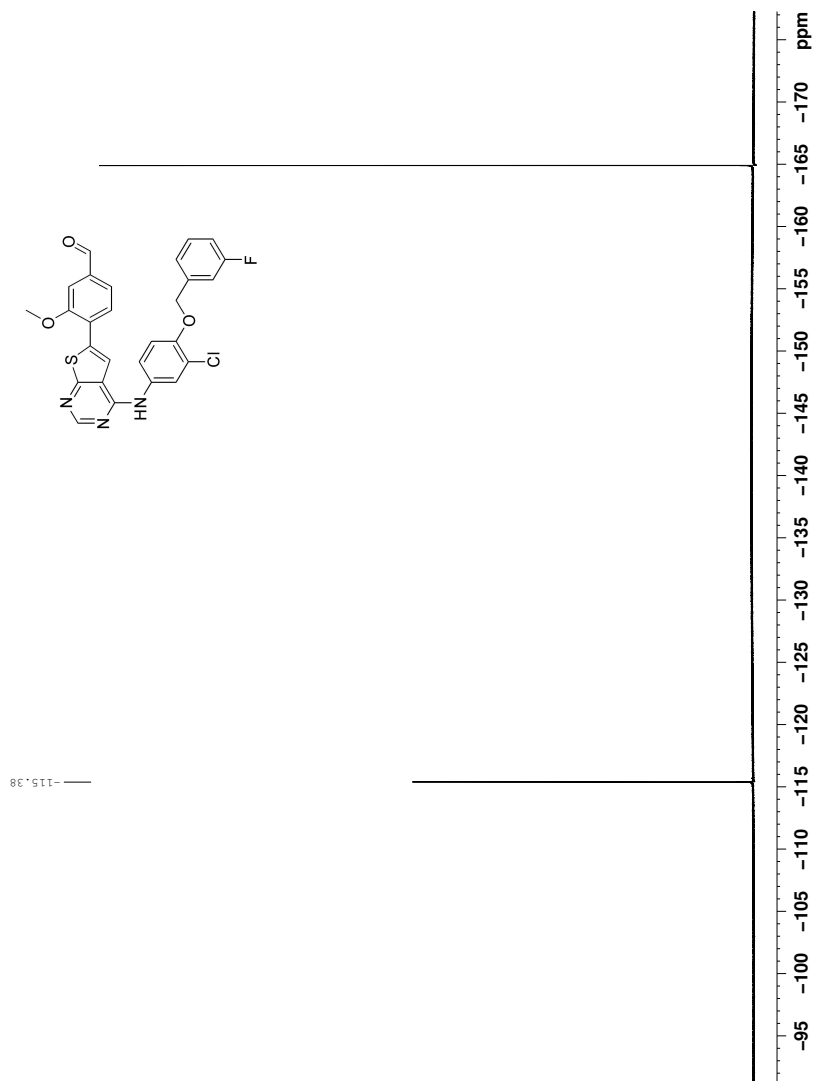


Figure I.2: ^{13}C -NMR spectrum of compound 14b.

Figure I.3: ^{19}F -NMR spectrum of compound **14b** (decoupled).

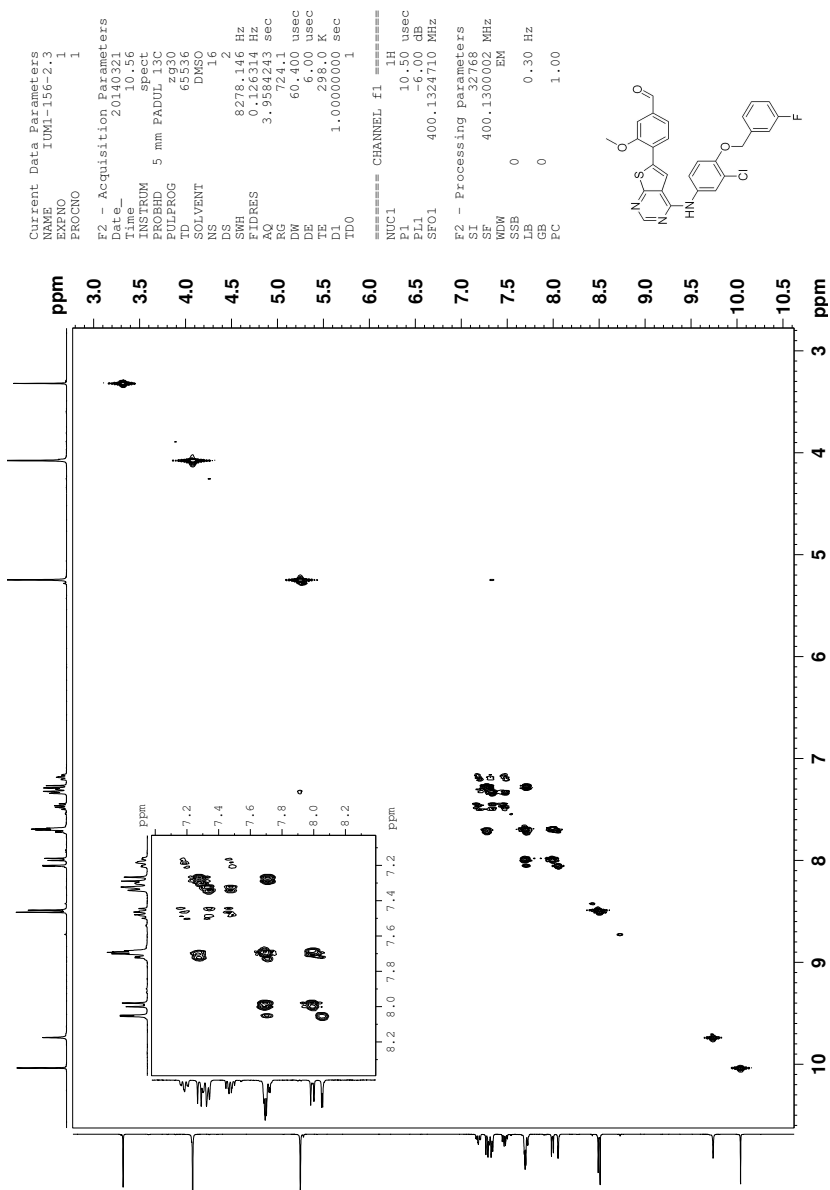


Figure I.4: COSY spectrum of compound 14b.

I SPECTROSCOPIC DATA - COMPOUND 14B

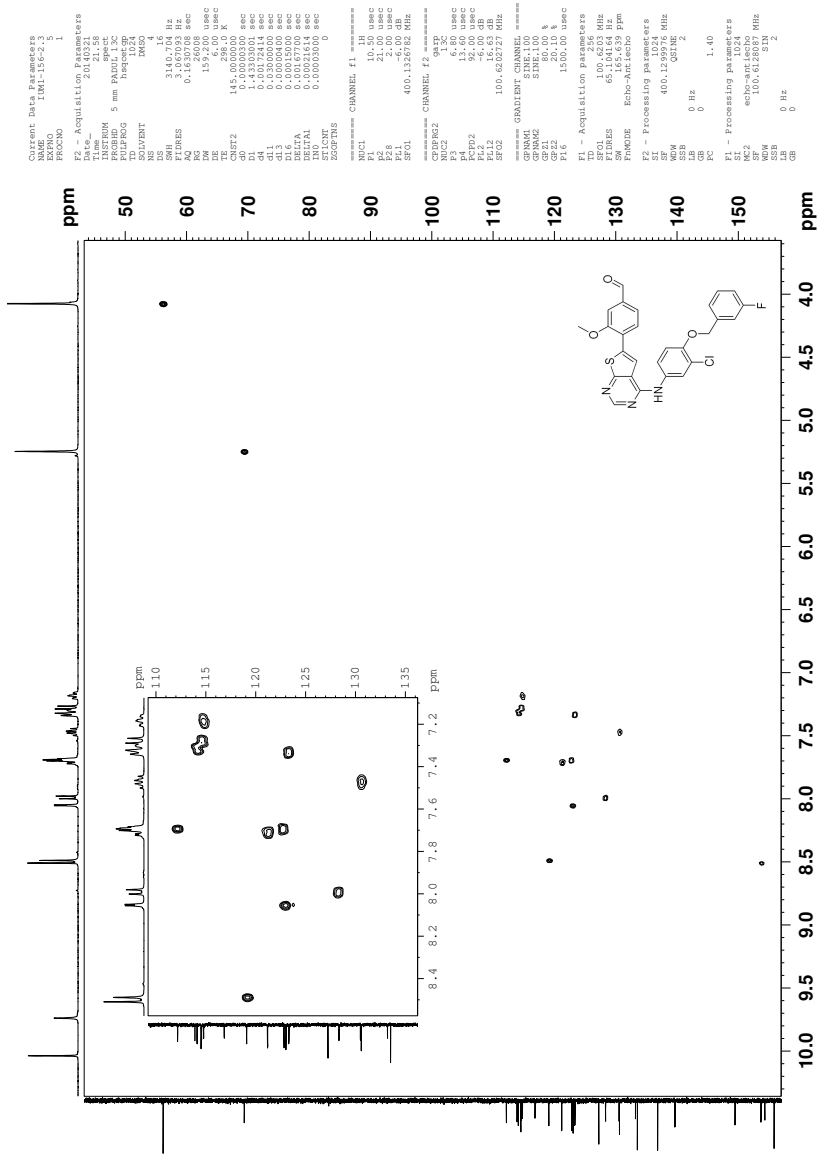


Figure I.5: HSQC spectrum of compound 14b.

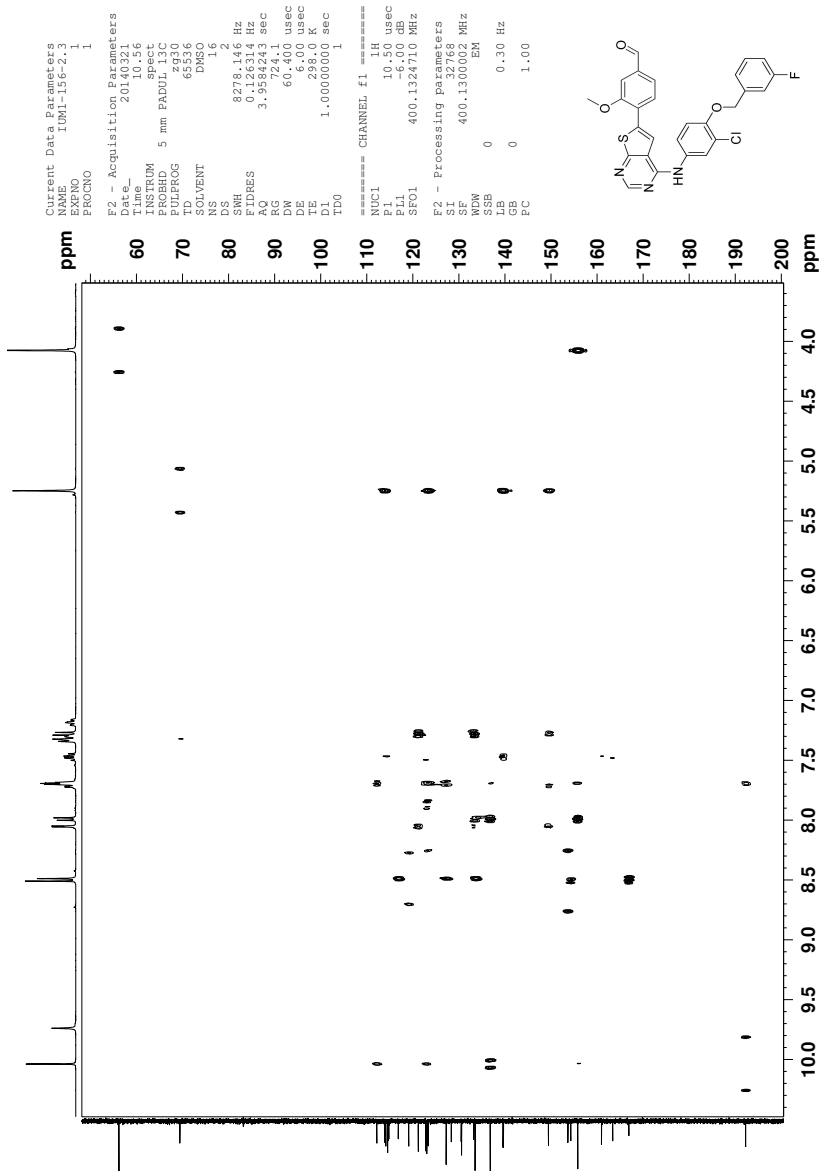


Figure I.6: HMBC spectrum of compound 14b.

I SPECTROSCOPIC DATA - COMPOUND 14B

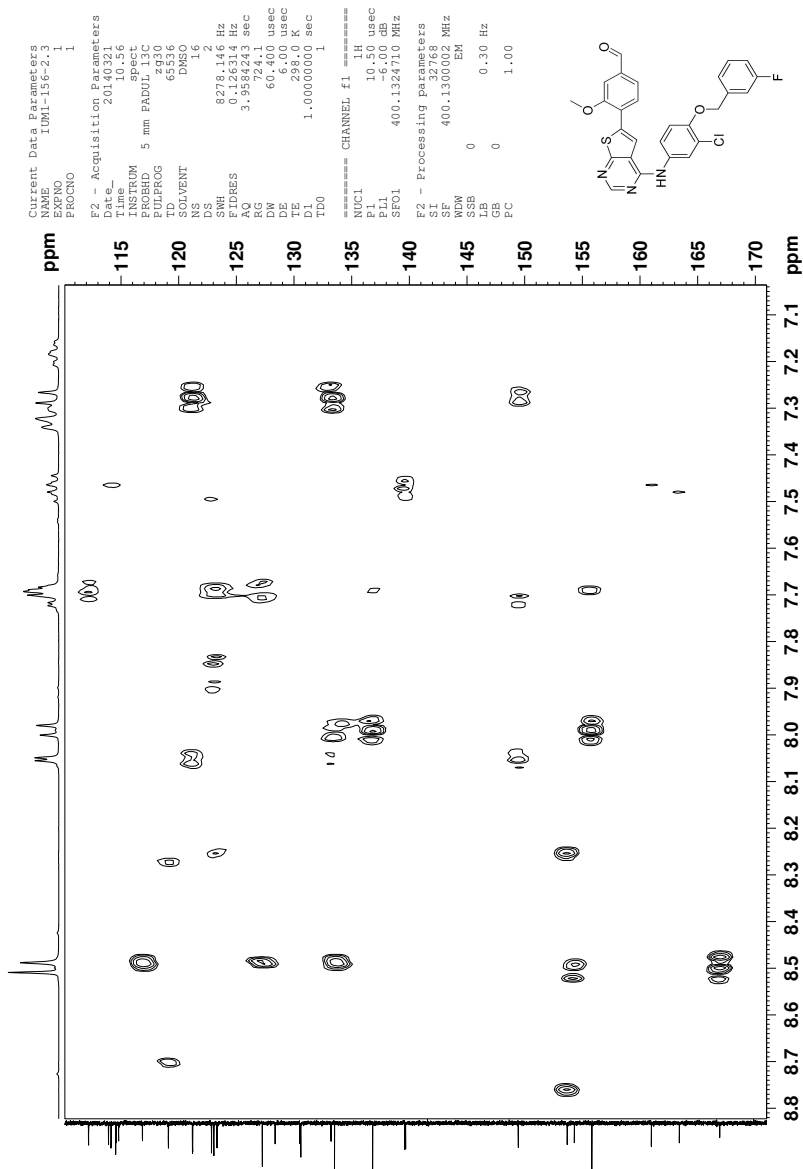


Figure I.7: Section of HMBC spectrum of compound 14b.

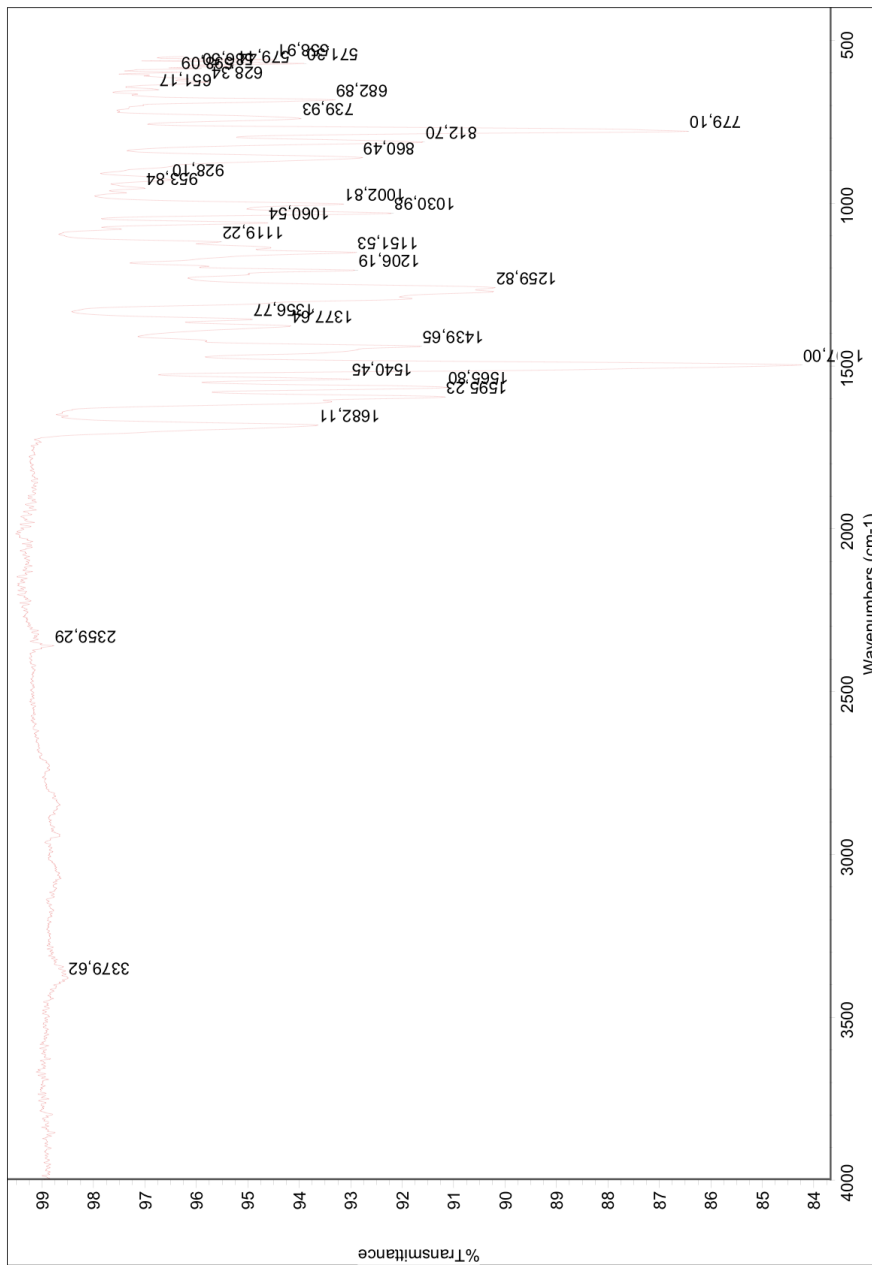


Figure I.8: IR spectrum of compound **14b**.

I SPECTROSCOPIC DATA - COMPOUND 14B

Elemental Composition Report

Page 1

Single Mass Analysis

Tolerance = 2.0 PPM / DBE: min = -1.5, max = 50.0

Element prediction: Off

Number of isotope peaks used for i-FIT = 3

Monoisotopic Mass, Even Electron Ions

58510 formula(e) evaluated with 138 results within limits (all results (up to 1000) for each mass)

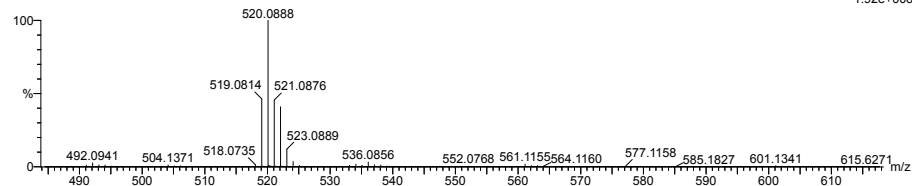
Elements Used:

C: 3-500 H: 0-1000 N: 0-100 O: 0-200 F: 0-3 S: 0-3 Cl: 0-2

NT-MSLAB-Operator-SVG

2014-75 182 (3.549) AM2 (Ar,35000.0,0.00,0.00); Cm (135:184)

1: TOF MS ASAP+
1.92e+006



Minimum: -1.5
Maximum: 50.0

Mass	Calc. Mass	mDa	PPM	DBE	i-FIT	Norm	Conf(%)	Formula
520.0888	520.0893	-0.5	-1.0	31.5	1106.0	0.222	80.10	C38 H15 N C1
	520.0886	0.2	0.4	32.5	1117.8	11.990	0.00	C36 H11 N3 O F
	520.0898	-1.0	-1.9	28.5	1118.2	12.425	0.00	C33 H12 N3 O2 F2
	520.0887	0.1	0.2	22.5	1110.3	4.499	1.11	C30 H19 N3 O2 S Cl
	520.0883	0.5	1.0	18.5	1114.5	8.709	0.02	C29 H21 N O3 F Cl2
	520.0889	-0.1	-0.2	24.5	1110.5	4.649	0.96	C28 H13 N7 F2 Cl
	520.0880	0.8	1.5	23.5	1114.9	9.079	0.01	C28 H15 N5 O3 F S
	520.0893	-0.5	-1.0	23.5	1118.1	12.270	0.00	C27 H14 N5 O7
	520.0880	0.8	1.5	14.5	1114.9	9.080	0.01	C27 H23 N F3 S Cl2
	520.0898	-1.0	-1.9	18.5	1111.7	5.899	0.27	C27 H20 N3 O3 F S Cl
	520.0889	-0.1	-0.2	17.5	1114.3	8.529	0.02	C27 H22 N O6 S2
	520.0894	-0.6	-1.2	14.5	1115.1	9.282	0.01	C26 H22 N O4 F2 Cl2
	520.0882	0.6	1.2	25.5	1117.8	11.955	0.00	C26 H9 N9 O F3
	520.0880	0.8	1.5	18.5	1117.9	12.073	0.00	C26 H18 N O11
	520.0886	0.2	0.4	13.5	1113.7	7.892	0.04	C25 H24 N O3 F2 S3
	520.0878	1.0	1.9	18.5	1114.4	8.628	0.02	C25 H20 N7 S Cl2
	520.0896	-0.8	-1.5	14.5	1112.3	6.526	0.15	C25 H22 N3 F3 S2 Cl
	520.0891	-0.3	-0.6	19.5	1115.4	9.631	0.01	C25 H16 N5 O4 F2 S
	520.0880	0.8	1.5	29.5	1117.2	11.380	0.00	C24 H6 N15 O
	520.0887	0.1	0.2	15.5	1112.3	6.460	0.16	C24 H18 N3 O5 F3 Cl
	520.0878	1.0	1.9	14.5	1115.2	9.366	0.01	C24 H20 N O8 F2 S
	520.0893	-0.5	-1.0	18.5	1111.8	5.984	0.25	C23 H19 N9 S2 Cl
	520.0891	-0.3	-0.6	14.5	1118.3	12.532	0.00	C23 H19 N O12 F
	520.0898	-1.0	-1.9	24.5	1111.4	5.622	0.36	C23 H11 N13 O Cl
	520.0880	0.8	1.5	13.5	1112.2	6.430	0.16	C22 H23 N5 O4 S2 Cl
	520.0889	-0.1	-0.2	14.5	1114.8	8.998	0.01	C22 H21 N7 O F S Cl2
	520.0898	-1.0	-1.9	9.5	1114.6	8.769	0.02	C22 H25 N O4 F3 S3
	520.0885	0.3	0.6	8.5	1115.4	9.577	0.01	C22 H29 N3 F S3 Cl2
	520.0885	0.3	0.6	19.5	1111.6	5.844	0.29	C22 H15 N9 O5 Cl
	520.0889	-0.1	-0.2	10.5	1115.8	10.014	0.00	C21 H21 N O9 F3 S
	520.0891	-0.3	-0.6	25.5	1117.6	11.793	0.00	C21 H7 N15 O2 F
	520.0886	0.2	0.4	19.5	1113.8	8.044	0.03	C21 H15 N11 O F S2
	520.0898	-1.0	-1.9	8.5	1115.7	9.932	0.00	C21 H28 N3 O4 S2 Cl2
	520.0890	-0.2	-0.4	9.5	1115.2	9.395	0.01	C20 H24 N3 O9 Cl2
	520.0883	0.5	1.0	15.5	1112.0	6.186	0.21	C20 H17 N9 O2 F2 S Cl
	520.0878	1.0	1.9	9.5	1112.8	7.032	0.09	C20 H25 N5 O F2 S3 Cl
	520.0878	1.0	1.9	20.5	1117.5	11.692	0.00	C20 H11 N11 O6 F
	520.0895	-0.7	-1.3	13.5	1114.0	8.224	0.03	C20 H22 N7 O4 S3
	520.0896	-0.8	-1.5	4.5	1115.8	10.039	0.00	C19 H30 N3 O F2 S3 Cl2
	520.0887	0.1	0.2	14.5	1115.1	9.301	0.01	C19 H18 N7 O9 S
	520.0891	-0.3	-0.6	9.5	1113.1	7.289	0.07	C19 H24 N5 O5 F S2 Cl
	520.0882	0.6	1.2	8.5	1114.0	8.165	0.03	C19 H26 N3 O8 S3
	520.0879	0.9	1.7	11.5	1114.6	8.843	0.01	C19 H19 N7 O3 F3 Cl2
	520.0896	-0.8	-1.5	15.5	1112.8	7.039	0.09	C19 H16 N9 O6 F Cl
	520.0898	-1.0	-1.9	15.5	1114.6	8.843	0.01	C18 H16 N11 O2 F2 S2
	520.0883	0.5	1.0	10.5	1113.1	7.262	0.07	C18 H20 N5 O10 F Cl
	520.0887	0.1	0.2	5.5	1115.4	9.597	0.01	C18 H26 N3 O6 F2 S Cl2
	520.0878	1.0	1.9	4.5	1113.5	7.713	0.04	C18 H28 N O9 F S2 Cl
	520.0889	-0.1	-0.2	16.5	1117.9	12.094	0.00	C17 H12 N11 O7 F2
	520.0892	-0.4	-0.8	4.5	1114.1	8.250	0.03	C17 H27 N O13 S Cl
	520.0885	0.3	0.6	10.5	1114.4	8.569	0.02	C17 H20 N7 O6 F2 S2
	520.0894	-0.6	-1.2	11.5	1112.9	7.142	0.08	C17 H18 N9 O3 F3 S Cl
	520.0889	-0.1	-0.2	5.5	1113.5	7.656	0.05	C17 H26 N5 O2 F3 S3 Cl

Figure I.9: MS spectrum of compound 14b, page 1.

Elemental Composition Report

Single Mass Analysis

Tolerance = 2.0 PPM / DBE: min = -1.5, max = 50.0

Element prediction: Off

Number of isotope peaks used for i-FIT = 3

Monoisotopic Mass, Even Electron Ions

58510 formula(e) evaluated with 138 results within limits (all results (up to 1000) for each mass)

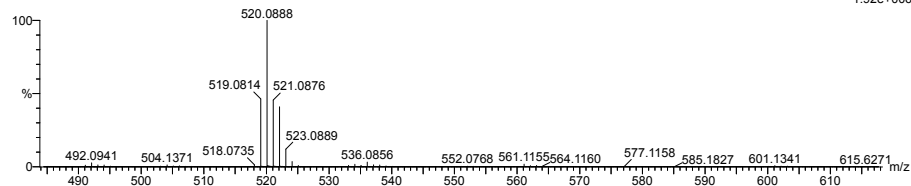
Elements Used:

C: 3-500 H: 0-1000 N: 0-100 O: 0-200 F: 0-3 S: 0-3 Cl: 0-2

NT-MSLAB-Operator-SVG

2014-75 182 (3.549) AM2 (Ar,35000,0,0,00,0,00); Cm (135:184)

1: TOF MS ASAP+
1.92e+006



Minimum: -1.5
Maximum: 50.0

Mass	Calc. Mass	mDa	PPM	DBE	i-FIT	Norm	Conf(%)	Formula
520.0881	0.7	1.3	6.5	1113.3	7.539	0.05		C16 H22 N5 O7 F3 S Cl
520.0893	-0.5	-1.0	4.5	1114.7	8.892	0.01		C16 H27 N3 O9 F S3
520.0898	-1.0	-1.9	10.5	1115.9	10.061	0.00		C16 H19 N7 O10 F S
520.0883	0.5	1.0	21.5	1111.3	5.508	0.41		C16 H8 N19 F Cl
520.0887	0.1	0.2	9.5	1112.8	6.968	0.09		C15 H23 N11 O2 S3 Cl
520.0889	-0.1	-0.2	0.5	1114.3	8.457	0.02		C15 H29 N O10 F2 S2 Cl
520.0894	-0.6	-1.2	6.5	1114.0	8.219	0.03		C15 H21 N5 O11 F2 Cl
520.0885	0.3	0.6	5.5	1115.6	9.787	0.01		C15 H23 N3 O14 F S
520.0892	-0.4	-0.8	15.5	1112.2	6.396	0.17		C15 H15 N15 O3 S Cl
520.0898	-1.0	-1.9	5.5	1118.7	12.864	0.00		C14 H22 N3 O18
520.0883	0.5	1.0	5.5	1114.8	9.002	0.01		C14 H25 N9 O3 F S2 Cl2
520.0878	1.0	1.9	10.5	1112.6	6.821	0.11		C14 H19 N11 O7 S Cl
520.0881	0.7	1.3	1.5	1114.4	8.611	0.02		C14 H25 N O15 F2 Cl
520.0898	-1.0	-1.9	21.5	1114.3	8.505	0.02		C14 H7 N21 F S
520.0896	-0.8	-1.5	6.5	1115.1	9.291	0.01		C14 H21 N7 O7 F3 S2
520.0888	0.0	0.0	11.5	1114.2	8.380	0.02		C14 H17 N13 O4 F Cl2
520.0880	0.8	1.5	10.5	1113.6	7.814	0.04		C13 H19 N13 O3 F S3
520.0894	-0.6	-1.2	17.5	1112.1	6.259	0.19		C13 H9 N19 O F2 Cl
520.0892	-0.4	-0.8	-0.5	1115.6	9.827	0.01		C13 H32 N5 O6 S3 Cl2
520.0885	0.3	0.6	16.5	1113.6	7.753	0.04		C13 H11 N17 O4 F S
520.0889	-0.1	-0.2	11.5	1112.4	6.550	0.14		C13 H17 N15 F2 S2 Cl
520.0887	0.1	0.2	7.5	1118.2	12.392	0.00		C13 H17 N7 O12 F3
520.0896	-0.8	-1.5	5.5	1115.2	9.417	0.01		C13 H24 N9 O7 S Cl2
520.0883	0.5	1.0	1.5	1115.0	9.226	0.01		C13 H25 N3 O11 F3 S2
520.0885	0.3	0.6	7.5	1114.2	8.377	0.02		C12 H19 N13 O F3 S Cl2
520.0881	0.7	1.3	12.5	1112.2	6.434	0.16		C12 H13 N15 O5 F2 Cl
520.0894	-0.6	-1.2	10.5	1114.2	8.400	0.02		C12 H18 N13 O7 S2
520.0896	-0.8	-1.5	1.5	1116.4	10.561	0.00		C12 H24 N3 O15 F2 S
520.0898	-1.0	-1.9	16.5	1117.8	11.994	0.00		C12 H10 N17 O8
520.0881	0.7	1.3	1.5	1114.9	9.141	0.01		C12 H27 N9 F3 S3 Cl2
520.0898	-1.0	-1.9	5.5	1113.5	7.691	0.05		C12 H24 N11 O3 F S3 Cl
520.0883	0.5	1.0	0.5	1115.3	9.520	0.01		C12 H28 N5 O11 S Cl2
520.0894	-0.6	-1.2	1.5	1115.1	9.294	0.01		C11 H26 N9 O4 F2 S2 Cl2
520.0885	0.3	0.6	0.5	1113.6	7.819	0.04		C11 H28 N7 O7 F S3 Cl
520.0882	0.6	1.2	12.5	1113.8	7.997	0.03		C11 H13 N17 O F3 S2
520.0880	0.8	1.5	5.5	1114.0	8.238	0.03		C11 H22 N9 O11 S2
520.0885	0.3	0.6	11.5	1117.7	11.861	0.00		C11 H14 N13 O12
520.0890	-0.2	-0.4	6.5	1113.1	7.304	0.07		C11 H20 N11 O8 F S Cl
520.0887	0.1	0.2	18.5	1116.4	10.625	0.00		C11 H5 N21 O2 F3
520.0891	-0.3	-0.6	6.5	1113.9	8.121	0.03		C10 H20 N13 O4 F2 S3
520.0896	-0.8	-1.5	12.5	1114.2	8.427	0.02		C10 H12 N17 O5 F2 S
520.0878	1.0	1.9	5.5	1114.1	8.312	0.02		C10 H24 N15 S3 Cl2
520.0886	0.2	0.4	2.5	1114.7	8.903	0.01		C10 H22 N9 O9 F2 Cl2
520.0883	0.5	1.0	11.5	1113.2	7.383	0.06		C10 H16 N19 O S Cl2
520.0892	-0.4	-0.8	8.5	1112.7	6.883	0.10		C9 H14 N15 O6 F3 Cl
520.0885	0.3	0.6	22.5	1115.0	9.196	0.01		C9 H2 N27 O2
520.0887	0.1	0.2	2.5	1113.1	7.247	0.07		C9 H22 N11 O5 F3 S2 Cl
520.0890	-0.2	-0.4	1.5	1114.1	8.260	0.03		C9 H23 N7 O16 Cl
520.0883	0.5	1.0	7.5	1113.7	7.906	0.04		C9 H16 N13 O9 F2 S
520.0880	0.8	1.5	16.5	1113.1	7.340	0.06		C9 H10 N23 O S2
520.0878	1.0	1.9	1.5	1114.1	8.298	0.02		C9 H24 N9 O8 F2 S3
520.0879	0.9	1.7	3.5	1112.9	7.144	0.08		C8 H18 N11 O10 F3 Cl
520.0896	-0.8	-1.5	7.5	1118.2	12.394	0.00		C8 H15 N13 O13 F
520.0892	-0.4	-0.8	1.5	1114.4	8.595	0.02		C8 H23 N9 O12 F S2

Figure I.10: MS spectrum of compound 14b, page 2.

Elemental Composition Report

Page 3

Single Mass Analysis

Tolerance = 2.0 PPM / DBE: min = -1.5, max = 50.0

Element prediction: Off

Number of isotope peaks used for i-FIT = 3

Monoisotopic Mass, Even Electron Ions

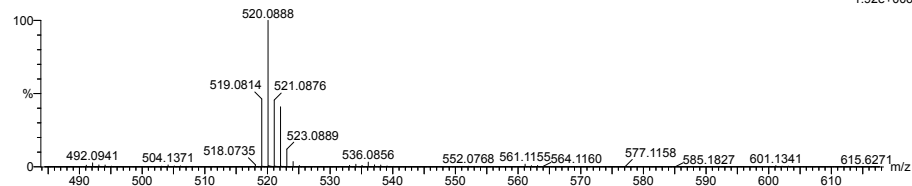
58510 formula(e) evaluated with 138 results within limits (all results (up to 1000) for each mass)

Elements Used:

C: 3-500 H: 0-1000 N: 0-100 O: 0-200 F: 0-3 S: 0-3 Cl: 0-2

NT-MSLAB-Operator-SVG

2014-75 182 (3.549) AM2 (Ar,35000.0,0.00,0.00); Cm (135:184)

1: TOF MS ASAP+
1.92e+006

Minimum: -1.5
Maximum: 50.0

Mass	Calc. Mass	mDa	PPM	DBE	i-FIT	Norm	Conf(%)	Formula
520.0898	-1.0	-1.9	11.5	1111.9	6.114	0.22	C8 H15 N21 O S2 Cl	
520.0890	-0.2	-0.4	1.5	1113.7	7.876	0.04	C7 H25 N15 O F S3 Cl2	
520.0894	-0.6	-1.2	7.5	1113.1	7.283	0.07	C7 H17 N19 O2 F S Cl2	
520.0883	0.5	1.0	2.5	1118.1	12.268	0.00	C7 H19 N9 O17 F	
520.0885	0.3	0.6	6.5	1111.8	5.951	0.26	C7 H19 N17 O5 S2 Cl	
520.0897	-0.9	-1.7	-1.5	1115.0	9.239	0.01	C7 H23 N9 O10 F3 Cl2	
520.0890	-0.2	-0.4	12.5	1110.9	5.086	0.62	C7 H11 N21 O6 Cl	
520.0892	-0.4	-0.8	12.5	1112.7	6.890	0.10	C6 H11 N23 O2 F S2	
520.0894	-0.6	-1.2	3.5	1114.1	8.305	0.02	C6 H17 N13 O10 F3 S	
520.0896	-0.8	-1.5	18.5	1115.6	9.836	0.01	C6 H3 N27 O3 F	
520.0879	0.9	1.7	14.5	1110.6	4.749	0.87	C6 H6 N25 F3 Cl	
520.0881	0.7	1.3	2.5	1113.1	7.302	0.07	C6 H21 N15 O6 F S Cl2	
520.0883	0.5	1.0	13.5	1116.6	10.804	0.00	C5 H7 N23 O7 F	
520.0883	0.5	1.0	2.5	1111.7	5.857	0.29	C5 H21 N17 O2 F2 S3 Cl	
520.0895	-0.7	-1.3	2.5	1113.1	7.312	0.07	C5 H20 N15 O10 Cl2	
520.0881	0.7	1.3	-1.5	1113.7	7.943	0.04	C5 H21 N9 O14 F3 S	
520.0888	0.0	0.0	8.5	1110.3	4.504	1.11	C5 H13 N21 O3 F2 S Cl	
520.0897	-0.9	-1.7	9.5	1111.5	5.703	0.33	C5 H11 N23 F3 Cl2	
520.0878	1.0	1.9	7.5	1112.5	6.716	0.12	C5 H15 N19 O6 F S2	
520.0896	-0.8	-1.5	2.5	1111.5	5.696	0.34	C4 H20 N17 O6 F S2 Cl	
520.0887	0.1	0.2	1.5	1112.1	6.285	0.19	C4 H22 N15 O9 S3	
520.0894	-0.6	-1.2	-1.5	1118.6	12.813	0.00	C4 H20 N9 O18 F2	
520.0894	-0.6	-1.2	14.5	1112.7	6.915	0.10	C4 H5 N27 F3 S	
520.0884	0.4	0.8	4.5	1111.0	5.219	0.54	C4 H15 N19 O4 F3 Cl2	
520.0879	0.9	1.7	-1.5	1112.8	7.006	0.09	C4 H23 N15 O3 F3 S2 Cl2	
520.0892	-0.4	-0.8	7.5	1111.6	5.783	0.31	C4 H14 N19 O10 S	
520.0892	-0.4	-0.8	-1.5	1111.7	5.907	0.27	C3 H22 N15 O7 F2 S Cl2	
520.0888	0.0	0.0	3.5	1109.4	3.576	2.80	C3 H16 N17 O11 F Cl	
520.0895	-0.7	-1.3	13.5	1109.3	3.480	3.08	C3 H8 N29 Cl2	
520.0878	1.0	1.9	2.5	1111.5	5.738	0.32	C3 H18 N15 O14 S	
520.0881	0.7	1.3	9.5	1111.4	5.564	0.38	C3 H9 N23 O4 F3 S	

Figure I.11: MS spectrum of compound 14b, page 3.

J Spectroscopic Data - Compound 14c

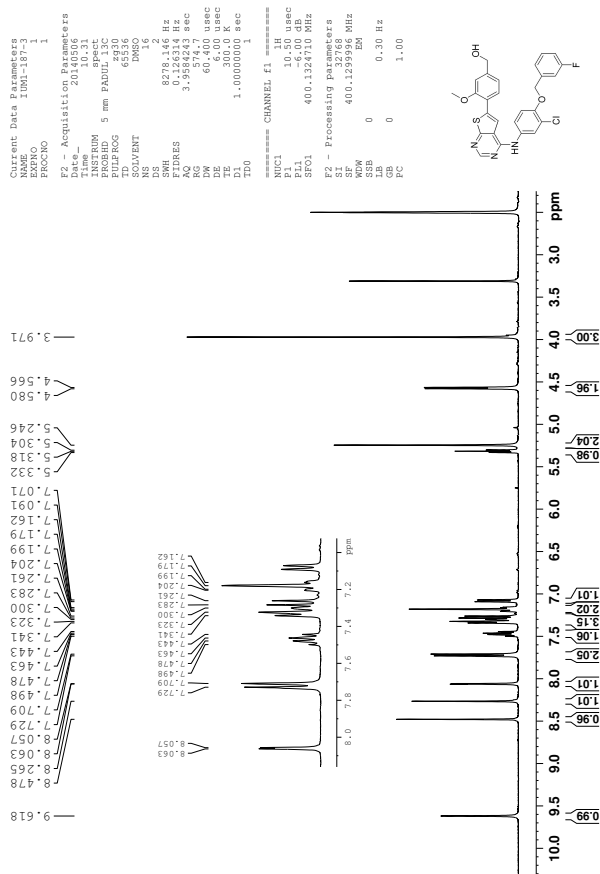


Figure J.1: ¹H-NMR spectrum of compound 14c.

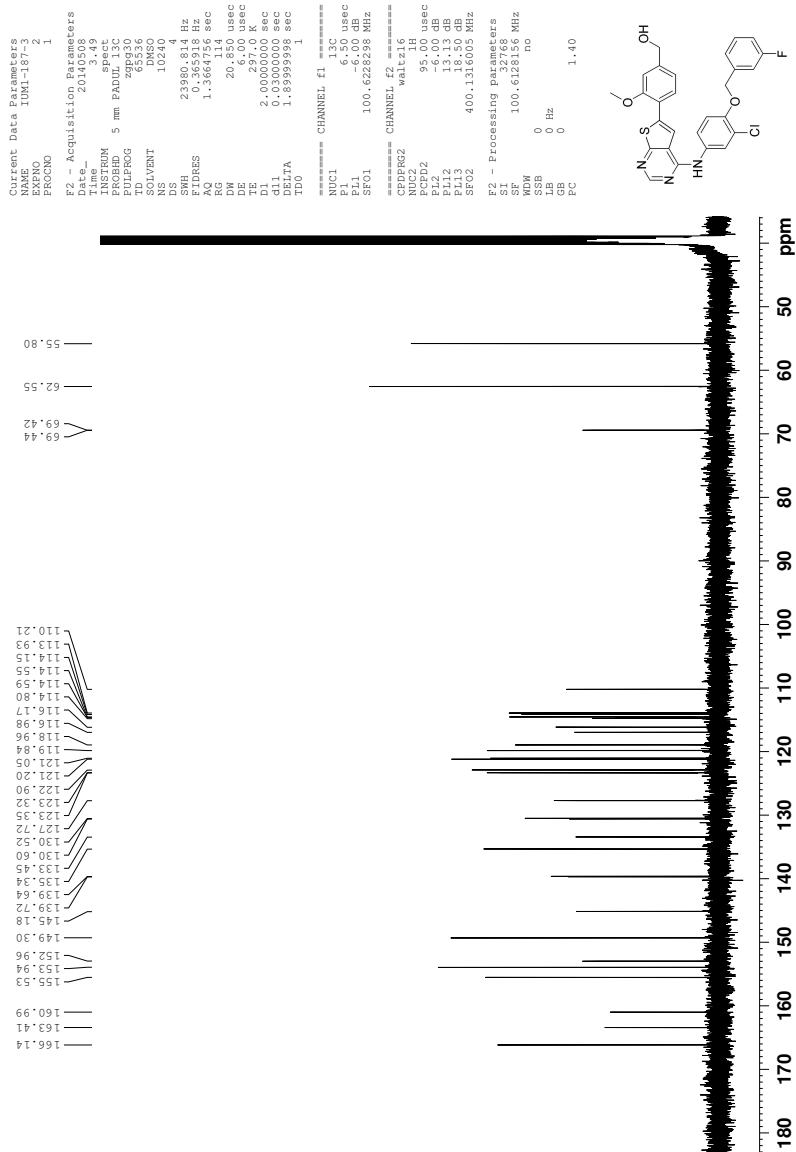


Figure J.2: ¹³C-NMR spectrum of compound 14c.

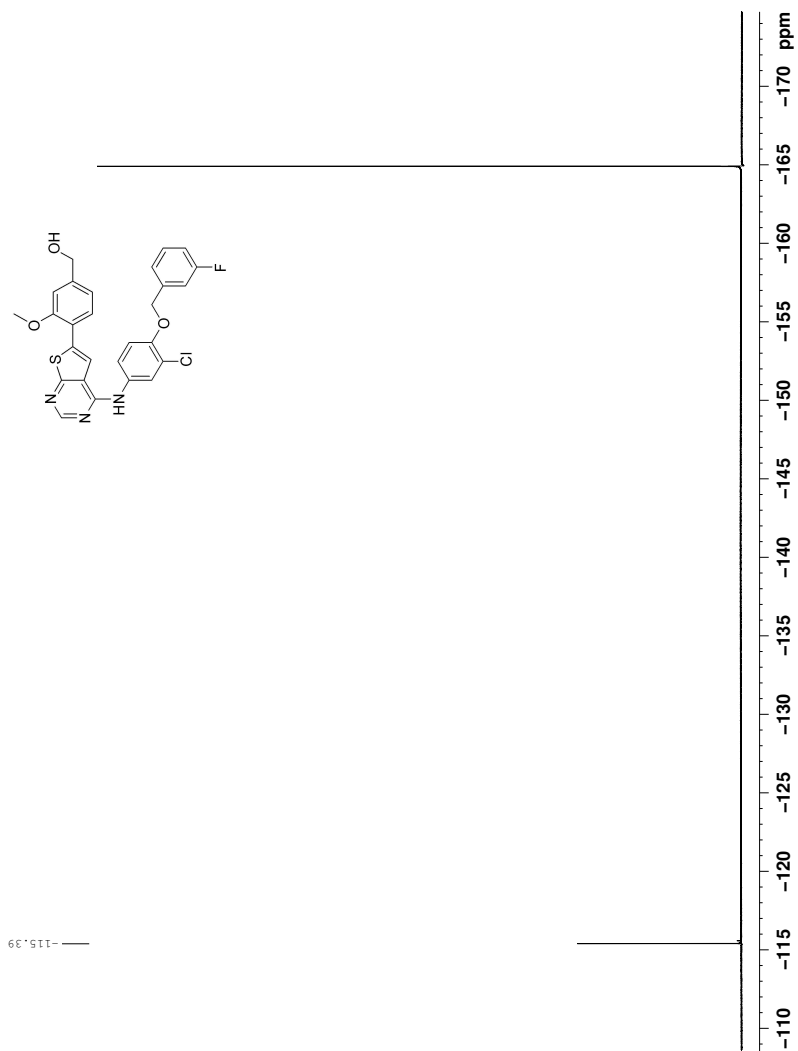


Figure J.3: ^{19}F -NMR spectrum of compound 14c (decoupled).

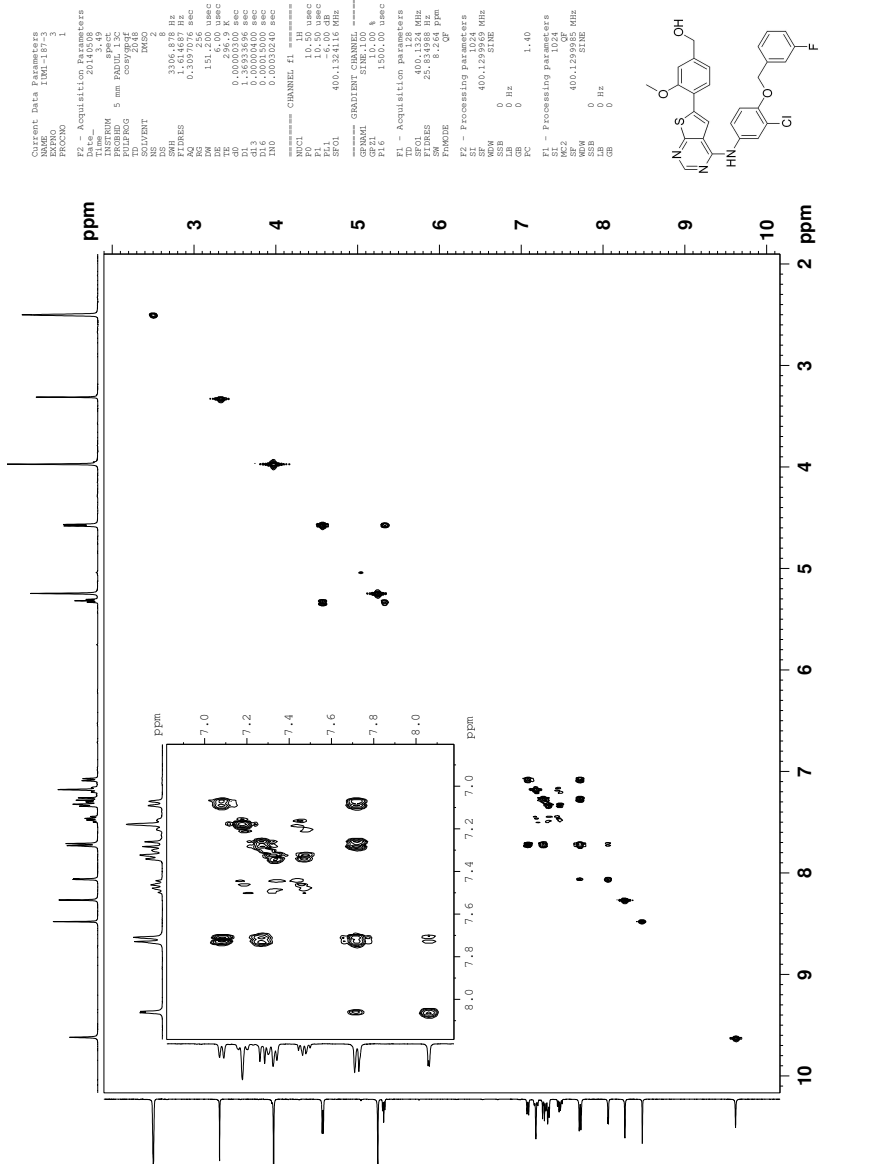


Figure J.4: COSY spectrum of compound 14c.

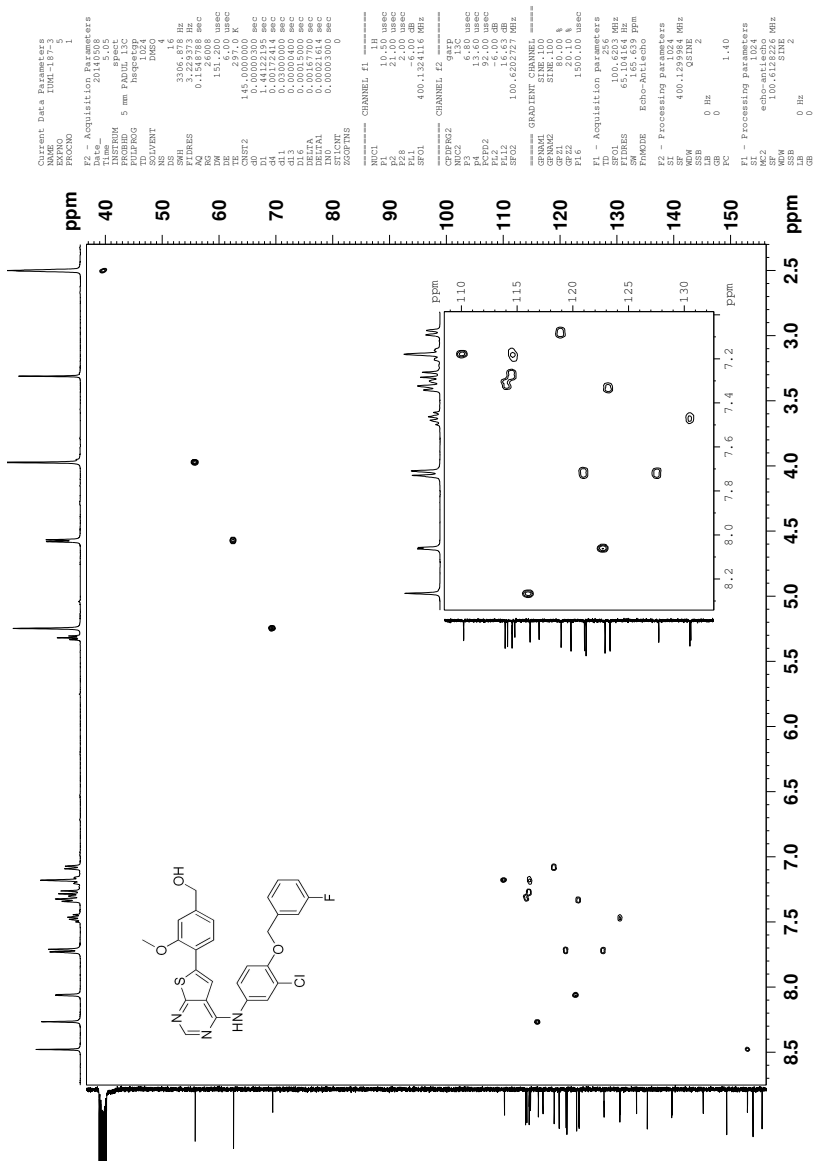


Figure J.5: HSQC spectrum of compound 14c.

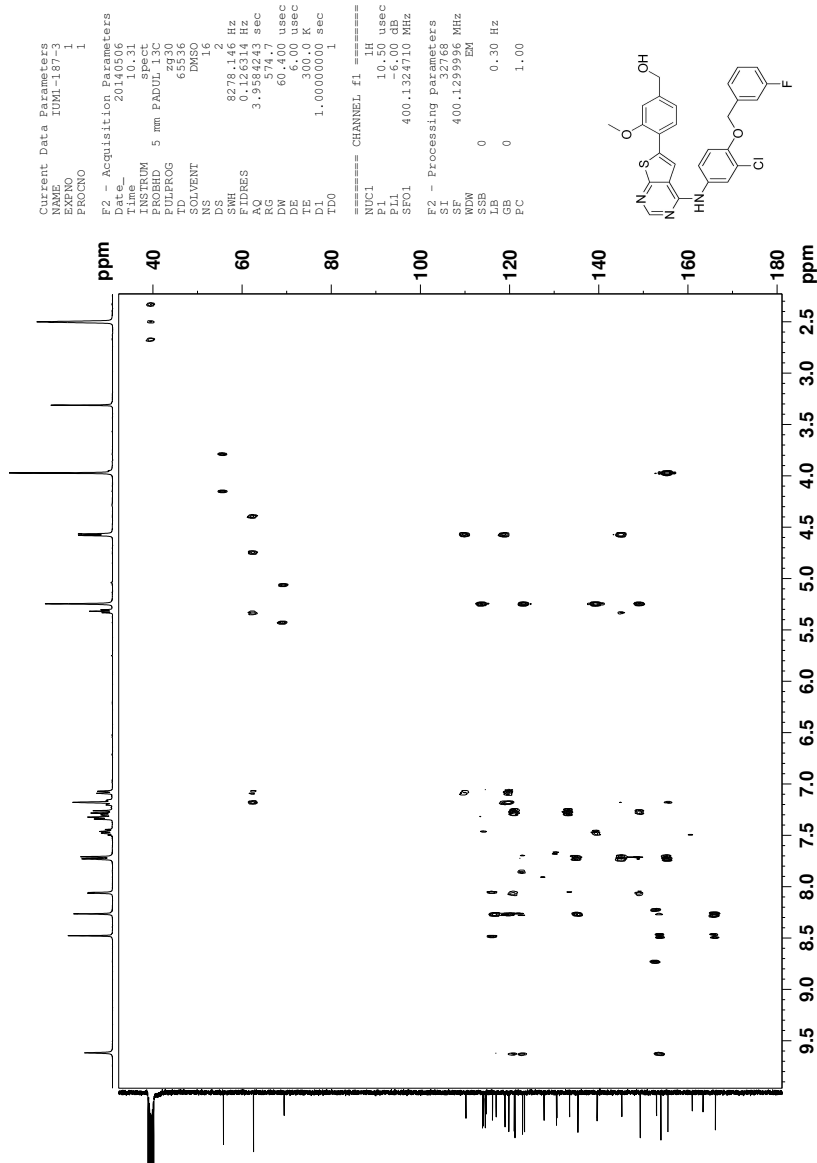


Figure J.6: HMBC spectrum of compound 14c.

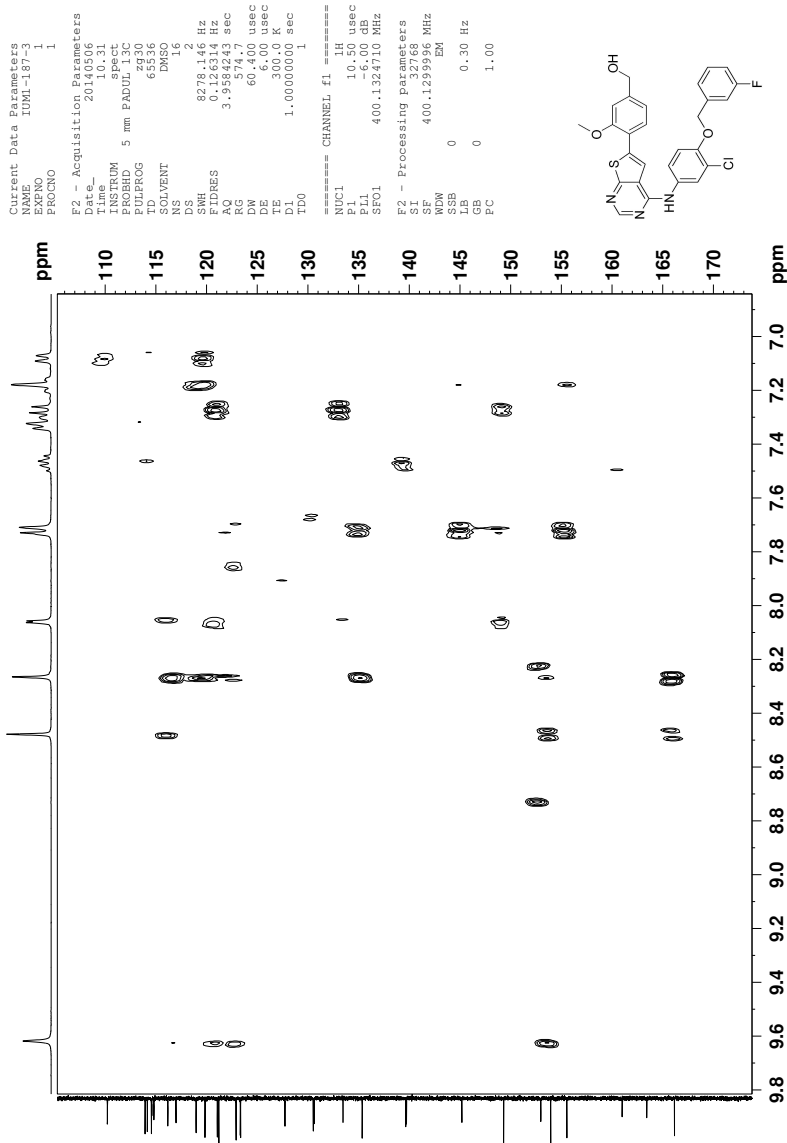


Figure J.7: Section of HMBC spectrum of compound 14c.

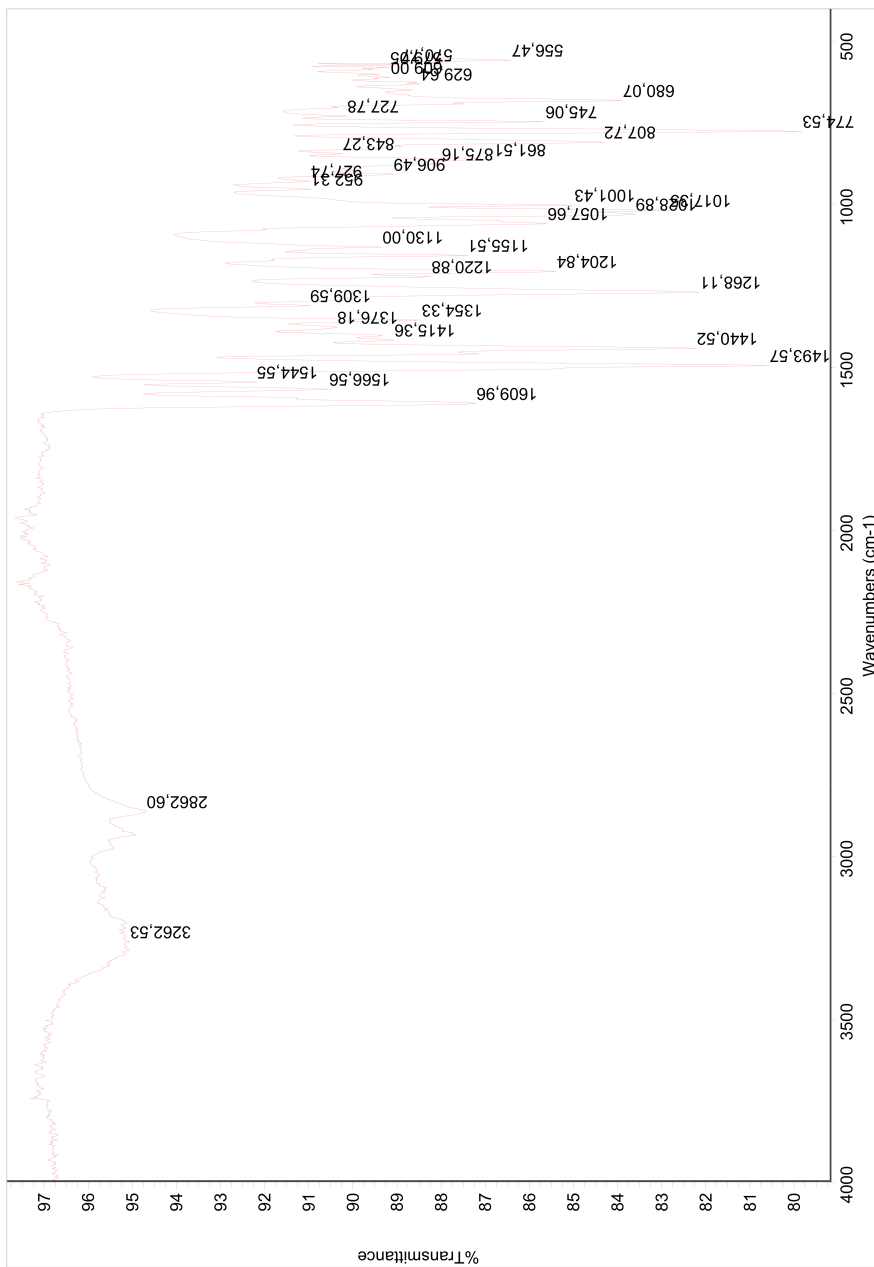


Figure J.8: IR spectrum of compound 14c.

Elemental Composition Report

Single Mass Analysis

Tolerance = 2.0 PPM / DBE: min = -1.5, max = 50.0

Element prediction: Off

Number of isotope peaks used for i-FIT = 3

Monoisotopic Mass, Even Electron Ions

59192 formula(e) evaluated with 123 results within limits (all results (up to 1000) for each mass)

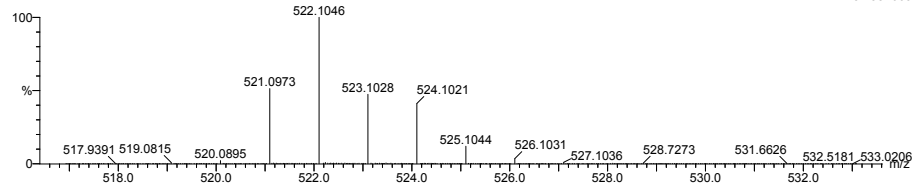
Elements Used:

C: 3-500 H: 0-1000 N: 0-100 O: 0-200 F: 0-3 S: 0-3 Cl: 0-2

NT-MSLAB-Operator-SVG

2014-74 141 (2.757) AM2 (Ar,35000.0,0.00,0.00); Cm (140:176)

1: TOF MS ASAP+
8.28e+005



Minimum: -1.5
Maximum: 50.0

Mass	Calc. Mass	mDa	PPM	DBE	i-FIT	Norm	Conf(%)	Formula
522.1046	522.1050	-0.4	-0.8	30.5	1042.6	0.540	58.28	C38 H17 N C1
	522.1043	0.3	0.6	31.5	1052.5	10.511	0.00	C36 H13 N3 O F
	522.1054	-0.8	-1.5	27.5	1053.0	10.942	0.00	C33 H14 N3 O2 F2
	522.1043	0.3	0.6	21.5	1045.8	3.767	2.31	C30 H21 N3 O2 S Cl1
	522.1039	0.7	1.3	17.5	1049.7	7.628	0.05	C29 H23 N O3 F Cl2
	522.1036	1.0	1.9	22.5	1049.9	7.921	0.04	C28 H17 N5 O3 F S
	522.1046	0.0	0.0	23.5	1045.9	3.919	1.99	C28 H15 N7 F2 Cl1
	522.1037	0.9	1.7	13.5	1049.9	7.882	0.04	C27 H25 N F3 S Cl2
	522.1050	-0.4	-0.8	22.5	1052.9	10.835	0.00	C27 H16 N5 O7
	522.1045	0.1	0.2	16.5	1049.4	7.421	0.06	C27 H24 N O6 S2
	522.1054	-0.8	-1.5	17.5	1047.1	5.055	0.64	C27 H22 N3 O3 F S Cl1
	522.1039	0.7	1.3	24.5	1052.5	10.503	0.00	C26 H11 N9 O F2
	522.1050	-0.4	-0.8	13.5	1050.1	8.109	0.03	C26 H24 N O4 F2 Cl2
	522.1036	1.0	1.9	17.5	1052.7	10.680	0.00	C26 H20 N O11
	522.1048	-0.2	-0.4	18.5	1050.5	8.497	0.02	C25 H18 N5 O4 F2 S
	522.1052	-0.6	-1.1	13.5	1047.6	5.575	0.38	C25 H24 N3 F3 S2 Cl1
	522.1043	0.3	0.6	12.5	1048.9	6.850	0.11	C25 H26 N O3 F2 S3
	522.1044	0.2	0.4	14.5	1047.5	5.520	0.40	C24 H20 N3 O5 F3 Cl1
	522.1036	1.0	1.9	28.5	1052.0	9.959	0.00	C24 H8 N15 O
	522.1050	-0.4	-0.8	17.5	1047.2	5.139	0.59	C23 H21 N9 S2 Cl1
	522.1055	-0.9	-1.7	23.5	1046.8	4.800	0.82	C23 H13 N13 O Cl1
	522.1048	-0.2	-0.4	13.5	1053.1	11.100	0.00	C23 H21 N O12 F
	522.1041	0.5	1.0	7.5	1050.5	8.441	0.02	C22 H31 N3 F S3 Cl2
	522.1054	-0.8	-1.5	8.5	1049.7	7.665	0.05	C22 H27 N O4 F3 S3
	522.1041	0.5	1.0	18.5	1047.1	5.037	0.65	C22 H17 N9 O5 Cl1
	522.1036	1.0	1.9	12.5	1047.5	5.499	0.41	C22 H25 N5 O4 S2 Cl2
	522.1046	0.0	0.0	13.5	1049.9	7.847	0.04	C22 H23 N7 O F S Cl2
	522.1043	0.3	0.6	18.5	1049.0	7.006	0.09	C21 H17 N11 O F S2
	522.1046	0.0	0.0	9.5	1050.9	8.845	0.01	C21 H23 N O9 F3 S
	522.1048	-0.2	-0.4	24.5	1052.4	10.372	0.00	C21 H9 N15 O2 F
	522.1055	-0.9	-1.7	7.5	1050.7	8.711	0.02	C21 H30 N3 O4 S2 Cl2
	522.1046	0.0	0.0	8.5	1050.3	8.276	0.03	C20 H26 N3 O9 Cl2
	522.1039	0.7	1.3	14.5	1047.4	5.354	0.47	C20 H19 N9 O2 F2 S Cl1
	522.1052	-0.6	-1.1	12.5	1049.2	7.131	0.08	C20 H24 N7 O4 S3
	522.1053	-0.7	-1.3	14.5	1048.1	6.043	0.24	C19 H18 N9 O6 F Cl1
	522.1039	0.7	1.3	7.5	1049.1	7.076	0.08	C19 H28 N3 O8 S3
	522.1048	-0.2	-0.4	8.5	1048.3	6.306	0.18	C19 H26 N5 O5 F S2 Cl1
	522.1053	-0.7	-1.3	3.5	1050.9	8.824	0.01	C19 H32 N3 O F2 S3 Cl2
	522.1043	0.3	0.6	13.5	1050.3	8.258	0.03	C19 H20 N7 O9 S
	522.1044	0.2	0.4	4.5	1050.5	8.487	0.02	C18 H28 N3 O6 F2 S Cl2
	522.1039	0.7	1.3	9.5	1048.4	6.332	0.18	C18 H22 N5 O10 F Cl1
	522.1054	-0.8	-1.5	14.5	1049.7	7.714	0.04	C18 H18 N11 O2 F2 S2
	522.1048	-0.2	-0.4	3.5	1049.2	7.176	0.08	C17 H29 N O13 S Cl1
	522.1041	0.5	1.0	9.5	1049.5	7.509	0.05	C17 H22 N7 O6 F2 S2
	522.1046	0.0	0.0	4.5	1048.6	6.614	0.13	C17 H28 N5 O2 F3 S3 Cl1
	522.1046	0.0	0.0	15.5	1052.7	10.702	0.00	C17 H14 N11 O7 F2
	522.1050	-0.4	-0.8	10.5	1048.2	6.160	0.21	C17 H20 N9 O3 F3 S Cl1
	522.1055	-0.9	-1.7	9.5	1051.0	8.929	0.01	C16 H21 N7 O10 F S
	522.1039	0.7	1.3	20.5	1046.7	4.671	0.94	C16 H10 N19 F Cl1
	522.1050	-0.4	-0.8	3.5	1049.9	7.828	0.04	C16 H29 N3 O9 F S3
	522.1037	0.9	1.7	5.5	1048.5	6.513	0.15	C16 H24 N5 O7 F3 S Cl1
	522.1055	-0.9	-1.7	0.5	1051.0	8.968	0.01	C15 H29 N3 O7 F3 S Cl2
	522.1041	0.5	1.0	4.5	1050.7	8.714	0.02	C15 H25 N3 O14 F S

Figure J.9: MS spectrum of compound 14c, page 1.

Elemental Composition Report

Single Mass Analysis

Tolerance = 2.0 PPM / DBE: min = -1.5, max = 50.0

Element prediction: Off

Number of isotope peaks used for i-FIT = 3

Monoisotopic Mass, Even Electron Ions

59192 formula(e) evaluated with 123 results within limits (all results (up to 1000) for each mass)

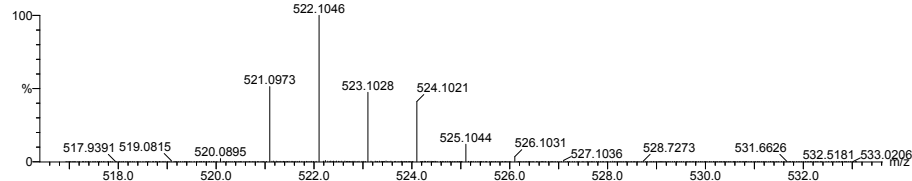
Elements Used:

C: 3-500 H: 0-1000 N: 0-100 O: 0-200 F: 0-3 S: 0-3 Cl: 0-2

NT-MSLAB-Operator-SVG

2014-74 141 (2.757) AM2 (Ar,35000.0,0.00,0.00); Cm (140:176)

1: TOF MS ASAP+
8.28e+005



Minimum: -1.5
Maximum: 50.0

Mass	Calc. Mass	mDa	PPM	DBE	i-FIT	Norm	Conf (%)	Formula
522.1046	0.0	0.0	0.0	-0.5	1049.4	7.359	0.06	C15 H31 N O10 F2 S2 Cl
522.1048	-0.2	-0.4	14.5	1047.5	5.466	0.42		C15 H17 N15 O3 S Cl
522.1043	0.3	0.6	8.5	1048.0	5.988	0.25		C15 H25 N11 O2 S3 Cl
522.1051	-0.5	-1.0	5.5	1049.2	7.169	0.08		C15 H23 N5 O11 F2 Cl
522.1039	0.7	1.3	4.5	1050.0	7.937	0.04		C14 H27 N9 O3 F S2 Cl2
522.1055	-0.9	-1.7	20.5	1049.5	7.476	0.06		C14 H9 N21 F S
522.1052	-0.6	-1.1	5.5	1050.3	8.245	0.03		C14 H23 N7 O7 F3 S2
522.1055	-0.9	-1.7	4.5	1053.5	11.489	0.00		C14 H24 N3 O18
522.1044	0.2	0.4	10.5	1049.4	7.348	0.06		C14 H19 N13 O4 F Cl2
522.1037	0.9	1.7	0.5	1049.6	7.581	0.05		C14 H27 N O15 F2 Cl
522.1044	0.2	0.4	6.5	1053.1	11.038	0.00		C13 H19 N7 O12 F3
522.1051	-0.5	-1.0	16.5	1047.5	5.454	0.43		C13 H11 N19 O F2 Cl
522.1048	-0.2	-0.4	-1.5	1050.7	8.666	0.02		C13 H34 N5 O6 S3 Cl2
522.1053	-0.7	-1.3	4.5	1050.3	8.256	0.03		C13 H26 N9 O7 S Cl2
522.1036	1.0	1.9	9.5	1048.8	6.794	0.11		C13 H21 N13 O3 F S13
522.1039	0.7	1.3	0.5	1050.2	8.179	0.03		C13 H27 N3 O11 F3 S2
522.1046	0.0	0.0	10.5	1047.7	5.635	0.36		C13 H19 N15 F2 S2 Cl
522.1041	0.5	1.0	15.5	1049.0	6.997	0.09		C13 H13 N17 O4 F S
522.1055	-0.9	-1.7	15.5	1052.6	10.597	0.00		C12 H12 N17 O8
522.1055	-0.9	-1.7	4.5	1048.6	6.620	0.13		C12 H26 N11 O3 F S3 Cl
522.1037	0.9	1.7	11.5	1047.7	5.642	0.35		C12 H15 N15 O5 F2 Cl
522.1040	0.6	1.1	-0.5	1050.4	8.420	0.02		C12 H30 N5 O11 S Cl2
522.1050	-0.4	-0.8	9.5	1049.4	7.404	0.06		C12 H20 N13 O7 S2
522.1053	-0.7	-1.3	0.5	1051.4	9.406	0.01		C12 H26 N3 O15 F2 S
522.1037	0.9	1.7	0.5	1050.0	7.978	0.03		C12 H29 N9 F3 S3 Cl2
522.1042	0.4	0.8	6.5	1049.4	7.400	0.06		C12 H21 N13 O F3 S Cl2
522.1041	0.5	1.0	10.5	1052.5	10.519	0.00		C11 H16 N13 O12
522.1051	-0.5	-1.0	0.5	1050.2	8.222	0.03		C11 H28 N9 O4 F2 S2 Cl2
522.1037	0.9	1.7	4.5	1049.3	7.276	0.07		C11 H24 N9 O11 S2
522.1041	0.5	1.0	-0.5	1048.8	6.789	0.11		C11 H30 N7 O7 F S3 Cl
522.1046	0.0	0.0	5.5	1048.4	6.370	0.17		C11 H22 N11 O8 F S Cl
522.1044	0.2	0.4	17.5	1051.4	9.370	0.01		C11 H7 N21 O2 F3
522.1039	0.7	1.3	11.5	1049.0	6.927	0.10		C11 H15 N17 O F3 S2
522.1055	-0.9	-1.7	6.5	1049.8	7.790	0.04		C11 H20 N13 O5 F2 Cl2
522.1053	-0.7	-1.3	11.5	1049.6	7.538	0.05		C10 H14 N17 O5 F2 S
522.1048	-0.2	-0.4	5.5	1049.1	7.063	0.09		C10 H22 N13 O4 F2 S3
522.1039	0.7	1.3	10.5	1048.5	6.459	0.16		C10 H18 N19 O S Cl2
522.1055	-0.9	-1.7	-0.5	1049.3	7.314	0.07		C10 H29 N7 O11 S2 Cl
522.1042	0.4	0.8	1.5	1049.9	7.836	0.04		C10 H24 N9 O9 F2 Cl2
522.1046	0.0	0.0	0.5	1049.3	7.315	0.07		C9 H25 N7 O16 Cl
522.1049	-0.3	-0.6	7.5	1048.0	5.969	0.26		C9 H16 N15 O6 F3 Cl
522.1039	0.7	1.3	6.5	1049.1	7.106	0.08		C9 H18 N13 O9 F2 S
522.1044	0.2	0.4	1.5	1048.3	6.286	0.19		C9 H24 N11 O5 F3 S2 Cl
522.1041	0.5	1.0	21.5	1050.0	7.985	0.03		C9 H4 N27 O2
522.1037	0.9	1.7	15.5	1048.3	6.288	0.19		C9 H12 N23 O S2
522.1048	-0.2	-0.4	0.5	1049.7	7.712	0.04		C8 H25 N9 O12 F S2
522.1055	-0.9	-1.7	10.5	1047.2	5.210	0.55		C8 H17 N21 O S2 Cl
522.1053	-0.7	-1.3	6.5	1053.0	11.008	0.00		C8 H17 N13 O13 F
522.1042	0.4	0.8	5.5	1047.1	5.120	0.60		C7 H21 N17 O5 S2 Cl
522.1046	0.0	0.0	0.5	1048.9	6.851	0.11		C7 H27 N15 O F S3 Cl2
522.1051	-0.5	-1.0	6.5	1048.3	6.317	0.18		C7 H19 N19 O2 F S Cl2
522.1046	0.0	0.0	11.5	1046.6	4.544	1.06		C7 H13 N21 O6 Cl
522.1039	0.7	1.3	1.5	1052.9	10.877	0.00		C7 H21 N9 O17 F
522.1053	-0.7	-1.3	17.5	1050.6	8.548	0.02		C6 H5 N27 O3 F

Figure J.10: MS spectrum of compound 14c, page 2.

Elemental Composition Report

Single Mass Analysis

Tolerance = 2.0 PPM / DBE: min = -1.5, max = 50.0

Element prediction: Off

Number of isotope peaks used for i-FIT = 3

Monoisotopic Mass, Even Electron Ions

59192 formula(e) evaluated with 123 results within limits (all results (up to 1000) for each mass)

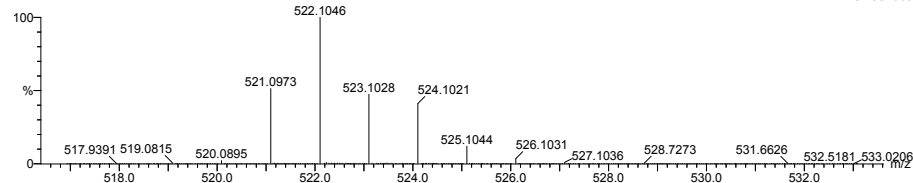
Elements Used:

C: 3-500 H: 0-1000 N: 0-100 O: 0-200 F: 0-3 S: 0-3 Cl: 0-2

NT-MSLAB-Operator-SVG

2014-74 141 (2.757) AM2 (Ar,35000.0,0.00,0.00); Cm (140:176)

1: TOF MS ASAP+
8.28e+005

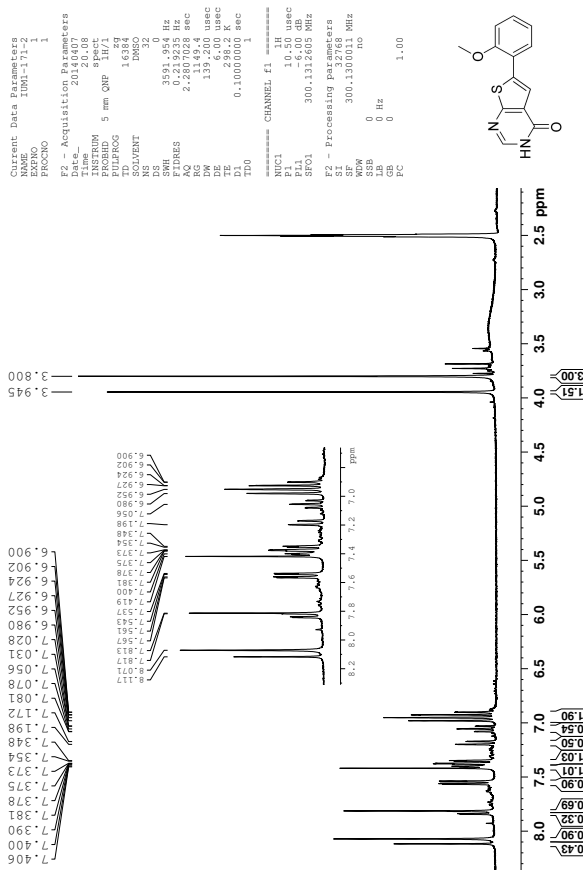


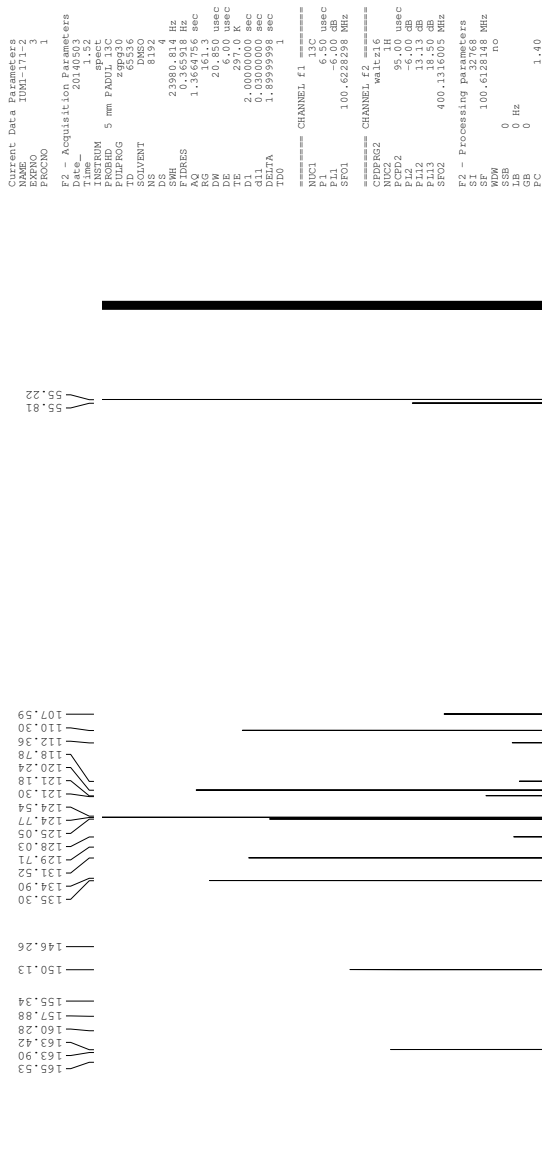
Minimum: -1.5
Maximum: 50.0

Mass	Calc. Mass	mDa	PPM	DBE	i-FIT	Norm	Conf (%)	Formula
522.1051	-0.5	-1.0	2.5	1049.6	7.524	0.05	C6 H19 N13 O10 F3 S	
522.1038	0.8	1.5	1.5	1048.4	6.346	0.18	C6 H23 N15 O6 F S Cl2	
522.1048	-0.2	-0.4	11.5	1047.9	5.908	0.27	C6 H13 N23 O2 F S2	
522.1039	0.7	1.3	1.5	1046.8	4.811	0.81	C5 H23 N17 O2 F2 S3 Cl	
522.1039	0.7	1.3	12.5	1051.4	9.387	0.01	C5 H9 N23 O7 F	
522.1051	-0.5	-1.0	1.5	1048.5	6.451	0.16	C5 H22 N15 O10 Cl2	
522.1053	-0.7	-1.3	8.5	1047.1	5.051	0.64	C5 H13 N23 F3 Cl2	
522.1044	0.2	0.4	7.5	1045.8	3.744	2.37	C5 H15 N21 O3 F2 S Cl	
522.1051	-0.5	-1.0	13.5	1047.7	5.678	0.34	C4 H7 N27 F3 S	
522.1040	0.6	1.1	3.5	1046.6	4.595	1.01	C4 H17 N19 O4 F3 Cl2	
522.1048	-0.2	-0.4	6.5	1047.6	5.543	0.39	C4 H16 N19 O10 S	
522.1044	0.2	0.4	0.5	1047.6	5.572	0.38	C4 H24 N15 O9 S3	
522.1053	-0.7	-1.3	1.5	1046.9	4.853	0.78	C4 H22 N17 O6 F S2 Cl	
522.1044	0.2	0.4	2.5	1045.4	3.359	3.48	C3 H18 N17 O11 F Cl	
522.1037	0.9	1.7	8.5	1046.3	4.249	1.43	C3 H11 N23 O4 F3 S	
522.1051	-0.5	-1.0	12.5	1044.3	2.250	10.54	C3 H10 N29 Cl2	

Figure J.11: MS spectrum of compound 14c, page 3.

K Spectroscopic Data - Compound 20

Figure K.1: $^1\text{H-NMR}$ spectrum of compound 20.

Figure K.2: ^{13}C -NMR spectrum of compound 20.

K SPECTROSCOPIC DATA - COMPOUND 20

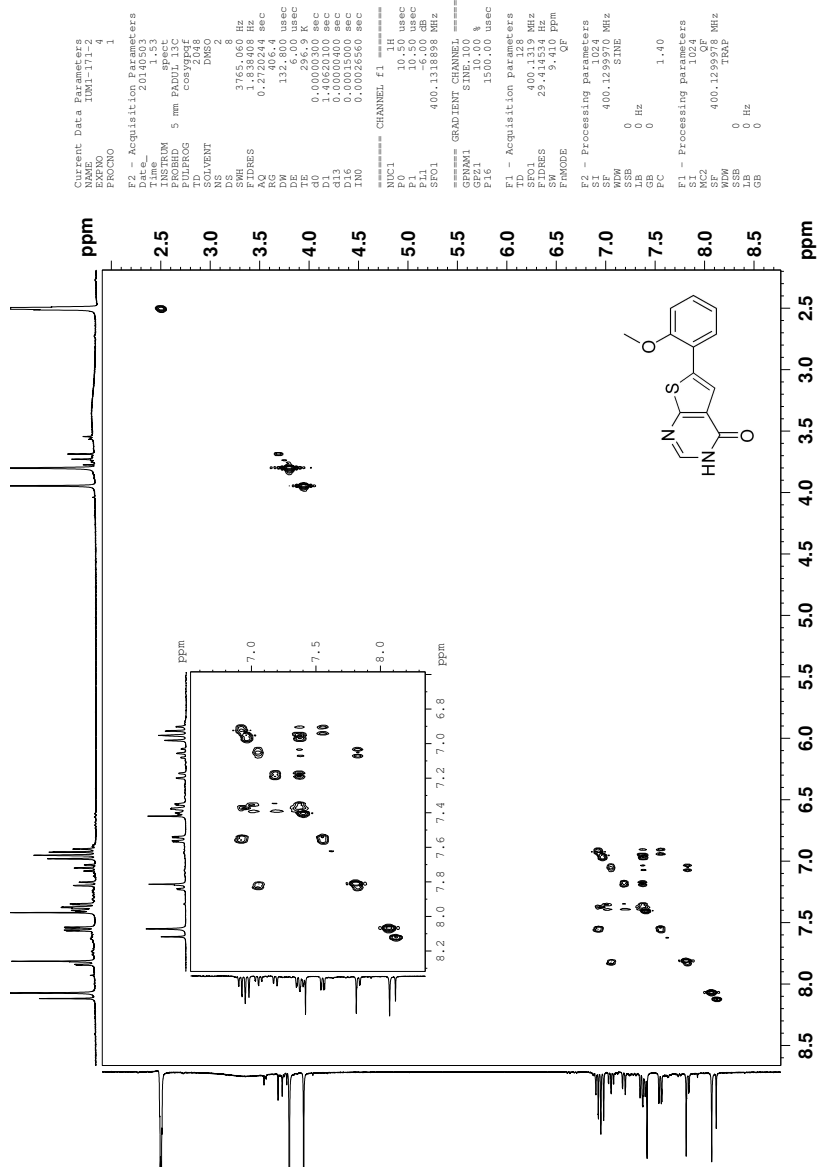


Figure K.3: COSY spectrum of compound 20.

K SPECTROSCOPIC DATA - COMPOUND 20

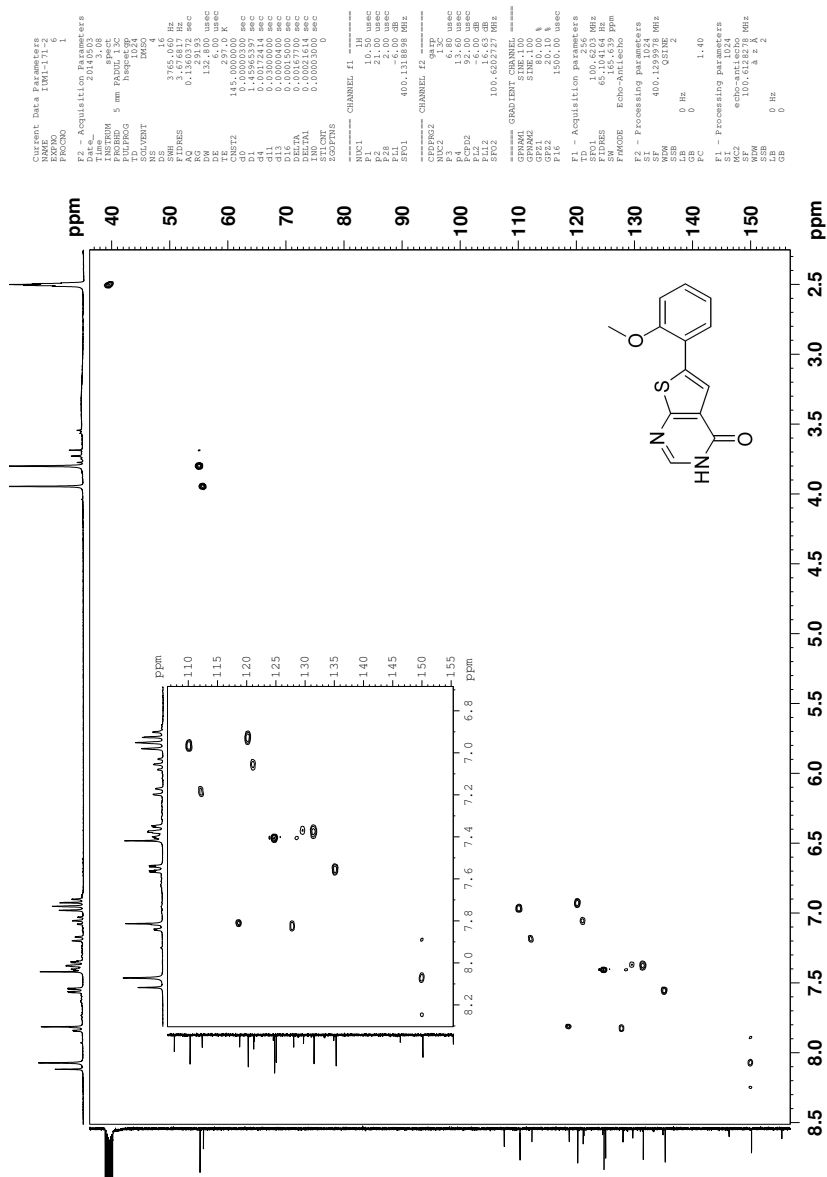


Figure K.4: HSQC spectrum of compound 20.

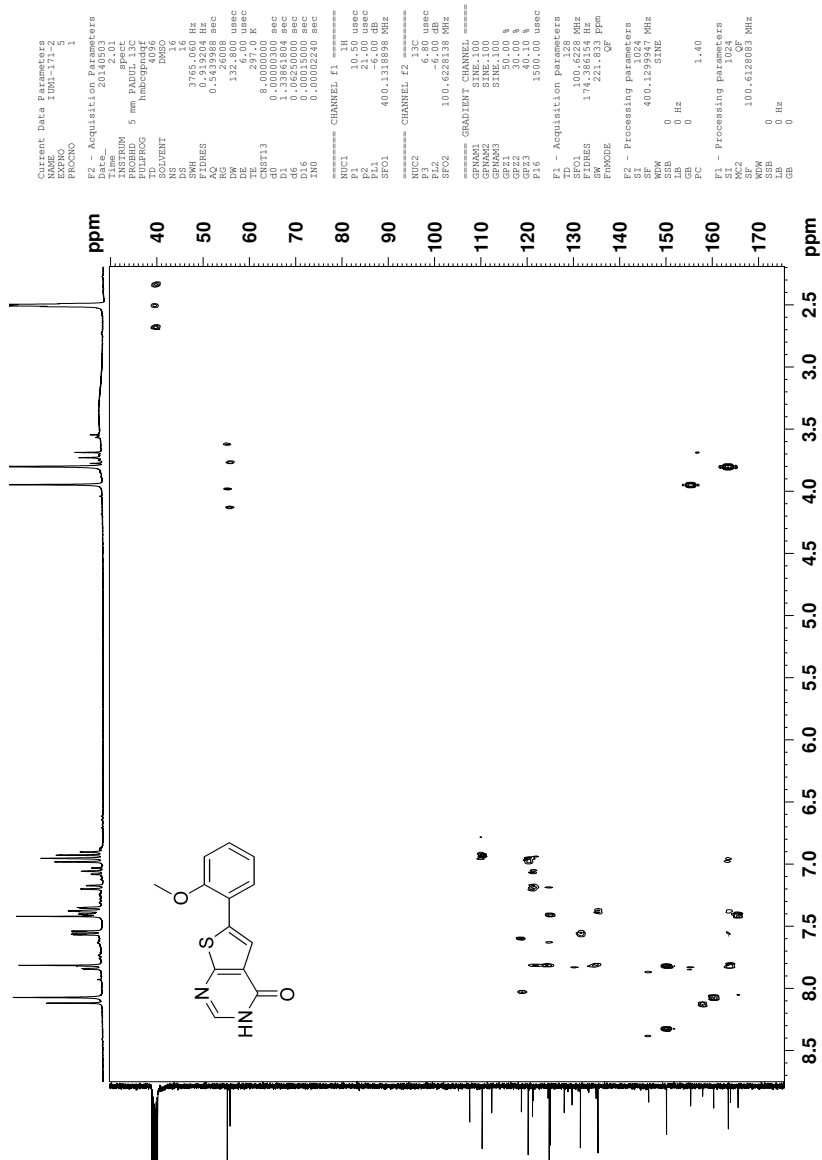


Figure K.5: HMBC spectrum of compound 20.

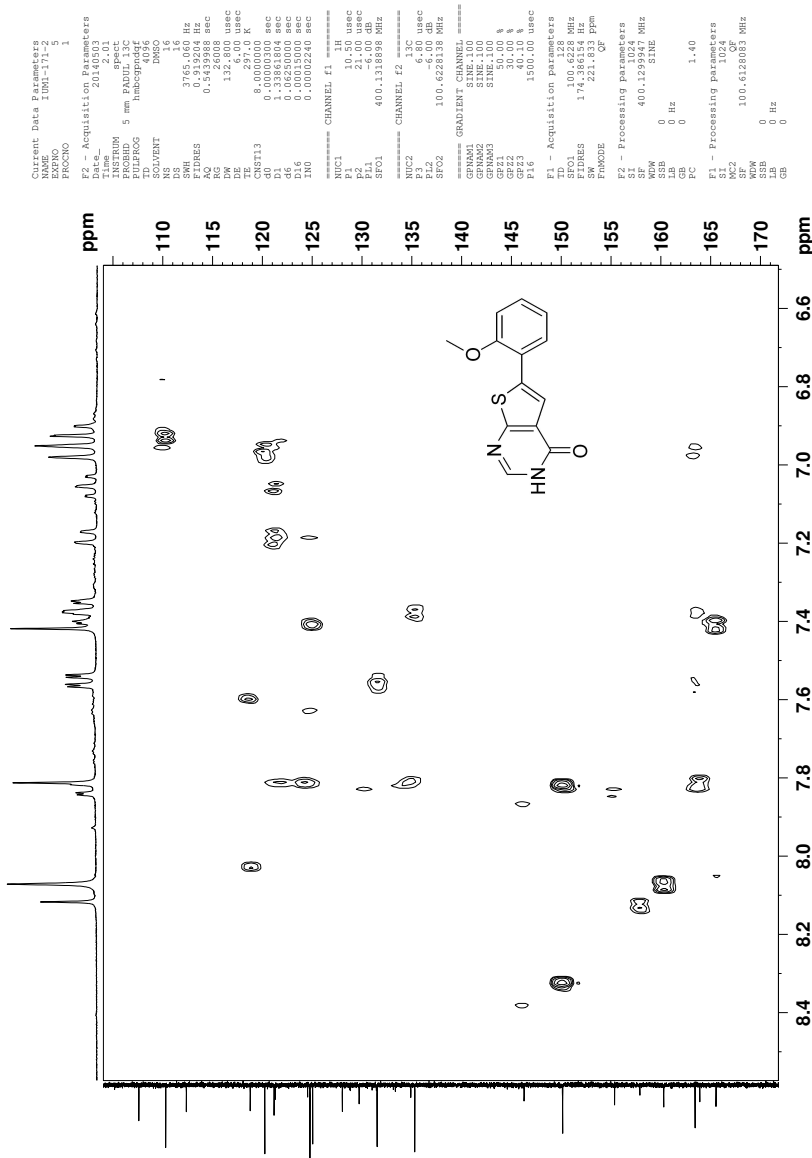


Figure K.6: Section of HMBC spectrum of compound 20.

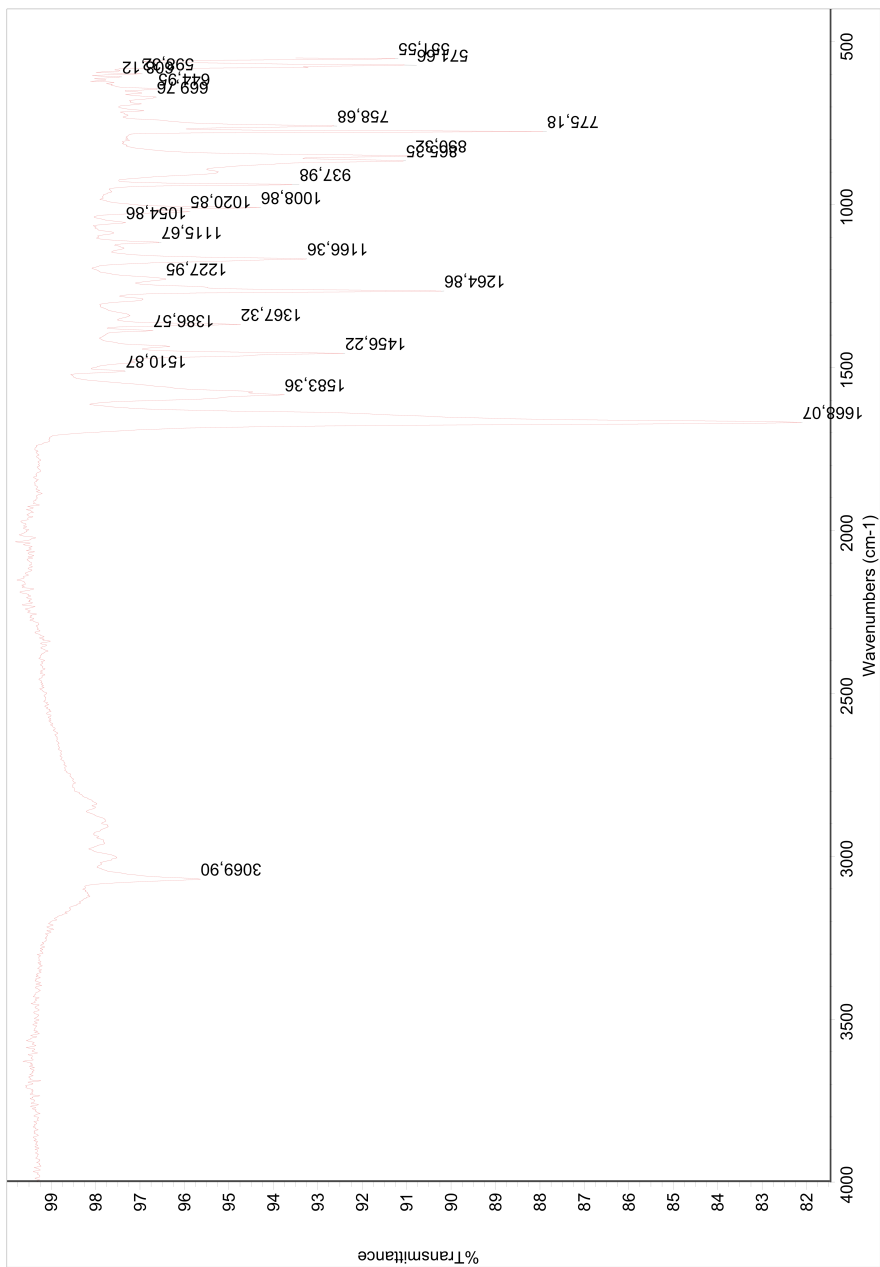


Figure K.7: IR spectrum of compound 20.

LXXXVI

Elemental Composition Report

Page 1

Single Mass Analysis

Tolerance = 2.0 PPM / DBE: min = -1.5, max = 50.0

Element prediction: Off

Number of isotope peaks used for i-FIT = 3

Monoisotopic Mass, Even Electron Ions

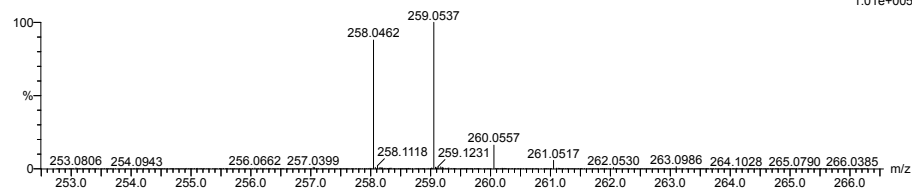
944 formula(e) evaluated with 3 results within limits (up to 1000) for each mass

Elements Used:

C: 3-500 H: 0-1000 N: 0-100 O: 0-200 S: 0-3

NT-MSLAB-Operator-SVG

2014-88 299 (5.823) AM2 (Ar,35000.0,0.00,0.00)

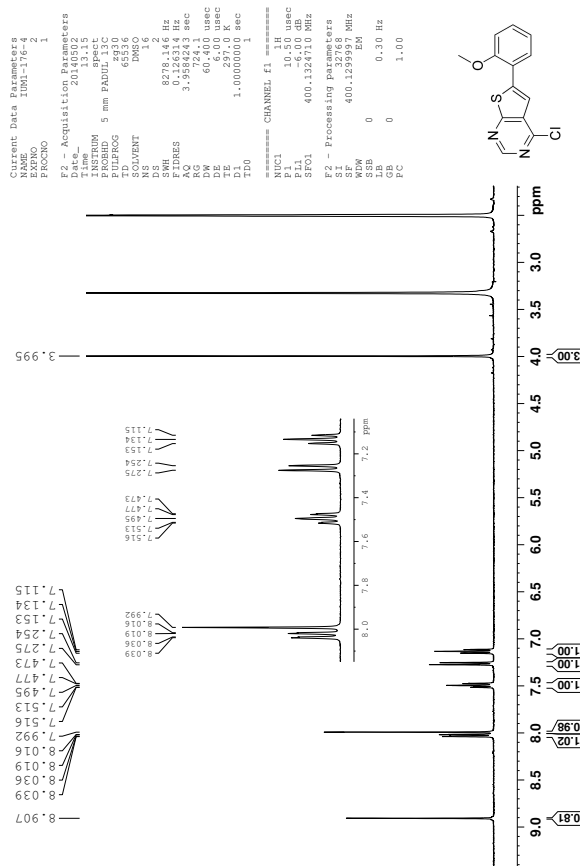
1: TOF MS ASAP+
1.01e+005Minimum: -1.5
Maximum: 50.0

Mass	Calc. Mass	mDa	PPM	DBE	i-FIT	Norm	Conf(%)	Formula
259.0537	259.0539	-0.2	-0.8	6.5	1098.7	17.626	0.00	C5 H7 N8 O5
	259.0535	0.2	0.8	0.5	1092.6	11.514	0.00	C5 H15 N4 O4 S2
	259.0541	-0.4	-1.5	9.5	1081.1	0.000	100.00	C13 H11 N2 O2 S

Figure K.8: MS spectrum of compound 20.

LXXXVII

L Spectroscopic Data - Compound 21

Figure L.1: $^1\text{H-NMR}$ spectrum of compound 21.

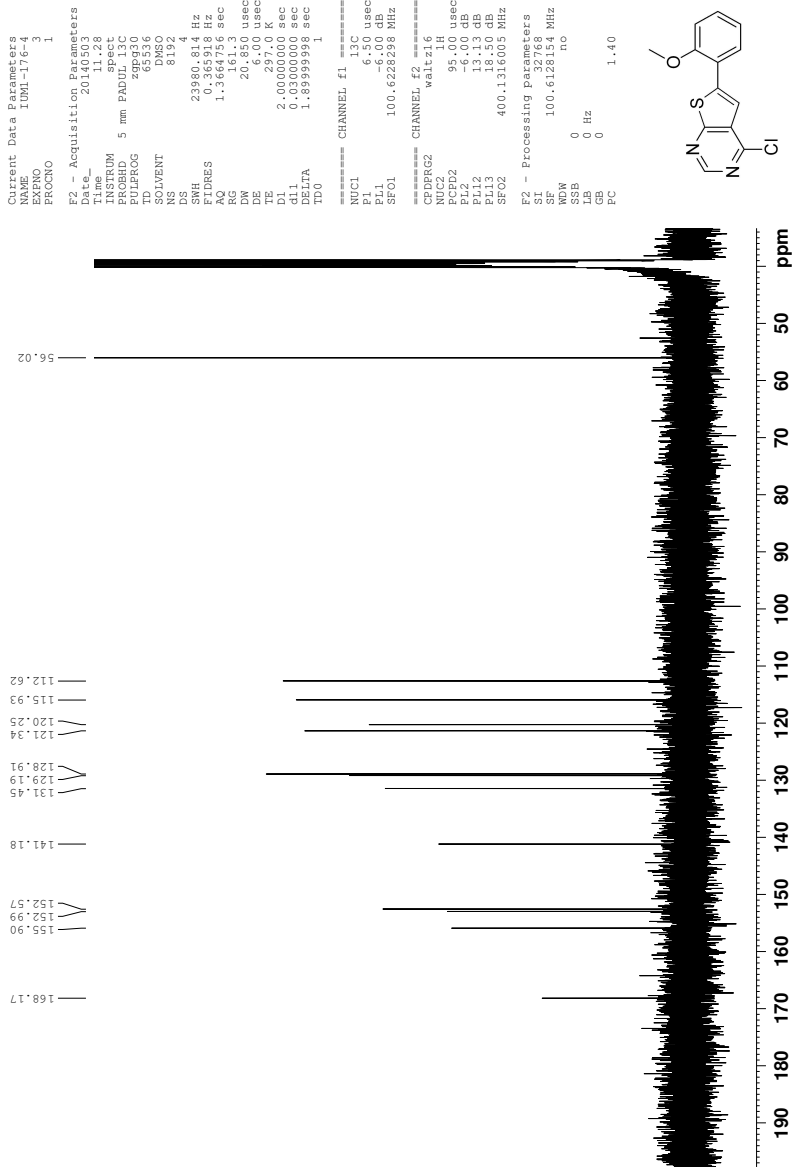


Figure L.2: ¹³C-NMR spectrum of compound 21.

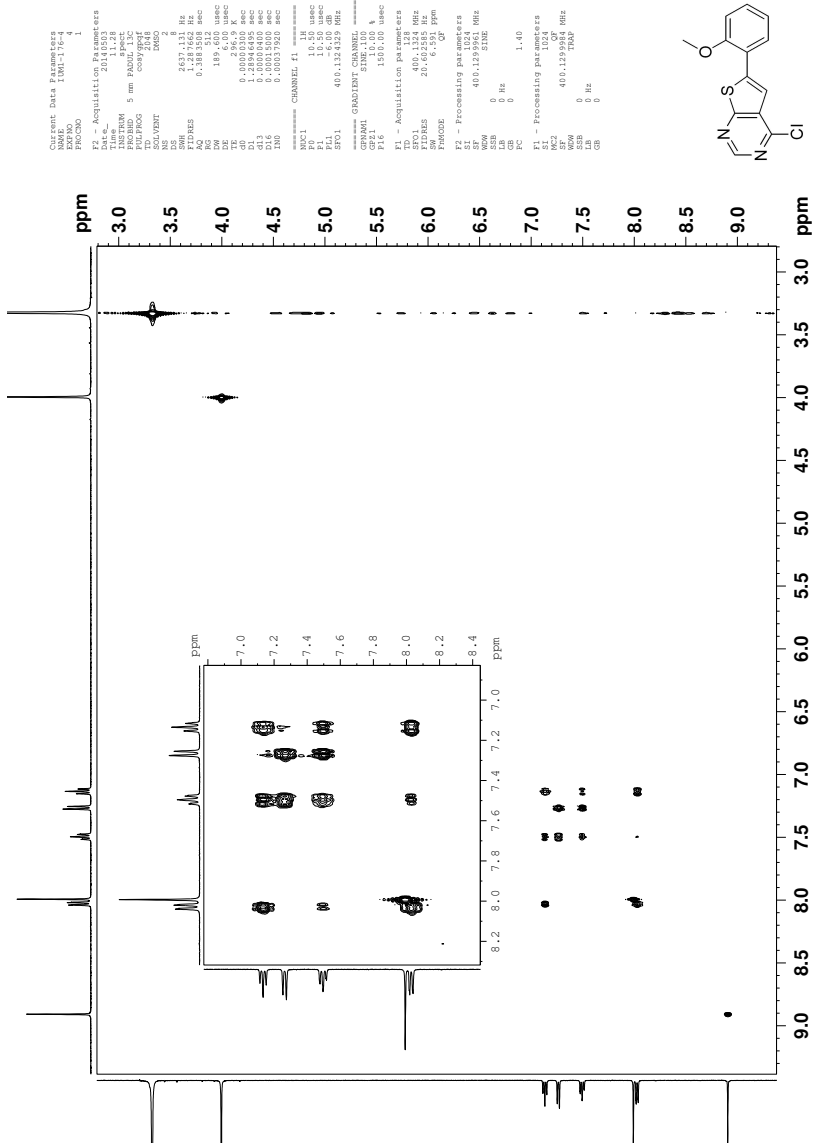


Figure L.3: COSY spectrum of compound 21.

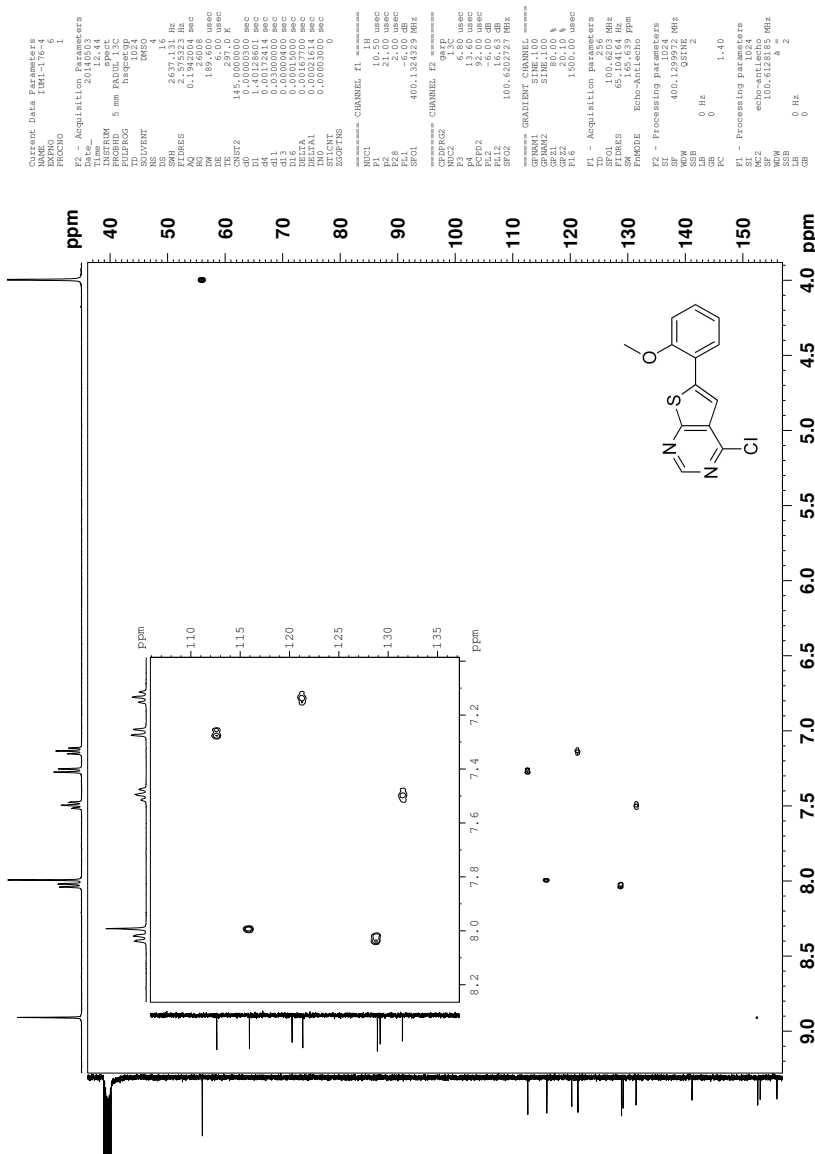


Figure L.4: HSQC spectrum of compound 21.

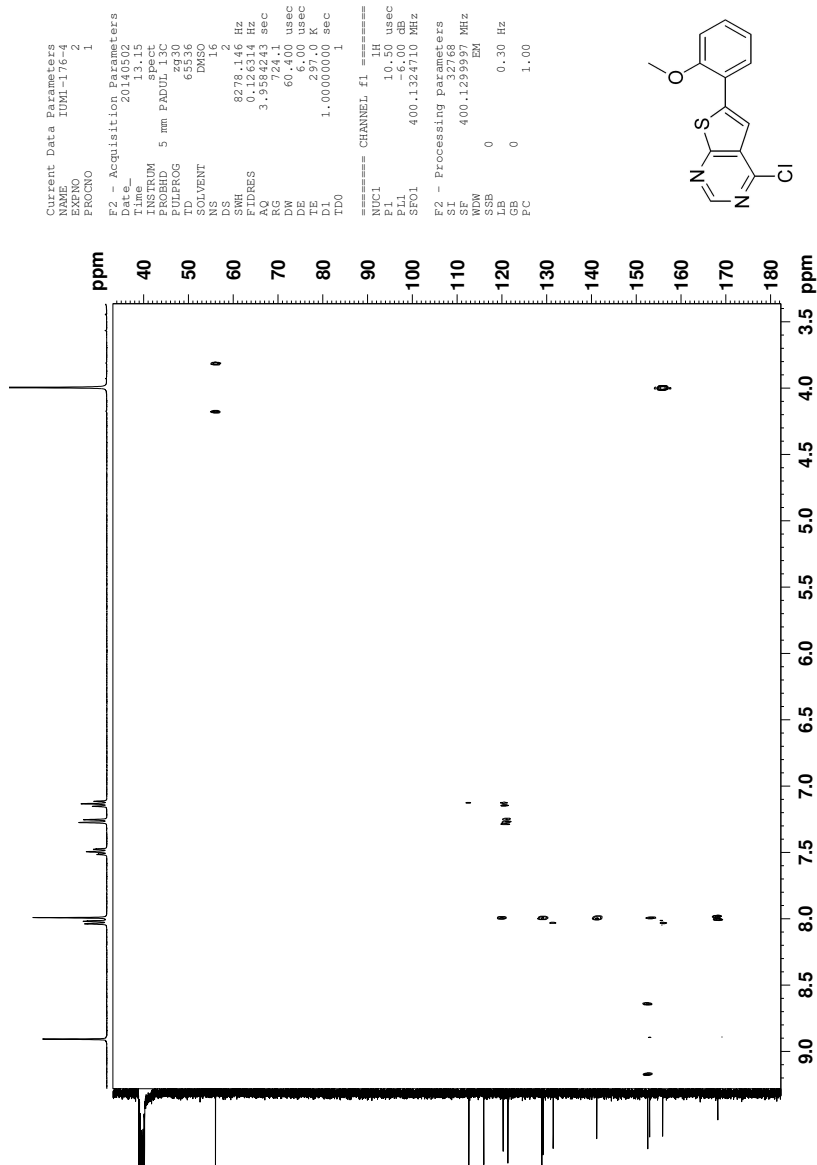


Figure L.5: HMBC spectrum of compound 21.

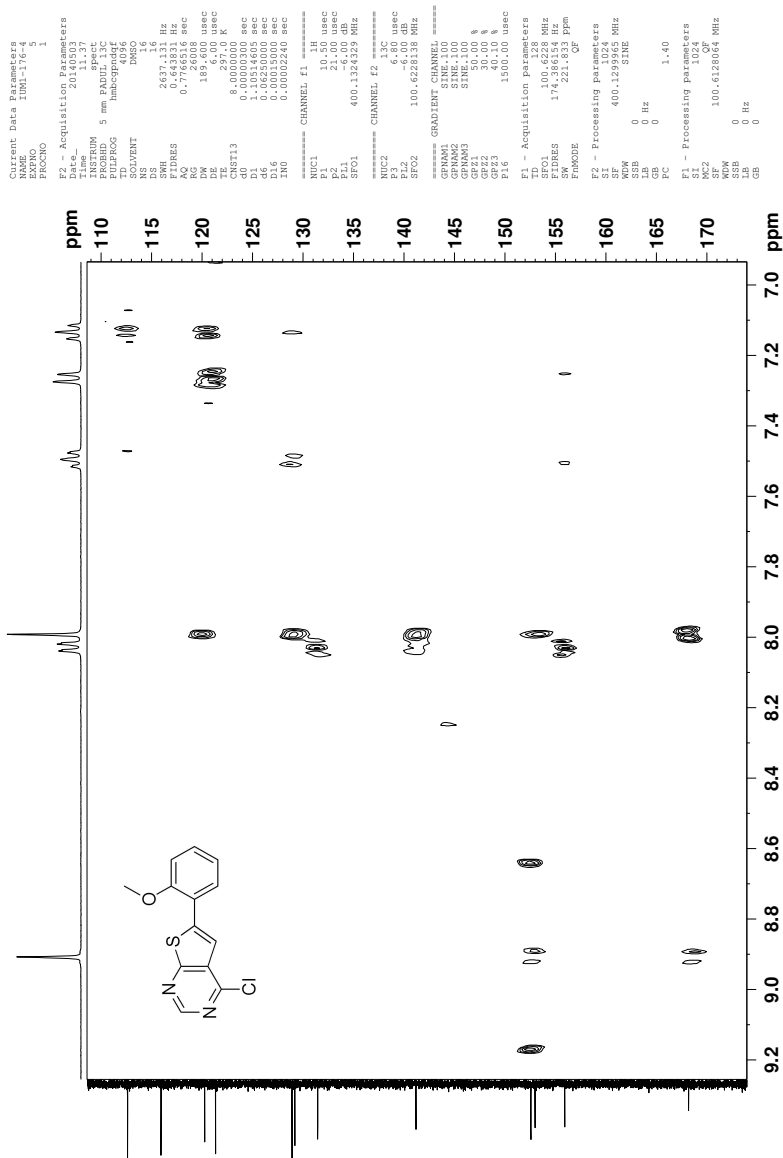


Figure L.6: Section of HMBC spectrum of compound 21.

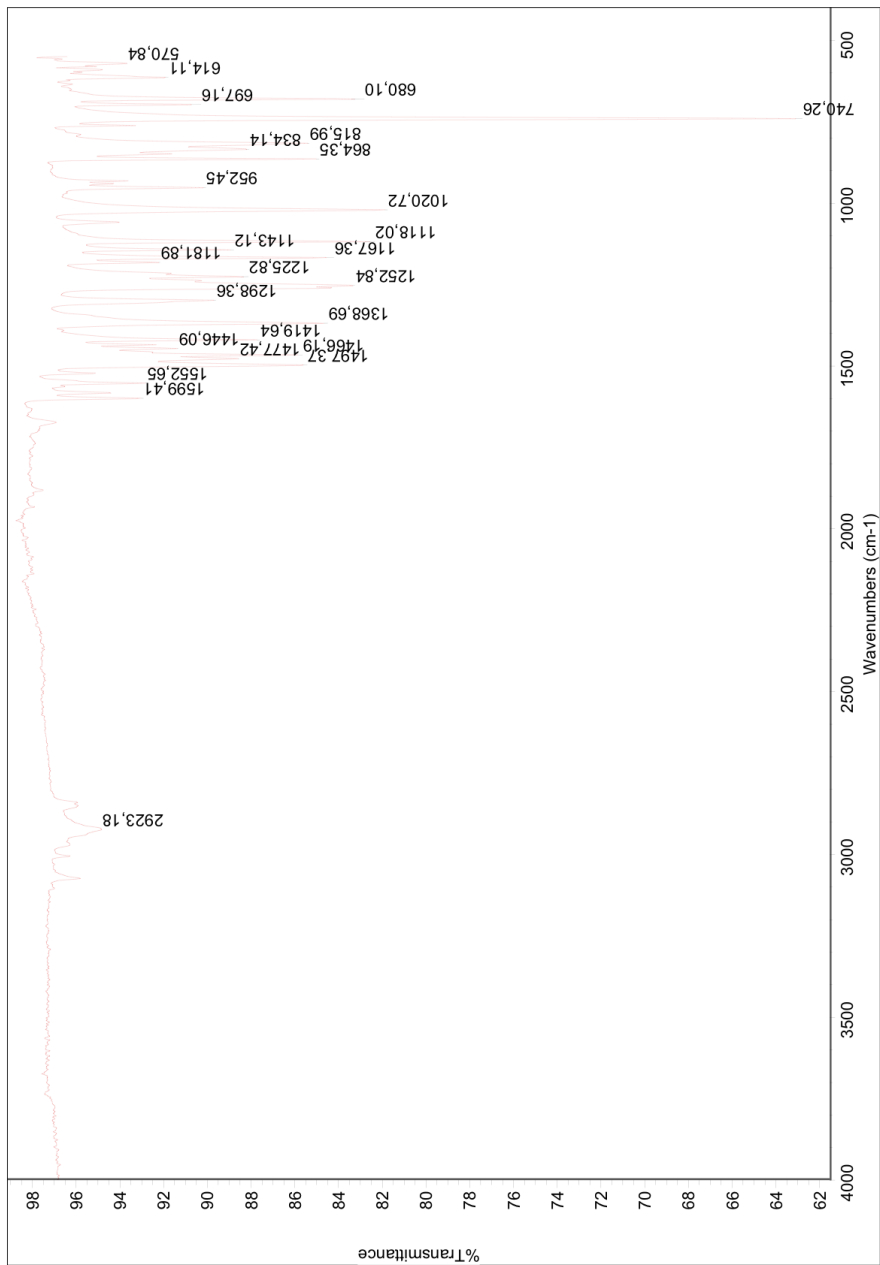


Figure L.7: IR spectrum of compound 21.

Elemental Composition Report

Page 1

Single Mass Analysis

Tolerance = 2.0 PPM / DBE: min = -1.5, max = 50.0

Element prediction: Off

Number of isotope peaks used for i-FIT = 3

Monoisotopic Mass, Even Electron Ions

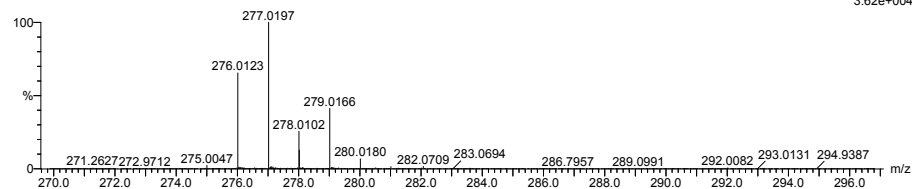
2339 formula(e) evaluated with 4 results within limits (up to 1000) for each mass

Elements Used:

C: 3-500 H: 0-1000 N: 0-100 O: 0-200 S: 0-3 Cl: 0-2

NT-MSLAB-Operator-SVG

2014-89 166 (3.239) AM2 (Ar,35000,0,0,0,0,0)

1: TOF MS ASAP+
3.62e+004

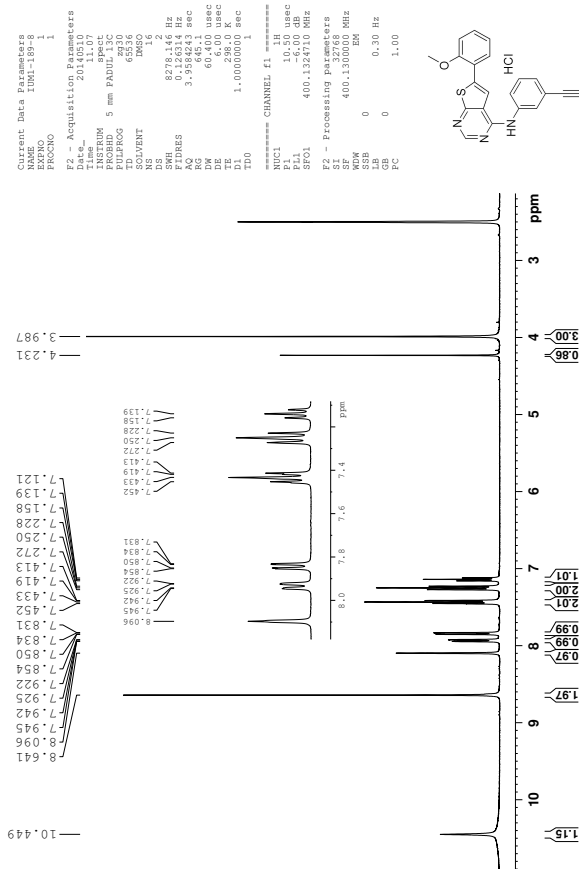
Minimum: -1.5
Maximum: 50.0

Mass	Calc. Mass	mDa	PPM	DBE	i-FIT	Norm	Conf(%)	Formula
277.0197	277.0202	-0.5	-1.8	9.5	972.1	0.034	96.62	C13 H10 N2 O S Cl
	277.0196	0.1	0.4	0.5	975.6	3.511	2.99	C5 H14 N4 O3 S2 Cl
	277.0201	-0.4	-1.4	6.5	977.6	5.542	0.39	C5 H6 N8 O4 Cl
	277.0196	0.1	0.4	5.5	988.0	15.959	0.00	C9 H9 O10

Figure L.8: MS spectrum of compound 21.

XCV

M Spectroscopic Data - Compound 15a·HCl

Figure M.1: $^1\text{H-NMR}$ spectrum of compound 15a·HCl.

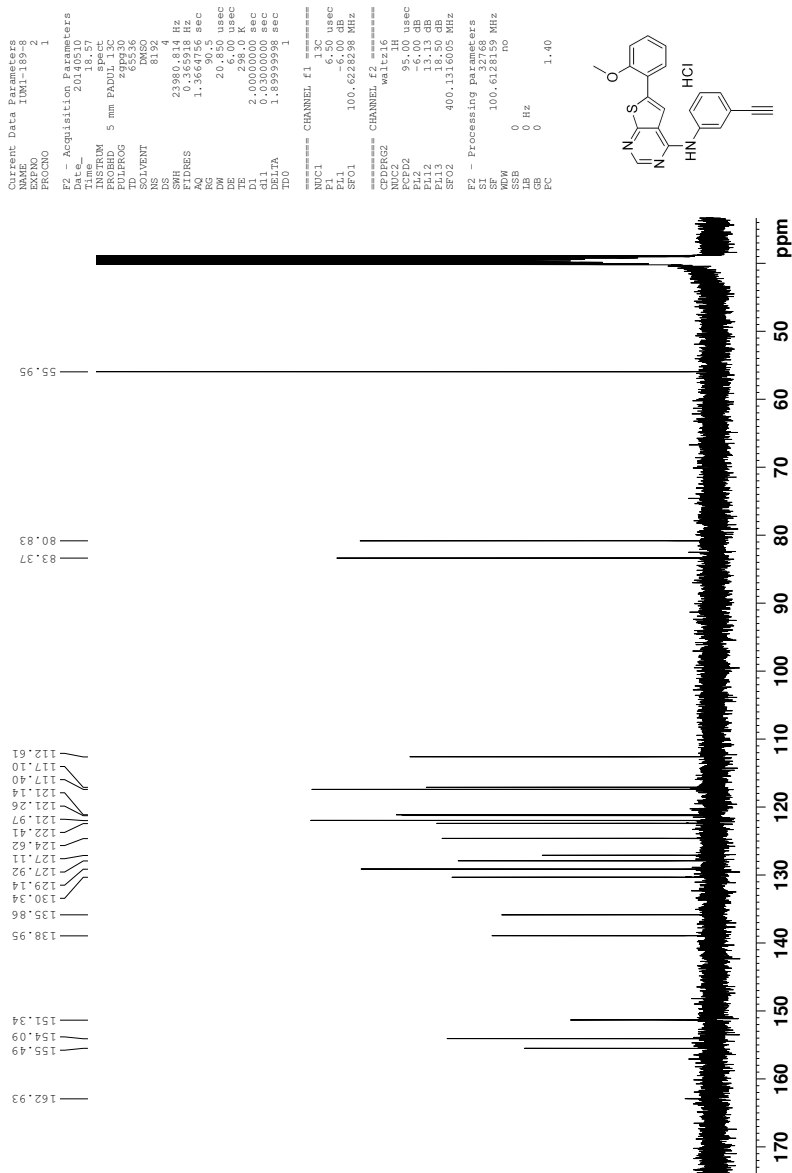


Figure M.2: ¹³C-NMR spectrum of compound 15a·HCl.

M SPECTROSCOPIC DATA - COMPOUND 15A·HCL

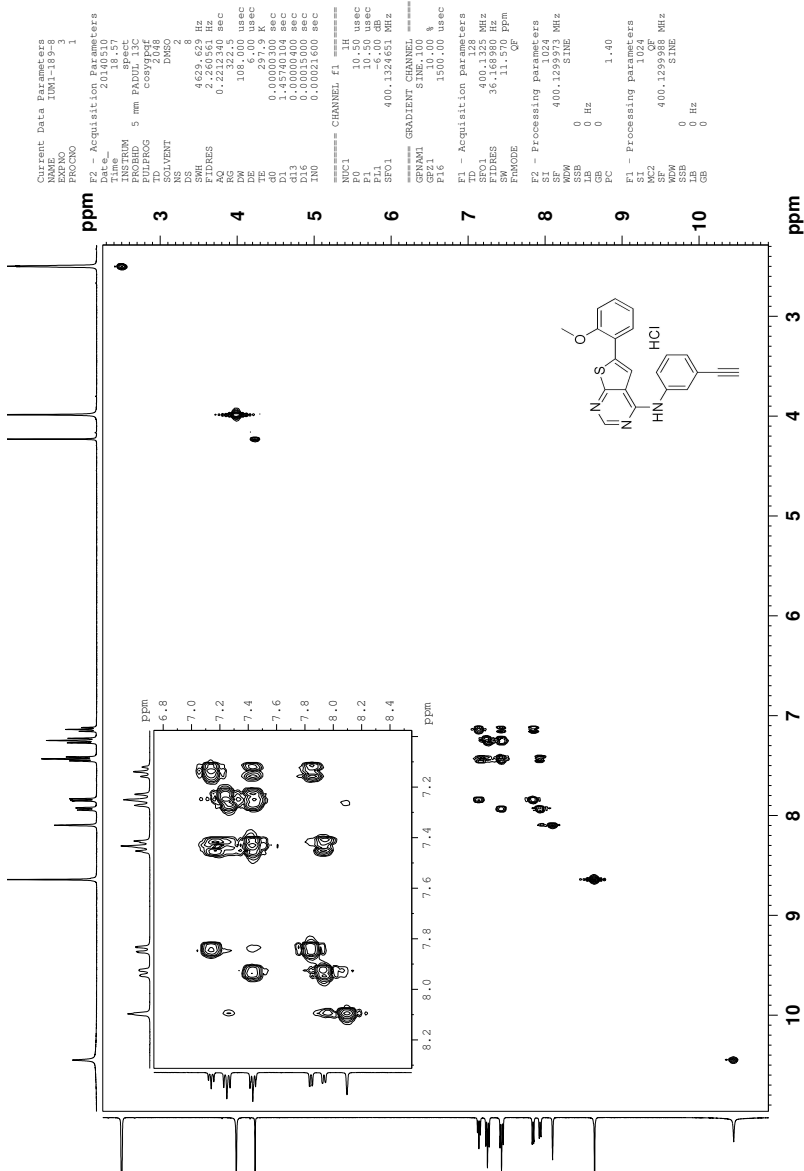


Figure M.3: COSY spectrum of compound 15a·HCl.

M SPECTROSCOPIC DATA - COMPOUND 15A·HCL

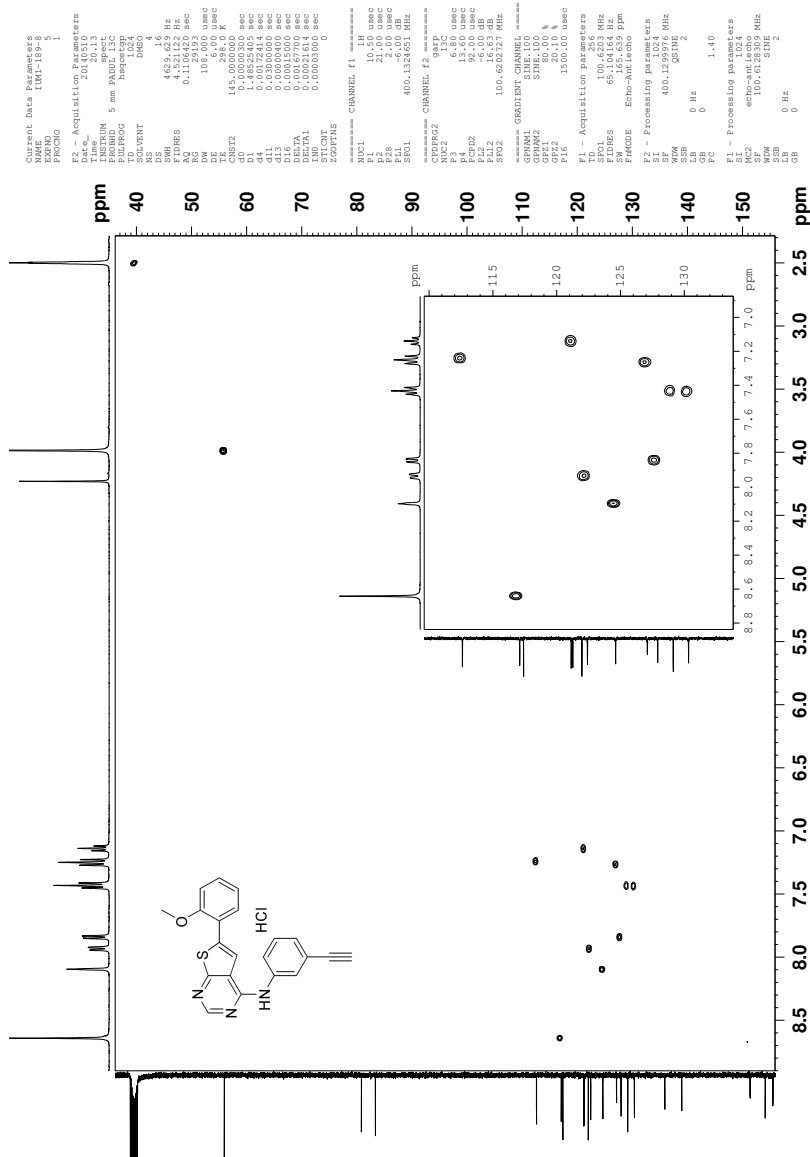


Figure M.4: HSQC spectrum of compound 15a·HCl.

M SPECTROSCOPIC DATA - COMPOUND 15A·HCL

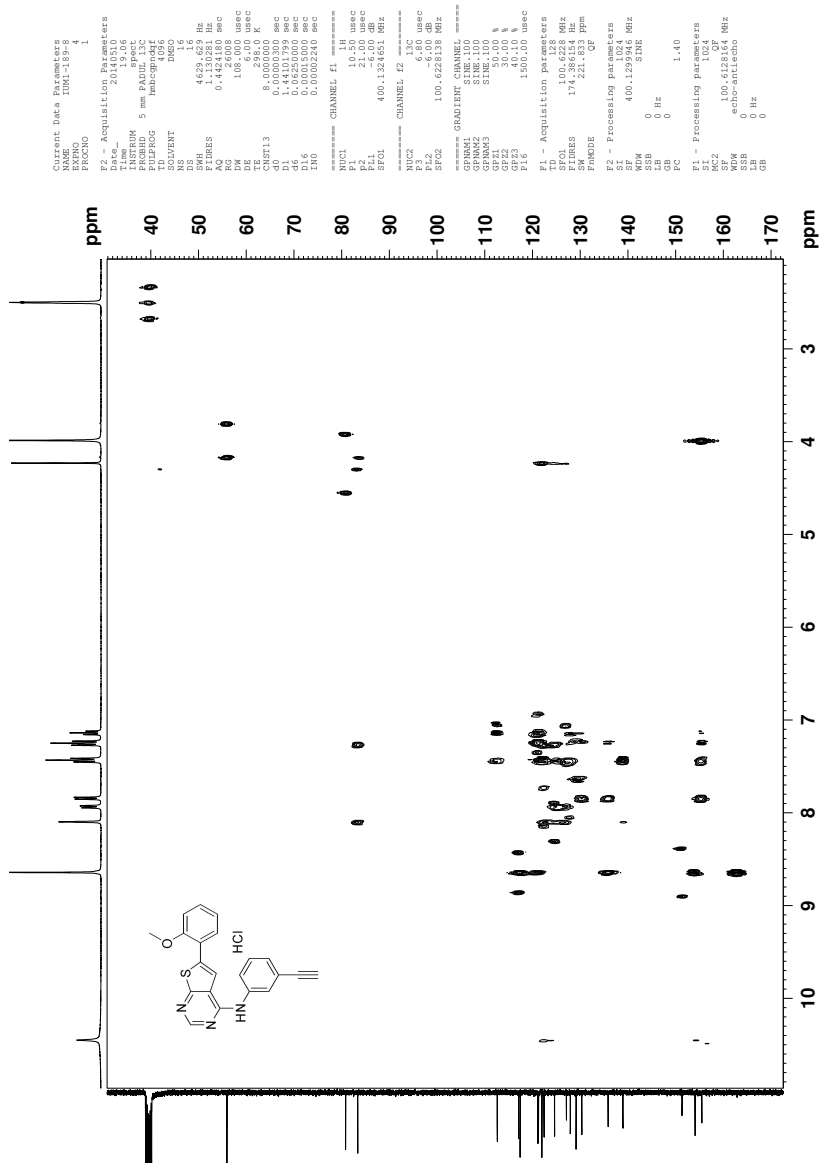


Figure M.5: HMBC spectrum of compound 15a·HCl.

Elemental Composition Report

Page 1

Single Mass Analysis

Tolerance = 2.0 PPM / DBE: min = -1.5, max = 50.0

Element prediction: Off

Number of isotope peaks used for i-FIT = 3

Monoisotopic Mass, Even Electron Ions

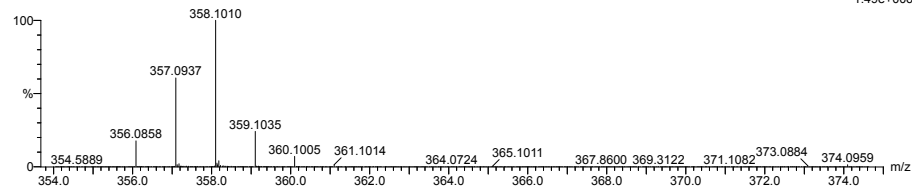
2394 formula(e) evaluated with 5 results within limits (all results (up to 1000) for each mass)

Elements Used:

C: 3-500 H: 0-1000 N: 0-100 O: 0-200 S: 0-3

NT-MSLAB-Operator-SVG

2014-91 159 (3.101) AM2 (Ar,35000.0,0.00,0.00)

1: TOF MS ASAP+
1.49e+006

Minimum: -1.5
Maximum: 50.0

Mass	Calc. Mass	mDa	PPM	DBE	i-FIT	Norm	Conf(%)	Formula
358.1010	358.1014	-0.4	-1.1	15.5	1216.1	0.000	100.00	C21 H16 N3 O S
	358.1008	0.2	0.6	6.5	1228.3	12.255	0.00	C13 H20 N5 O3 S2
	358.1006	0.4	1.1	3.5	1229.8	13.718	0.00	C5 H16 N11 O6 S
	358.1014	-0.4	-1.1	2.5	1232.0	15.903	0.00	C6 H20 N11 O S3
	358.1012	-0.2	-0.6	12.5	1232.2	16.114	0.00	C13 H12 N9 O4

Figure M.6: MS spectrum of compound 15a·HCl.

CI

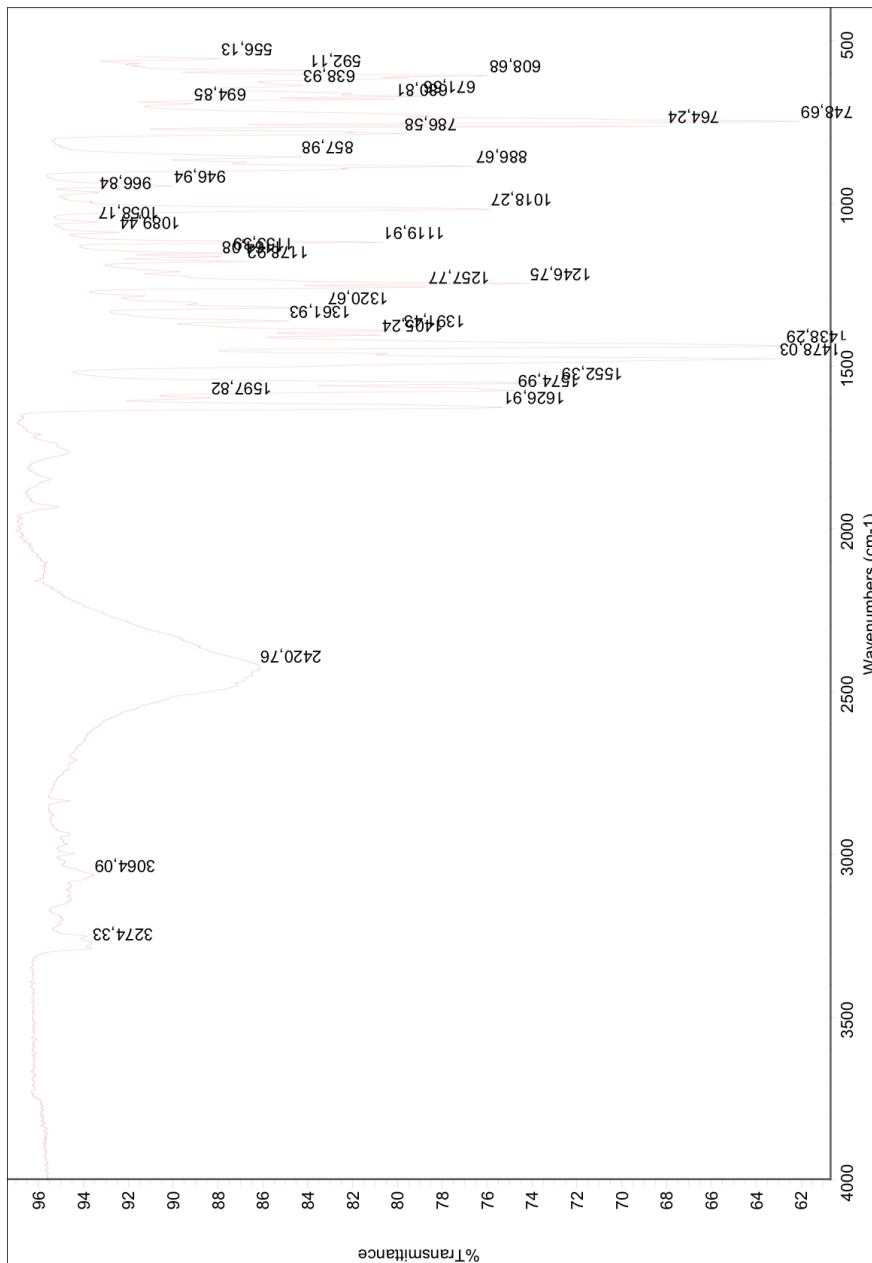


Figure M.7: IR spectrum of compound **15a**·HCL.

N SPECTROSCOPIC DATA - COMPOUND 15B

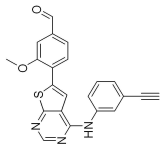
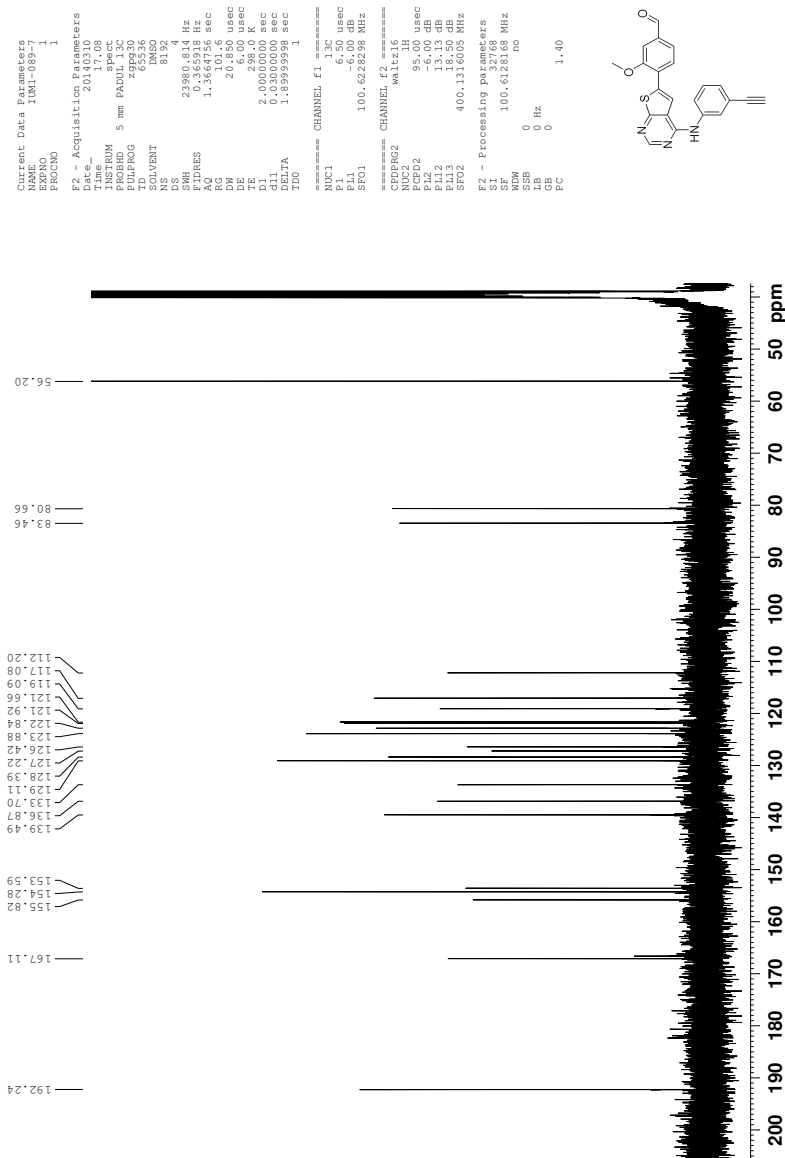


Figure N.2: ¹³C-NMR spectrum of compound 15b.

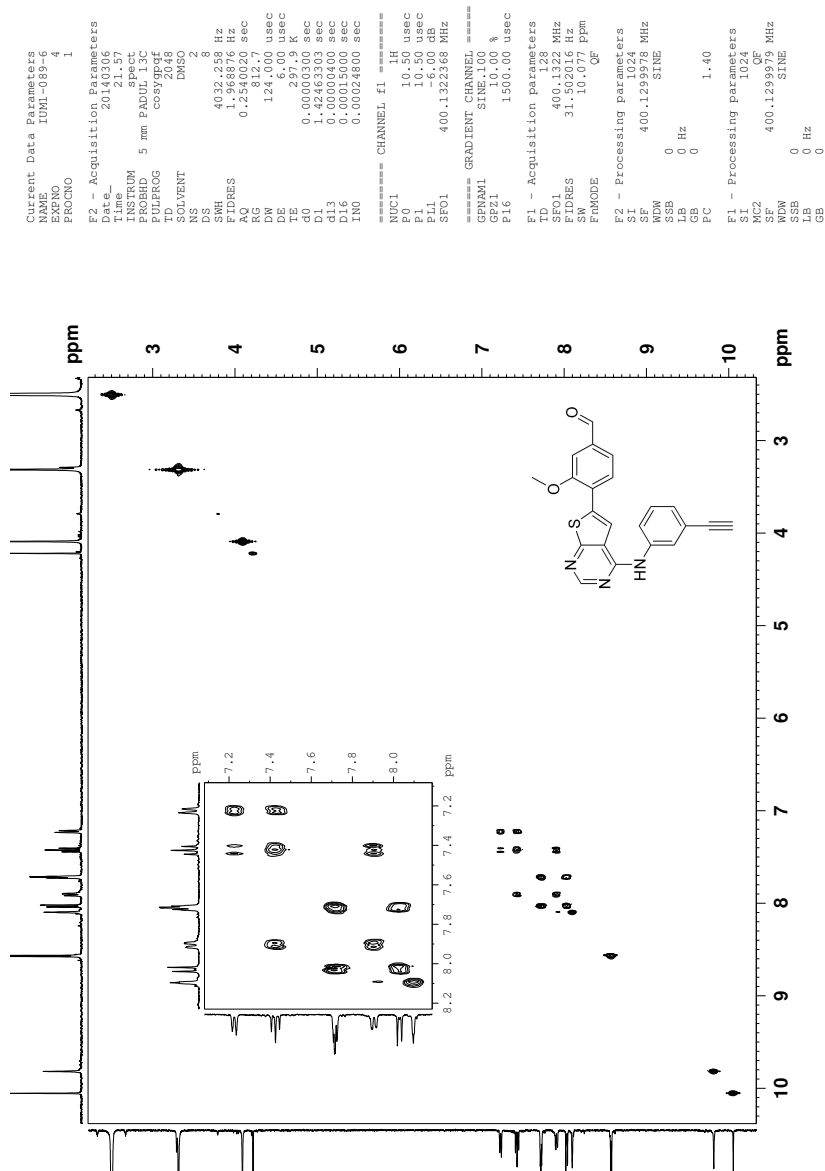


Figure N.3: COSY spectrum of compound 15b.

N SPECTROSCOPIC DATA - COMPOUND 15B

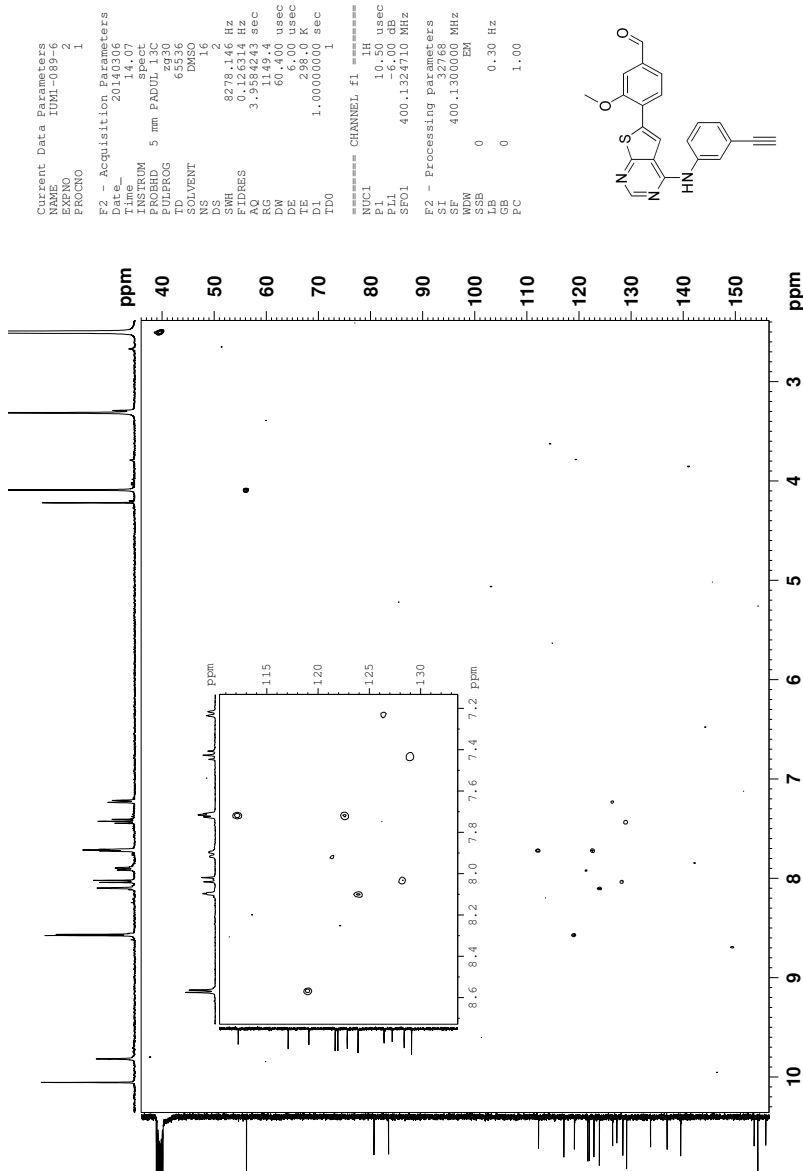


Figure N.4: HSQC spectrum of compound 15b.

N SPECTROSCOPIC DATA - COMPOUND 15B

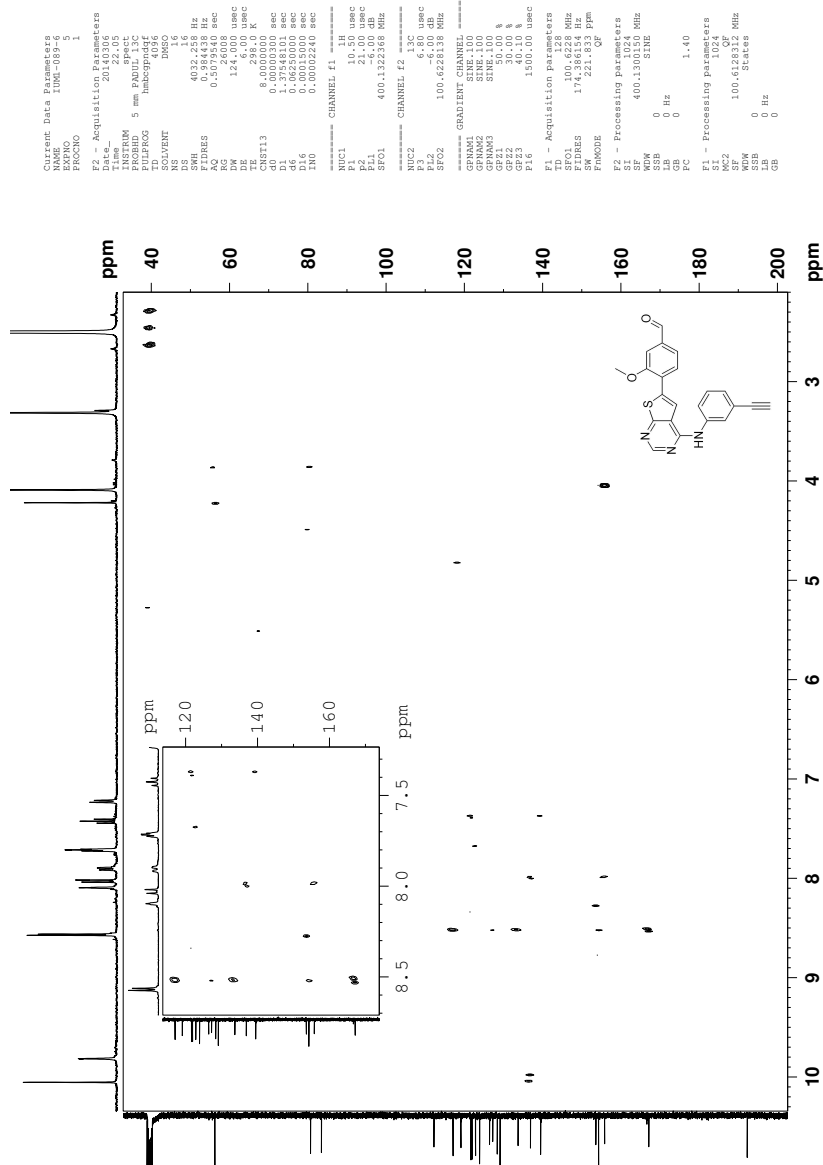


Figure N.5: HMBC spectrum of compound 15b.

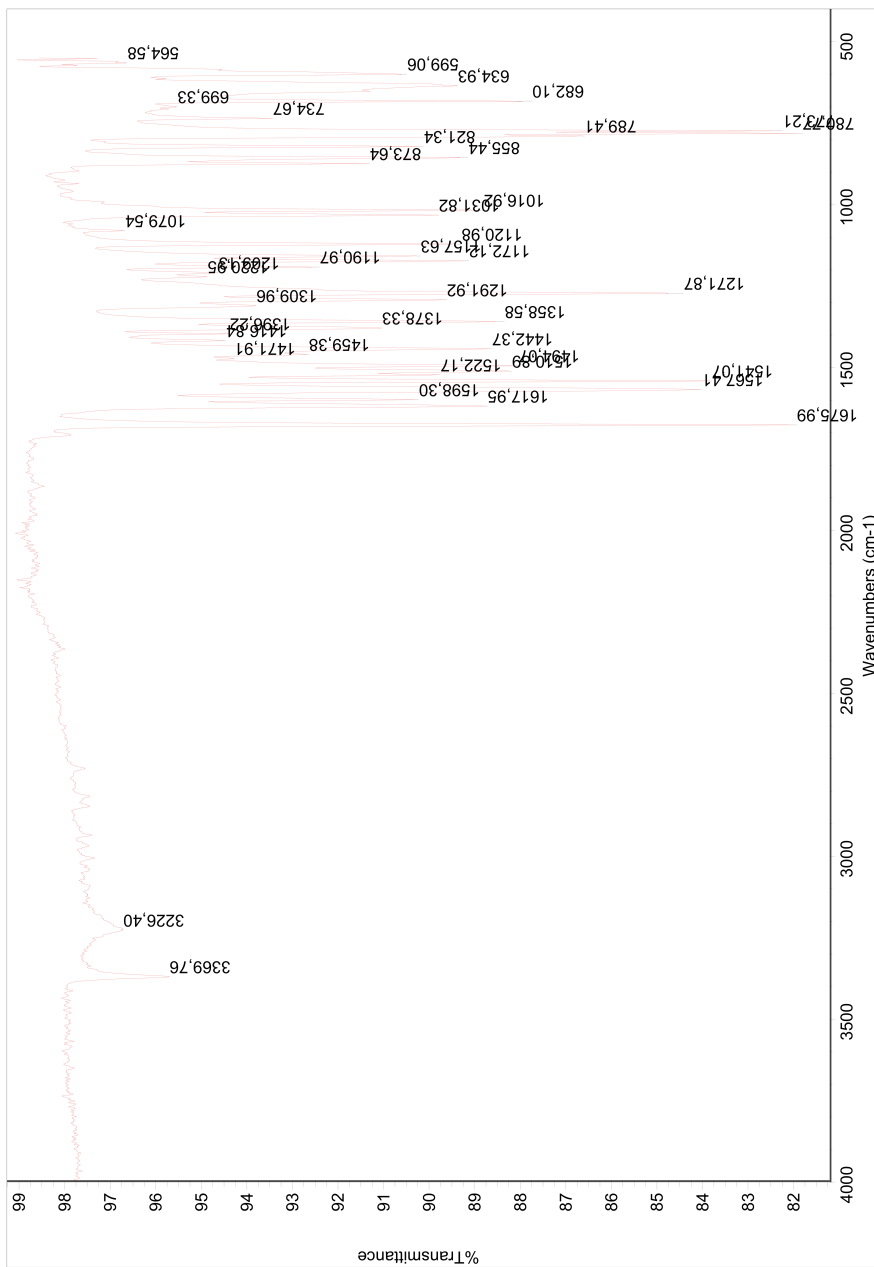


Figure N.6: IR spectrum of compound **15b**.

Elemental Composition Report

Single Mass Analysis

Tolerance = 3.0 PPM / DBE: min = -1.5, max = 50.0

Element prediction: Off

Number of isotope peaks used for i-FIT = 3

Monoisotopic Mass, Even Electron Ions

2517 formula(e) evaluated with 9 results within limits (all results (up to 1000) for each mass)

Elements Used:

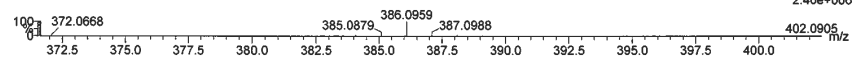
C: 0-500 H: 0-1000 N: 3-100 O: 0-100 S: 0-3

21-Feb-2014

2016-18 237 (4.617) AM2 (Ar,35000.0,0.00,0.00); Cm (233:240)

1: TOF MS ASAP+

2.40e+006



Minimum: -1.5
Maximum: 50.0

Mass	Calc. Mass	mDa	PPM	DBE	i-FIT	Norm	Conf(%)	Formula
386.0959	386.0961	-0.2	-0.5	13.5	39.5	17.819	0.00	C14 H12 N9 O5
	386.0957	0.2	0.5	7.5	36.3	14.686	0.00	C14 H20 N5 O4 S2
	386.0963	-0.4	-1.0	16.5	21.6	0.000	100.00	C22 H16 N3 O2 S ← [M+H] ⁺
	386.0955	0.4	1.0	4.5	37.9	16.254	0.00	C6 H16 N11 O7 S
	386.0964	-0.5	-1.3	3.5	40.1	18.445	0.00	C7 H20 N11 O2 S3
	386.0950	0.9	2.3	-1.5	40.9	19.280	0.00	C6 H24 N7 O6 S3
	386.0968	-0.9	-2.3	9.5	37.2	15.606	0.00	C7 H12 N15 O3 S
	386.0948	1.1	2.8	8.5	39.6	17.999	0.00	C13 H16 N5 O9
	386.0970	-1.1	-2.8	12.5	35.2	13.582	0.00	C15 H16 N9 S2

Figure N.7: MS spectrum of compound 15b.

O Spectroscopic Data - Compound 15c

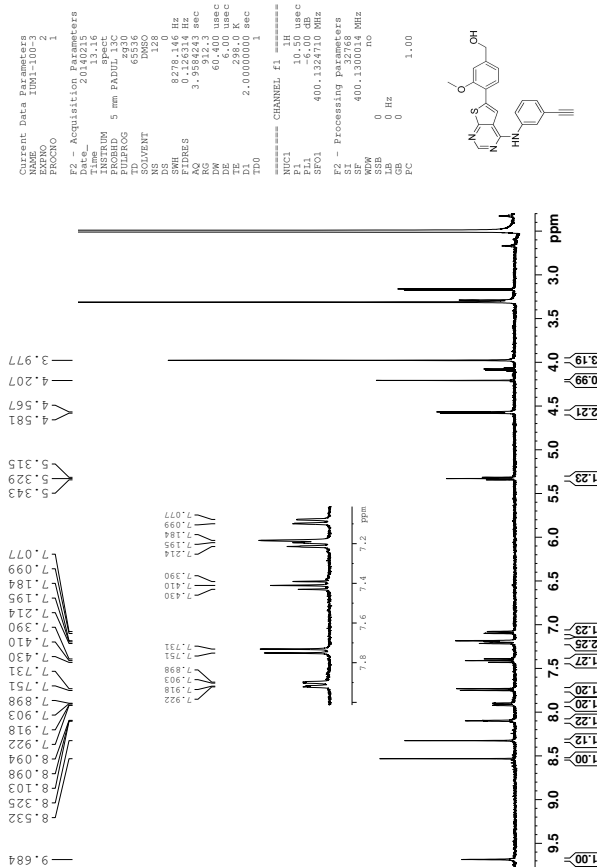


Figure O.1: ¹H-NMR spectrum of compound 15c.

O SPECTROSCOPIC DATA - COMPOUND 15C

```

Current Data Parameters
NAME      TUMI-100-5
PROCNO    1
Date_ Acquisition Parameters
Time      20140311
INSTRUM   spect
PROBHD    5 mm PDPUR30
PULPROG   zgpg30
TD         65536
AQ         81.92
RG         8192
DS         2390.814 Hz
SFO1       100.6282598 MHz
FIDRES     1.36664756 sec
AQ         1.36664756 sec
RG         20.850 usec
DE         6.00 usec
TE         298.0 K
D1         0.03000000 sec
DELTA     1.89599998 sec
TD0        1
===== CHANNEL f1 =====
NUC1       13C
P1         6.50 usec
PL1        -6.00 dB
SFO1       100.6282598 MHz
===== CHANNEL f2 =====
WALTZ16
NUC2       13C
P2         95.00 usec
PL2        -6.00 dB
PL12       18.50 dB
PL13       18.50 dB
SFO2       400.1316005 MHz
F2 - Processing parameters
SI         32768
SF         100.6128164 MHz
WDW        HM
SSB        0 Hz
LB         0
GB         0
PC         1.40
  
```

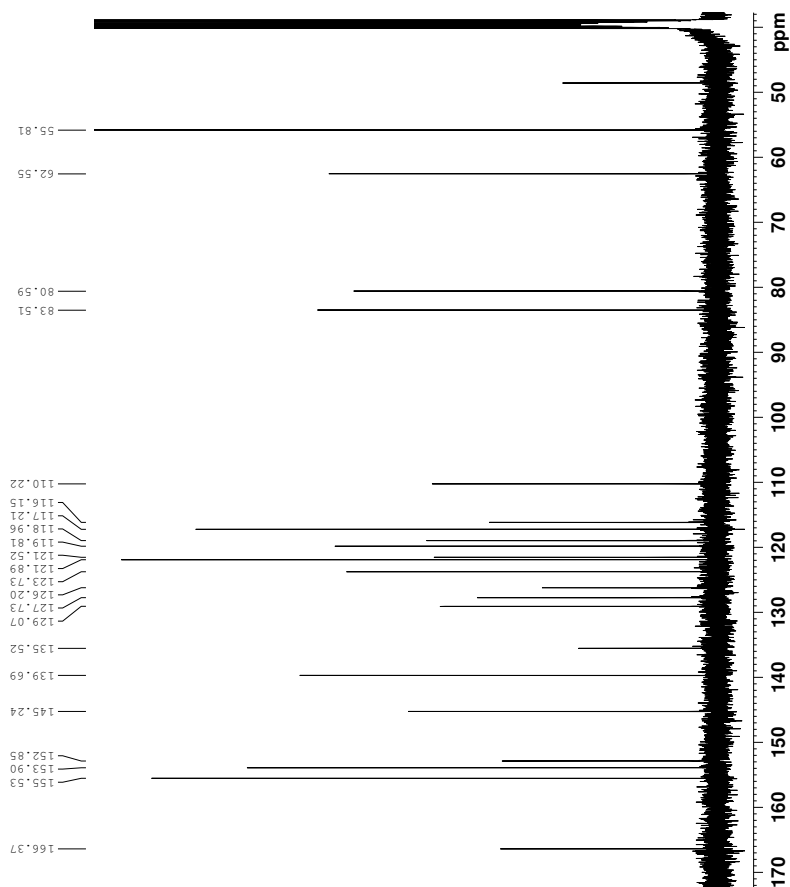
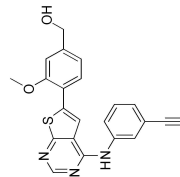


Figure O.2: ¹³C-NMR spectrum of compound 15c.

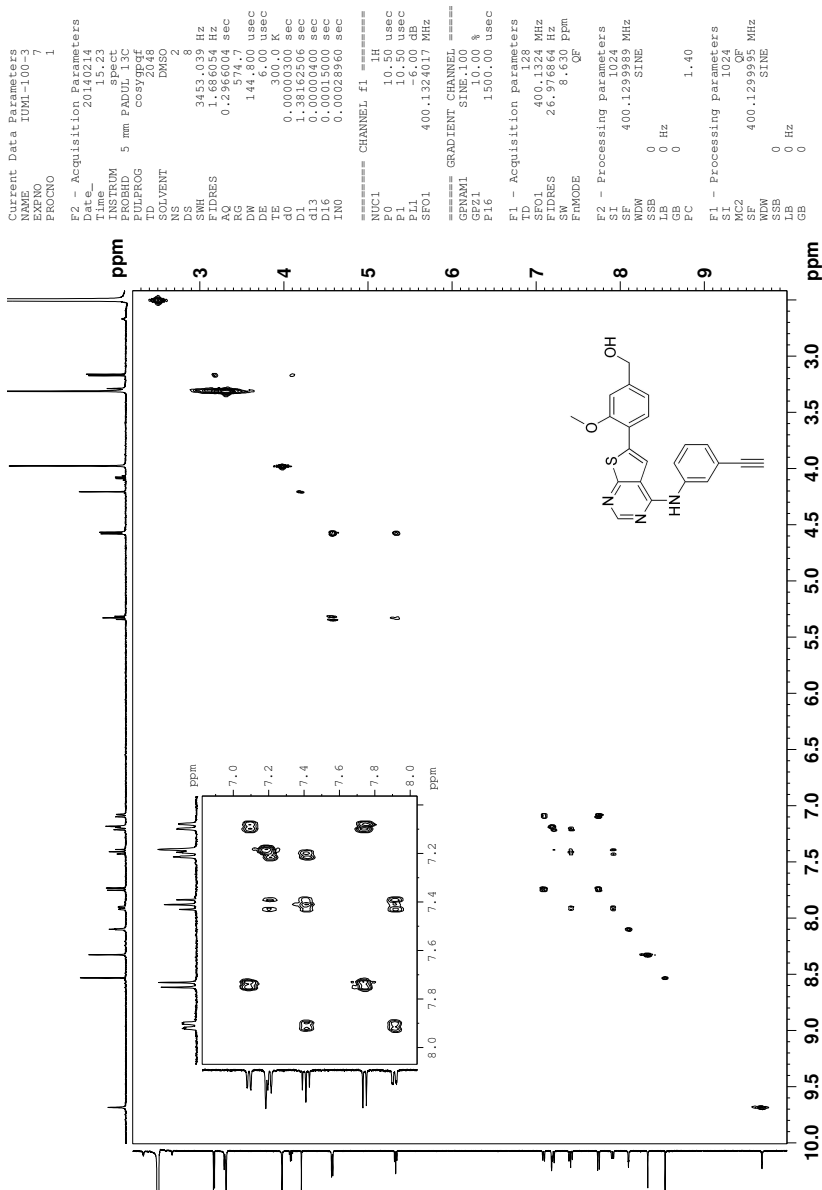


Figure O.3: COSY spectrum of compound 15c.

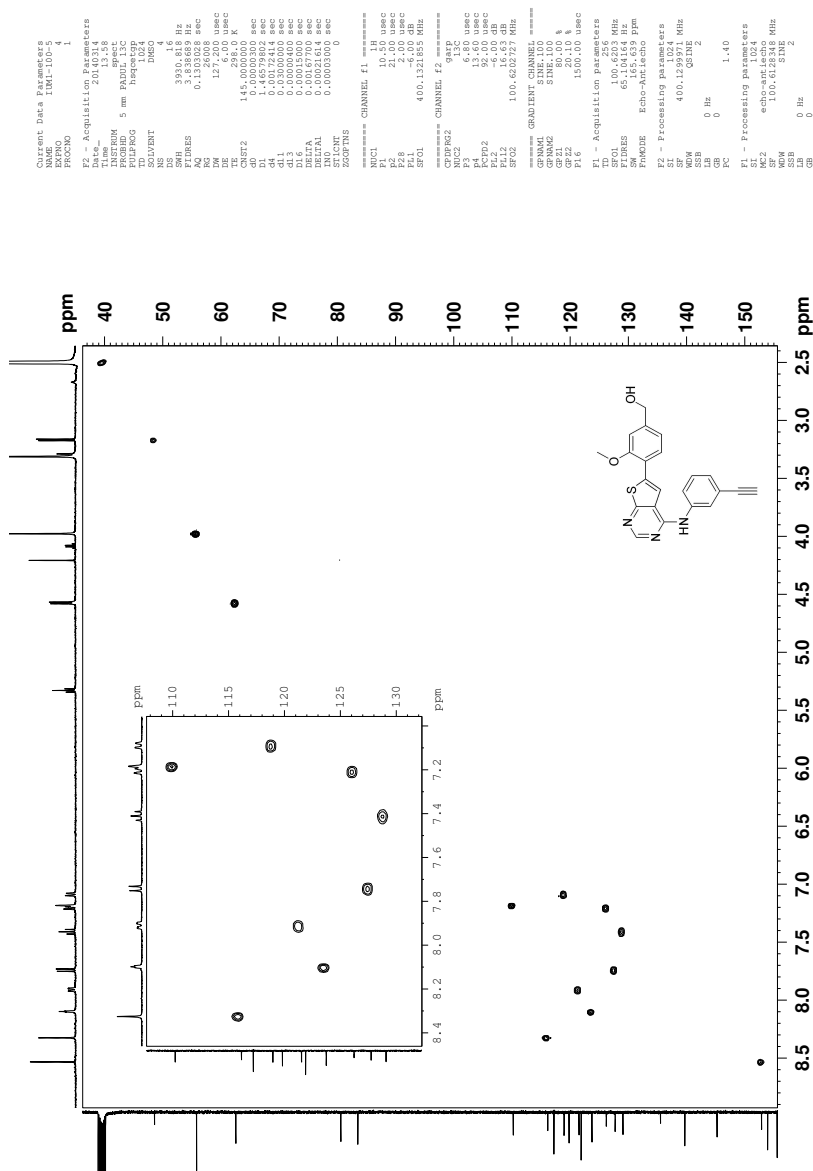


Figure O.4: HSQC spectrum of compound 15c.

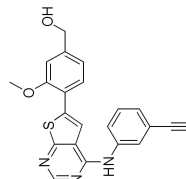
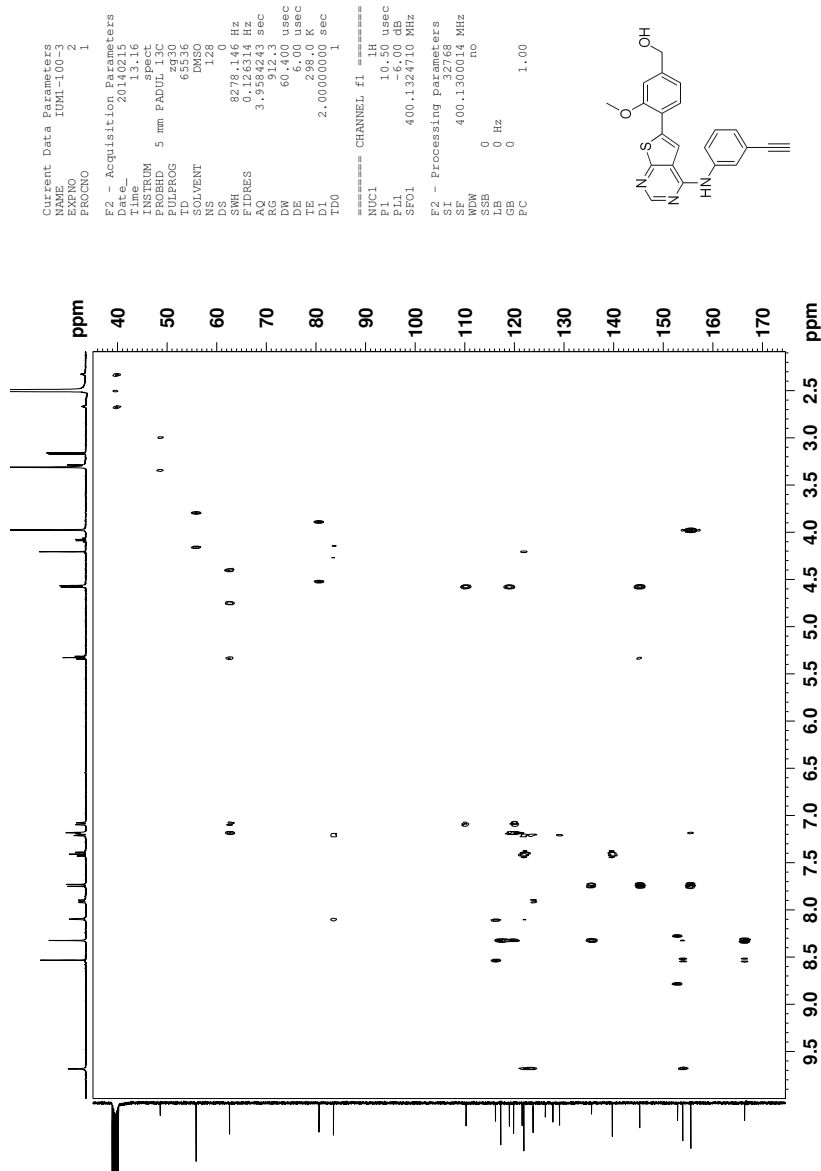


Figure O.5: HMBC spectrum of compound 15c.

O SPECTROSCOPIC DATA - COMPOUND 15C

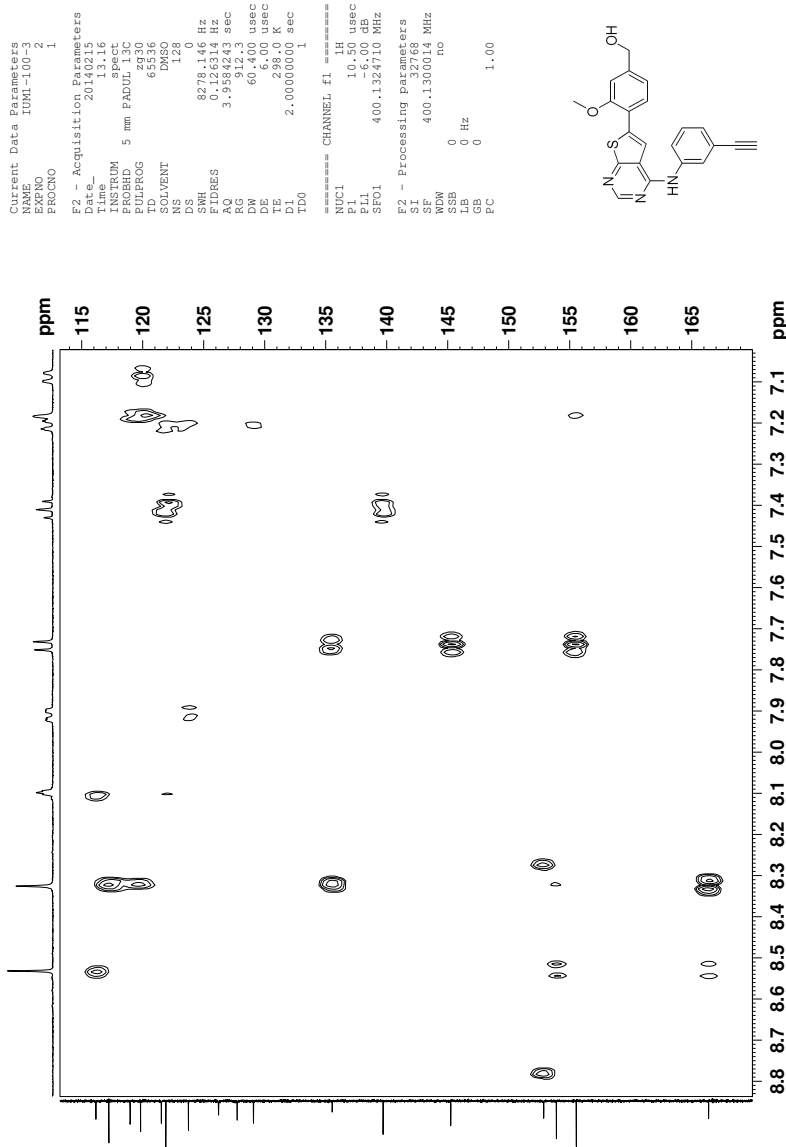
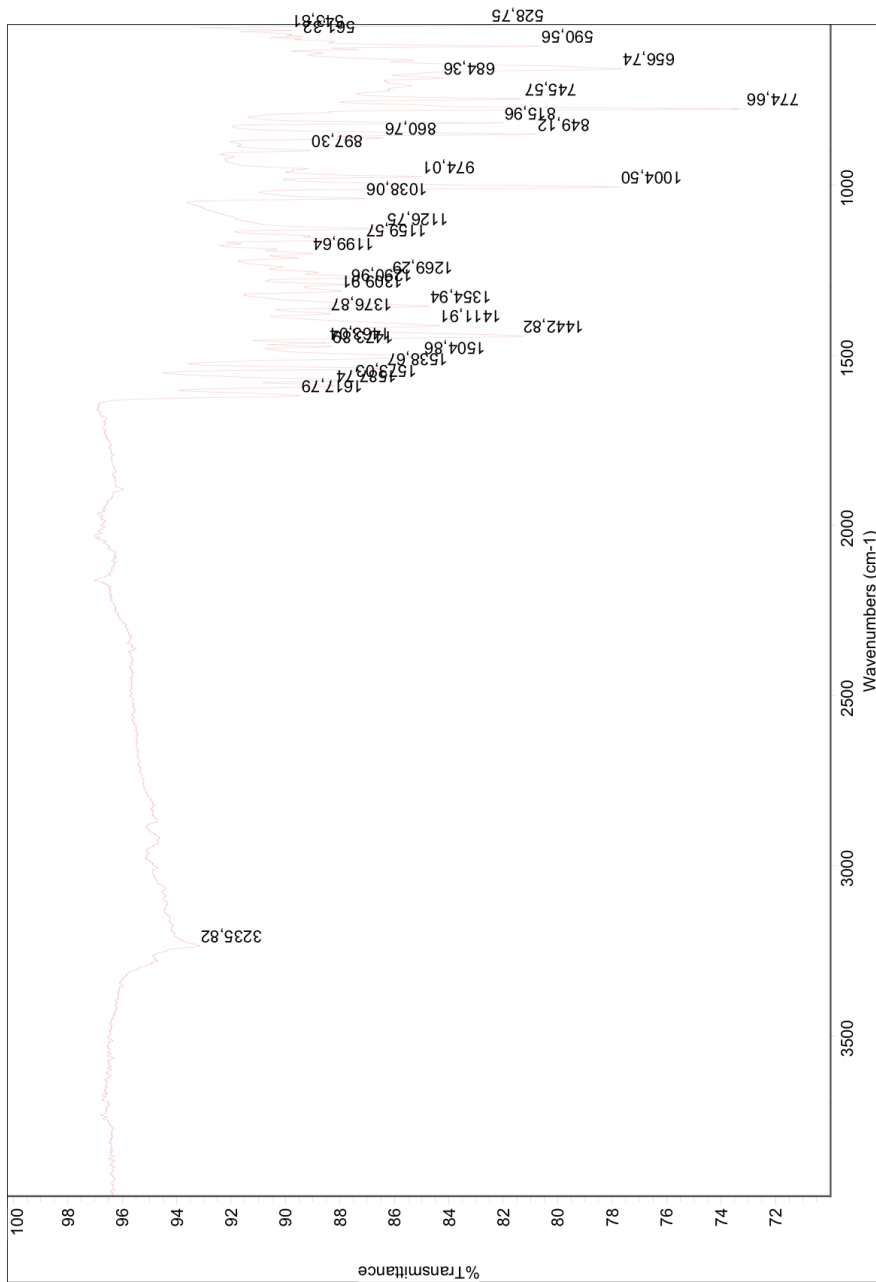


Figure O.6: Section of HMBC spectrum of compound 15c.

Figure O.7: IR spectrum of compound **15c**.

CXVI

Elemental Composition Report

Page 1

Single Mass Analysis

Tolerance = 2.0 PPM / DBE: min = -1.5, max = 50.0

Element prediction: Off

Number of isotope peaks used for i-FIT = 3

Monoisotopic Mass, Even Electron Ions

3325 formula(e) evaluated with 5 results within limits (up to 20 closest results for each mass)

Elements Used:

C: 0-500 H: 0-1000 N: 0-100 O: 0-100 S: 0-3

21-Feb-2014

2016-19 228 (4.445) AM2 (Ar:35000.0,0.00,0.00); Cm (165:228)

1: TOF MS ASAP+

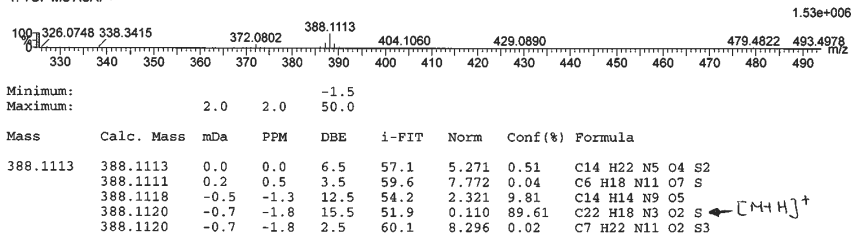


Figure O.8: MS spectrum of compound 15c.

CXVII

P Risk Assessment Form

NTNU		Utarbeidet av		Nummer		Dato	
HMS		HMS-avd.		HMSRV2601		22.02.2011	
		Godkjent av		Eksperter		Etablering	
		Hoff		Hoff		01.12.2008	

Kartlegging av risikofylt aktivitet

Dato: 30.01.2014

Enhet: Institutt for Kjemi
Linjeleder: Marie L. Oliver
Deltakere ved kartleggingen (m/ funksjon): Romansvarlig og veilederførsteamanuensis Bård Heide Hoff, medveileder Steffen Bugge, masterstudent Ingri U. Moen
(Ansv. veileder, student, evt. medveiledere, evt. andre m. kompetanse)

Kort beskrivelse av hovedaktivitet/hovedprosess: Masteroppgave student: Ingri Ullestad Moen. Tittel på oppgaven.: Fragment based approach in the search for new kinase inhibitors

Er oppgaven rønt teoretisk? (JA/NEI): nei

risikovurdering, Besonr «JA»: Beskriv kort aktiviteten i kartleggingskjemaet under. Risikovurdering trenger ikke å fylles ut.

Signaturer: Ansvarlig veileder: _____

ID nr.	Aktivitet/prosess	Ansvarlig	Ekisterende dokumentasjon	Ekisterende sikringsstiltak	Lov, forskrift o.l.	Kommentar
S-1	Generell syntetisk organisk kjemi aktivitet	Hoff	Egen kartlegging og risikovurdering av generell syntetisk organisk kjemi aktivitet for lab D2-102 NTNU Lab og verksted håndbok	Arbeid i Avtrekk	AML Kjemikalieforskriften Farenstofforskriften Farenstoffsforurensningsforskriften Produktforskriften Merkelieforskriften Brennstoffforskriften eksplosjonsforskriften	Se egen kartlegging (vedlegg 2a) og risikovurdering (vedlegg 2b) av generell syntetisk organisk kjemi aktivitet for laboratorium D2-102
S-2	Organisk syntetisk aktivitet	Hoff /Ingri	Prosjektbeskrivelse Egen kartlegging og risikovurdering av generell syntetisk organisk kjemi aktivitet for lab D2-102 NTNU Lab og	Arbeid i avtrekk	AML Kjemikalieforskriften Farenstofforskriften Farenstoffsforurensningsforskriften Produktforskriften Merkelieforskriften Brennstoffforskriften eksplosjonsforskriften	Prosjektbeskrivelse (vedlegg). SJA analyser vil bli utført daglig og utarbejdet bli gjort opp i avtrekkskapet

Figure P.1: Risk assessment of the performed work, page 1.





 NTNU  HMS	Kartlegging av risikofylt aktivitet		Utarbeidet av HMS-avd.	Nummer HMSRV2601	Dato 22.03.2011	
			Godkjent av Rektor	Ersatter 01.12.2006		
S-3	Prosjektkjemikalier	Hoff	Inveiling av kjemikalier skjer under punktavsug eller i avtrekk	AML Kjemikalieforeskrif ten Forurensningsfore skriften Produktforeskrifte n Merkeforeskriften Brann og eksplosjonsforesk riften	Se egen liste over prosjektkjemikalie r (vedlegg)	
S-4	Gasskromatografi		verktøed håndbok Risikovurdert i EcoOnline NTNU Lab og verktøed håndbok			Se egen instruks For felleEllen Sab
S-5	HPLC	Hoff	AML og Kjemikalier forskrift	På benk	risikovurdering ? driftinstruks ? apparaturkort	Krever opplæring

Figure P.2: Risk assessment of the performed work, page 2.

NTNU		Risikovurdering		Utanleidt av		Nummer		Dato	
				HMS-avd.		HMSRV2601		22.03.2011	
HMS				Godkjent av				Ersatter	
				Rektor				01.12.2006	

Enhet: Institutt for Kjemi

Linjeleder: Marie L. Oliver

Deftakere ved kartleggingen (m/ funksjon): Romansvarlig og veileder/førsteamanuensis Bård Helge Hoff, medveileder Steffen Bugge, masterstudent Ingri U. Moen

(Ansv. Veileder, student, evt. medveiledere, evt. andre m. kompetanse)

Risikovurderingen gjelder hovedaktivitet: Masteroppgave student: Ingri Ullestad Moen Tittel på oppgaven: Fragment based approach in the search for new kinase inhibitors


Signaturer: Ansvarlig veileder:

Student:

Dato: 30.01.2014

ID nr	Aktivitet fra kartleggings-skjemaet	Mulig uønsket hendelse/ belastning	Vurdering av sannsynlighet (1-5)	Vurdering av konsekvens:				Risiko-Verdi (menneske)	Kommentarer/status Forslag til tiltak
				Menneske (A-E)	Ytre miljø (A-E)	Øk/ materiell (A-E)	Om- dømme (A-E)		
1	HPLC	Kjemikalissøl/eksponering	3	A	A	A	A	3A	Arbeid i avtrekk Std værneutstyr
2	Syntese aktivitet	Eksposering/kuttskader	3	B	A	A	A	3A	Arbeid i avtrekk Std værneutstyr
3	Organisk løsningsmidler	Eksposeringfare – søl Hudkontakt og innånding	3	B	A	A	A	3A/B	Bruker hansker som er kjemikaliebestandig Std værneutstyr Håndteres i avtrekkskap
		Sprut - øyeskade Brann i kjemikallet	3	C	A	A	A	3B / 3A	Påbudt med øyevern på laben
			2	B	A	A	A	2A/B	Det finnes ingen åpne brannkilder på laben Det jobbes kun med små mengder, opp til 2,5 L
4	Veie av farlig kjemikalier (vurdert som gul eller rød fra EcoOnline)	Eksposeringfare - Hudkontakt og innånding	2	A	A	A	A	2A	Hansker må bli brukt av rett kvalitet (se veiledning på Lab og verksted håndbok-hansker guide)

Figure P.3: Risk assessment of the performed work, page 3.

NTNU		Risikovurdering				Utarbeidet av	Nummer	Date
HMS						HMS-avd.	HMSRV2601	22.03.2011
		Godkjent av		Erstatler		01.12.2006		
		Rektor						

									Utveies i avtrekk Påbudt med labfrakken på laben
	Arylborsyrer	3	A	A	A	A	A	3A	Lite giftig Std værneutstyr
	Aniliner	3	B	A	A	A	A	3A	Håndteres i avtrekkskap 100-500 mg: liten mengde Avtrekkskap
	Fosforoksyklorid	2	A	A	A	A	A	2A	Rett type hansker
	Halogeneringsmidler	2	B	A	A	A	A	2A/B	Måles ut i avtrekk. Nøytralisering gjøres i avtrekk Rett type hansker
5	Palladiumforbindelser	3	A	A	A	A	A	3A	Måles ut i avtrekk. Nøytralisering gjøres i avtrekk Rett type hansker
6	Kjemikalier-reagenser og produkter	3	B	A	A	A	B	3B	Fast stoff, liten mengde 10- 200 mg.
									Små mengder: 1-100 mg Benytt støvmaske for faste stoffer



Sannsynlighet vurderes etter følgende kriterier:

Svært liten 1	Liten 2	Middels 3	Stor 4	Svært stor 5
1 gang pr. 50 år eller sjeldnere	1 gang pr. 10 år eller sjeldnere	1 gang pr. år eller sjeldnere	1 gang pr. måned eller sjeldnere	Skjer ukentlig

Konsekvens vurderes etter følgende kriterier:

Gradering	Menneske	Ytre miljø	ØK/materiell	Omdømme
-----------	----------	------------	--------------	---------

Figure P.4: Risk assessment of the performed work, page 4.

NTNU		Risikovurdering		Utarbeidet av		Nummer		Dato	
 HMS				HMS-avd.		HMSRV2601		22.05.2011	
				Godkjent av Rektor				Erstatler 01.12.2006	
									

	Vann, jord og luft				
E Svært Alvorlig	Død	Svært langvarig og ikke reversibel skade	Drifts- eller aktivitetsstans >1 år.	Troverdighet og respekt betydelig og varig svekket	
D Alvorlig	Alvorlig personskade. Mulig uførhet.	Langvarig skade. Lang restitusjonstid	Driftsstans > ½ år Aktivitetsstans i opp til 1 år	Troverdighet og respekt betydelig svekket	
C Moderat	Alvorlig personskade.	Mindre skade og lang restitusjonstid	Drifts- eller aktivitetsstans < 1 mnd	Troverdighet og respekt svekket	
B Liten	Skade som krever medisinsk behandling	Mindre skade og kort restitusjonstid	Drifts- eller aktivitetsstans < tuke	Negativ påvirkning på troverdighet og respekt	
A Svært liten	Skade som krever førstehjelp	Ubetydelig skade og kort restitusjonstid	Drifts- eller aktivitetsstans < 1dag	Liten påvirkning på troverdighet og respekt	

Risikoverdi = Sannsynlighet x Konsekvens

Beregn risikoverdi for Menneske. Enheten vurderer selv om de i tillegg vil beregne risikoverdi for Ytre miljø, Økonomimateriell og Omdømme. I så fall beregnes disse hver for seg.

Til kolonnen "Kommentarer/status, forslag til forebyggende og korrigerende tiltak":

Tiltak kan påvirke både sannsynlighet og konsekvens. Prioriter tiltak som kan forhindre at hendelsen inntreffer, dvs. sannsynlighetsreducerende tiltak foran skjerpet beredskap, dvs. konsekvensreducerende tiltak.

Figure P.5: Risk assessment of the performed work, page 5.

NTNU		Risikomatrixe		Nummer		Dato	
HMS/IKS				HMSRV2604		08.03.2010	
		Utsendelses- og godkjent av					
		Rektor				08.02.2010	

MATRISE FOR RISIKOVURDERINGER ved NTNU

KONSEKVENSENS	Svært alvorlig	E1	E2	E3	E4	E5
	Alvorlig	D1	D2	D3	D4	D5
	Moderat	C1	C2	C3	C4	C5
	Liten	B1	B2	B3	B4	B5
	Svært liten	A1	A2	A3	A4	A5
		Svært liten	Liten	Middels	Stor	Svært stor
SANNSYNLIGHET						

Prinsipp over akseptkriterium. Forklaring av fargene som er brukt i risikomatrixen.

Farge	Beskrivelse
Rød	Uakseptabel risiko. Tiltak skal gjennomføres for å redusere risikoen.
Gul	Vurderingsområde. Tiltak skal vurderes.
Grønn	Akseptabel risiko. Tiltak kan vurderes ut fra andre hensyn.

Figure P.6: Risk assessment of the performed work, page 6.